ISSN 0021-9673

VOL. 659 NO. 1 JANUARY 21, 1994

JOURNAL OF CHROMATOGRAPHY A

INCLUDING ELECTROPHORESIS AND OTHER SEPARATION METHODS

ELSEVIER

JOURNAL OF CHROMATOGRAPHY A

INCLUDING ELECTROPHORESIS AND OTHER SEPARATION METHODS

Scope. The *Journal of Chromatography A* publishes papers on all aspects of **chromatography, electrophoresis** and related methods. Contributions consist mainly of research papers dealing with chromatographic theory, instrumental developments and their applications. In the *Symposium volumes*, which are under separate editorship, proceedings of symposia on chromatography, electrophoresis and related methods are published. *Journal of Chromatography B: Biomedical Applications* —This journal, which is under separate editorship, deals with the following aspects: developments in and applications of chromatographic and electrophoretic techniques related to clinical diagnosis or alterations during medical treatment; screening and profiling of body fluids or tissues related to the analysis of active substances and to metabolic disorders; drug level monitoring and pharmacokinetic studies; clinical toxicology; forensic medicine; veterinary medicine; occupational medicine; results from basic medical research with direct consequences in clinical practice.

Submission of Papers. The preferred medium of submission is on disk with accompanying manuscript (see *Electronic manuscripts* in the Instructions to Authors, which can be obtained from the publisher, Elsevier Science B.V., P.O. Box 330, 1000 AH Amsterdam, Netherlands). Manuscripts (in English; *four* copies are required) should be submitted to: Editorial Office of *Journal of Chromatography A*, P.O. Box 681, 1000 AR Amsterdam, Netherlands, Telefax (+31-20) 5862 304, or to: The Editor of *Journal of Chromatography B: Biomedical Applications*, P.O. Box 681, 1000 AR Amsterdam, Netherlands. Review articles are invited or proposed in writing to the Editors who welcome suggestions for subjects. An outline of the proposed review should first be forwarded to the Editors for preliminary discussion prior to preparation. Submission of an article is understood to imply that the article is original and unpublished and is not being considered for publication elsewhere. For copyright regulations, see below.

Publication information. *Journal of Chromatography A* (ISSN 0021-9673): for 1994 Vols. 652–682 are scheduled for publication. *Journal of Chromatography B: Biomedical Applications* (ISSN 0378-4347): for 1994 Vols. 652–662 are scheduled for publication. Subscription prices for *Journal of Chromatography A*, *Journal of Chromatography B: Biomedical Applications* or a combined subscription are available upon request from the publisher. Subscriptions are accepted on a prepaid basis only and are entered on a calendar year basis. Issues are sent by surface mail except to the following countries where air delivery via SAL is ensured: Argentina, Australia, Brazil, Canada, China, Hong Kong, India, Israel, Japan, Malaysia, Mexico, New Zealand, Pakistan, Singapore, South Africa, South Korea, Taiwan, Thailand, USA. For all other countries airmail rates are available upon request. Claims for missing issues must be made within six months of our publication (mailing) date. Please address all your requests regarding orders and subscription queries to: Elsevier Science B.V., Journal Department, P.O. Box 211, 1000 AE Amsterdam, Netherlands. Tel.: (+31-20) 5803 642; Fax: (+31-20) 5803 598. Customers in the USA and Canada wishing information on this and other Elsevier journals, please contact Journal Information Center, Elsevier Science Inc., 655 Avenue of the Americas, New York, NY 10010, USA, Tel. (+1-212) 633 3750, Telefax (+1-212) 633 3764.

Abstracts/Contents Lists published in Analytical Abstracts, Biochemical Abstracts, Biological Abstracts, Chemical Abstracts, Chemical Titles, Chromatography Abstracts, Current Awareness in Biological Sciences (CABS), Current Contents/Life Sciences, Current Contents/Physical, Chemical & Earth Sciences, Deep-Sea Research/Part B: Oceanographic Literature Review, Excerpta Medica, Index Medicus, Mass Spectrometry Bulletin, PASCAL-CNRS, Referativnyi Zhurnal, Research Alert and Science Citation Index.

US Mailing Notice. *Journal of Chromatography A* (ISSN 0021-9673) is published weekly (total 52 issues) by Elsevier Science B.V., (Sara Burgerhartstraat 25, P.O. Box 211, 1000 AE Amsterdam, Netherlands). Annual subscription price in the USA US$ 4994.00 (US$ price valid in North, Central and South America only) including air speed delivery. Second class postage paid at Jamaica, NY 11431. **USA POSTMASTERS**: Send address changes to *Journal of Chromatography A*, Publications Expediting, Inc., 200 Meacham Avenue, Elmont, NY 11003. Airfreight and mailing in the USA by Publications Expediting.

See inside back cover for Publication Schedule, Information for Authors and information on Advertisements.

0021-9673/94/$07.00

Printed in the Netherlands

CONTENTS

(Abstracts/Contents Lists published in Analytical Abstracts, Biochemical Abstracts, Biological Abstracts, Chemical Abstracts, Chemical Titles, Chromatography Abstracts, Current Awareness in Biological Sciences (CABS), Current Contents/Life Sciences, Current Contents/Physical, Chemical & Earth Sciences, Deep-Sea Research/Part B: Oceanographic Literature Review, Excerpta Medica, Index Medicus, Mass Spectrometry Bulletin, PASCAL-CNRS, Referativnyi Zhurnal, Research Alert and Science Citation Index)

(Continued overleaf)

Contents (continued)

BOOK REVIEWS

JOURNAL OF CHROMATOGRAPHY A

VOL. 659 (1994)

JOURNAL OF CHROMATOGRAPHY A

INCLUDING ELECTROPHORESIS AND OTHER SEPARATION METHODS

ELSEVIER

AMSTERDAM — LONDON — NEW YORK — TOKYO

0021-9673/94/$07.00

Printed in the Netherlands

Journal of Chromatography A, 659 (1994) 1
Elsevier Science B.V., Amsterdam

CHROM. 25 684

Publisher's Note

Observant readers of this issue of the *Journal of Chromatography A* may have noticed an important change on the cover and title page: after having served the journal in various capacities for more than 30 years, Dr. Karel Macek has relinquished his position as editor of this section as from January 1994.

Karel Macek, who has been actively involved in chromatography since his university studies in the late 1940s, first joined the *Journal of Chromatography* in 1962 as editor of the Bibliography Section. This section, which has its roots in the *Handbook of Paper Chromatography* (by Drs. Ivo Hais and Karel Macek), has in the course of the years become perhaps the most complete survey of the literature on chromatography and electrophoresis.

After a stay in Rome at Michael Lederer's laboratory in 1968–1969, Karel Macek became associate editor of the *Journal of Chromatography* in 1969 and since 1989 he has been one of the editors of the main section of the journal.

Coming from a background in analytical biochemistry, Karel Macek recognized early on the important role that the separation sciences could play in biomedicine. This contributed to the establishment, in 1977, of a separate section, *Journal of Chromatography, Biomedical Applications*, of which Karel has been editor since its inception.

We have greatly valued our efficient and cordial collaboration with Karel Macek during the course of the many years. Fortunately, his departure as editor of the "blue" section does not bring this collaboration to an end: he will remain as one of the editors, together with Irving Wainer, of the *Journal of Chromatography B: Biomedical Applications*, where readers and contributors will continue to benefit from his dedication and critical judgement, and he will join the editorial board of the *Journal of Chromatography A*. Although the amount of extra free time that he will now have available may thus be limited, we hope Karel will enjoy it in good health and that it will allow him to devote more time to his other passions, such as the arts (in particular, opera), travelling and culinary delights.

SSDI 0021-9673(93)E1139-Q

Journal of Chromatography A, 659 (1994) 3–13
Elsevier Science B.V., Amsterdam

CHROM. 25 621

Review

Cross-axis coil planet centrifuge for the separation and purification of polar compounds

J.-M. Menet, D. Thiebaut* and R. Rosset

Laboratoire de Chimie Analytique (URA CNRS 437), École Supérieure de Physique et Chimie Industrielles, 10 Rue Vauquelin, 75231 Paris Cedex 05 (France)

(First received July 22nd, 1993; revised manuscript received October 4th, 1993)

ABSTRACT

A new counter-current chromatograph, named the cross-axis coil planet centrifuge, has been optimized through various versions since 1987. Features of this recently commercialized apparatus are reviewed. It allows the use of biphasic polar solvent systems, of aqueous solutions of polymers and systems containing an organic phase of small or moderate hydrophobicity. Separations and purifications achieved on the cross-axis device demonstrate that it provides a good efficiency and resolution with very high retention of the stationary phase at convenient flow-rates, whatever the solvent system used.

CONTENTS

1. INTRODUCTION

Counter-current chromatography (CCC) is a liquid–liquid partition chromatographic method. The stationary phase is liquid and is retained in the column by a chosen centrifugal force field. The mobile phase, immiscible to the stationary phase, percolates through the latter. At present, CCC has limitations related to the design of the devices. The type J coil planet centrifuge (CPC)

* Corresponding author.

0021-9673/94/$07.00
SSDI 0021-9673(93)E1049-6

allows the use of high flow-rates of the mobile phase but cannot be used reliably with biphasic polar solvent systems [1]. In contrast, the centrifugal droplet counter-current chromatograph (CDCCC) is able to retain these solvent systems but the flow-rates are limited because of the internal pressure [2].

The cross-axis CPC has emerged as a universal counter-current chromatograph. It combines the respective advantages of the two previous devices, *i.e.*, the use of high flow-rates and of biphasic polar solvent systems. Moreover, the column efficiency is at least comparable to or even higher than that of the type J CPC, which in turn is higher than that of the CDCCC.

This review describes the genesis and evolution of cross-axis devices, along with their principles and operation. Some applications are detailed, ranging from the purification of complex media, natural products and antibiotics to separations of biological interest. They allow comparison with the two other CCC devices and demonstrate the capability of the cross-axis device to provide faster separations without any loss of efficiency and resolution.

2. INSTRUMENTATION

2.1. Genesis

In 1981, Ito [3] built a new apparatus based on planetary motion, named the high-speed counter-current chromatograph (HSCCC) because of its ability to achieve fast separations. The central axis of the apparatus and the axis of the column are parallel. For all the devices described in this section, the chromatographic column is made of a PTFE tube wound around a cylindrical holder. The design is referred as a type J CPC [4] (coil planet centrifuge). Its principle is shown in Fig. 1A.

In 1986, he designed a new prototype, called the type J-L angle rotor CPC [5]. The motion is also planetary. However, the column axis and the central axis are no longer parallel; in this prototype they have a 25° angle to each other, as shown in Fig. 1B.

The obvious end for these designs was to incline the column axis so that it would be perpendicular to the central axis. Such a prototype was realized in 1987 by Ito, who named it the type X CPC [6], shown in Fig. 1C.

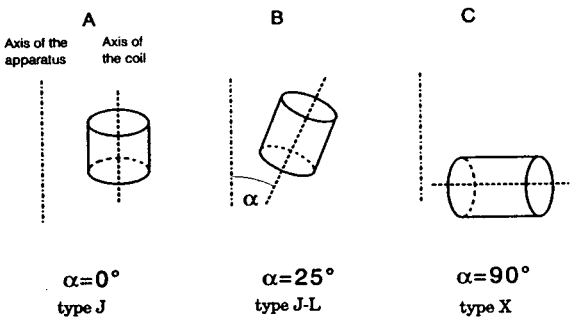

Fig. 1. Genesis of the cross-axis CPC.

2.2. General principle

The vertical axis of the apparatus and the horizontal axis of the coil are always kept perpendicular to each other at a fixed distance. The cylindrical column revolves around the central axis at the same rotational speed as it rotates on its own axis. As the PTFE inlet and outlet flow tubes can rotate on themselves without any twisting, the device is rotary seal free. Three parameters displayed in Fig. 2A explain the various versions of the cross-axis prototypes: r is the radius of the column holder, R is the distance between the two axes and L is the measure of the lateral shift of the column holder along its axis. The name of a cross-axis device is based on the ratio L/R, when defined. Types X and L represent the limits for the column positions; the first type involves no shifting of the column holder while the second corresponds to an infinite shift. Some examples of Ito's prototypes are shown in Fig. 2B. Table I gives the characteristics of the six cross-axis prototypes built by Ito and co-workers [6–11]. They have different L/R ratios, hence their various names.

Studies of the ratio β $(=r/R)$ led to various columns by varying the radius of the column holder. However, another idea was to change the holder configuration. Fig. 3 shows the two types of column holders used on type J and

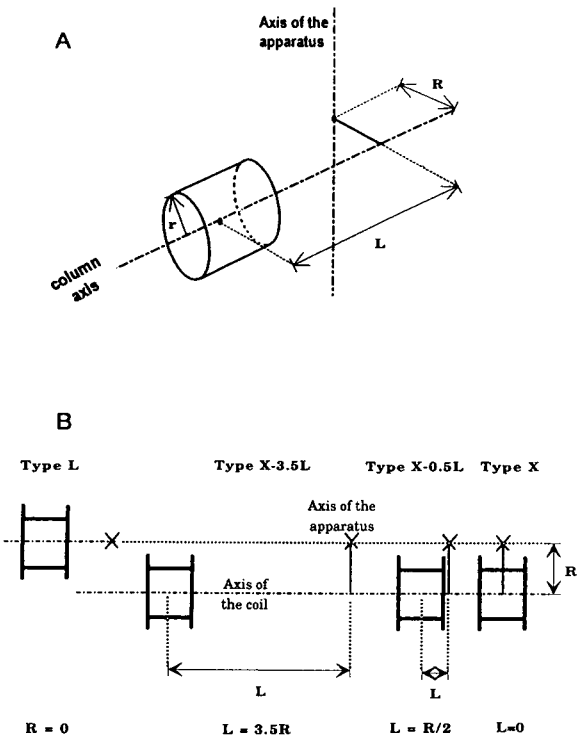

Fig. 2. General principle of various cross-axis CPCs. (A) All the fundamental parameters for the design of a cross-axis apparatus are shown. (B) Some examples of Ito's prototypes are displayed. Type X was built in 1987, type X-0.5L in 1988, type X-3.5L in 1991 and type L in 1992.

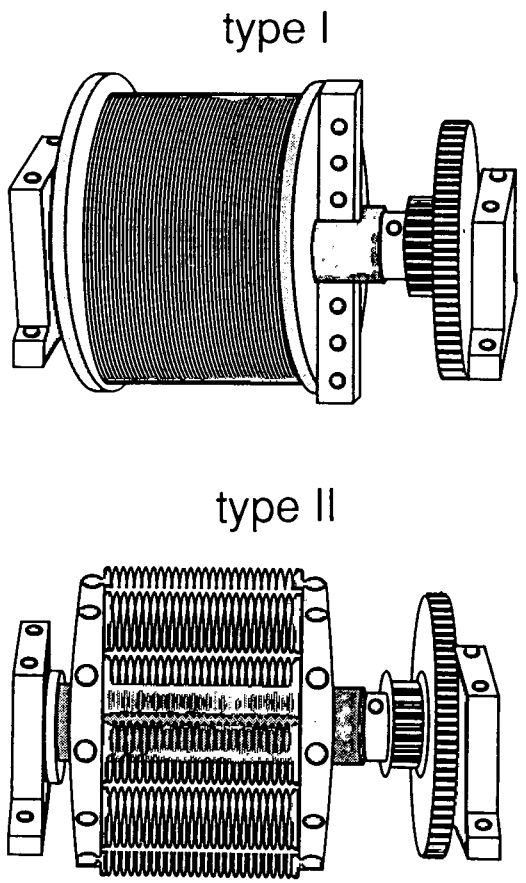

Fig. 3. Two types of columns used on type J and cross-axis CPCs (modified from ref. 11). The description is given in the text.

cross-axis prototypes. Type I is the best known and the simplest as the PTFE tube is directly wound on a cylinder. This standard type (Ia) consists of alternate layers of right- and left-handed coils. A second subtype (Ib), mainly used for cross-axis CPCs, consists of entirely left- or right-handed coils with interconnecting tubes between each layer. The type II column is an eccentric coil assembly [12]. It consists in a given number of column units, each prepared by winding a PTFE tube on a cylinder. The set of these units is arranged symmetrically around the holder; they are parallel to the holder axis, at the same distance. All of them are left- or right-handed coils. For this type of column, β is defined as the ratio of the radius of a cylinder forming a column unit on R. The purpose is to decrease β, which can be as low as 0.01. The internal volume of such columns is small (a few tens of millilitres) so that they have an analytical purpose. Moreover, using small β values increases the efficiency (number of theoretical plates) of the column [11].

Except for the first prototype, it was possible to assemble two columns in series. The advantage is to equilibrate continuously the whole apparatus, from a mechanical point of view.

The latest prototype [11] (X-1.5L type), commercialized by Countercurrent Technologies (CTI [13]), is shown in Fig. 4. All the parts are made of stainless steel, except for the gears and the cylindrical holders, which are of Delrin. Its external dimensions are 60 cm × 60 cm × 35 cm. A horizontal section, perpendicular to the central axis, is shown in Fig. 5. The two columns, made of several layers of PTFE tubing wound on

TABLE I
CHARACTERISTICS OF CROSS-AXIS CPCs

Year	Column position	L (cm)	R (cm)	β[a]	Column volume (ml)
1987 [6]	X	0	10	0.25	15
				0.50	15
				0.75	15
				0.5–0.8	400
				0.19–0.9	?
1988 [7]	X or X-0.5L	0 or 10	20	0.125	15 or 28
				0.375	15 or 28
				0.625	15 or 28
				0.375–0.625	800
1989 [8]	X-1.25L	12.5	10	0.5	28
				0.75–1.75	750
1991 [9]	X-LL	15.2	7.6	0.5	20–30
				1	20–30
				1.6	20–30
				0.25–0.60	280
				0.50–1.00	250
				1.00–1.20	450
1991 [10]	X-3.5L	13.5	3.8	0.50–1.30	150
				0.44–1.50	220
1992 [11]	X-1.5L or L	16.85	10.4 or 0	0.26 or 0.16	20
				0.48 or 0.30	41
				0.26–0.48 or 0.16–0.30	287
				0.10 or 0.06	18
				0.02 or 0.01	17

[a] β Calculated as defined in the text ($\beta = r/R$), except for the L position: $\beta = r/L$.

the cylindrical holder, are mounted in series. The inside diameter of the tube used for the columns is 2.6 mm. The rotational speed is regulated up to 1000 rpm, the usual operating speed being 750–800 rpm. The configurations of the stationary and planetary mitre gears and the pulleys and belts force the column to rotate around its own axis at the same speed as its revolution speed around the central axis. Two counter-axes, rotating due to the plastic gears, are required to prevent the twisting of the inlet and outlet PTFE tubes. The prototype was built to allow the counter-axis to be exchanged with the column holder. In that case, the type would be L.

3. ADVANTAGES

3.1. Retention of stationary phase

Ito [14] defined three solvent system groups, according to the hydrophobicity of the non-aqueous phase. The first, called "hydrophobic", includes solvent systems containing a hydrophobic organic phase, such as heptane–water or chloroform–water. Such systems are easily retained by the type J [15] and cross-axis CPCs [16] and by the CDCCC [17], as shown in Table II, with a particularly high value for the X-axis.

"Intermediate" solvent systems involve a more hydrophilic organic phase; examples are chloro-

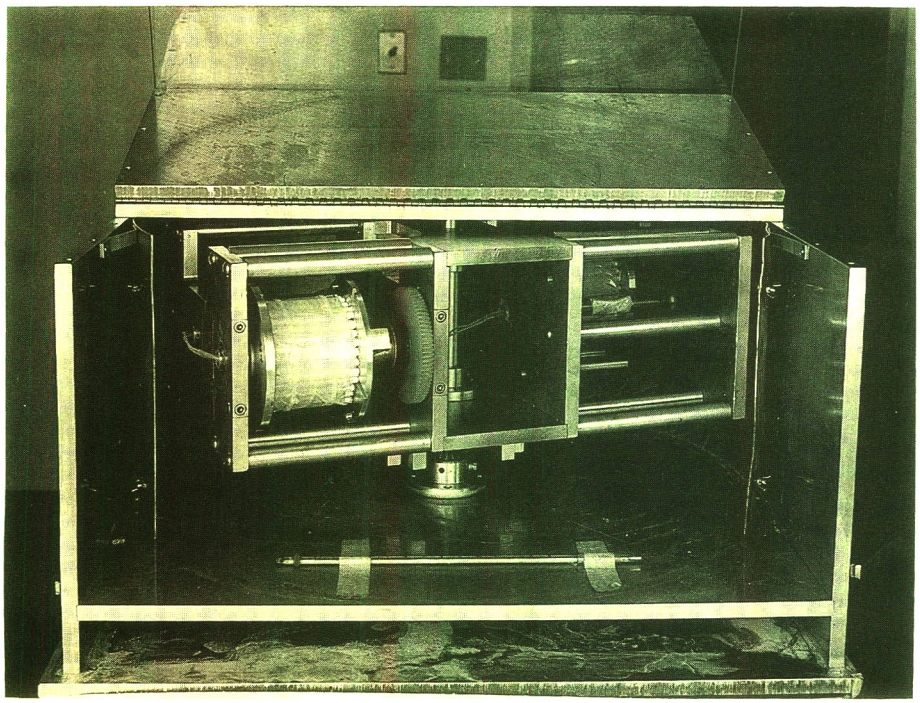

Fig. 4. Photograph of the type L and X-1.5L prototype (courtesy of Dr. Y. Ito). All the rotating parts are enclosed in a box. The pulley driven by a belt from the electric engine is at the bottom of the vertical central axis. Two cylindrical holders (white parts) are mounted in the X-1.5L position. The inlet and outlet PTFE tubes go through the upper part of the central axis. One counter-axis for each column is installed to prevent the twisting of the PTFE tubes. A small circular plate around the holder of the columns and the counter-axis decreases the required engine torque by 30%. Owing to the sufficient distance between one column axis and its counter-axis, the connecting tubes are reliable and do not need to be replaced often.

form–acetic acid–water and *n*-butanol–water. Their tendency to evolve after mixing to a more stable emulsion than the "hydrophobic" system decreases the retention of stationary phase. Type J CPC undergoes the highest decrease [15], whereas the other two devices show only a small decrease [16,17].

The "hydrophilic" group encompasses biphasic systems containing a polar phase, such as *n*-butanol–acetic acid–water and *sec.*-butanol–water. Their emulsions are nearly stable. Consequently, their stationary phase is even less retained in the column; the type J device leads to such low values that it can hardly be used with such systems [15]. The CDCCC allows good retention of the stationary phase [17] at a low flow-rate limited by the internal pressure drop due to the viscosity of the organic phase [2]. The cross-axis apparatus does not encounter such a limitation [11,16]; its internal pressure drop is similar to that observed inside the type J CPC, which is much smaller than that obtained on a CDCCC.

This advantage is magnified when systems containing at least one polymer phase are used. The retention of the stationary phase ranges from 30% to 70% at an average flow-rate of 3 ml/min [11] for the cross-axis CPC, whereas the CDCCC permits a smaller range but at a flow-rate lower than 1 ml/min [17]. The type J CPC using type I columns does not retain these solvent systems [18], whereas the use of type II columns allows a small retention of stationary phase (typically 20%) [19]. Therefore, all the values shown in Table II emphasize one of the advantages of the cross-axis CPC, *i.e.*, that it allows a universal choice of solvent systems without diminished flow-rates.

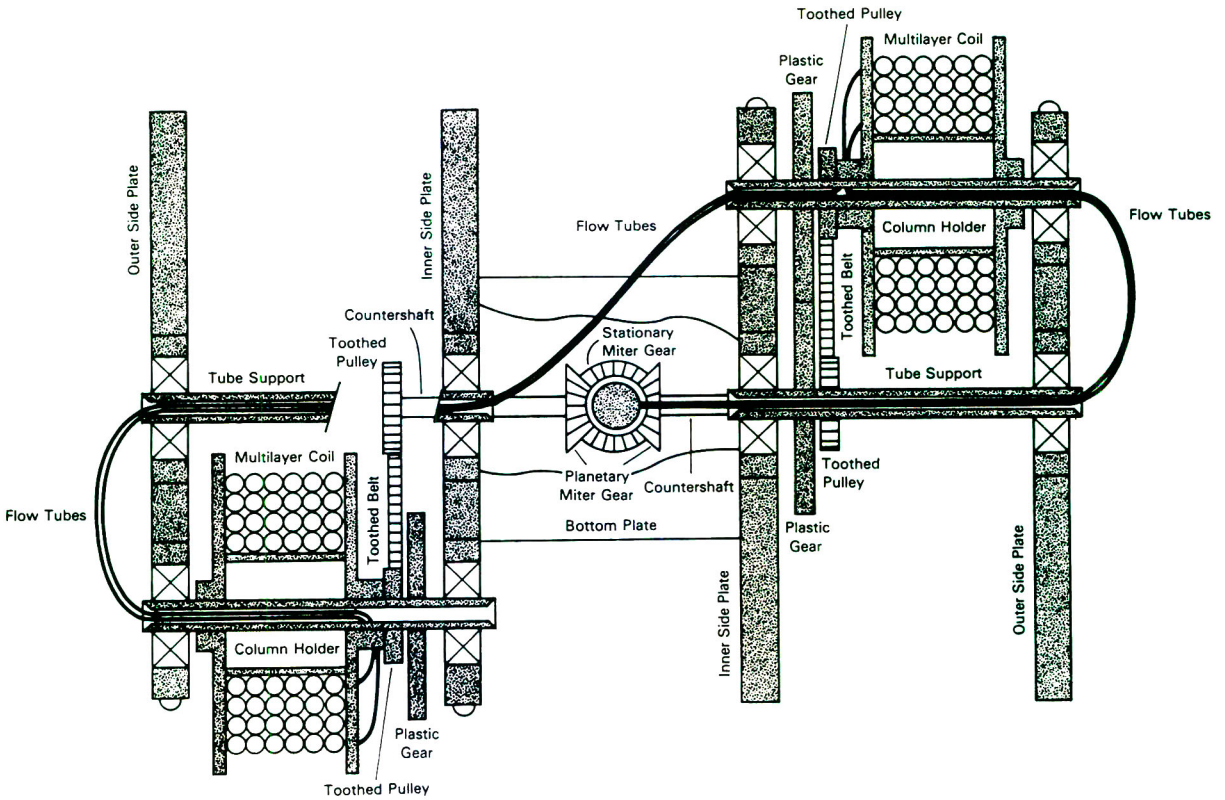

Fig. 5. Section of the latest cross-axis device [11]. The plane of the section is perpendicular to the central axis of the apparatus. The two columns and their counter axes are shown in the X-1.5L position. The paths for the PTFE tubes are shown. The inlet tube comes from the central axis, goes through one counter-axis and undergoes a small loop before entering the axis of the column. Then the outlet of the column goes to the counter-axis, undergoes the small loop and enters the axis of the second column. The outlet tube must take exactly the same reverse path otherwise twisting occurs.

TABLE II

MAXIMUM RETENTIONS OF STATIONARY PHASE FOR TYPE J AND CROSS-AXIS CPCs AND CDCCC

The retention of the stationary phase is given as a percentage of the total volume of the column. For hydrophilic systems and those containing a polymer phase, the values are obtained on the cross-axis CPC at an average flow-rate of 3 ml/min, whereas they are typically obtained at 1 ml/min on the CDCCC.

Solvent system group	Type J CPC	Cross-axis CPC	CDCCC
"Hydrophobic"	90 [15]	>95 [16]	75 [17]
"Intermediate"	50 [15]	>80 [16]	75 [17]
"Hydrophilic"	20–30 [15]	50–90 [11,16]	50–70 [17]
Containing a polymer phase	0 [18]	30–70 [11]	<50 [17]

3.2. Resolution and efficiency

According to the equation

$$R_s = 2V_s(K_2 - K_1)/(w_2 + w_1) \quad (1)$$

where R_s is the resolution between two adjacent peaks, K_2 and K_1 the partition coefficients of the separated solutes and w_2 and w_1 are the peak base widths in volume units, the resolution between two peaks is proportional to the volume of stationary phase (V_s) inside the column. As a result, the higher the retention of stationary phase, the higher is the resolution. The high retention of the stationary phase obtained with the cross-axis CPC is consequently particularly helpful in achieving good separations.

Using the same solvent system, a separation of three proteins (*e.g.*, cytochrome *c*, myoglobin and ovalbumin) allows a comparison of type J and cross-axis CPCs [19]. To obtain a sufficient retention of the polyethylene glycol (PEG)-rich stationary phase, type II columns were used with a type J CPC. However, the limited flow-rate of 0.65 ml/min leads to 19% retention of the stationary phase, which is low compared with the 49% obtained with the cross-axis at a flow-rate of 2 ml/min. The low flow-rate for the type J CPC increases the separation time to 10 h, as shown in Fig. 6A, two times longer than the experiments carried on the cross-axis CPC (Fig. 6B). Moreover, the latter shows a higher resolution, partly due to the increase in stationary phase retention. The efficiencies, measured as the number of theoretical plates using the myoglobin and ovalbumin peaks, are similar for the two devices.

3.3. Column choice

The cross-axis apparatus is very versatile because the volume of type I columns is easily chosen and adapted to the purpose of the separation. A small cylinder radius and inside diameter and one layer of PTFE tube lead to an "analytical" version. A multi-layer coil of a larger inside diameter allows a "semi-preparative" use. Type II columns are adapted to "analytical" separations, as they are made of several single-layer coils of low volume.

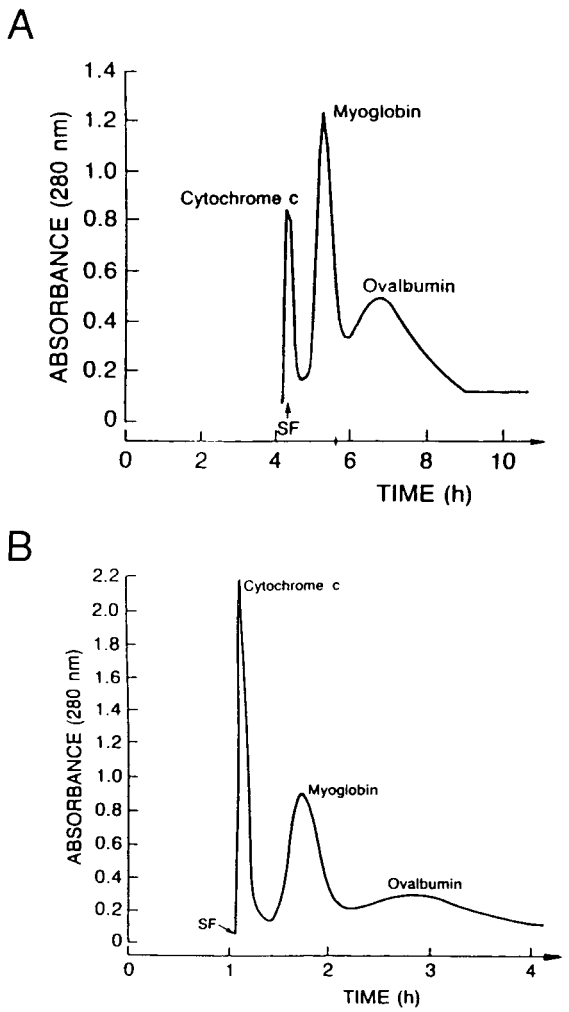

Fig. 6. Comparison of separations of a three-protein mixture achieved on type J and cross-axis CPCs (modified from ref. 19). (A) Type J CPC equipped with Type II columns with a 220-ml total capacity; sample, 10–100 mg of each protein; solvent system, 12.5% (w/w) PEG-1000–12.5% (w/w) K_2HPO_4 with a heavier mobile phase; flow-rate, 0.65 ml/min; rotational speed, 800 rpm. (B) Type X-LL cross-axis CPC with a 250-ml total capacity; two type Ib columns in series. Same experimental conditions as above, except flow-rate 2 ml/min and rotational speed 750 rpm.

4. OPERATION

4.1. Operating parameters

A cross-axis device is operated the same way as a type J CPC. However, more parameters intervene: they are displayed in Table III for

TABLE III

OPERATING PARAMETERS FOR TYPE J AND CROSS-AXIS CPCs

Available parameter	Type J CPC	Cross-axis CPC
Column type	×	×
Direction of winding	×	×
Rotation direction	×	×
Elution mode	×	×
Elution direction	–[a]	×
Column position	–[a]	×
Rotational speed	×	×
Flow-rate	×	×
Choice of a lighter or a heavier mobile phase	×	×

[a] Not available.

both CPCs. Related to the column fabrication are the *column types* already discussed and the *directions of winding*. The latter can be left- or right-handed. Both devices have two *rotation directions*, *i.e.*, clockwise or counter-clockwise, around the central axis, consequently setting the rotation direction of the column. Choosing the directions of winding and of column rotation allows the definition of the head and the tail of the column. When the column is rotated, a small solid ball introduced into the tube migrates towards one end, which is called the head. The tail is the other end. For type J and cross-axis CPCs, the choice of winding and of rotation direction around the central axis determines the head and tail of the column. The direction of the mobile phase pumped in the column is described by the head-to-tail or tail-to-head *elution mode*. Another parameter is consequently required: the *elution direction*. This indicates the direction of the mobile phase relative to the central axis, *i.e.*, inward or outward. The *position of the column* (X, L, X-L, . . .) is an additional parameter for the cross-axis.

Three other usual parameters are common to both devices: the *rotational speed*, ranging from 50 to 1000 rpm, the *flow-rate*, ranging from 0.2 to 10 ml/min, and the choice of a *lighter* or a *heavier mobile phase* are also important parameters influencing the efficiency of the column, the resolution and the retention of the stationary phase.

4.2. Separation procedure

The liquid phase chosen as the stationary is pumped in the column while the apparatus is stopped. When the columns are completely filled, the CPC is rotated at the desired speed and direction. The mobile phase is then pumped and the hydrodynamic equilibrium of the phases is achieved when the mobile phase emerges from the outlet tube. The sample can be introduced using an injection valve. The solutes are dissolved in the stationary phase, the mobile phase or the mixture of the latter, depending on the experiments.

Optimization for the best retention of the stationary phase is often required concerning the elution mode and direction, the choice of the mobile phase and the rotation direction [20]. Whatever the cross-axis CPC and the solvent system, the heavier mobile phase needs to be pumped in the outward elution direction, while a lighter mobile phase requires an inward elution direction. Type Ib columns consequently enhance the major influence of the elution direction as it is the same in each layer. In contrast, type Ia columns reduce this influence by alternately changing the elution direction for neighbouring layers. Other parameters are fixed before the experiment, such as the column position, its direction of winding and its type. An increase in rotational speed usually increases the retention of stationary phase, whereas a higher flow-rate always means a lower retention of stationary phase [11]. A study based on the experimental designs is now being carried out to evaluate the independent influence of each parameter, along with their multiple interactions [21].

For on-line solute monitoring, the outlet tube is connected to detectors which are widely used in liquid chromatography, such as a UV detector [22], a fluorimeter [23] or an evaporating light-scattering detector [24].

5. APPLICATIONS AND EXAMPLES

Table IV shows separations or purifications achieved with the various cross-axis prototypes. They have analytical or preparative purposes and can be classified into three groups. One en-

TABLE IV

EXAMPLES OF SEPARATIONS AND PURIFICATIONS

Separated compounds	Amount	Solvent system
DNP amino acids [25–28]	100 mg–10 g	Chloroform–acetic acid–0.1 *M* HCl
Dipeptides (containing a tyrosine moiety) [25,26]	100 mg–2.5 g	*n*-Butanol–dichloroacetic acid–0.1 *M* ammonium formate (100:1:100 to 100:0:100, v/v/v) or *n*-butanol–acetic acid–water
Indole auxins [27,28]	3 g	*n*-Hexane–ethyl acetate–methanol–water
Proteins (containing a haeme group, lipoproteins, globulins, histones, recombinant enzyme) [10,19,29]	10 mg–1 g	PEG-1000–potassium phosphate buffer or PEG-8000/Dextran T500 + potassium phosphate buffer
Polysaccharides [30]	–[a]	*n*-Butanol–0.13 *M* NaCl + HPC[b] (15 g/l)
Steroids (crude synthetic mixture) [27]	2.4 g	*n*-Hexane–ethyl acetate–methanol–water
Flavonoids (from a crude extract of sea buckthorn) [27]	100 mg	Chloroform–methanol–water
Antibiotics (bacitracin) [28]	5 g	Chloroform–95% ethanol–water

[a] Data not available.

[b] Hexadecylpyridinium chloride.

compasses the experiments carried out with biphasic polar solvent systems. Solutes separated include dipeptides and polysaccharides. Fig. 7 shows a chromatogram of the analytical separation of six dipeptides containing a tyrosine moiety [25], which was obtained on the first prototype (X type). The solvent system consisted of two polar phases, *i.e.*, a butanol-rich phase and an aqueous phase. A gradient of dichloroacetic acid from 0.01 to 0% (v/v) was used. The retention of the stationary phase was 55%, which is high for such a solvent system.

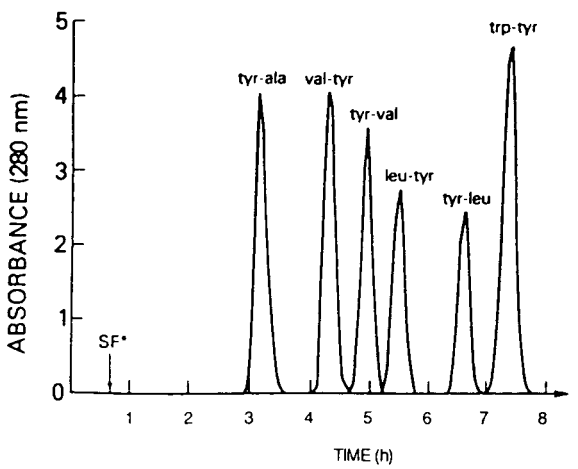

Fig. 7. Chromatogram of a dipeptide separation on a type X cross-axis CPC [25]. Amounts of 100 mg each of tyrosylalanine, valyltyrosine, tyrosylvaline, leucyltyrosine, tyrosylleucine and tryptophyltyrosine. Solvent system, *n*-butanol–dicloroacetic acid–0.1 *M* ammonium formate, with a gradient (100:1:100 to 100:0:100) with a heavier aqueous mobile phase; flow-rate, 120 ml/h; rotational speed, 800 rpm. One type Ia column, total volume 400 ml. Retention of stationary phase, 55%.

The second group of experiments concerned aqueous solutions of polymers. These systems have been extensively studied [31] because they are particularly suitable for the separation or extraction of cellular organelles and biological molecules. PEG–potassium phosphate buffer allows the pH for the two liquid phases to be fixed between 4 and 9. Moreover, varying the molecular mass of the polymer modifies the partition coefficient of the solute. Such a system was used on the cross-axis prototypes for various applications to proteins, all shown in Table IV. Another well known system is based on a PEG–dextran biphasic mixture. The partition coefficients of the solutes can also be adjusted by changing the molecular masses of the polymers; adding a phosphate buffer sets the pH. The very low interfacial tensions of these solvent systems (as low as 0.0001 dyn/cm) are suitable for fragile

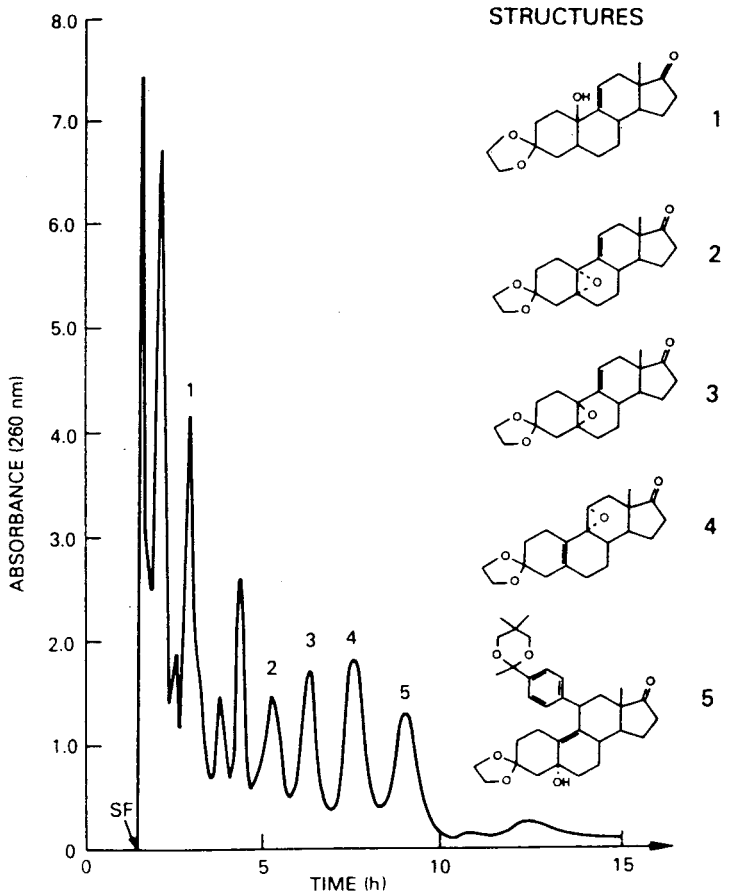

Fig. 8. Chromatogram of a steroid reaction mixture on a type X-0.5L cross-axis CPC [27]. A 2.4-g amount of a mixture of synthetic steroids was used. Solvent system, *n*-hexane–ethyl acetate–methanol–water (6:5:4:2, v/v) with a heavier aqueous mobile phase; flow-rate, 240 ml/h; rotational speed, 450 rpm. Two type Ia columns in series, total volume 1600 ml. Retention of stationary phase, 71%.

molecules, such as proteins in which the quaternary structure may be broken. A PEG-8000–dextran T500 system containing potassium phosphate buffer allowed the separation of various histones and globulins [10].

The third group of experiments included more "classical" solvent systems, based on a low-polarity organic phase and an aqueous phase. Fig. 8 shows a chromatogram of 2.4 g of a crude reaction mixture of synthetic steroids [27]. The semi-preparative separation was carried out at a high flow-rate of 4 ml/min. However, the retention of the stationary phase remained high (71%). Five products were identified by NMR spectroscopy and their formulae are given in Fig. 8. The same solvent system also separated a 3-g mixture of indole auxins [27,28]. Solvent systems based on a chloroform-rich organic phase were used to separate DNP-amino acids and flavonoids from a crude extract of sea buckthorn (*Hippophae rhamnoides*) [27]. An antibiotic, *i.e.*, bacitracin, was purified with the same system [28].

6. CONCLUSIONS

The cross-axis coil planet centrifuge is a useful counter-current chromatograph. Its design enhances the retention of the liquid stationary phase inside the chromatographic column for

biphasic polar solvent systems in comparison with previous CCC devices. As a result, the resolution is increased. The efficiency, which is at least similar to that of the type J CPC, is satisfactory, partly owing to three-dimensional mixing. Moreover, the choice of columns of small or large internal volume determines the analytical or preparative purpose of the device.

REFERENCES

1 W.D. Conway, *Countercurrent Chromatography —Apparatus, Theory and Applications*, VCH, New York, 1990, pp. 157–158.
2 W. Murayama, T. Kobayashi, Y. Kosuge, H. Yano, Y. Nunogaki and K.J. Nunogaki, *J. Chromatogr.*, 239 (1982) 643.
3 Y. Ito, *J. Chromatogr.*, 214 (1981) 122.
4 Y. Ito, in N.B. Mandava and Y. Ito (Editors), *Countercurrent Chromatography —Theory and Practice*, Marcel Dekker, New York, 1988, Ch. 3, p. 423.
5 Y. Ito, *J. Chromatogr.*, 358 (1986) 325.
6 Y. Ito, *Sep. Sci. Technol.*, 22 (1987) 1971.
7 Y. Ito and T.-Y. Zhang, *J. Chromatogr.*, 449 (1988) 135.
8 Y. Ito, H. Oka and J. Slemp, *J. Chromatogr.*, 463 (1989) 305.
9 Y. Ito, E. Kitazume, M. Bhatnagar and F. Trimble, *J. Chromatogr.*, 538 (1991) 59.
10 Y. Shibusawa and Y. Ito, *J. Liq. Chromatogr.*, 15 (1992) 2787.
11 K. Shinomyia, J.-M. Menet, H.M. Fales and Y. Ito, *J. Chromatogr.*, 644 (1993) 215.
12 J.L. Sandlin and Y. Ito, *J. Liq. Chromatogr.*, 11 (1988) 55.
13 *Type X-1.5L High-Speed Countercurrent Chromatograph*, Countercurrent Technologies, Research Triangle Park, NC, 1993.
14 Y. Ito, *J. Chromatogr.*, 301 (1984) 377.
15 Y. Ito, *J. Chromatogr.*, 301 (1984) 387.
16 Y. Ito, *J. Chromatogr.*, 538 (1991) 67.
17 M.-C. Rolet, *Thèse de Doctorat*, Université Paris VI, Paris, 1993.
18 Y. Ito, in N.B. Mandava and Y. Ito (Editors), *Countercurrent Chromatography —Theory and Practice*, Marcel Dekker, New York, 1988, p. 648.
19 Y. Shibusawa and Y. Ito, *J. Chromatogr.*, 550 (1991) 695.
20 J.-M. Menet, K. Shinomyia and Y. Ito, *J. Chromatogr.*, 644 (1993) 239.
21 J. Goupy, J.-M. Menet, K. Shinomiya and Y. Ito, in W.D. Conway and R. Petroski (Editors), *Symposium Monograph on Countercurrent Chromatography*, American Chemical Society, Washington, DC, in press.
22 H. Oka, F. Oka and Y. Ito, *J. Chromatogr.*, 479 (1989) 53.
23 S. Drogue, *Thèse de Doctorat*, Université Paris VI, Paris, 1992.
24 S. Drogue, M.-C. Rolet, D. Thiébaut and R. Rosset, *J. Chromatogr.*, 538 (1991) 91.
25 Y. Ito, *Sep. Sci. Technol.*, 22 (1987) 1989.
26 Y. Ito and T.-Y. Zhang, *J. Chromatogr.*, 449 (1988) 153.
27 T.-Y. Zhang, Y.-W. Lee, Q.C. Fang, R. Xiao and Y. Ito, *J. Chromatogr.*, 454 (188) 185.
28 M. Bhatnagar, H. Oka and Y. Ito, *J. Chromatogr.*, 463 (1989) 317.
29 Y. Shibusawa, Y. Ito, K. Ikewaki, D.J. Rader and H.B. Brewer, *J. Chromatogr.*, 596 (1992) 118.
30 Y. Ito, personal communication.
31 P.-E. Albertsson, *Partition of Cell Particles and Macromolecules*, Wiley, New York, 3rd ed., 1986.

Journal of Chromatography A, 659 (1994) 15–25
Elsevier Science B.V., Amsterdam

CHROM. 25 484

Shock layer thickness and optimum linear velocity in displacement chromatography

Jie Zhu and Georges Guiochon*

Department of Chemistry, University of Tennessee, Knoxville, TN 37996-1501 (USA) and Division of Analytical Chemistry, Oak Ridge National Laboratory, Oak Ridge, TN 37831-6120 (USA)

(First received April 14th, 1993; revised manuscript received July 14th, 1993)

ABSTRACT

The width of the mixed zones between two successive bands in the isotachic train represents the loss in recovery yield achieved in displacement chromatography. Intuitively, this width depends on the mobile phase flow velocity, but no systematic study of this effect has yet been performed. On the other hand, constant pattern behavior and the theory of shock layer are well known in chemical engineering. Using this approach, and assuming competitive Langmuir isotherm behavior, an analytical equation is derived which relates the shock layer thickness (SLT) in displacement chromatography and the column design and operating parameters. Using this equation, it is possible to investigate the dependence of the SLT between two consecutive bands in the isotachic train on the mobile phase velocity, the concentration and the retention factor of the displacer and the separation factor of the two components. In displacement chromatography, the optimum mobile phase linear velocity (u^{S}_{opt}) for minimum shock layer thickness, or maximum recovery yield depends not only on the coefficients of axial dispersion and mass transfer resistance of the two components, as does the optimum mobile phase velocity (u^{L}_{opt}) in linear chromatography, but also on the retention factor and the concentration of the displacer. The results of the study of this analytical equation are in excellent agreement with those of numerical calculations.

INTRODUCTION

Although suggested by Tswett [1], displacement chromatography was really introduced by Tiselius and Claeson [2] and Spedding [3] in the 1940s. Glückauf [4] developed its theory soon afterwards in the case of Langmuir isotherm behavior. He also recognized that a self-sharpening effect of thermodynamic origin (due to the non-linear behavior of the isotherm) counteracts the band spreading due to the finite rate of mass transfer [5]. Later, Helfferich and Klein [6] and Rhee and Amundson [7] completed the theoretical study of displacement in the framework of the ideal model. No general theory is available in the equilibrium-dispersive and kinetic models, although numerical solutions have been published and studied [8–10]. Although displacement has been widely used in the past for preparative applications [2,3,11], it fell into oblivion as a practical technique shortly after World War II. In spite of systematic efforts [12,13] to reintroduce it as a preparative method of separation, its renaissance is considerably slowed by the lack of understanding of many issues of critical importance in actual practice. One of them is related to the mixed zone between consecutive bands in the isotachic train.

The ideal model predicts that two consecutive bands are separated by a concentration shock. There are no mixed zones between consecutive bands, hence complete recovery of the feed as separated products is possible. This ideal situa-

* Corresponding author. Address for correspondence: Department of Chemistry, University of Tennessee, Knoxville, TN 37994-1501, USA.

0021-9673/94/$07.00
SSDI 0021-9673(93)E0869-V

tion is, of course, not observed with actual columns. A mixed zone of finite width takes place between consecutive bands. Calculations show that, under experimental conditions giving a high value of the production rate, the recovery yield achieved in displacement chromatography because of the finite width of this mixed zone is as low as, or even lower than, the recovery yield in overloaded elution chromatography [14]. Admittedly, the isotachic train is not yet formed under these conditions, which contributes much to the reduced yield. Nevertheless, as most practitioners seem to prefer performing displacement separations under isotachic conditions and would like to improve recovery yields as much as possible, it is important to study the parameters which control the width of these mixed bands. Unfortunately, little information and much contradiction is found on this topic in the literature.

Horváth and co-workers [12,13,15,16] reported that the resolution between adjacent bands decreases with increasing flow-rate. They suggested that displacement development should be carried out at a flow-rate 2–10 times lower than that used in elution under linear conditions [13]. They also reported that operating the column at high flow-rates, in order to increase the production rate, is done at the expense of a markedly decreased recovery yield [13], and recommended flow-rates much lower than those used typically in elution with similar columns. This result is in agreement with the observation made by Cardinali *et al.* [17] that the overlap between the last component and the displacer decreases markedly with decreasing flow-rate. On the other hand, Subramanian and co-workers [8,18] reported an opposite result. They observed that the flow-rate does not affect much the band profile in the flow-rate range 0.1–1 ml/min (for a 4.6 mm I.D. column). Similarly, from the results of Cardinali *et al.* [17], the degree of overlap between successive bands of the isotachic train seems to be little affected by the change in flow-rate made by these workers. These apparent contradictions deserve some clarification.

We know that the concentration shocks predicted by the ideal model for the chromatograms obtained with infinitely efficient columns cannot actually take place. Real columns have a finite efficiency. The concentration shocks that nonlinear equilibrium isotherms tend to build up are eroded by the effects of axial dispersion and of the finite rate of the mass transfer kinetics. Very steep fronts, in which the concentrations of one or several components change rapidly, take place instead. These regions are called shock layers. When adsorption isotherms are convex upwards, as they should be in displacement chromatography, the breakthrough curves observed in frontal analysis have a very steep front [11,19]. Similarly, the boundaries between successive zones in displacement chromatography are also very steep. When the isotachic train has been formed, it propagates unchanged. This means that a constant pattern or steady-state, dynamic equilibrium is reached between the self-sharpening trend driven by thermodynamics and the dispersive effects of the finite column efficiency. The boundaries between two successive bands are binary shock layers. The simplest and most useful model for the profiles of these layers has been derived and studied by Rhee and co-workers [20–23]. This theory results into a fairly simple expression for the shock layer thickness (SLT) in the case of Langmuir adsorption behavior [23].

In a previous paper [24], we presented the results of a theoretical and experimental investigation of the dependence of the SLT in single component frontal analysis on the two main operating parameters which control it, the mobile phase velocity and the height of the concentration step injected into the column. The SLT is simply related to the column height equivalent to a theoretical plate (HETP), the height of the concentration step and the isotherm. While there is an optimum linear velocity, u^{L}_{opt}, for minimum HETP in linear chromatography, there is an optimum linear velocity, u^{S}_{opt}, for minimum SLT in frontal analysis. Both velocities are related, but may be very different. u^{S}_{opt} depends strongly on the limit retention factor or initial slope of the isotherm [24]. Therefore, a similar investigation made in displacement chromatography could help in understanding the factors controlling the thickness of the intermediate, mixed zones between successive bands in the isotachic train in displacement chromatography.

The theory of multi-component shock layers

has been developed by Rhee and Amundson [23] and applied by them to the study of shock layer profiles in multi-component frontal analysis. Recently, Guiochon and co-workers [24–27] used these results to study the accuracy of isotherm measurements by binary frontal analysis, the optimization of the experimental conditions and some related problems. In this paper, we apply the analytical equation derived by Rhee and Amundson for the calculation of SLT to the study of the width of intermediate mixed zones in displacement chromatography, for mixtures of components following the competitive Langmuir isotherm model. We discuss the influence on the SLT of the mobile phase velocity, the concentration and the retention factor of the displacer and the separation factor between the two components.

THEORY

We first recall the definition of shock layers, and briefly explain how the work of Rhee and Amundson [21] on single-component shock layers can be extended to binary shock layers [23]. Then, we derive an analytical equation relating the SLT in displacement chromatography and the experimental conditions. Throughout the discussion, we assume competitive Langmuir isotherms. For the sake of simplicity, the isotherm is written as

$$q_i = \frac{q_s \Gamma_i}{1 + \Gamma_1 + \Gamma_2} \tag{1}$$

where q_i is the concentration of component i at equilibrium in the stationary phase, q_s is the saturation capacity of the stationary phase and $\Gamma_i = b_i C_i$, b_i being the coefficient of the Langmuir isotherm and C_i the mobile phase concentration of i.

Because the shock layer theory, as all theoretical models of chromatography so far, consider the column as radially homogeneous, and hence neglects the possible influence of radial perturbations in the packing density, we consider only the abscissa in discussing column properties. Similarly, the mobile phase flow velocity, not its flow-rate, is significant in the study of the mass transfer resistance. Therefore, we give the shock layer thickness in time and distance units, not in volume as suggested by a reviewer. Multiplication by the appropriate value of the column cross-sectional area would supply easily these data, when needed.

The SLT in single-component frontal analysis

In frontal analysis, a stream of constant concentration is injected into the column. Assuming that the column is initially empty, the front or breakthrough curve propagates along the column at a constant velocity, U_s [4–7]:

$$U_s = \frac{u}{1 + K} \tag{2}$$

with

$$K = \frac{k'_0}{1 + \Gamma_0} \tag{3}$$

where u is the mobile phase velocity, k'_0 is the retention factor, $a = k'_0/F$ and b are the parameters of the Langmuir isotherm, F is the phase ratio and C_0 is the step concentration injected. The SLT is the distance, $\Delta\eta_x$, between two concentrations C_1^* and C_r^* inside the column (Fig. 1), or the time, $\Delta\eta_t$, separating the elution of these two concentrations:

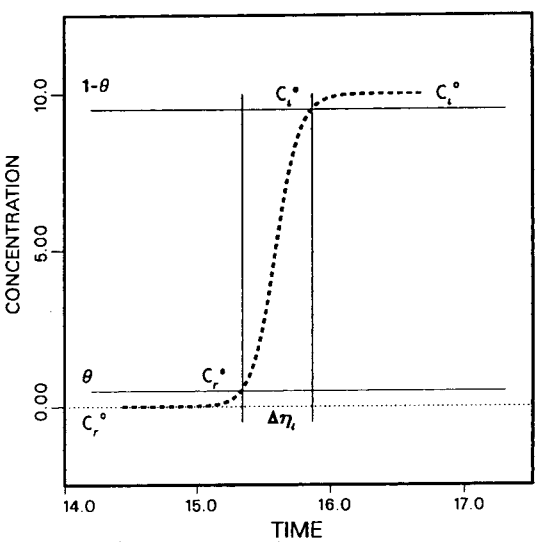

Fig. 1. Definition of the shock layer thickness (SLT). The curve shows the concentration profile, $C(t)$, of the breakthrough curve in single-component frontal analysis obtained for the injection of a step from $C = 0$ to $C = C_0 = 10$ mM. Concentration in mM, time in min.

$$C_r^* = \theta C_0 \quad (4a)$$

$$C_l^* = (1-\theta)C_0 \quad (4b)$$

where θ is an arbitrary number lower than 0.5, usually between 0.01 and 0.05. The SLT can be calculated by introducing the dimensionless moving coordinate:

$$\xi = \frac{x - tU_s}{L} \quad (5)$$

The SLT is given by

$$\Delta\xi = \xi(C_r^*) - \xi(C_l^*) \quad (6a)$$

$$\Delta\eta_x = L\,\Delta\xi \quad (6b)$$

$$\Delta\eta_t = \frac{L}{U_s} \cdot \Delta\xi \quad (6c)$$

where L is the column length.

Rhee and Amundson [21] have shown that the SLT is given by the following equation:

$$\Delta\xi = \left[\frac{D_a(1+K)}{KuL} + \frac{u}{(1+K)k_f L}\right]\frac{\Gamma_0 + 2}{\Gamma_0} \cdot \ln\left|\frac{1-\theta}{\theta}\right| \quad (7a)$$

$$\Delta\eta_x = \left[\frac{D_a(1+K)}{Ku} + \frac{u}{(1+K)k_f}\right]\frac{\Gamma_0 + 2}{\Gamma_0} \ln\left|\frac{1-\theta}{\theta}\right| \quad (7b)$$

$$\Delta\eta_t = \left[\frac{D_a(1+K)^2}{Ku^2} + \frac{1}{k_f}\right]\frac{\Gamma_0 + 2}{\Gamma_0} \cdot \ln\left|\frac{1-\theta}{\theta}\right| \quad (7c)$$

where D_a is the axial dispersion coefficient, including the effects of molecular axial diffusion, tortuosity and eddy diffusion [28,29], and k_f is a lumped mass transfer coefficient [20–23,30]. $\Gamma_0 = bC_0$ is the dimensionless sample injection concentration.

The SLT in multi-component displacement chromatography

When the formation of the isotachic train is achieved in displacement chromatography, all the bands migrate at the same velocity as the displacer front. A constant pattern, *i.e.*, an asymptotic solution, has been reached and there is a shock layer between two consecutive bands. The train moves at the velocity

$$U_{sd} = \frac{u}{1+K_d} = \frac{u}{1 + \dfrac{k'_{0,d}}{1+\Gamma_d}} \quad (8)$$

The plateau concentration of each band in the isotachic train is determined by the displacer concentration. It is given by

$$C_{p,i} = \frac{1}{b_i}\left[\frac{a_i}{a_d}(1+\Gamma_d) - 1\right] \quad (9)$$

where $\Gamma_d = b_d C_d$ and b_d and C_d are the Langmuir isotherm parameter and the injection concentration of the displacer, respectively.

All the previous results are given by the ideal model. They are still valid with actual columns having a finite efficiency. However, the rear boundary of each band in the isotachic train is mixed with the front boundary of the following band (Fig. 2). The SLT is given by the same definition as for a single component (compare Figs. 1 and 2). By replacing the plateau injection concentration, C_0, in eqn. 6 by the plateau

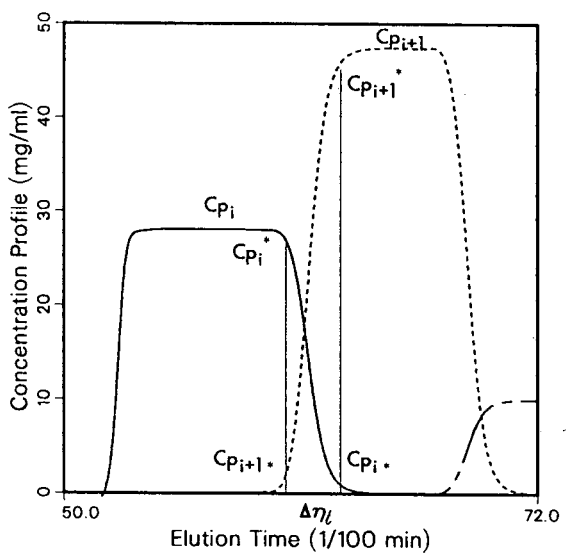

Fig. 2. Definition of the shock layer thickness (SLT) between two bands of the isotachic train in displacement chromatography. C_{p_1} and C_{p_2} are the plateau concentrations; $C^*_{p,i} = (1-\theta)C_{p,i}$, $C_{p,i,*} = \theta C_{p,i}$, $C^*_{p,i+1} = (1-\theta)C_{p,i+1}$, $C_{p,i+1,*} = \theta C_{p,i+1}$. $\Delta\eta_t$ is the shock layer thickness in time unit.

concentration, $C_{p,i}$, we obtain for the SLT in multi-component displacement chromatography

$$\Delta\xi = \xi(C^*_{p,i}) - \xi(C_{p,i*}) = \xi(C^*_{p,i+1}) - \xi(C_{p,i+1,*}) \quad (10)$$

where

$$C^*_{p,i} = \theta C_{p,i};\ C_{p,i,*} = (1-\theta)C_{p,i} \quad (11a)$$

$$C^*_{p,i+1} = \theta C_{p,i+1};\ C_{p,i+1,*} = (1-\theta)C_{p,i+1} \quad (11b)$$

Rhee and Amundson [23] have shown that the concentration profiles in the shock layers in each mixed zone are described by the following partial differential equation:

$$-\frac{\lambda}{PeSt}\cdot\frac{d^2C_i}{d\xi^2} + \left[\frac{1}{Pe} + \frac{\lambda(1-\lambda)}{St}\right]\frac{dC_i}{d\xi} = \lambda F\mathcal{F}(C_i, C_{p,i}, C_{i+1}, C_{p,i+1}) \quad (12)$$

where i is the rank of the component in the train, between 1 and n. The function $\mathcal{F}(C_i, C_{p,i}, C_{i+1}, C_{p,i+1})$ depends on the parameters of the multi-component isotherm. Pe and St are the Peclet and Stanton numbers, respectively.

Using the hodograph transform, Rhee and Amundson [23] have also shown that a plot of C_i *versus* C_{i+1} is a straight line (solid line in Fig. 3), provided that these two components have the same apparent dispersion coefficient, D_a, and the same rate coefficient, k_f, in addition to the competitive Langmuir isotherm behavior. The equation of this straight line is

$$C_i = -\frac{C_{p,i}}{C_{p,i+1}}\cdot C_{i+1} + C_{p,i} \quad (13)$$

Therefore, the function $\mathcal{F}(C_i, C_{p,i}, C_{i+1}, C_{p,i+1})$ can be decoupled into two functions, $\mathcal{F}(C_i, C_{p,i}, C_{p,i+1})$ and $\mathcal{F}(C_{i+1}, C_{p,i}, C_{p,i+1})$, and the following equations give the SLT in displacement chromatography:

$$|\Delta\xi| = \frac{1+K_d}{K_d}\left[\frac{D_a}{uL} + \frac{K_d u}{(1+K_d)^2 k_f L}\right] \times \left|\frac{1+\alpha}{1-\alpha}\right| \ln\left|\frac{1-\theta}{\theta}\right| \quad (14a)$$

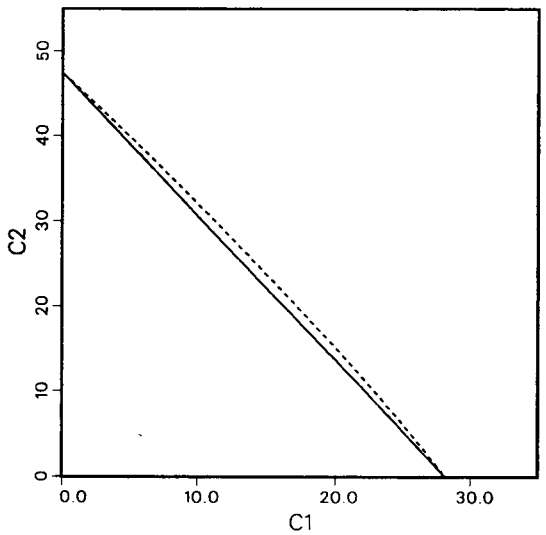

Fig. 3. Hodograph plot of the three chromatograms in Fig. 4. Solid line: $k_{f,1} = k_{f,2} = k_{f,d} = 20$ min^{-1} and $k_{f,1} = k_{f,2} = k_{f,d} = 200$ min^{-1}. Dashed line: $k_{f,1} = 20$ min^{-1}, $k_{f,2} = 200$ min^{-1}, $k_{f,d} = 100$ min^{-1}. Concentrations in mg/ml.

$$|\Delta\eta_x| = \frac{1+K_d}{K_d}\left[\frac{D_a}{u} + \frac{K_d u}{(1+K_d)^2 k_f}\right] \times \left|\frac{1+\alpha}{1-\alpha}\right| \ln\left|\frac{1-\theta}{\theta}\right| \quad (14b)$$

$$|\Delta\eta_t| = \left[\frac{(1+K_d)^2 D_a}{K_d u^2} + \frac{1}{k_f}\right]\left|\frac{1+\alpha}{1-\alpha}\right| \ln\left|\frac{1-\theta}{\theta}\right| \quad (14c)$$

Hence, the SLT in displacement chromatography depends on the axial dispersion coefficient, the mass transfer coefficient and the separation factor, α, of the two adjacent band components, and on the injection concentration and retention factor, k'_0 of the displacer. The SLT does not depend on the retention factor or the feed concentration of either adjacent components. Obviously, when the isotachic train is formed, the concentration of each band reaches a plateau concentration which is determined by the concentration of the displacer.

The values of the SLT given by eqn. 14b are compared in Table I with those derived from chromatograms obtained by numerical integration of the system of equations of the transport-

TABLE I

SHOCK LAYER THICKNESS AND MASS TRANSFER COEFFICIENT

Parameter[a]	Shock layer thickness (min)[b]				Mass transfer coefficient k_f (min^{-1})[c]		
	1r	2f	2r	d	Component 1	Component 2	Displacer
N	2.175	2.175	2.020	2.020	20	20	20
T	2.033	2.033	2.033	2.033			
N	1.691	1.691	1.619	1.619	200	200	200
T	1.513	1.513	1.513	1.513			
N	1.918	1.905	1.640	1.640	20	200	100

[a] N = SLT from numerical calculation; T = SLT from eqn. 14b.
[b] 1r = Rear shock for the first component; 2f = front shock for the second component; 2r = rear shock for the second component; d = front shock for the displacer (see Fig. 2).
[c] D_L 0.00137 cm^2/min.

dispersive model [31]. The calculated chromatograms are shown in Fig. 4. It is seen in Table I that, when the two adjacent components have the same axial dispersion and kinetic coefficients, the SLT of the rear shock of the less retained band is the same as the SLT of the front shock of the more retained band. The SLT changes from pair to pair of components, but it is the same for all pairs having the same separation factor.

If the two adjacent components do not have the same axial dispersion and kinetic coefficients, the plot of C_i *versus* C_{i+1} is not a straight line (see chain line in Fig. 3), and the decoupling of $\mathcal{F}(C_i, C_{p,i}, C_{i+1}, C_{p,i+1})$ is not possible, even in the case of the competitive Langmuir isotherm model. In this case, no simple analytical solution for the SLT can be derived. However, the SLT will be between the two values calculated using eqn. 14 with the smaller k_f (*e.g.*, 20 in Table I) and the larger k_f (200 in Table I). Therefore, a good approximation of the SLT can still be obtained from eqn. 14.

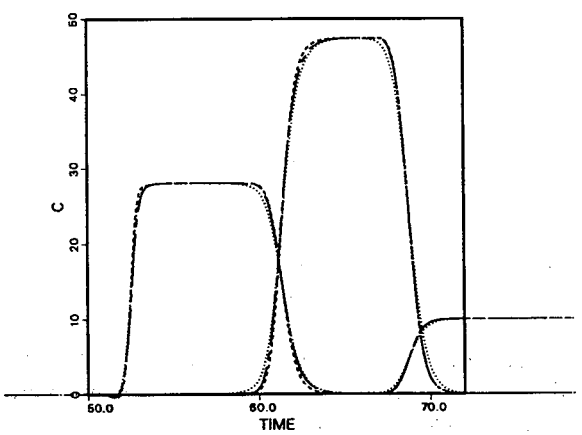

Fig. 4. Overlay of three displacement chromatograms (θ = 0.1). Dotted line: $k_{f,1} = k_{f,2} = k_{f,d} = 20\ min^{-1}$. Dashed line: $k_{f,1} = k_{f,2} = k_{f,d} = 200\ min^{-1}$. Chain dashed line: $k_{f,1} = 20$, $k_{f,2} = 200$, $k_{f,d} = 100\ min^{-1}$. The axial dispersion coefficient is the same for all the components, 0.00137 cm^2/min. Langmuir isotherm parameters: $a_1 = 7.0$, $a_2 = 11.2$, $a_d = 17.9$, $b_1 = 0.07$, $b_2 = 0.079$, $b_d = 0.66$. Concentration in mg/ml, time in min.

DISCUSSION

We now discuss the consequences of eqn. 14, the dependence of the SLT on the characteristics of the displacer, the mobile phase velocity and the separation factor.

Dependence of the SLT on the retention factor and the concentration of the displacer

The SLT in displacement chromatography does not depend directly on the retention factors of either the components involved or their concentrations, but it does depend on them indirectly, through K_d. The condition for achievement of the isotachic train is that the value of K (eqn. 3) is the same for all the components of the mixture, and for the displacer:

$$K_1 = K_2 = K_i = \cdots = \frac{k'_{0,d}}{1+\Gamma_d} \quad (15)$$

Hence, the plateau concentration of each component in theisotachic train is obtained by solving eqn. 15 for $C_{p,i}$. This explains why in displacement, unlike in frontal analysis, the retention factors and the concentrations of the sample components do not appear in eqn. 14.

Figs. 5 and 6 illustrate the dependence of the SLT on the retention factor, $k'_{0,d}$ (Fig. 5), and on the injection concentration, C_d (Fig. 6), of the displacer. We see (Fig. 5) that, as the retention factor of the displacer increases, the SLT decreases rapidly at first. Then, $\Delta\eta_x$ tends slowly towards 0 as $k'_{0,d}$ increases indefinitely. $\Delta\eta_t$, on the other hand, reaches a minimum beyond which it starts to increase slowly, with a slanted asymptote. Differentiation of eqn. 14c by respect to K_d shows that the optimum value of $k'_{0,d}$ for minimum SLT_t (SLT in time units) corresponds to

$$K_d = 1 \quad (16a)$$

$$k'_{0,d} = 1 + b_d C_d \quad (16b)$$

$$C_d = \frac{k'_{0,d} - 1}{b_d} \quad (16c)$$

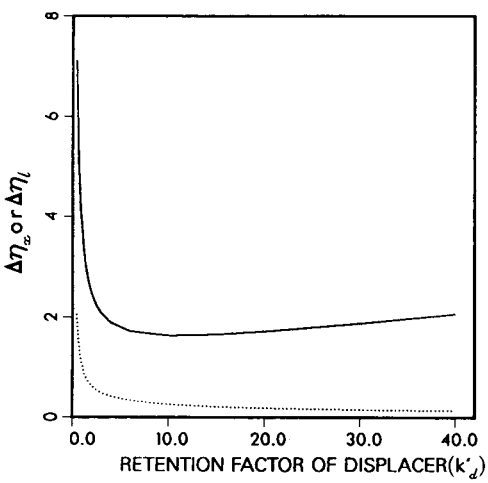

Fig. 5. Plot of the SLT *versus* the retention factor of the displacer, $k'_{0,d}$, based on eqn. 14b or 14c. $D_a = 0.00137$ cm^2/min, $k_f = 20$ min^{-1}, $u = 0.3$ cm/min, $\theta = 0.05$, $C_d = 20$ mg/ml, $\alpha = 1.5$. Langmuir isotherm parameter $b_d = 0.5$ ml/mg. Dotted line: $\Delta\eta_x$ *versus* $k'_{0,d}$. Solid line: $\Delta\eta_t$ *versus* $k'_{0,d}$.

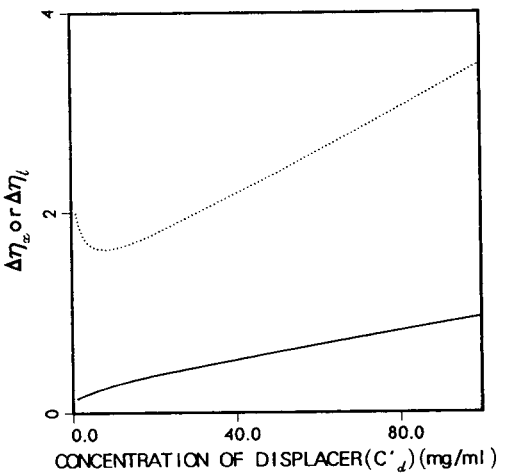

Fig. 6. Plot of the SLT *versus* the displacer concentration, C_d, based on eqn. 14b or 14c. $D_a = 0.00137$ cm^2/min, $k_f = 20$ min^{-1}, $u = 0.3$ cm/min, $\theta = 0.05$, $k'_{0,d} = 5$, $\alpha = 1.5$. Langmuir parameter $b = 0.5$ ml/mg. Solid line: $\Delta\eta_x$ *versus* C_d. Dotted line: $\Delta\eta_t$ *versus* C_d.

Depending whether the choice of the displacer is restricted or not, these equations define an optimum of the displacer retention factor (Fig. 5) or of its concentration (Fig. 6) for achieving minimum $\Delta\eta_t$, but there are no minima for $\Delta\eta_x$. As illustrated in Fig. 6, $\Delta\eta_x$ always increases with increasing displacer concentration. This result is important because it is just the opposite of what happens in single-component frontal analysis, where the SLT decreases with increasing feed concentration.

Dependence of the SLT on the mobile phase linear velocity

Fig. 7 shows three overlaid displacement chromatograms. The profiles of the isotachic train were calculated at three different mobile phase linear velocities. The values of $\Delta\eta_x$ and $\Delta\eta_t$ derived from these chromatograms are compared with those given by eqns. 14b and 14c in Figs. 8 and 9 respectively, showing the expected agreement. Fig. 8 shows the plot of $\Delta\eta_x$ *versus* the linear velocity, u. The curve obtained is very similar to the plot of the column HETP *versus* u in linear chromatography. Both curves exhibit a minimum, demonstrating the existence of an optimum mobile phase velocity for which the separation performance will be best.

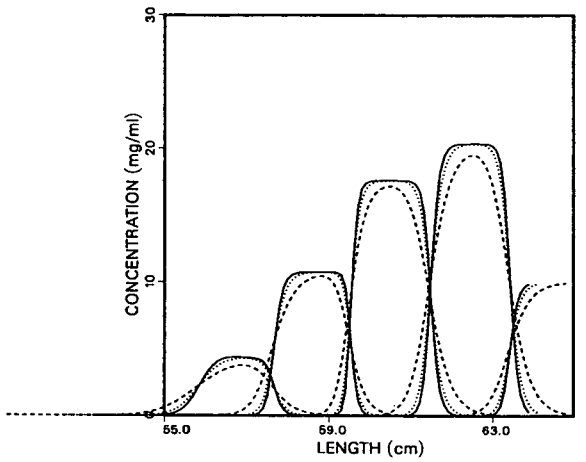

Fig. 7. Four-component displacement separations at three different mobile phase velocities. Chain line, $u = 2$ cm/min; dotted line, $u = 1$ cm/min; solid line, $u = 0.2$ cm/min. $D_a = 0.00137$ cm^2/min, $k_f = 20$ min^{-1}. Langmuir isotherm parameters: $a_1 = 1.5$, $a_2 = 2.25$, $a_3 = 4.0$, $a_4 = 6.0$, $a_d = 9.0$, $b_1 = 0.04$, $b_2 = 0.07$, $b_3 = 0.12$, $b_4 = 0.18$, $b_d = 0.6$.

The dependence of D_a on the mobile phase velocity has been discussed abundantly in linear chromatography. We assume in this work that the molecular diffusion coefficients and the kinetic coefficients are independent of the concentration. The classical equations of Van Deemter *et al.* [28] and Knox and Saleem [29] give, respectively,

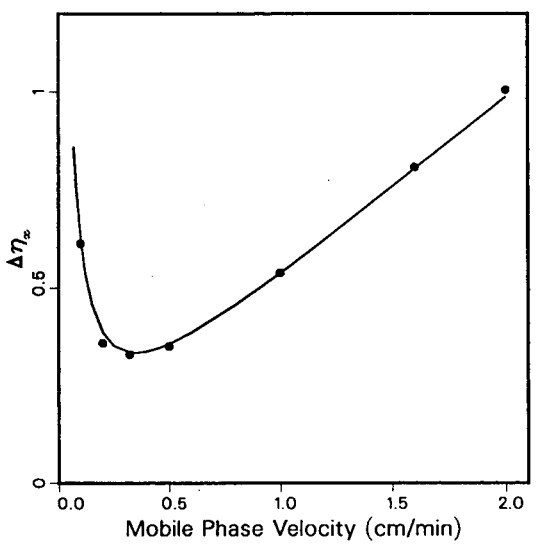

Fig. 8. $\Delta\eta_x$ *versus* mobile phase velocity. Solid line: calculation from eqn. 14b ($\alpha = 1.5$, $\theta = 0.05$). Symbols: $\Delta\eta_x$ from the numerical calculations in Fig. 7.

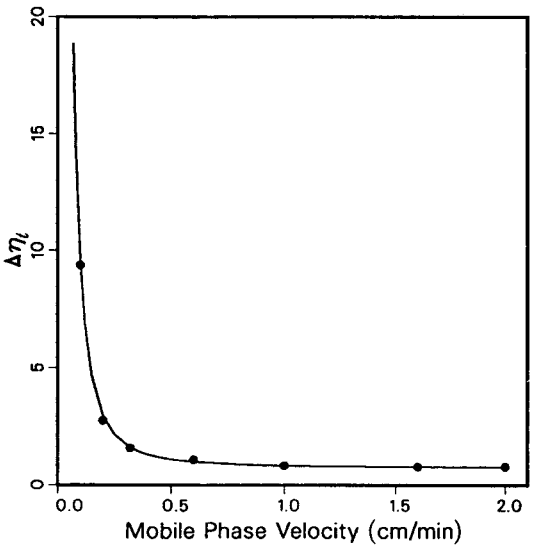

Fig. 9. Same as Fig. 8, but $\Delta\eta_t$ *versus* mobile phase velocity.

$$2D_a = Au + B \tag{17a}$$

$$2D_a = B + Au^{1/3} \tag{17b}$$

We use here the former, Van Deemter equation. Differentiation of eqn. 14b with respect to u shows that the SLT is minimum for the following value of the linear velocity:

$$u_{opt}^{S} = \sqrt{\frac{D_a(1 + K_d)^2 k_f}{K_d}} \tag{18}$$

where K_d refers to the displacer and the coefficients D_a and k_f are those of the two components considered. Note that in the derivation of eqn. 14 it was assumed that these coefficients are the same for two successive components. Remarkably, this equation is otherwise the same as that found in frontal analysis. The optimum velocity for minimum shock layer thickness in displacement chromatography is the velocity for which the SLT of the displacer breakthrough curve is also a minimum. Both equations have for the limit when C_d tends towards zero the optimum linear velocity in linear chromatography.

We observe in Fig. 7 that the SLT of the front

shock of the first band is larger than the others. The reason is due to the difference in the dependence of single-component and binary SLT on the height of the concentration step. The opposite result could also be observed. Fig. 7 shows also that the SLT does not vary much as long as the linear velocity remains close to u^S_{opt}. However, unlike the band width in linear chromatography, the SLT broadens rapidly when the linear velocity increases well above u^S_{opt}. This explains the phenomenon reported by Horváth and co-workers [12,16] of the existence of an optimum in the purity of the product collected when the flow-rate is decreased. The flow-rate below which the purity degrades rapidly corresponds to the optimum velocity given by eqn. 18.

The optimum velocity depends also on the values of the axial dispersion coefficient, D_a, and the kinetic coefficient, k_f. However, apart from using small particles with well accessible pores, such as the packings developed for high-performance liquid chromatography, there is little we can do to achieve higher values of u^S_{opt}.

Dependence of the optimum velocity u^S_{opt} on the retention factor and concentration of the displacer

As shown by eqn. 18, the optimum velocity for minimum SLT depends on the K_d, and hence on the concentration and the retention factor of the displacer selected. The dependence of u^S_{opt} on the retention factor of the displacer is illustrated in Fig. 10. Differentiation of eqn. 18 shows that u^S_{opt} is minimum for

$$k'_{0,d} = 1 + \Gamma_d \tag{19}$$

u^S_{opt} is equal to u^L_{opt}, the optimum velocity for minimum HETP in linear chromatography, for

$$k'_{0,d} = \sqrt{1 + \Gamma_d} \tag{20}$$

We see in Fig. 10, where plots of u^S_{opt} and u^L_{opt} *versus* $k'_{0,d}$ are shown, that u^S_{opt} is larger than u^L_{opt} when $k'_{0,d}$ is smaller than $\sqrt{1 + b_d C_d}$. In practice, this value of the retention factor of the displacer is nearly impossible to achieve, since it is almost always lower than 2. $k'_{0,d} = 2$ requires $b_d C_d = 3$, a value of the displacer concentration for which the equilibrium concentration of the

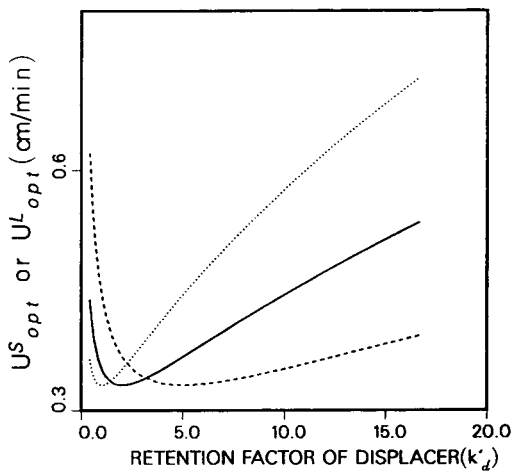

Fig. 10. Dependence of u^S_{opt} on $k'_{0,d}$ for two displacer concentrations, 20 mg/ml (solid line) and 40 mg/ml (dashed line). $b_d = 0.1$ ml/mg, $D_a = 0.00137$ cm^2/min, $k_f = 20$ min^{-1}. The dotted line shows u^L_{opt} versus k'_0.

displacer in the stationary phase is $q = 3q_s/4$, or 75% of the saturation capacity. Hence, in almost all cases, u^S_{opt} is smaller than u^L_{opt}, and often much smaller. In almost all the reports on separations made with displacement chromatography, the displacers chosen have very large retention factors (about 10–15) [15,32]. This is why the optimum linear velocity u^S_{opt} in displacement is very low compared with the optimum linear velocity u^L_{opt} in linear chromatography, and why the production rate in displacement chromatography cannot be as large as anticipated.

Fig. 11 shows the dependence of u^S_{opt} on the concentration of the displacer for two values of its retention factor, 2 and 10. The dependence of u^S_{opt} on the displacer concentration is very different for the two values of $k'_{0,d}$ in the whole accessible concentration range, although both curves have minima. Rearrangement of eqn. 19 shows that $\Delta\eta_x$ is minimum for

$$K = 1 \tag{21a}$$

thus

$$C_d = \frac{k'_{0,d} - 1}{b_d} \tag{21b}$$

u^S_{opt} is equal to u^L_{opt} (*cf.*, straight lines in Fig. 11) at the displacer concentration [24]

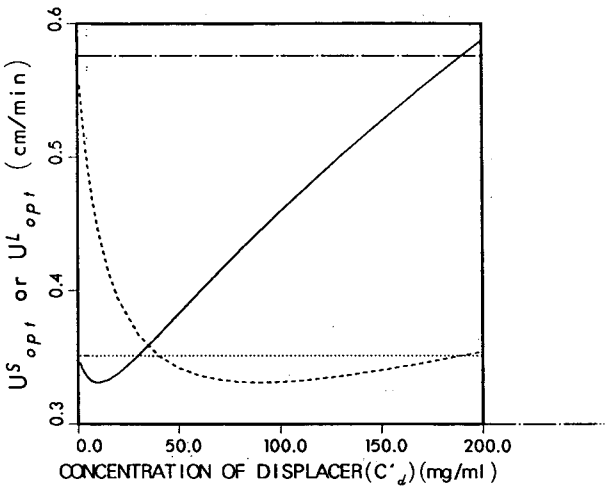

Fig. 11. Dependence of u^S_{opt} on the injection concentration of the displacer for two values of $k'_{0,d}$, 2 (solid line) and 10 (dashed line). $b_d = 0.1$ ml/mg, $D_a = 0.00137$ cm^2/min, $k_f = 20$ min^{-1}. Dotted line: u^L_{opt} for $k'_0 = 2$. Chain dashed line: u^L_{opt} for $k'_0 = 10$.

$$C_d = \frac{k'^2_{0,d} - 1}{b_d} \qquad (22)$$

For the lower value of $k'_{0,d}$, the optimum velocity increases nearly linearly with increasing concentration above *ca.* 30 mg/ml. For the higher value, in contrast, the optimum velocity remains nearly constant in that concentration range.

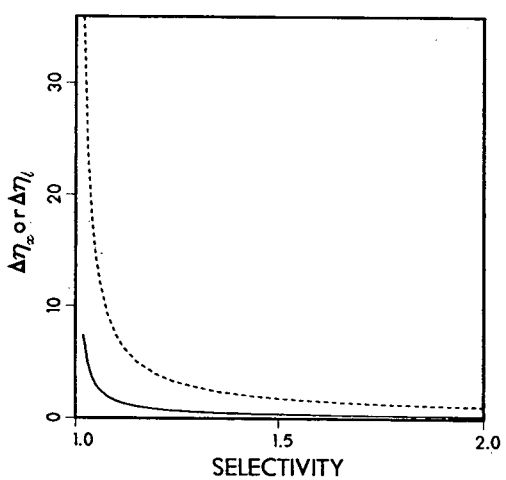

Fig. 12. Dependence of the SLT on the separation factor. $D_a = 0.00137$ cm^2/min, $k_f = 20$ min^{-1}, $\theta = 0.05$, $K_d = 0.45$. Solid line: $\Delta\eta_\infty$ *versus* α. Dotted line: $\Delta\eta_l$ *versus* α.

Dependence of the SLT on the separation factor

Fig. 12 shows the dependence of the SLT on the separation factor $\alpha = k'_2/k'_1$ of the two components. The SLT decreases dramatically as α increases from 1 to 1.3. For higher values of α, it slowly tends towards zero with increasing value of α.

CONCLUSIONS

This work has shown that the shock layer theory permits a detailed investigation of the optimization of the experimental conditions in displacement chromatography for the separation of multi-component mixtures which follow competitive Langmuir isotherm behavior. The theory explains the various empirical conclusions previously reported, including the apparent contradictions between results obtained under different conditions.

The conclusions of this work are extremely simple to apply, as it is not necessary to measure the isotherm parameters for the sample components. Only the single Langmuir isotherm parameters for the displacer and the separation factor at infinite dilution are required in all the equations. The results apply only to the isotachic train. Obviously, the production rate will be maximum if the sample size injected is such that this train is just formed when it reaches the outlet of the column.

Obviously, the conclusions of this work, like those of most of the theoretical work published so far in chromatography, assume that the column is radially homogeneous, hence that the column packing is homogeneous and perfect distribution of the sample takes place at the column inlet. These are ideal assumptions which have proved to be surprisingly satisfactory in liquid chromatography. Nevertheless, when preparative columns are used which have a diameter comparable to their length, new effects may arise owing to the random fluctuations which occur in the packing density. A detailed analysis of the phenomena which take place in actual columns will be published soon [33].

ACKNOWLEDGEMENTS

This work was supported in part by grant CHE-9201663 from the National Science Foundation and by the cooperative agreement between the University of Tennessee and the Oak Ridge National Laboratory. We acknowledge support of our computational effort by the University of Tennessee Computing Center.

REFERENCES

1 M.S. Tswett, *Ber. Dtsch. Bot. Ges.*, 24 (1906) 316 and 384.
2 A. Tiselius and S. Claeson, *Ark. Kemi Mineral. Geol.*, 16A (1943) 18.
3 F.H. Spedding, *Discuss. Faraday Soc.*, 7 (1949) 38.
4 E. Glückauf, *Proc. R. Soc. London, Ser. A*, 186 (1946) 35.
5 E. Glückauf and J.I. Coates, *J. Chem. Soc.*, (1947) 1315.
6 F. Helfferich and G. Klein, *Multicomponent Chromatography—A Theory of Interference*, Marcel Dekker, New York, 1970.
7 H.K. Rhee and N.R. Amundson, *AIChE J.*, 28 (1982) 423.
8 G. Subramanian, M.W. Phillips and S.M. Cramer, *J. Chromatogr.*, 454 (1988) 1.
9 A.M. Katti and G. Guiochon, *Anal. Chem.*, 61 (1989) 982.
10 S. Golshan-Shirazi and G. Guiochon, *Anal. Chem.*, 61 (1989) 1960.
11 F. Helfferich, *Ion Exchange*, Vol. 2, McGraw-Hill, New York, 1962, Ch. 9.
12 Cs. Horváth, A. Nahum and J.H. Frenz, *J. Chromatogr.*, 218 (1981) 365.
13 J.H. Frenz and Cs. Horvath, in Cs. Horváth (Editors), *High Performance Liquid Chromatography—Advances and Perspectives*, Vol. 5, Academic Press, New York, 1988, p. 211.
14 A. Felinger and G. Guiochon, *Biotechnol. Bioeng.*, 41 (1993) 134.
15 Cs. Horváth, J.H. Frenz and Z. El Rassi, *J. Chromatogr.*, 255 (1983) 273.
16 J.H. Frenz, Ph. Van der Schriek and Cs. Horváth, *J. Chromatogr.*, 330 (1985) 1.
17 F. Cardinali, A. Ziggiotti and G.C. Viscomi, *J. Chromatogr.*, it 499 (1990) 37.
18 G. Subramanian and S.M. Cramer, *Biotechnol. Prog.*, (1989) 1.
19 T. Vermeulen, *Adv. Chem. Eng.*, 2 (1981) 147.
20 H.-K. Rhee, B.F. Bodin and N.R. Amundson, *Chem. Eng. Sci.*, 26 (1971) 1571.
21 H.-K. Rhee and N.R. Amundson, *Chem. Eng. Sci.*, 27 (1972) 199.
22 H.-K. Rhee and N.R. Amundson, *Chem. Eng. Sci.*, 28 (1973) 55.
23 H.-K. Rhee and N.R. Amundson, *Chem. Eng. Sci.*, 29 (1974) 2049.
24 J. Zhu and G. Guiochon, *J. Chromatogr.*, 636 (1993) 189.
25 Z. Ma and G. Guiochon, *J. Chromatogr.*, 603 (1992) 13.
26 Z. Ma, *Ph.D. Dissertation*, University of Tennessee, Knoxville, TN, 1992.
27 Z. Ma and G. Guiochon, *J. Chromatogr.*, 609 (1992) 19.
28 J.J. Van Deemter, F.J. Zuiderweg and A. Klinkenberg, *Chem. Eng. Sci.*, 5 (1956) 271.
29 J.H. Knox and M. Saleem, *J. Chromatogr. Sci.*, 7 (1969) 745.
30 J.C. Giddings, *Dynamics of Chromatography*, Marcel Dekker, New York, 1964.
31 S. Golshan-Shirazi and G. Guiochon, *J. Chromatogr.*, 603 (1992) 1.
32 G. Vigh, G. Quintero and G. Farkas, *J. Chromatogr.*, 481 (1989) 237.
33 G. Guiochon, T. Farkás, M. Sarker and T. Yun, in preparation.

Journal of Chromatography A, 659 (1994) 27–41
Elsevier Science B.V., Amsterdam

CHROM. 25 485

Theoretical study of the accuracy and precision of the measurement of single-component isotherms by the elution by characteristic point method

Hong Guan, Brett J. Stanley and Georges Guiochon*

Department of Chemistry, University of Tennessee, Knoxville, TN, 37996-1501 (USA) and Division of Analytical Chemistry, Oak Ridge National Laboratory, Oak Ridge, TN 37831-6120 (USA)

(First received March 4th, 1993; revised manuscript received July 21st, 1993)

ABSTRACT

Using the equilibrium-dispersive model of chromatography, band profiles corresponding to a known Langmuir isotherm are calculated. A noise sequence is added to the calculated profile to simulate an actual chromatogram. The elution by characteristic point (ECP) method of isotherm calculation is then applied to this profile, and the derived isotherm is compared with the initial one. Significant differences between the "true" and the "measured" isotherms are observed at low or moderate column efficiencies. The direct method of determination of the isotherm from the band profile based on the numerical solution of the inverse mathematical problem gives more accurate results than ECP, especially at low column efficiency. It is recommended to use the ECP method only when the column efficiency exceeds markedly 2000 theoretical plates.

INTRODUCTION

The method of elution by characteristic points (ECP) is widely used for the determination of equilibrium isotherms. Arising from the work of Glueckauf [1,2], it was developed by Cremer and Huber over 30 years ago [3]. This method is based on the use of a simple equation that gives the profile of the diffuse part of an overloaded elution band. However, this equation is derived from the ideal model, and the ideal model assumes that the column has an infinite efficiency. As real columns have a finite efficiency, which broadens the diffuse parts of elution profiles, the ECP method contains a definite model error, and its use is recommended only with columns having a sufficient efficiency [3,4]. So far, no efficiency threshold has been defined, and there is no information available regarding the dependence of the model error on the column efficiency. In the past, several workers have attempted to make corrections to this method, but only limited success has been achieved.

Because of its simplicity, however, the ECP method is very attractive and has become widely popular for the determination of single-component adsorption isotherms [4,5]. It can be used with any conventional liquid chromatograph without requiring any modification of the hardware. The sample size required is low compared with the amounts needed in the frontal analysis (FA) and frontal analysis by characteristic point (FACP) methods. Although accurate detector calibration is required in the range of mobile phase composition studied, the possibility of deriving a large number of isotherm data points from a single run gives a good precision, which is sometimes mistakenly assumed to mean a high

* Corresponding author. Address for correspondence: Department of Chemistry, University of Tennessee, Knoxville, TN, 37996-1501, USA.

0021-9673/94/$07.00
SSDI 0021-9673(93)E0870-Z

accuracy. Because of the model error and of our current lack of understanding of its actual importance, the accuracy of the ECP method remains in doubt and careful experimentalists rightly prefer frontal analysis, which is highly accurate as it is based on the measurement of the retention times of a series of self-sharpening fronts, results which are not affected by any model errors.

The major advantages of the ECP method, the rapidity of data acquisition and the small amount of component required, seem compelling to us. Because of increasing pressure from regulatory agencies to force waste reduction, we feel that the ECP method will be used more often in the future than it has been in the past. Further, our current interest is in the investigation of the relationships between (i) equilibrium isotherms in a diphasic system, (ii) band profiles in nonlinear chromatography and (iii) the production rates and recovery yields of purified products achieved in preparative chromatography. The determination of adsorption isotherms is one of the critical problems that have to be solved to proceed successfully to any practical application [5–7]. Considering the fact that most relevant problems involve complex and expensive chemicals, the ECP method is especially attractive [6,7].

We have decided to re-examine the ECP method and its fundamental background. We know that the equilibrium-dispersive model of chromatography [5,8] permits the calculation of the profiles of bands eluted from columns having a finite efficiency, provided that the equilibrium isotherms and the column efficiency are known. The result obtained is accurate when the column efficiency exceeds 100 theoretical plates [8]. Therefore, we can use a computer to simulate an entire experiment. We first assume an isotherm, and calculate the band profile that would be recorded in the ECP method with a known column, for a known amount of that component. By adding an appropriate noise sequence, a chromatogram like that recorded by an actual detector is obtained. The ECP method can then be applied to this chromatogram. The comparison between the "true" (*i.e.*, assumed) and the "measured" (*i.e.*, ECP-calculated) isotherms gives the model error. Repeating the same determination with different noise sequences gives the precision of the method. If needed, the effect of flow-rate or temperature fluctuations could also be included [9].

We report here on the results of this study. A forthcoming paper [10] will discuss experimental reproducibility.

THEORY

When a large-size sample is injected into a chromatographic column, an unsymmetrical band is eluted [5]. For a convex-upwards isotherm, by far the most frequent type, the band front is steep and the band rear is diffuse. The ideal model of chromatography, which assumes that the column efficiency is infinite, gives the equation of the diffuse part of the profile [11]:

$$t_R(C) = t_p + t_0\left(1 + F \cdot \frac{dq}{dC}\right) \quad (1)$$

where $t_R(C)$ is the retention time of the mobile phase concentration C, t_p is the width of the injected pulse (assumed to have a rectangular profile), t_0 is the hold-up time ($t_0 = L/u$, L = column length, u = mobile phase velocity), F is the phase ratio [$V_s/V_m = (1-\epsilon)/\epsilon$, V_s and V_m being the volumes of the stationary and mobile phase, respectively, and ϵ the packing porosity] and $q(C)$ is the equilibrium isotherm.

The direct use of eqn. 1 serves as the basis of the ECP method. This equation is solved for dq/dC, and the result is integrated as a function of C, hence the isotherm. In practice (Fig. 1), the isotherm is calculated from the elution profile of a large-size sample using the relationship

$$q = \frac{1}{V_a}\sum_0^C (V - V_0)\delta_i C \quad (2)$$

where q is the amount of the compound adsorbed on the stationary phase in equilibrium with the mobile phase at concentration C, V_a is the volume of adsorbent in the column, V_0 is the hold-up volume, V is the retention volume of the characteristic point of the diffuse profile at concentration C, and $\delta_i C$ is the concentration increment (with $\Sigma\delta_i C = C$).

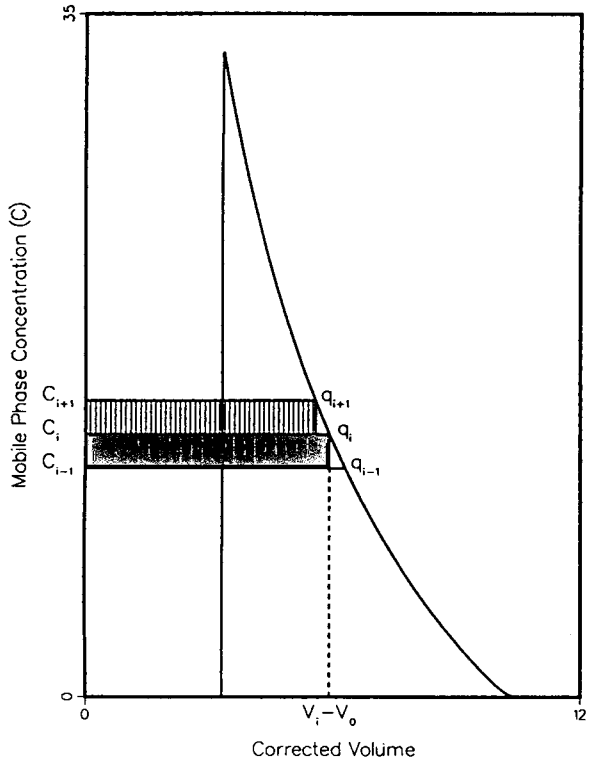

Fig. 1. Elution by characteristic point (ECP). Concentration in mg/ml; volume in ml.

As the efficiency of actual columns is finite, eqn. 1 does not give the true profile of an elution band. This profile can be calculated with excellent accuracy by using the equilibrium-dispersive model [8] which takes the finite column efficiency into account [5–8,11]. Unfortunately, this model has no analytical solutions. Numerical solutions are easy to calculate using one of the algorithms previously described [8]. Figs. 2 and 3 show the profiles calculated for columns of different efficiencies, using two different sample sizes. The isotherm used is the Langmuir model:

$$q = \frac{q_s bC}{1 + bC} \tag{3}$$

where q_s is the saturation capacity of the adsorbent and b a coefficient related to the adsorption energy. This equation can be normalized by using a reduced concentration, $\Gamma = bC$. Instead of reporting the absolute sample size, it is more convenient and meaningful to report the loading factor, L_f, or ratio of the sample size to the column saturation capacity (*i.e.*, the amount of component needed to make a complete monolayer on the surface of the column packing).

RESULTS AND DISCUSSION

In the following, we refer to the concentration profiles derived from the equilibrium-dispersive model as calculated profiles and to the profiles obtained after addition of noise sequences as chromatograms. We refer to the initial Langmuir isotherm as the true isotherm, to the isotherms derived by ECP from the band profiles or the chromatograms as the ECP isotherms and to the isotherms fitted to the Langmuir equation with the coefficients derived from the ECP isotherm as the fitted isotherm. Correspondingly, there are two types of errors considered in this study: (1) the error between the true isotherm and that of ECP and (2) the error between the ECP isotherm and the fitted Langmuir model, which is the model error.

Derivation of the isotherm from calculated band profiles

The elution profiles of large-size samples were calculated on columns having 200, 500, 1000, 2000 and 5000 plates, using a true Langmuir isotherm with $b = 0.024$ ml/mg and $q_s = 500$ mg/ml. The profiles obtained for loading factors of 0.05 and 0.20 are shown in Figs. 2 and 3, respectively. The first value corresponds to a moderate degree of column overloading and the second to a strong overloading. The column dimensions were 25 cm × 4.6 mm I.D., the flow-rate was 1 ml/min and the phase ratio was 0.25. The profiles obtained are typically Langmuirian. Their widths decrease with increasing column efficiency, the fronts become steeper and the tailing of their diffuse rear part becomes less important.

As a first step, the equilibrium isotherm was calculated by applying the ECP method described above to the elution band profiles shown in Figs. 2 and 3, before noise sequences were added. The ECP isotherms derived from the low-efficiency profiles in Fig. 3 ($L_f = 0.20$) are shown in Fig. 4. Similar results were obtained for a loading factor of 0.05. We see in Fig. 4 that

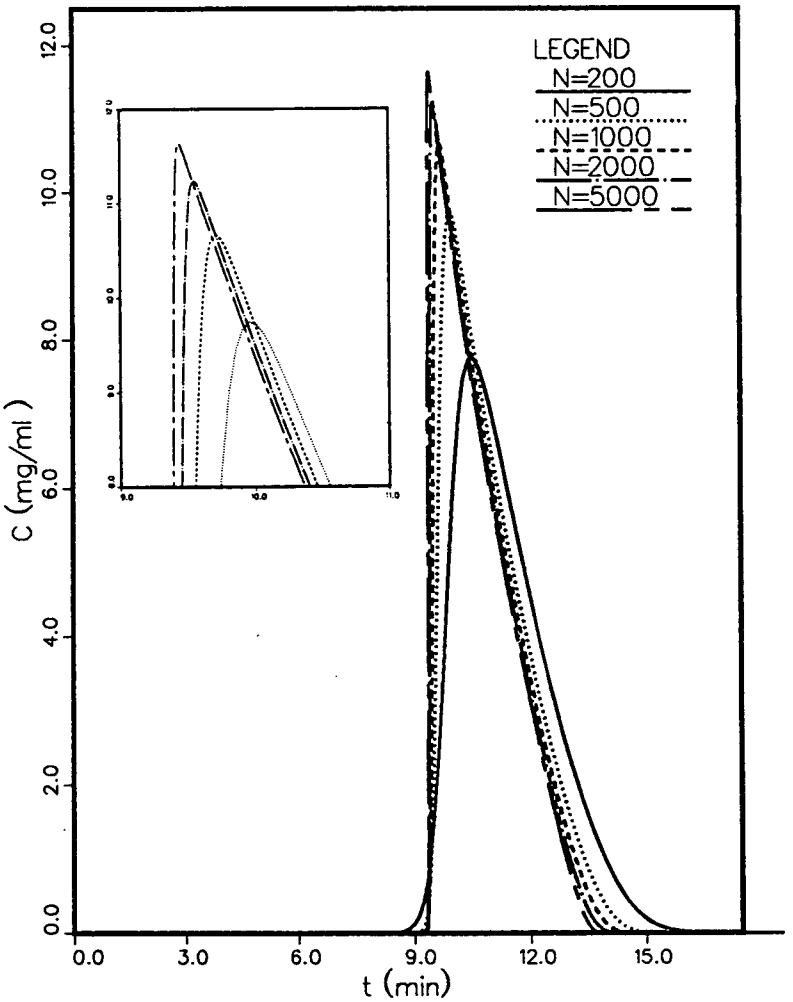

Fig. 2. Band profiles for $L_f = 0.05$ and $a/b = 500$. Inset: enlargement of the area around the top of the band profiles.

there are important, systematic differences between the "true" isotherm and the ECP isotherms derived from the profiles calculated with efficiencies of 200, 500 and 1000 theoretical plates. The ECP isotherm is always above the true isotherm.

Similar results were obtained for the profiles calculated with 2000 and 5000 theoretical plates. As the differences between ECP and true isotherms are now smaller, however, we show in Fig. 5 the ratio of the ECP to the true isotherm as a function of the sample concentration in the mobile phase. We see that, even at the highest efficiency considered (5000 theoretical plates), the ECP isotherm is nearly 5% higher than the true one at very low concentrations, and still approximately 2% higher for $bC = 0.024$. Another striking feature of Fig. 5 is that the amount of solute adsorbed by the stationary phase at equilibrium is always overestimated, by approximately 1% for a column having as many as 5000 plates and by 3% for a column having 1000 plates.

Illustration of the model error is provided in Fig. 6, where the model error is plotted *versus* the concentration, C, in the case of the profile calculated with 2000 theoretical plates. The model error is shown as the residual, or the difference between the value of the adsorbed amount at equilibrium obtained from the fitted

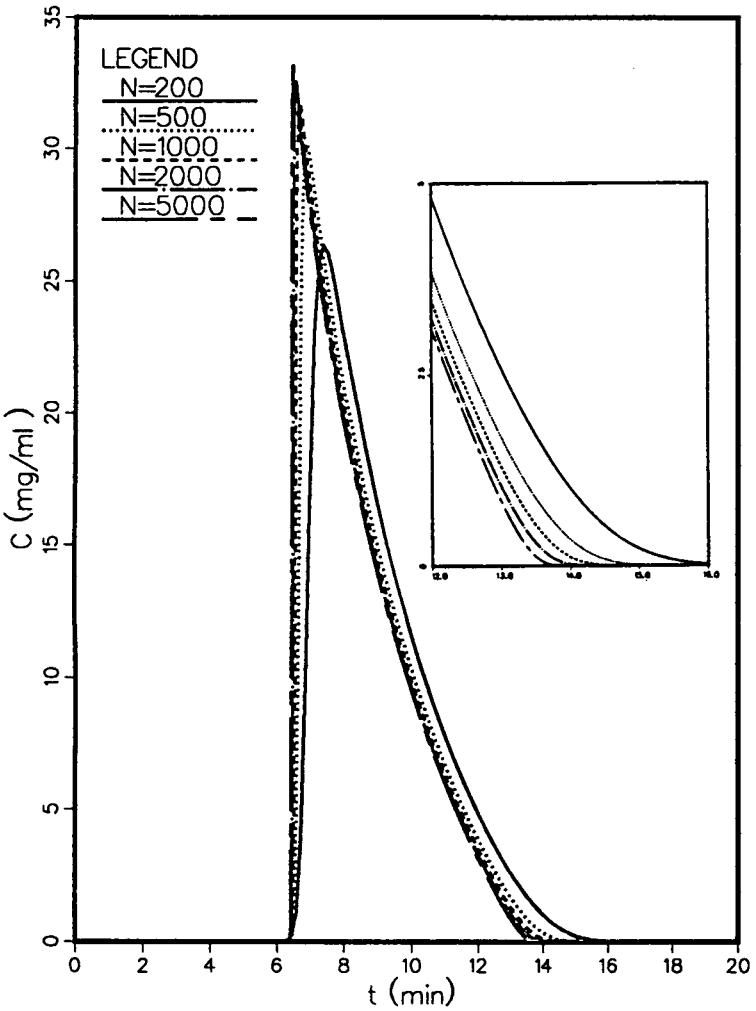

Fig. 3. Band profiles for $L_f = 0.20$ and $a/b = 500$. Inset: enlargement of the area around the tail of the band profiles.

Langmuir isotherm, and the value given by the ECP isotherm at the same concentration. The systematic error is important. Because of it, the ECP isotherm is not a Langmuir isotherm, and the fitting of the ECP isotherm data to the Langmuir equation will result in systematic errors on the coefficients q_s and b.

These errors could explain, at least in part, the difficulties encountered in previous studies with the accurate determination of adsorption isotherms of proteins in reversed-phase systems, and in the prediction of their elution band profiles in gradient elution [7]. The use of high-efficiency columns which have at least 5000 theoretical plates appears to be necessary in order to limit the systematic errors made to an extent compatible with the precision required in the prediction of band profiles for the optimization of the experimental conditions in preparative separations.

Derivation of the isotherm parameters from chromatograms

In the second step, noise sequences were added to the profiles shown in Figs. 2 and 3. These noise sequences were derived from a generator which gives random numbers, *RN*, between 0 and 1. A scale factor *SF* of 4σ was

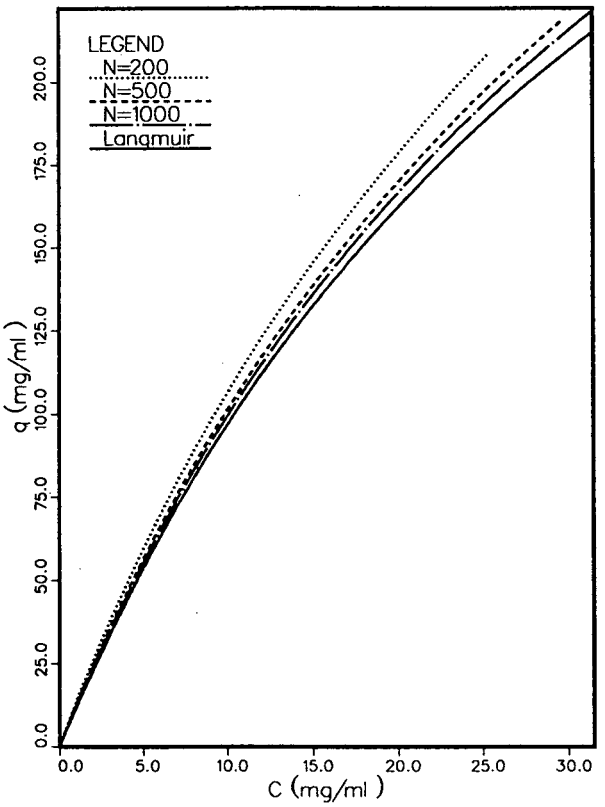

Fig. 4. Comparison between ECP isotherms and the true Langmuir isotherm for columns with low efficiencies (L_f = 0.20; a/b = 500).

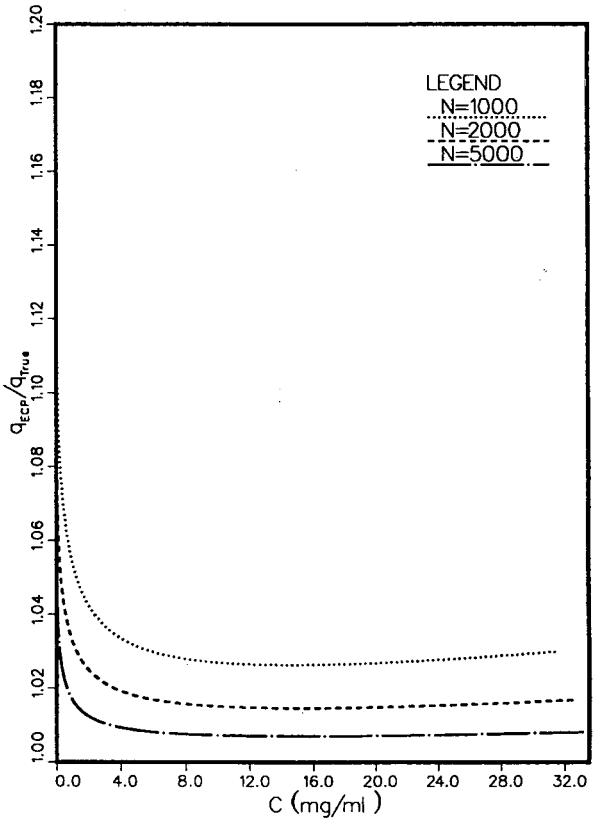

Fig. 5. Comparison between ECP isotherms and the true Langmuir isotherm for columns with high efficiencies (L_f = 0.20; a/b = 500).

multiplied to these random numbers to achieve the desired signal-to-noise ratio (*SNR*), which is defined here as the peak height obtained in the case while no noise signal was introduced divided by σ, the standard deviation of each point in the chromatogram. The number of data points, M, is neglected in this definition of *SNR* for reasons of clarity, because of its dependence on the number of theoretical plates as dictated by the algorithm and the arbitrary nature of SNR definitions. The number of points for each experiment are as follows: N = 5000, 2000, 1000, 500 and 200 plates correspond to M = 1498, 650, 356, 201 and 101 points (for L_f = 0.20) and M = 953, 439, 256, 156 and 88 points (for L_f = 0.05). However, the trends observed in this study are independent of M. The baseline estimate was taken as the numerical average of the above generated random numbers, R_{ave}. For each point of the band profile supplied by the equilibrium-dispersive model algorithm, a noise signal with the value $(RN \cdot SF - R_{ave})$, which is approximately $(RN - 0.5) \cdot h \cdot 4/SNR$[a], was added. The operation was repeated nine times, generating a total of ten chromatograms. For each chromatogram, the ECP isotherm was calculated, then the isotherm data points were fitted to the Langmuir model and the best values for the coefficients of the model were calculated. This provided a series of ten values for each coefficient and the final result was taken as the average of these ten values.

There are several ways to derive the best

[a] Statistical study shows that the rectangular probability density function with width $4h/SNR$ gives a standard deviation of $4h/SNR\sqrt{12} \approx 1.15h/SNR$. Compared with the σ chosen in our paper, which is defined as h/SNR, there is no significant difference between these two.

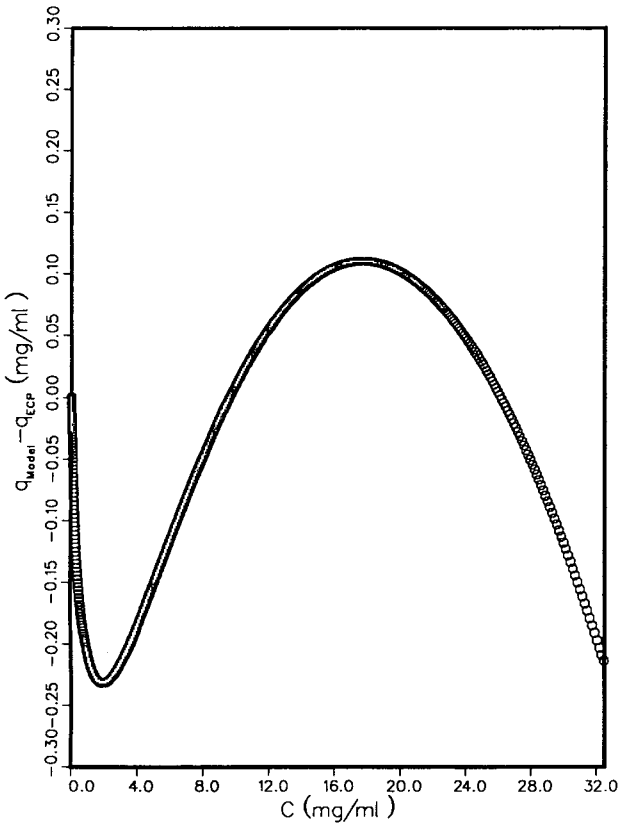

Fig. 6. Plot of the residual *versus* mobile phase concentration C. $L_f = 0.20$, $N = 2000$.

values of the model coefficients. First, the data points may or may not be smoothed prior to further calculations, and there are many smoothing algorithms. In our case, when the data were smoothed, a seven-point moving method, which takes the average of five points between the maximum and minimum, was used. Second, we can linearize eqn. 3 into several forms [12], the most popular being

$$q = aC - bqC \tag{4}$$

with $a = bq_s$. By use of the conventional least-squares method, b and a (hence $q_s = a/b$) can be expressed by

$$a = \frac{\sum_i q_i C_i + b \sum_i q_i C_i^2}{\sum_i C_i^2} \tag{5}$$

and

$$b = \frac{\sum_i q_i^2 C_i \sum_i C_i^2 - \sum_i q_i C_i \sum_i q_i C_i^2}{\left(\sum_i q_i C_i^2\right)^2 - \sum_i (q_i C_i)^2 \sum_i C_i^2} \tag{6}$$

Equations may also be similarly derived to yield the standard deviation of the coefficients a and b and the standard deviation around the regression [13].

Alternatively, a non-linear regression that is directly based on the Langmuir model in eqn. 3 can be used. For this, the appropriate routine of the SAS software available at the University of Tennessee Computing Center was used. Our calculations were performed for five different signal-to-noise ratios: 200, 500, 1000, 2000 and 5000.

Table I summarizes all the calculations performed. For comparison, linear regression results derived for a and b from the band profiles without noise are given in Table II and non-linear regression results in Table III. The results obtained from the series of noisy chromatograms are reported in Figs. 7–13.

We find in Tables II and III that no matter what regression method is used, there is always a positive systematic error on the ECP yielded results for the coefficient a whereas for the coefficient b the error may be either positive or negative, depending on which regression method is used. For a moderate sample size ($L_f = 5\%$), the positive error for the coefficient a is 14% when the column has a poor efficiency (200 plates) and decreases to slightly more than 1% for an efficient 5000-plate column. The error is reduced by approximately one third when the larger sample size is used ($L_f = 20\%$). The b values derived from large size sample band profiles are accurate when the column efficiency is above 200 theoretical plates.

Influence of signal noise on measurement of the coefficient a. Figs. 7–10 illustrate the influence of the noise on the coefficient a. Each figure corresponds to a different procedure of analyzing the simulated experimental data (Table I), and contains five curves, one for each value of the column efficiency. In each figure, for each column efficiency, the numerical average of a de-

TABLE I

COMBINATIONS OF PARAMETERS CONSIDERED IN THE ECP SIMULATIONS

Column efficiency (number of theoretical plates) $N = 200$, 500, 1000, 2000, 5000. Signal-to-noise ratio $SNR = h/\sigma = 200$, 500, 1000, 2000, 5000.

L_f [a] = 0.05				L_f [a] = 0.20			
SD[b]		NSD[c]		SD[b]		NSD[c]	
LR[d]	NLR[e]	LR[d]	NLR[e]	LR[d]	NLR[e]	LR[d]	NLR[e]

[a] Loading factor.
[b] Data smoothed first.
[c] Data non-smoothed.
[d] Linear regression.
[e] Non-linear regression.

TABLE II

PARAMETERS DERIVED BY ECP FROM CALCULATED BAND PROFILES (*SNR* INFINITE) (LINEAR REGRESSION)

True values: $a = 12.00$; $b = 0.024$; $q_s = a/b = 500$.

L_f	Parameter[a]	$N = 200$	$N = 500$	$N = 1000$	$N = 2000$	$N = 5000$
0.05	a	13.737	12.826	12.479	12.271	12.132
	B	32.519	27.533	25.984	25.112	24.531
0.20	a	13.277	12.566	12.319	12.178	12.084
	B	24.508	23.947	23.920	23.955	23.968

[a] $B = b \cdot 100$.

rived from a series of ten chromatograms is plotted *versus* the logarithm of the signal-to-noise ratio. For the high and low N values, error bars corresponding to the standard deviation based on the ten simulated a values are given, to indicate the influence of the noise on the precision of the derived coefficients. The higher is *SNR*, and as for the data in Table II the higher

TABLE III

PARAMETERS DERIVED BY ECP FROM CALCULATED BAND PROFILES (*SNR* INFINITE) (NON-LINEAR REGRESSION)

True values: $a = 12.00$; $b = 0.024$; $q_s = a/b = 500$.

L_f	Parameter[a]	$N = 200$	$N = 500$	$N = 1000$	$N = 2000$	$N = 5000$
0.05	a	13.755	12.838	12.487	12.276	12.135
	B	32.807	27.705	26.091	25.176	24.565
0.20	a	13.318	12.594	12.337	12.189	12.090
	B	24.784	24.121	24.030	24.021	24.003

[a] $B = b \cdot 100$.

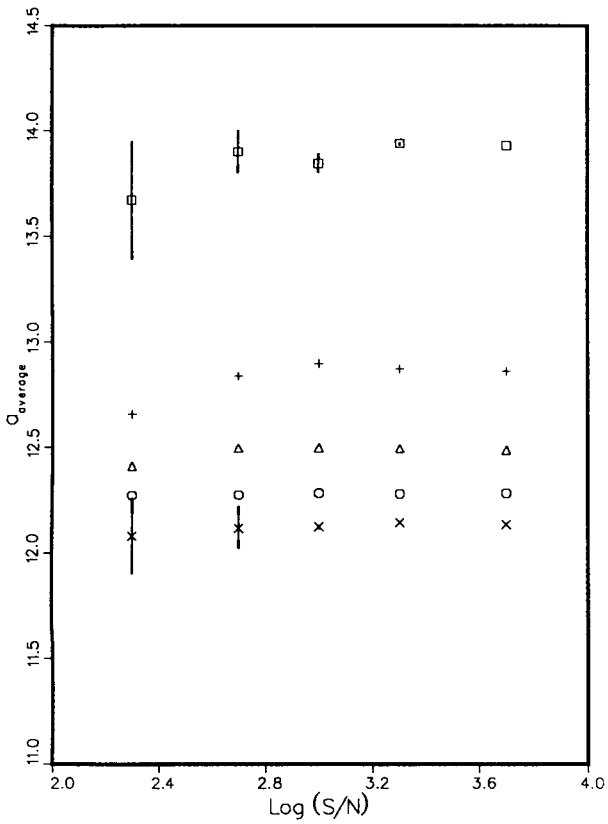

Fig. 7. Parameter *a* yielded by linear regression for smoothed data *versus* the logarithm of the signal-to-noise ratio ($L_f = 0.05$). N = (□) 200; (+) 500; (△) 1000; (○) 2000; (×) 5000.

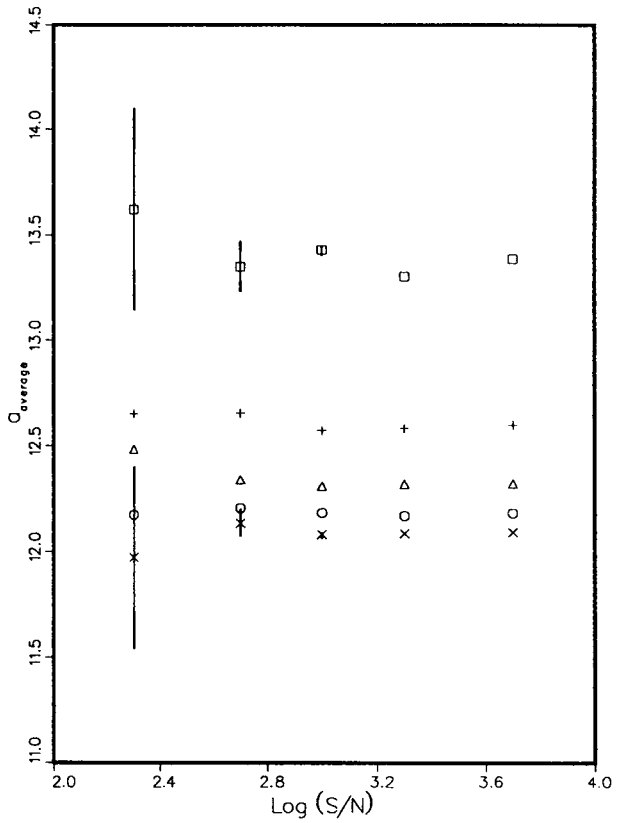

Fig. 8. Parameter *a* yielded by linear regression for smoothed data *versus* the logarithm of the signal-to-noise ratio ($L_f = 0.20$). N = (□) 200; (+) 500; (△) 1000; (○) 2000; (×) 5000.

the column efficiency, the more accurate are the results. However, the reproducibility at high efficiency tends to be slightly less than at low efficiency.

Figs. 7 and 8 show the results obtained by linear regression using eqn. 4 for two different loading factors, 0.05 and 0.20, respectively. Compared with the results shown in Table II, we see that the accuracy is better for the larger loading factor, when a chromatogram or a profile without noise was used. The improvement is more significant at very low efficiency than at high efficiency. On the other hand, the precision is poorer for the larger loading factor because the peak is now higher, hence the baseline noise is higher for a given *SNR*. This causes wider fluctuations of the end time of the integration.

Figs. 8 and 9 show the results obtained with the same series of data when using linear (Fig. 8) and non-linear (Fig. 9) regression methods. There is virtually no difference, which shows that in this case there does not seem to be any particular advantage in using the slightly more complex approach of non-linear regression. It must be noted, however, that the results from linear and non-linear regression are different at the 95% confidence level.

Finally, a comparison between Figs. 8 and 10 illustrates the influence of smoothing data before undergoing the regression calculation. As expected, when no smoothing was involved, there appears to be a larger scatter of *a* values (Fig. 10). Actually, the standard deviation for *a* values when $SNR = 200$ (*ca.* 11.90, not shown) now becomes comparable to the true *a* value (12.00). This scatter is such that, at low *SNR*, the

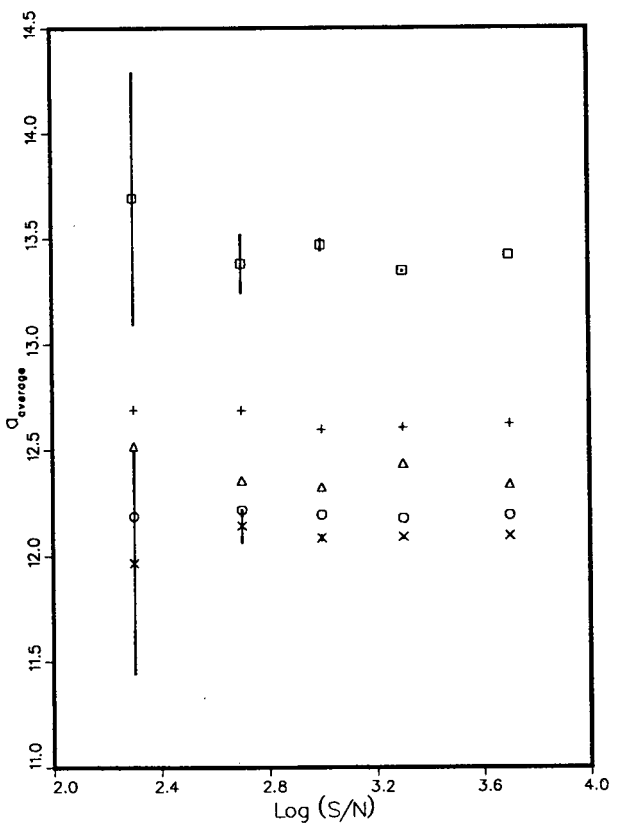

Fig. 9. Parameter *a* yielded by non-linear regression for smoothed data *versus* the logarithm of the signal-to-noise ratio ($L_f = 0.20$). N = (□) 200; (+) 500; (△) 1000; (○) 2000; (×) 5000.

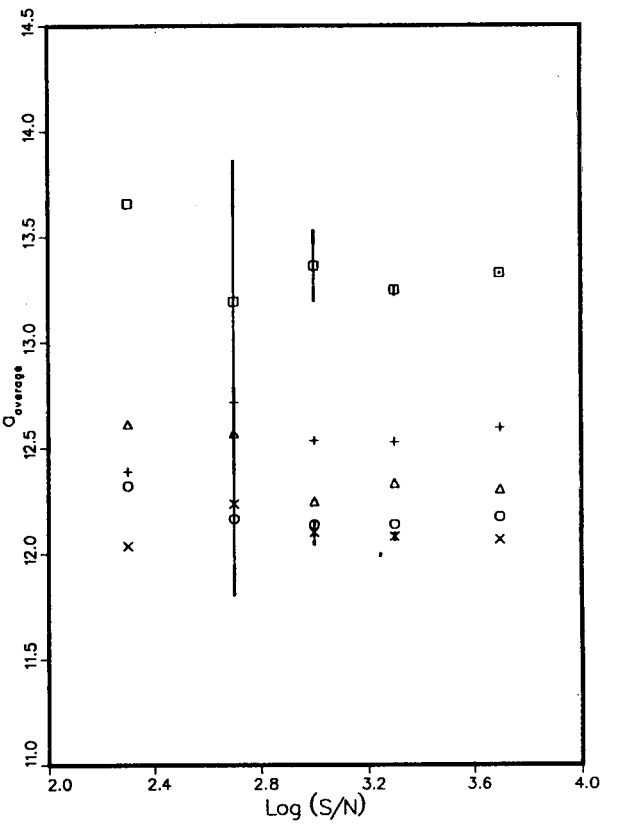

Fig. 10. Parameter *a* yielded by linear regression for non-smoothed data *versus* the logarithm of the signal-to-noise ratio ($L_f = 0.20$). N = (□) 200; (+) 500; (△) 1000; (○) 2000; (×) 5000.

systematic error which appears on the derivation of *a* does not necessarily decrease with increasing column efficiency. Inversion of the order takes place between *SNR* of 200 and 500. Similar results were obtained also for the loading factor of 0.05.

Influence of signal noise on measurement of the coefficient b. Figs. 11–13 show similar results for the coefficient *b* of the Langmuir model. These figures demonstrate that even when *SNR* is small, the noise signal does not seem to affect the average *b* value estimate to a large extent. The calculated standard deviations for each *SNR* based on ten simulated *b* values are less than 10^{-4}. Also, all the *b* values derived for columns having 500 theoretical plates or higher are identical within the limits of error. Similar results regarding both the accuracy and the precision are obtained no matter whether the data are smoothed (Fig. 12) or not (Fig. 13) in advance. Data obtained from non-linear regression (not shown) lead to the same conclusions as before. Once again, we can see that the precision of the results derived from non-smoothed data is lower than that from smoothed data.

Influence of integration path in the ECP method

In all the above studies, the ECP integration, (eqn. 2) was evaluated directly from the chromatograms. However, numerical integration is typically performed with the independent (or "known") variable as the integration variable, and the dependent (or "measured") variable is placed in the integrand. In eqn. 2, the indepen-

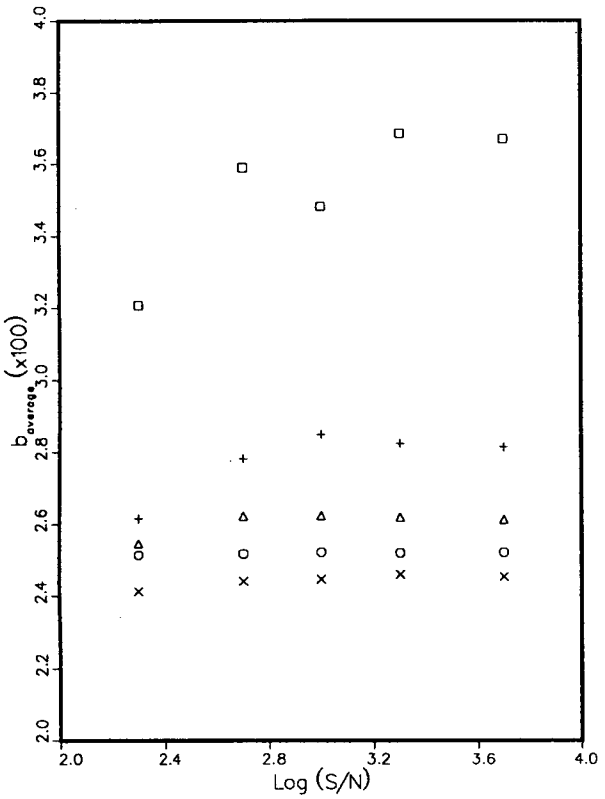

Fig. 11. Parameter b yielded by linear regression for smoothed data *versus* the logarithm of the signal-to-noise ratio ($L_f = 0.05$). N = (□) 200; (+) 500; (△) 1000; (○) 2000; (×) 5000.

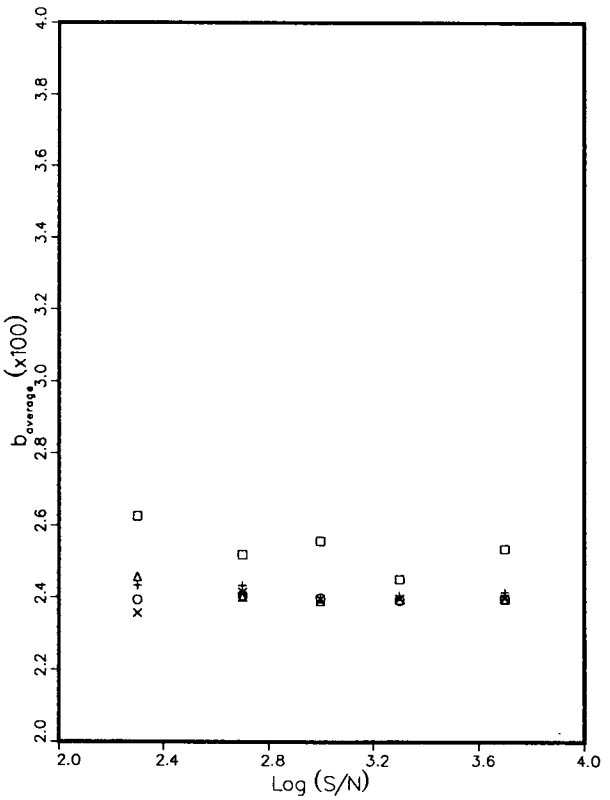

Fig. 12. Parameter b yielded by linear regression for smoothed data *versus* the logarithm of the signal-to-noise ratio ($L_f = 0.20$). N = (□) 200; (+) 500; (△) 1000; (○) 2000; (×) 5000.

dent variable (concentration) is in fact measured. Hence a noisy step length, $\delta_t C$, is used in the integration. An alternative way of evaluating eqn. 2 is to order the entire data set in terms of increasing concentration instead of increasing time. This is easily performed with vector ordering algorithms commonly supplied in many software packages. This procedure effectively transfers the experimental noise from the concentration variable to the time variable, so that the integration can proceed with a noise-free step length. Further, as negative concentrations do not make any sense, the tail of the data may be cut at the first occurrence of a negative concentration at the beginning of the algorithm, immediately after baseline correction.

The effect of cutting and integrating the data in this manner greatly increases the precision of the computed isotherm, in effect better preserving the low-pass filtering characteristic of integration. In Table IV the ECP results are shown for $L_f = 0.20$, $N = 2000$ and $SNR = 500$ and 1000, where the parameters were determined by simplex optimization. These results clearly show that transferring the noise to the time variable increases the precision of the results. Further, the accuracy of b is retained at lower SNR. The two orders of magnitude increase in precision is due to the effect of a smoothly varying integration variable, which subsequently filters the isotherm more effectively. Integrating in this manner eliminates the need for data smoothing and the performance of several sample trials in order to reduce the effect of random noise. The accuracy for any one trial, on average, will always be greater than if noise is allowed on the integration variable.

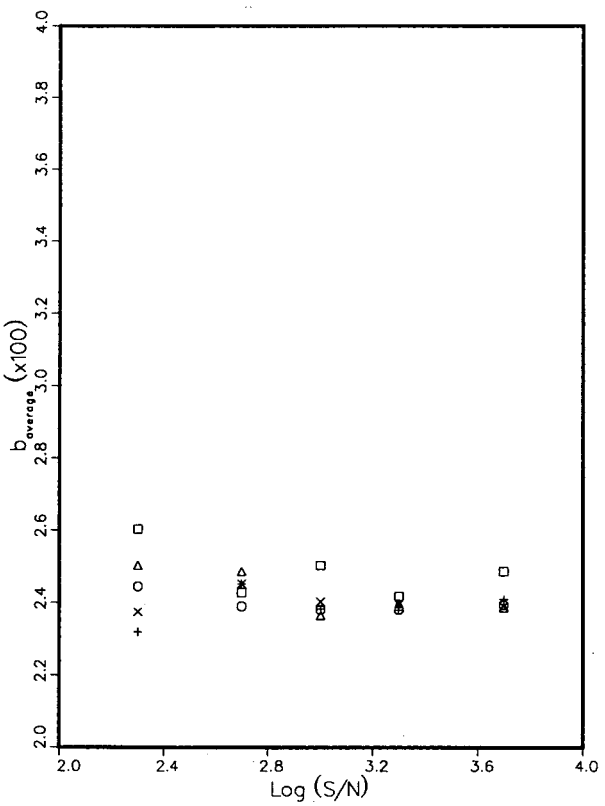

Fig. 13. Parameter b yielded by linear regression for non-smoothed data *versus* the logarithm of the signal-to-noise ratio ($L_f = 0.20$). N = (□) 200; (+) 500; (△) 1000; (○) 2000; (×) 5000.

Effect of determining a *independently from the retention time at infinite dilution*

With an infinite dilution experiment, an accurate measure of the retention factor, k', can be obtained. The accuracy and precision of this measure depends on *SNR*, the data density and the fluctuation of the experimental parameters (*i.e.*, pressure drop, temperature, etc.). With a value of the phase ratio, F, the initial slope of the true isotherm, $a = k'/F$, can be determined more accurately than that yielded by the ECP method for columns of less than 5000 plates (often to within 0.05%) [14]. The effect of fixing this measure of a and then determining b from the ECP isotherm is to place the systematic error arising from the finite efficiency on the b coefficient.

This effect is illustrated for $N = 1000$ plates, $SNR = 1000$ and $L_f = 0.20$ in the residual plot of Fig. 14. In this figure, the fitted Langmuir isotherms (obtained via simplex optimization of the coefficients with respect to the ECP isotherm) are compared with the true isotherm and the ECP isotherm in terms of their relative error, $r = [q_{fit}(C) - q(C)]/q(C)$, where $q_{fit}(C)$ is the fitted isotherm. The solid line represents the true isotherm prediction error when both a and b are optimized. The upper dashed line represents the true isotherm prediction error when a is fixed to the infinite dilution value (assumed as the correct

TABLE IV

PARAMETERS DERIVED FROM ECP METHOD WITH DIFFERENT CONCENTRATION INTEGRATION PATHS

$L_f = 0.20$, $N = 2000$. True values: $a = 12.00$; $b = 0.024$; $q_s = a/b = 500$.

Statistic	Parameter	$SNR = 500$		$SNR = 1000$	
		c-Noise[a]	*t*-Noise[a]	*c*-Noise[a]	*t*-Noise[a]
Mean	a	12.0	12.175	12.2	12.176
	b	0.023	0.02400	0.024	0.024003
Standard deviation	σ_a	0.3	0.005	0.2	0.001
	σ_b	0.001	0.00002	0.001	0.000005
Error (%)	a	0	+1.46	+1	+1.46
	b	−3	0	0	+0.01

[a] *c*-Noise refers to evaluating eqn. 2 as is, allowing the noise to reside on the concentration data. *t*-Noise refers to transferring the concentration errors to the time or volume variable by ordering the concentration data monotonically from low to high.

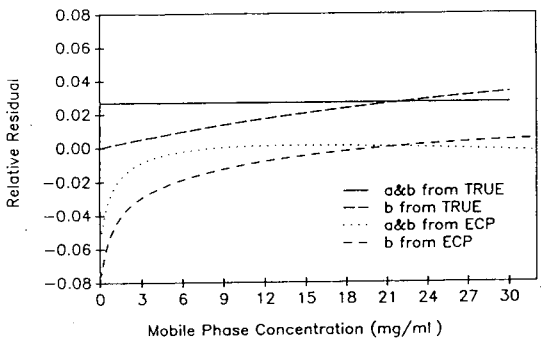

Fig. 14. Relative residual error of the predicted isotherms. Solid and upper dashed lines correspond to the predicted error with respect to the true isotherm ($a = 12.0$, $b = 0.024$); solid line corresponds to conventional ECP analysis, where both a and b are fitted to the ECP isotherm; upper dashed line corresponds to accurately determining a independently and fitting b to the ECP isotherm. Dotted and lower dashed lines correspond to the respective residuals of estimation of the ECP analyses (with respect to the fit ECP isotherm).

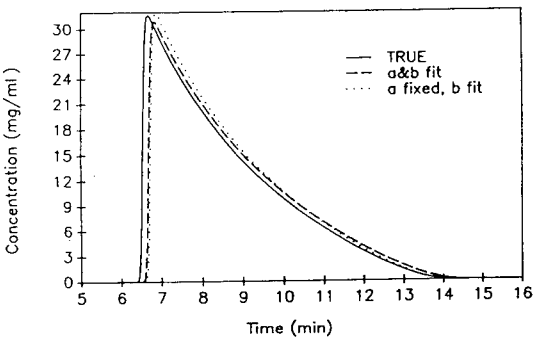

Fig. 15. Band profiles corresponding to the predicted isotherms derived by the different methods in this study. Solid line represents the "true" chromatogram. Dashed line originates from the isotherm determined by fitting both a and b in ECP analysis. Dotted line originates from the isotherm determined by accurately measuring a independently and fitting b to the ECP isotherm.

value here), and only b is fitted to the ECP isotherm. The dotted and lower dashed lines represent the corresponding residual errors from the optimizations (with respect to the ECP isotherm). The a and b fit isotherm is shifted above the true isotherm by an approximately constant amount, whereas the b fit isotherm converges to the true isotherm at low C. The statistical results of these determinations are given in Table V. The effect of these results on the predicted band profiles are shown in Fig. 15.

From these results, it is apparent that at low efficiencies most of the positive systematic error is placed on the a coefficient when conventional regression on ECP isotherms is performed (for high loading factors). If a is determined accurately beforehand, and b is fitted to the ECP isotherm, a negative systematic error is placed on b. Although the former method fits the data better (ECP isotherm), it does not cumulatively reflect the true isotherm any better until large mobile phase concentrations are encountered (>21.5 mg/ml, which corresponds to a loading factor of approximately 12% in the above simulation). However, as the error in the b term inherently increases as the loading factor decreases, the advantage of determining a separately is not great. This is illustrated by the

TABLE V

COMPARISON OF DIFFERENT METHODS OF OPTIMIZATION OF THE LANGMUIR PARAMETERS

$L_f = 0.20$, $N = 1000$, $SNR = 1000$. True values: $a = 12.00$; $b = 0.024$; $q_s = a/b = 500$.

Result	Parameter	a and b fitted	a fixed, b fitted b fitted	Fit to band profile
Coefficients	a	12.32	12.00	11.85
	b	0.02399	0.02216	0.02530
Error (%)	a	+2.7	0.0	−1.2
	b	−0.04	−7.7	+5.4
σ_{fit} [a]		0.01598	0.02942	0.01231

[a] Defined as the relative root-mean-squared (rms) value of fit. Defined for the predicted and ECP isotherms for the first two columns and for the predicted and observed chromatograms for the last column.

similarity of the aggregate error in the predicted chromatograms shown in Fig. 15.

Analysis by fit of the band profile

Dose *et al.* [15] showed that the isotherm parameters can be determined from the band profile data by simulating the band profile with a known efficiency and optimizing the isotherm coefficients with a careful simplex routine. If this algorithm is applied to the above data $L_f = 0.20$, $SNR = 1000$ and $N = 1000$, the results in Table V and Fig. 15 ("fit to band profile") are obtained. The predicted chromatogram is overlaid with the true chromatogram on the scale of Fig. 15. However, the error in the Langmuir coefficients remains significant. The effects of underestimating a and overestimating b cancel each other. This false minimum is obtained because of the systematic direction of convergence of the simplex and the shallow nature of the chi-squared surface. The initial estimates for this algorithm were obtained from the a and b fit of the ECP isotherm.

This method of analysis exhibits high precision, but the gain in accuracy over the ECP analysis in terms of the isotherm parameters decreases as the column efficiency increases. The accuracy with respect to the observed band profile, however, is always good. Therefore, this is a good practical method for predicting nonlinear chromatograms, although it bears the stigma of a circular argument, and for this reason must be used cautiously. As the convergence of this algorithm can be prohibitively slow, and little advantage exists for the high-efficiency cases, the use of this program is advised for low efficiency columns only (<2000 plates).

CONCLUSIONS

The experimental requirements to achieve the precision and accuracy which are needed in the determination of isotherms by ECP are more stringent than generally believed. The column efficiency should exceed 2000 and preferably be close to 5000 theoretical plates. The signal-to-noise ratio (maximum height of the band divided by the standard deviation of the noise) should exceed 500. A large size sample should be injected, corresponding to a loading factor of about 0.20, to achieve a better estimate of the coefficient a. Smoothing the raw data in advance can reduce the large scatter of the results to a certain extent, but integrating the data with the error placed on the time variable eliminates the scatter more effectively. Finally, the detector response should be linear in the range of concentrations sampled, or it should be accurately calibrated.

The independent determination of the retention factor at infinite dilution can be performed by the injection of a sample small enough to be eluted under linear conditions. This procedure provides often a value of the initial slope of the isotherm that is more accurate than the value derived from the ECP method for $N < 5000$ plates. There are cases, however, where these values are difficult to reconcile, for example because of the existence of a low density of active sites on the surface [16].

ACKNOWLEDGEMENTS

We are grateful to Charles Bayne (ACD, ORNL) and Eric Dose (Ross Laboratories, Columbus, OH) for their useful comments. This work was supported in part by grant CHE-9201663 from the National Science Foundation and by the cooperative agreement between the University of Tennessee and the Oak Ridge National Laboratory. We acknowledge support of our computational effort by the University of Tennessee Computing Center.

REFERENCES

1 E. Glueckauf, *Nature*, 156 (1945) 748.
2 E. Glueckauf, *Proc. R. Soc. London, Ser. A*, 186 (1946) 35.
3 E. Cremer and J.F.K. Huber, *Angew. Chem.*, 73 (1961) 461.
4 J. Conder and J. Young, *Physicochemical Measurement by Gas Chromatography*, Wiley, New York, 1979, p. 353.
5 A.M. Katti and G. Guiochon, *Adv. Chromatogr.*, 31 (1991) 1.
6 M.Z. El Fallah and G. Guiochon, *Anal. Chem.*, 63 (1991) 2244.
7 M.Z. El Fallah and G. Guiochon, *Biotechnol. Bioeng.*, 39 (1992) 877.

8 S. Golshan-Shirazi and G. Guiochon, in F. Dondi and G. Guiochon (Editors), *Theoretical Advancement in Chromatography and Related Separation Techniques (NATO ASI, Series C*, Vol. 383), Kluwer, Dordrecht, 1992, pp. 61–92.
9 J. Roles and G. Guiochon, *J. Phys. Chem.*, 95 (1991) 4098.
10 H. Guan and G. Guiochon, in preparation.
11 S. Golshan-Shirazi and G. Guiochon, in F. Dondi and G. Guiochon (Editors), *Theoretical Advancement in Chromatography and Related Separation Techniques (NATO ASI, Series C*, Vol. 383), Kluwer, Dordrecht, 1992, pp. 1–33.
12 F. Harrison and S.K. Katti, *Chemometr. Intell Lab. Syst.*, 9 (1990) 249.
13 R.L. Anderson, *Practical Statistics for Analytical Chemists*, Van Nostrand, New York, 1987, pp. 89–121.
14 M. Goedert and G. Guiochon, *Chromatographia*, 6 (1973) 39.
15 E.V. Dose, S. Jacobson and G. Guiochon, *Anal. Chem.*, 63 (1991) 833.
16 M. Diack and G. Guiochon, *Anal. Chem.*, 63 (1991) 2608.

Journal of Chromatography A, 659 (1994) 43–56
Elsevier Science B.V., Amsterdam

CHROM. 25 561

Accurate measurements of solubility and thermodynamic transfer quantities using reversed-phase liquid–liquid chromatography

Rebecca Silveston and Bengt Kronberg*

Institute for Surface Chemistry, P.O. Box 5607, S-114 86 Stockholm (Sweden)

(First received July 12th, 1993; revised manuscript received September 14th, 1993)

ABSTRACT

A reversed-phase high-performance liquid chromatographic system, consisting of polydimethylsiloxane coated on non-porous glass beads as the stationary phase and pure water as the mobile phase, was used to measure the absolute solubility and the temperature dependence of the solubility of a series of alkylbenzenes in water in the temperature range 0–80°C. The system and the method of analysis provide accurate values of the molar free energy, enthalpy, entropy and reasonable values of the heat capacity of transfer of the alkylbenzenes from their own liquids into water. The thermodynamic data were analysed in terms of the Flory–Huggins theory giving combinatorial and non-combinatorial, *i.e.*, interactional, contributions to the free energy of transfer. All the data were found to agree very well with literature values. The success of the system is attributed to the liquid nature of the stationary phase, the low surface area-to-volume ratio offered by the support material chosen and the availability of the absolute value of the volume of the stationary phase to calculate the phase ratio.

INTRODUCTION

In reversed-phase high-performance liquid chromatography (RP-HPLC), the stationary phase is less polar than the mobile phase, which is often a mixture of water and an organic solvent (modifier). Chromatographic retention is due to the equilibrium distribution of a probe molecule between the stationary phase and the mixed mobile phase. This retention is expressed in terms of a capacity factor, k', relating the retention volume to the hold-up volume in the system. This in turn is related to the partitioning of the probe between the stationary phase and the mobile phase. Therefore, thermodynamics under equilibrium conditions can be applied to chromatographic retention [1–4]. Liquid and gas chromatography have in fact been shown to be very powerful tools for obtaining thermodynamic functions of mixtures [5,6]. However, extracting thermodynamic information is often hampered by the lack of knowledge of the volume of the stationary phase required to calculate the partition coefficient. Hence one has to be content with the dependence of a relative quantity, *e.g.*, the capacity factor, k', on parameters such as the mixing ratio of water and organic modifier in the mobile phase or the temperature. In the first case, for weak interactions between the probe molecules and the molecules in the mixed mobile phase, log k' is linearly dependent on the composition of the mixed phase. However, this dependence has been found to become non-linear as the water content of the mobile phase is increased [2]. Less attention has been paid to pure aqueous systems, which are of interest in this work. The advantage of using temperature as a parameter is that the enthalpy change can be obtained directly from k' for the process of

* Corresponding author.

0021-9673/94/$07.00
SSDI 0021-9673(93)E1000-P

transferring a probe molecule between the stationary phase and the mobile phase. However, absolute values of the free energy and the entropy of transfer require a knowledge of the total volume of the stationary phase in order to relate the capacity factor to the partition coefficient through the phase ratio.

In this paper we show that it is indeed possible to obtain meaningful and absolute values of all the thermodynamic transfer functions and also the solubility, by virtue of a high-molecular mass stationary phase, which is a non-polar liquid, and an accurate independent measurement of the phase ratio. These thermodynamic data for hydrocarbons at infinite dilution in pure water can be used to examine hydrocarbon–water interactions.

The interaction of non-polar parts of molecules with water is an important factor in several common physico-chemical processes, such as micellization of surfactants and protein denaturation. These interactions are usually determined by measuring the solubility of alkyl derivatives in water. The model compounds often contain one polar part, which makes only a minor contribution to the solubility of a homologous series in dilute aqueous solution [7]. However, there are experimental problems associated with measuring the solubility of even these alkyl derivatives in water owing to their low aqueous solubility. These problems are largely circumvented by the use of chromatography.

This study extends our previous work [8] on the transfer of toluene and ethylbenzene from a non-polar liquid to water by measuring benzene and propylbenzene on the same HPLC set-up, which consists of water as the mobile phase and a non-polar liquid, *viz.*, polydimethylsiloxane (PDMS), coated on non-porous glass beads as the stationary phase. The volume of the polydimethylsiloxane stationary phase is characterized by elemental analysis such that the phase ratio and thereby the free energy, entropy and enthalpy are obtained for the transfer process.

EXPERIMENTAL

Chemicals and column preparation

The stationary phase consisted of a polymer coated on non-porous glass beads (30–60 μm) from Werner Glass (Stockholm, Sweden). The polymer was PDMS, a secondary standard used as received from Aldrich (*M ca.* 600 000). The polymer is a liquid over the whole temperature range investigated, *i.e.*, 0–80°C. The fact that the polymer is very hydrophobic together with the high molecular mass prevents bleeding of the stationary phase. The PDMS was deposited on the non-porous glass beads by first dissolving it in toluene and mixing the solution with the glass beads for 15 min, and then evaporating the toluene in a Rotavapor. The glass beads, used as the support material, were precleaned by washing with water and 95% ethanol to remove organic material before drying at 110°C overnight to remove traces of water.

The coated beads were slurried in water containing about 10% of chromatographic-grade methanol in order to improve the dispersion. The slurry was packed with this water–methanol mixture as the packing fluid in a Magnus Scientific Instruments slurry packer at *ca.* 350 atm (1 atm = 101 325 Pa). The packing process was complete after 2 l of packing solution had passed through the column, then the methanol was rinsed out with another 2 l of deaerated water, equivalent to about 200 column dead volumes.

The water used in the above processes was purified with a modified Millipore Milli-Q purification system. The feed water was purified by the following steps: decalcination, prefiltration with activated charcoal, reverse osmosis, treatment with two mixed-bed ion exchangers, activated charcoal, an in-line filter (0.2 μm), an Organex cartridge and finally filtration through a 0.2-μm cationic nylon filter. All purification units were Millipore products, except the final filter, which was obtained from Zetapore.

The probe liquids were chromatographic-grade benzene and propylbenzene from Merck and Aldrich. A saturated solution of the probe in water was mixed daily, and the water-rich part was diluted 2–4-fold with water before use. Sodium nitrate was added to this diluted solution to mark the column hold-up or dead volume. A knowledge of the exact concentration of the probe sample was not necessary for our purposes once it had been verified that the retention volumes were independent of probe concentration.

Characterization of the stationary phase

In order to obtain the phase ratio, it is necessary to determine the volume of the liquid polymer in the stationary phase. The initial mass of the polymer on the glass beads unfortunately could not be used as a measure of the amount of PDMS deposited on the beads as a certain amount of the polymer was lost both in the preparation of the packing and during the packing process with methanol–water. The amount was instead determined by elemental analysis, performed by MikroKemi (Uppsala, Sweden), of 200-mg samples of the column material removed after the experiment. This was found to be a more accurate method of determining the amount of PDMS in the column than the differential thermal analysis method used in our previous work on toluene and ethylbenzene [8]. We therefore re-measured the packing of the previous column (No. 3) and recalculated the resulting thermodynamic quantities for toluene and ethylbenzene to be presented here together with the results for benzene and propylbenzene.

Four different columns were used for retention measurements of benzene, toluene, ethylbenzene and propylbenzene. For benzene we joined columns 1 and 2 in series in order to obtain large enough retention volumes that could be measured accurately. Column 3 was used for toluene and ethylbenzene and column 4 for propylbenzene. The total amounts of PDMS in columns 1 + 2, 3 and 4 were found to be 0.0819 ± 0.0009, 0.0264 ± 0.0003 and 0.00105 ± 0.00001 g, respectively. The resulting thickness of the layer of polymer on the glass bead support material was calculated to be 800–1400 Å for columns 1 + 2, 500–800 Å for column 3 and 10–20 Å for column 4. Both the volume of polymer used and the resulting thickness decreased as the alkyl chain length increased to ensure reasonable retention times. The phase ratio, *i.e.*, the ratio of the volume of the stationary to that of the mobile phase in the chromatographic system, was calculated to be 0.048, 0.036 and 0.0023 for columns 1 + 2, 3 and 4, respectively.

Analysis of the column performance gave about 400 theoretical plates for columns 1 + 2 and 3 and 30 theoretical plates for column 4. This corresponds to a height equivalent to a theoretical plate (HETP) of 0.8 mm for columns 1 + 2 and 3 and 1.8 mm for column 4. The high HETP value for the latter column is probably due to dispersion effects caused by the pure, non-coated glass beads (see below).

Apparatus and chromatographic procedure

Stainless-steel columns with 0.5-mm end frits of various lengths and widths were used to obtain reasonable retention times for both benzene and propylbenzene. Two 4.6 mm I.D. columns were used in series for benzene, one 5 cm (No. 1) and one 25 cm long (No. 2). For propylbenzene, a 4 cm × 2.1 mm I.D. column (No. 4) was used and packed with 50% cleaned, non-coated glass beads. A reference column was packed with only cleaned glass beads in order to verify that there was no interaction of the propylbenzene with the glass surface. Stainless-steel tubing of 3-ml volume was inserted between the water source and the injector to ensure a well thermostated mobile phase. The stainless-steel tubing from the injector to the column was 1/16 in. O.D. (1 in. = 2.54 cm) and 0.01 mm I.D. and that from the column to the detector was 1/16 in. O.D. and 0.007 mm I.D., and was insulated in order to reduce any local temperature effects of the laboratory. The latter tubing was kept as short as possible in order to minimize peak spreading. The column temperature was controlled by regulating a water-bath to ±0.25°C. The 20-μl loop of a Rheodyne Model 7125 injector and part of the injector itself were immersed in the water-bath. The loop was flushed with several volumes of the temperature-equilibrated probe solution before filling and finally left for a period of time in order to come to temperature equilibrium before injection. The eluate was detected with a Waters Model 410 Millipore refractive index meter. A pressure of 50 ± 15 atm from an LKB Model 2150 HPLC mini-pump ensured a constant flow-rate of 1.00 ± 0.005 ml/min. The eluate was collected in a beaker and weighed continuously in order to determine the retention volume. The detector output was recorded on a chart recorder and the peak maxima of the probe and marker were recorded [9]. The primary information was obtained as the difference in retention volumes of the probe and the salt marker, $V^N = V^R - V^{MK}$

(a full list of the symbols used is given at the end of the paper).

Treatment of experimental data

In chromatography, the most commonly measured parameter is the capacity factor, defined as

$$k' = (V_R - V^{MK})/V^{MK} = V^N/V^{MK} \quad (1)$$

where V^N is the net retention volume, *i.e.*, the difference between the retention volume of the probe, V^R, and the retention volume of a marker, V^{MK}, *e.g.*, a non-retarding molecule such as a salt, giving the mobile phase hold-up volume.

The retention mechanism in our system involves both absorption of the probe molecules into the stationary polymer liquid and adsorption at the polymer–water interface. The net retention volume can therefore be written as

$$V^N = K_c V^P + K_{ads} A^P \quad (2)$$

where V^P is the total volume of the stationary polymer phase, A^P is the total interfacial area of the polymer being exposed to the water and K_c and K_{ads} are the partition coefficients of the probe for the absorption and adsorption processes, respectively. In our system the adsorption term was found to be negligible, *i.e.*,

$$K_c \approx V^N/V^P = k'/\phi \quad (3)$$

where ϕ is the phase ratio. This was shown by measuring the net retention volume as a function of polymer loading, V^P, with an approximately constant polymer surface area, A^P, shown in Fig. 1 in ref. 8. The straight line passing through the origin indicates the negligible importance of the last term in eqn. 2. This result is a consequence of the experimental design in using non-porous, and relatively large, glass beads as the support for the PDMS polymer, thus giving a minimum surface-to-volume ratio of the polymer stationary phase.

The future usefulness of eqn. 3 depends on the correctness of the following three assumptions:
(i) The LC system is operating at equilibrium, *i.e.*, the partition coefficient is established quickly in comparison with the length of the column. This assumption was checked by verifying that the retention volume of a probe is independent of flow-rate, as shown in Fig. 1.

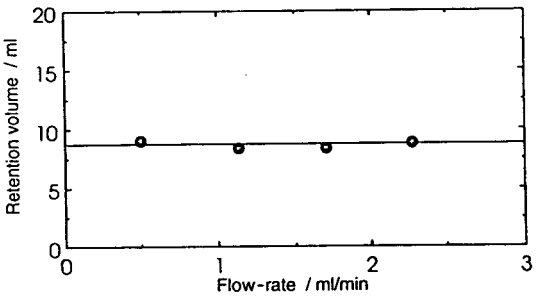

Fig. 1. Retention volume of toluene as a function of flow-rate.

(ii) The partitioning is constant throughout the column. This assumption is true as long as we can verify that we are operating in the linear portion of the partition equilibrium. We found that the retention volume of a probe is independent of probe concentration (Fig. 2 in ref. 8), thus ensuring infinite probe dilution conditions, *i.e.*, the system is operating in the Henry's law range.
(iii) The stationary and mobile liquid phases are mutually immiscible such that they can be considered as a pure water and a pure PDMS phase. This ensures that one is determining the difference in behaviour of two binary mixtures (probe–PDMS and probe–water) as opposed to two ternary mixtures. The correctness of this assumption was not checked, but the precaution was taken of using a very high-molecular-mass polymer. Also, no changes in retention volume were detected as a function of time, which would be the case if the polymer had a slight solubility in the water (bleeding).

We shall now link the partition coefficient to meaningful thermodynamic quantities.

THERMODYNAMIC BACKGROUND

The fundamental quantity in eqn. 3 is the equilibrium partition coefficient, K_c, describing the partitioning of the probe (component 1) between the two immiscible phases, in our sys-

tem the water mobile phase (W) and the non-polar polymer stationary phase (P). The partition coefficient, K_c, is at any temperature defined as the ratio of the probe molar concentration $[1]^i$ in either phase i. The concentration is thus expressed in moles of probe (n_1) per unit volume, *i.e.*, n_1^P/V^P for the polymer phase and n_1^W/V^W for the aqueous phase, and the partition coefficient is

$$K_c = \frac{[1]^P}{[1]^W} = \frac{n_1^P/V^P}{n_1^W/V^W} \tag{4}$$

where V^P and V^W are the volumes of the polymer and water phase, respectively.

From fundamental thermodynamics, the partition ceofficient, K_c, defined using molar concentrations of the probe, is obtained by defining the activity coefficient of component 1, γ_1, as

$$\gamma_1 = \frac{a_1}{[1]} \tag{5}$$

where a_1 is the activity. Thus, the chemical potential is expressed as

$$\frac{\mu_1^i - \mu_1^0}{RT} = \ln a_1^i = \ln [1]^i + \ln \gamma_1^i , \tag{6}$$

valid for both the polymer and aqueous phase, *i.e.*, i = P or W. The standard state, μ_1^0, throughout this work refers to the pure components. At equilibrium between the two phases we obtain

$$\ln \gamma_1^W - \ln \gamma_1^P = \ln \frac{[1]^P}{[1]^W} = \ln K_c$$

$$= \frac{\Delta_P^W G_c}{RT} = \ln \frac{V^R - V^{MK}}{V^P} \tag{7}$$

where we have defined the molar free energy of transfer (using molar concentrations), $\Delta_P^W G_c$, in terms of the difference of the logarithm of the activity coefficients of the probe at infinite dilution in the two liquids. Another definition of the activity coefficient in eqn. 5 is possible using the volume fraction as the concentration variable [8,10], rendering K_φ and a free energy of transfer, $\Delta_P^W G_\varphi$, as

$$\frac{\Delta_P^W G_\varphi}{RT} \equiv \ln \frac{\varphi_1^P}{\varphi_1^W} = \ln K_\varphi$$

$$= \ln \frac{V_R - V^{MK}}{V^P} + \ln \frac{\bar{V}_1^P(\infty)}{\bar{V}_1^W(\infty)} \tag{8}$$

where $V_1^P(\infty)$, and $V_1^W(\infty)$ are the partial molar volumes of the probe at infinite dilution in the polymer and water phase, respectively.

Eqns. 7 and 8 suffer from the drawback, however, that the free energies defined contain both information from the difference in molecular interaction that the probe experiences in the two different phases and information from the difference in molecular sizes. It is of interest to isolate the molecular interaction from other contributions to the transfer functions in order to obtain information on solute–solvent interactions. This can be accomplished using the Flory–Huggins expressions for the chemical potential where the activity coefficient is split up into a combinatorial part, stemming from the difference in molecular sizes, and an interactional or non-combinatorial, part [11]. Hence we can take advantage of this expression in order to eliminate the combinatorial contribution to the entropy of mixing molecules of different sizes. In the Flory–Huggins theory, the chemical potential is expressed as

$$\frac{\Delta\mu_1^i}{RT} = \frac{\mu_1^i - \mu_1^0}{RT} = \ln \varphi_1^i + (1 - \varphi_1^i)\left(1 - \frac{\bar{V}_1^i}{\bar{V}_i}\right)$$

$$+ \chi_1^i (1 - \varphi_1^i)^2 \tag{9}$$

which is applied to both the polymer and aqueous phase, *i.e.*, i = P or W. In the equation, $\bar{V}_1^i$ is the partial molar volume of the probe in the solvent phase i, $\bar{V}_i$ is the molar volume of the solvent i and χ_1^i is the interaction parameter between the probe and solvent molecules. χ_1^W and χ_1^P represent the residual chemical potential in excess over the combinatorial contribution. We note in passing that $\bar{V}_P$ is strictly not defined due to the polydispersity of the polymer. However, this is not a problem when using very high-molecular mass polymers, because then the $\bar{V}_1^P/\bar{V}_P$ ratio is negligibly small, irrespective of the precise value of $\bar{V}_P$.

When equilibrium conditions prevail between the polymer and aqueous phase we are able to define a non-combinatorial free energy of transfer, $\Delta_P^W G'_\varphi$ in terms of the difference in χ_1^i parameters. In other words,

$$\frac{\Delta_P^W G'_\varphi}{RT} \equiv \chi_1^W - \chi_1^P = \ln\frac{\varphi_1^P}{\varphi_1^W} + \frac{\bar{V}_1^W(\infty)}{\bar{V}_W}$$

$$= \ln\frac{V_R - V^{MK}}{V^P} + \ln\left[\frac{\bar{V}_1^P(\infty)}{\bar{V}_1^W(\infty)}\right] + \frac{\bar{V}_1^W(\infty)}{\bar{V}_W} \quad (10)$$

Eqn. 10 is derived under the assumption of (i) equilibrium between the two phases, (ii) infinite dilute concentration of the probe and (iii) an infinitely high molecular mass of the PDMS polymer.

For the sake of clarity, we repeat that in our notation the non-combinatorial quantity denoted by $\Delta_P^W G'_\varphi$ is extracted from experimental retention volumes using a combinatorial contribution calculated according to the Flory–Huggins theory on a volume fraction basis.

The relationship between the non-combinatorial free energy of transfer, $\Delta_P^W G'_\varphi$, and the free energy of transfer, $\Delta_P^W G_\varphi$, defined by eqn. 8, is then

$$\Delta_P^W G'_\varphi = \Delta_P^W G_\varphi + \frac{\bar{V}_1^W(\infty)}{\bar{V}_w} \quad (11)$$

Pressure effects

Since HPLC operates at elevated pressures, one needs to consider the effect of pressure on the thermodynamic information obtained. This was pioneered by Locke and co-workers [4,12]. The $\mu_1^0(T, P)$ of eqn. 6 can be expressed at a standard pressure, P^*, of 1 atm as

$$\mu_1^0(T, P) = \mu_1^*(T, P^*) + (P - P^*)\bar{V}_1^0 \quad (12)$$

where $\bar{V}_1^0$ is the molar volume of the pure probe assuming that $(\partial\bar{V}_1^0/\partial P)_T = 0$. Following the development given in refs. 4 and 12, eqn. 12 can be applied to the polymer (P) and water (W) phases at equilibrium conditions, where $\Delta\mu_1^P(T, P) = \Delta\mu_1^W(T, P)$, to give

$$\frac{\Delta_P^W G(P)}{RT} = \frac{\Delta_P^W G(P^*)}{RT} + \frac{(P - P^*)}{RT}[\bar{V}_1^W(\infty) - \bar{V}_1^P(\infty)] \quad (13)$$

Note that the column pressure, P, is the mean pressure in the column, assuming a linear pressure gradient, as discussed in ref. 12. As eqn. 13 is applied at infinite dilution of the probe, $\bar{V}_1^0$ was replaced with $\bar{V}_1^i(\infty)$, *i.e.*, the partial molar volume of the probe in the solvent i at infinite dilution. Eqn. 13 shows explicitly the effects operating the HPLC system above atmospheric pressure in the term $[(P - P^*)/RT][\bar{V}_1^W(\infty) - \bar{V}_1^P(\infty)]$.

Transfer of the probe to PDMS

In order to compare our chromatographic results with solubility measurements we need to fill in the missing gap, *i.e.*, the transfer of the probe from the pure probe liquid to the PDMS polymer, illustrated below:

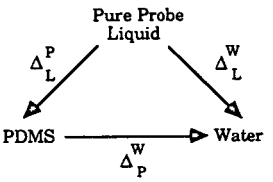

Thus $\Delta_L^W G = \Delta_L^P G + \Delta_P^W G$. The standard free energy of transfer of the probe from the pure liquid to the PDMS solution can be experimentally determined from vapour pressure or osmotic pressure measurements as well as GLC. The relative vapour pressure of the probe is related to its chemical potential according to

$$\frac{(\mu_1^P - \mu_1^0)}{RT} = \ln a_1^i = \ln\frac{p_1^P}{p_1^0}$$

$$= \ln\varphi_1^P + \left[1 - \frac{\bar{V}_1^P(\infty)}{\bar{V}_P}\right](1 - \varphi_1^P) + \chi_1^P(1 - \varphi_1^P)^2 \quad (14)$$

The free energy of transfer of the probe from the pure probe liquid to liquid PDMS, where $[\bar{V}_1^P(\infty)/\bar{V}_P] \approx 0$, and at the limit of infinite dilution, $\varphi_1^P \to 0$, is then

$$\frac{\Delta_L^P G_\varphi}{RT} = \ln\frac{1}{\varphi_1^P} = \chi_1^P + 1 \quad (15)$$

The corresponding non-combinatorial free energy of transfer is

$$\frac{\Delta_L^P G'_\varphi}{RT} = \chi_1^P \quad (16)$$

It is now possible to express the free energy of transfer from the pure probe to water according to the schematic triangle above, *i.e.*, from eqns. 8 and 15 we have

$$\frac{\Delta_L^W G_\varphi}{RT} = \ln\left(\frac{\varphi_1^P}{\varphi_1^W}\right) + \chi_1^P + 1$$

$$= \ln\frac{V^R - V^{MK}}{V^P} + \ln\left[\frac{\bar{V}_1^P(\infty)}{\bar{V}_1^W(\infty)}\right]$$

$$+ \chi_1^P + 1 + \frac{P-1}{RT}[\bar{V}_1^W(\infty) - \bar{V}_1^P(\infty)] \quad (17)$$

The corresponding non-combinatorial free energy is obtained from eqns. 10 and 16:

$$\frac{\Delta_L^W G'_\varphi}{RT} = (\chi_1^W - \chi_1^P) + \chi_1^P$$

$$= \ln\left(\frac{V^R - V^{MK}}{V^P}\right) + \frac{\bar{V}_1^W(\infty)}{\bar{V}_W} + \chi_1^P$$

$$+ \ln\left[\frac{\bar{V}_1^P(\infty)}{\bar{V}_1^W(\infty)}\right]$$

$$+ \frac{P-1}{RT}[\bar{V}_1^W(\infty) - \bar{V}_1^P(\infty)] \quad (18)$$

Solubility

One of the purposes of this work was to relate the thermodynamic quantities measured chromatographically to literature data on the solubility, in particular for the homologous series of alkylbenzenes. Solubility measurements can be considered as a transfer of the probe from the pure probe liquid, L, to water, W, and therefore we apply eqn. 9 to this system. At the solubility limit, the chemical potential of the hydrocarbon probe is equal to the chemical potential of the pure probe, provided that water has a limited solubility in the probe liquid, which is the case for hydrocarbons. The result, at the limit of infinite dilution of the probe in water, is then

$$\frac{\Delta_L^W G_\varphi}{RT} = \ln K_\varphi = -\ln[\varphi_1^W(\text{sat})]$$

$$= \left[1 - \frac{\bar{V}_1^W(\infty)}{\bar{V}_W}\right] + \chi_1^W \quad (19)$$

where $\varphi_1^W(\text{sat})$ is the saturation limit of the probe in water expressed in volume fraction. In terms of non-combinatorial quantities, the standard free energy of transferring the probe from its own liquid to water can thus be obtained from solubility measurements, *viz.*,

$$\frac{\Delta_L^W G'_\varphi}{RT} = -\ln[\varphi_1^W(\text{sat})] - \left(1 - \frac{\bar{V}_1^W(\infty)}{\bar{V}_W}\right)$$

$$= \chi_1^W \quad (20)$$

As most solubility measurements in the literature are given in mole fractions, we convert eqns. 19 and 20 to

$$-\ln x_1(\text{sat}) = \frac{\Delta_L^W G_\varphi}{RT} + \ln\left[\frac{\bar{V}_1^W(\infty)}{\bar{V}_W}\right] + 1 \quad (21a)$$

$$-\ln x_1(\text{sat}) = \frac{\Delta_L^W G'_\varphi}{RT} + \ln\left[\frac{\bar{V}_1^W(\infty)}{\bar{V}_W}\right]$$

$$+ 1 - \frac{\bar{V}_1^W(\infty)}{\bar{V}_W} \quad (21b)$$

It is now possible to compare the solubility, in terms of $\ln[x_1(\text{sat})]$, and the results from the chromatographic experiments. Combining eqn. 17 or 18 with eqn. 19 or 20, respectively, we obtain

$$-\ln[x_1(\text{sat})] = \ln\left[\frac{\bar{V}_1^W(\infty)}{\bar{V}_W}\right] + \chi_1^P + 1$$

$$+ \ln\left(\frac{V^R - V^{MK}}{V^P}\right) + \ln\left[\frac{\bar{V}_1^P(\infty)}{\bar{V}_1^W(\infty)}\right]$$

$$+ \frac{P-1}{RT}(\bar{V}_1^W(\infty) - \bar{V}_1^P(\infty)] \quad (22)$$

Note that eqn. 22 is independent of the route, *i.e.*, through ${}^W_L G_\varphi$ or ${}^W_L G'_\varphi$.

RESULTS AND DISCUSSION

Primary data

Table I shows the equilibrium partition coefficient, K_c, and the calculated non-combinatorial free energy at the experimental temperatures. For each probe, the $\Delta_L^W G'_\varphi$ data were plotted against temperature and fitted to a third-degree polynomial. The $T\Delta_L^W S'_\varphi$ data were obtained

TABLE I

PARTITION COEFFICIENT AND NON-COMBINATORIAL FREE ENERGY OF TRANSFER OF THE PROBE FROM THE PURE LIQUID TO WATER AT THE EXPERIMENTAL TEMPERATURES

Benzene			Toluene			Ethylbenzene			Propylbenzene		
T (°C)	K_c	$\Delta G'_\varphi$ (kJ/mol)	T (°C)	K_c	$\Delta G'_\varphi$ (kJ/mol)	T (°C)	K_c	$\Delta G'_\varphi$ (kJ/mol)	T (°C)	K_c	$\Delta G'_\varphi$ (kJ/mol)
0.1	89.4	22.2	2.6	297.4	27.2	2.6	911.6	31.6	1.6	3017.4	36.1
4.9	92.6	22.7	3.8	302.6	27.3	3.6	931.4	31.8	5.1	3153.0	36.7
10.0	95.0	23.2	5.5	307.2	27.5	5.5	934.3	32.0	10.1	3204.4	37.5
20.0	98.0	24.1	9.3	324.8	28.1	9.3	939.9	32.5	15.2	3331.1	38.3
25.0	97.8	24.5	9.8	311.8	28.0	9.8	949.1	32.5	20.1	3206.6	38.9
30.0	96.6	25.0	15.2	322.3	28.7	15.3	949.7	33.2	24.8	3185.0	39.5
39.3	92.9	25.6	20.1	307.2	29.1	20.1	927.8	33.7	29.9	3231.5	40.2
50.1	87.0	26.4	26.2	300.8	29.6	26.2	904.3	34.4	39.9	3056.8	41.5
60.3	80.3	27.1	35.0	285.6	30.4	35.0	850.8	35.3	50.0	2636.9	42.5
69.8	72.1	27.5	45.2	268.0	31.3	45.0	784.2	36.3	60.4	2295.6	43.5
80.1	64.4	28.1	55.0	244.6	32.0	55.0	708.5	37.2	70.2	1918.5	44.3
89.4	56.6	28.4	65.0	215.8	32.7	65.0	610.3	37.9	80.1	1570.6	45.0
			75.0	201.2	33.5	75.0	567.5	38.9	89.8	1373.9	45.9
			85.0	168.9	34.0	85.0	459.6	39.4			

from $\partial(\Delta_L^W G'_\varphi)/\partial T$ and $\Delta_L^W H'_\varphi$ was found using the fundamental equation $\Delta_L^W G'_\varphi = \Delta_L^W H'_\varphi - T\Delta_L^W S'_\varphi$. Finally, the heat capacity, $\Delta_L^W C'_{p_\varphi}$ ($=\partial\Delta_L^W H'_\varphi/\partial T$), was also calculated. The results are given in Table II for the experimental range 0–80°C; the values listed were calculated at convenient temperature intervals.

Importance of terms

It is of interest to investigate the different contributions to $\Delta_L^W G'_\varphi$ in eqn. 18. Table III shows the magnitude and sign, at 25°C, of each term, and its estimated error, as it appears on the right-hand side of eqn. 18.

The first term is equal to $RT \ln K_c$ according to eqn. 3 and varies between *ca.* 11 and 20 kJ/mol on going from benzene to propylbenzene. This term consists of the primary chromatographic data whereas all other terms were calculated from data collected from literature.

The second term, *i.e.*, $RT \ln [\bar{V}_1^W(\infty)/\bar{V}_W]$ was found to vary from 12 to 20 kJ/mol on going from benzene to propylbenzene. This is a substantial quantity and is of the same sign and size as the first term, involving the partition coefficient. Hence we conclude that $\Delta_L^W G_\varphi$ from eqn. 8, as opposed to the interactional free energy, $\Delta_L^W G'_\varphi$ from eqn. 10, *i.e.*, the free energy that is corrected for the combinatorial contribution, represents only about half of the interactional free energy. It is therefore essential to analyse the data in such a way as to take account of the combinatorial contributions arising from the size difference of the molecules if one wants the interactional, or non-combinatorial, contribution to the free energy of transfer. The $\bar{V}_1^W(\infty)/\bar{V}_W$ ratio was calculated in the following manner. First, the $\bar{V}_1^W(\infty)$ values were taken from Makhatadze and Privalov [13] for benzene and toluene in the temperature range 5–80°C. Second, the ratio $\bar{V}_1^W(\infty)/\bar{V}_1$ was calculated and found to be constant and equal to 0.913 for both benzene and toluene over the entire experimental temperature range. We therefore assume that this ratio has the same value also for ethylbenzene and propylbenzene. This factor was then multiplied by $\bar{V}_1/\bar{V}_W$ for which data are available from density measurements in the literature.

The third term in Table III, containing the χ_1^P parameter, is the non-combinatorial part of the free energy of transfer of the probe from its pure liquid to PDMS, and has previously been de-

TABLE II

NON-COMBINATORIAL THERMODYNAMIC QUANTITIES, $\Delta_L^W X'_\varphi$, FOR THE PURE PROBE LIQUID (L) TO WATER (W) TRANSFER, OBTAINED BY APPLYING FLORY–HUGGINS EXPRESSIONS ON EXPERIMENTAL HPLC DATA, *I.E.*, WITH THE USE OF EQN. 18, AND THE CONVENTIONAL THERMODYNAMIC QUANTITIES, $\Delta_L^W X_x$, OBTAINED FROM EQNS. 23 AND 24

Compound	Temperature (°C)	$\Delta G'_\varphi$ (kJ/mol)	$T\Delta S'_\varphi$ (kJ/mol)	$\Delta H'_\varphi$ (kJ/mol)	$\Delta C'_{p\varphi}$ (kJ/mol)	ΔG_x (kJ/mol)	$T\Delta S_x$ (kJ/mol)
Benzene	0	22.2	−28.9	−6.7	243	17.8	−22.0
	5	22.7	−28.2	−5.5	243	18.2	−21.2
	10	23.2	−27.5	−4.3	243	18.6	−20.3
	15	23.6	−26.7	−3.1	243	18.9	−19.5
	20	24.1	−26.0	−1.9	243	19.2	−18.6
	25	24.5	−25.2	−0.7	242	19.6	−17.7
	30	24.9	−24.4	0.5	241	19.8	−16.8
	40	25.7	−22.8	2.9	239	20.4	−14.9
	50	26.4	−21.1	5.3	237	20.8	−13.1
	60	27.0	−19.3	7.7	234	21.2	−11.2
	70	27.6	−17.6	10.0	230	21.5	−9.3
	80	28.0	−15.8	12.3	225	21.7	−7.4
Toluene	0	26.9	−32.4	−5.5	299	21.0	−23.7
	5	27.5	−31.5	−4.0	292	21.4	−22.6
	10	28.0	−30.6	−2.6	283	21.8	−21.6
	15	28.6	−29.8	−1.2	274	22.2	−20.6
	20	29.1	−28.9	0.1	265	22.5	−19.7
	25	29.5	−28.1	1.4	255	22.8	−18.7
	30	30.0	−27.3	2.7	245	23.1	−17.8
	40	30.9	−25.8	5.0	223	23.7	−16.1
	50	31.7	−24.5	7.1	199	24.2	−14.5
	60	32.4	−23.4	9.0	174	24.6	−13.1
	70	33.1	−22.5	10.6	146	25.0	−12.0
	80	33.7	−21.8	11.9	116	25.3	−11.1
Ethylbenzene	0	31.3	−36.3	−5.0	275	26.8	−33.7
	5	31.9	−35.5	−3.6	273	27.4	−32.0
	10	32.5	−34.8	−2.3	271	27.9	−30.4
	15	33.1	−34.1	−0.9	268	28.4	−28.8
	20	33.7	−33.3	0.4	266	28.9	−27.2
	25	34.3	−32.6	1.7	263	29.4	−25.6
	30	34.8	−31.8	3.0	260	29.8	−24.1
	40	35.8	−30.2	5.6	253	30.5	−21.2
	50	36.7	−28.7	8.1	245	31.1	−18.5
	60	37.6	−27.1	10.5	236	31.7	−16.0
	70	38.4	−25.6	12.8	226	32.1	−13.8
	80	39.1	−24.1	15.0	215	32.5	−11.9
Propylbenzene	0	35.8	−46.3	−10.5	463	23.8	−25.4
	5	36.6	−44.9	−8.2	453	24.3	−24.6
	10	37.4	−43.4	−6.0	443	24.7	−23.8
	15	38.2	−42.0	−3.8	432	25.1	−22.9
	20	38.9	−40.5	−1.7	420	25.5	−22.1
	25	39.6	−39.1	0.4	408	25.9	−21.2
	30	40.2	−37.8	2.4	395	26.2	−20.3
	40	41.4	−35.1	6.2	367	26.9	−18.6
	50	42.5	−32.7	9.8	337	27.4	−16.8
	60	43.4	−30.4	13.0	304	27.9	−15.0
	70	44.3	−28.5	15.8	268	28.3	−13.2
	80	45.1	−26.8	18.3	230	28.7	−11.5

TABLE III

COMPARISON OF THE MAGNITUDE AND SIGN OF THE TERMS, AT 25°C, CONTRIBUTING TO $\Delta_L^W G'_\varphi$ IN EQN. 18

All values in kJ/mol.

Compound	$RT \ln \frac{V^R - V^{MK}}{V^P}$ (±0.14)	$RT\left[\frac{\bar{V}_1^W(\infty)}{\bar{V}_W}\right]$ (±0.02)	$RT\chi_1^P$ (±0.02)	$RT \ln \frac{\bar{V}_1^P(\infty)}{\bar{V}_1^W(\infty)}$ (±0.003)	$(P-1)[\bar{V}_1^W(\infty) - \bar{V}_1^P(\infty)]$ (±0.003)
Benzene	11.44	11.19	1.90	0.090	−0.065
Toluene	14.28	13.36	1.90	0.090	−0.065
Ethylbenzene	16.99	15.38	1.90	0.090	−0.065
Propylbenzene	20.13	17.53	1.90	0.090	−0.065

termined [5,14] for benzene, toluene and ethylbenzene at two temperatures, 25 and 55°C. Although χ_1^P might be expected to increase with molecular size, it showed no discernible size dependence in this selection of probe sizes. Analysis of published data shows that $\chi = 1.9/RT$. Within the Flory–Huggins theory for polymer solutions based on a lattice model, $\chi = z\,\Delta w/kT$, where z is the coordination number and Δw is the molecular contact interaction energy. Thus, z and Δw were found to be approximately independent of temperature and probe size for all the probes in this study. Thereby the correction term, $RT\chi$, amounts to 1.90 kJ/mol, which is only *ca.* 2% of the free energy of transfer in eqn. 18. This is an important finding since the HPLC set-up, with the PDMS polymer coating, for the transfer from pure probe liquid to water is as such a good approximation even without taking into account the contribution from the transfer of the probe from its own liquid to PDMS. This is probably a consequence of the very hydrophobic properties of PDMS, such that the interaction between the probe molecules and the polymer is primarily due to dispersion interactions which are small and relatively independent of temperature in comparison with the probe–water interaction.

Compared with the first three terms, the last two terms are minor and serve only as very small correction terms. As for the fourth term, the ratio of $\bar{V}_1^W(\infty)$, from ref. 13, and $\bar{V}_1^P(\infty)$, determined using the Prigogine–Flory theory for non-polar polymer solutions in ref. 15, was found to be constant, independent of probe (benzene and toluene) or temperature, and equal to 1.037. This value differs from that previously published by us [8], 1.13, which was found to be in error. The ratio was, however, still found to be constant for these two probes and were also used for ethylbenzene and propylbenzene. The correction term, $RT \ln [\bar{V}_1^P(\infty)/\bar{V}_1^W(\infty)]$ amounts to 0.090 kJ/mol, which is only *ca.* 0.4% of the free energy of transfer defined in eqn. 18.

We find that the last term in Table III, the pressure contribution at our HPLC operating conditions of *ca.* 50 atm and with the standard pressure $P^* = 1$ atm, amounts to *ca.* −0.065 kJ/mol. Hence this contribution to the free energy of transfer is very small, as predicted by Locke and co-workers [4,12], and amounts to *ca.* 0.3% of the total free energy of transfer. We note that the last two terms almost completely cancel and that the net difference is of the same order of magnitude (or less) as the error in the total free energy of transfer. The last two terms were therefore ignored in the calculation of the non-combinatorial thermodynamic transfer functions, shown in Table II and in the calculation of solubilities (see below).

Thermodynamic transfer functions

Fig. 2 shows the Van 't Hoff plot for the benzene data, *i.e.*, where ln K_c is plotted as a function of the inverse of temperature. First we note that the function has a pronounced maxi-

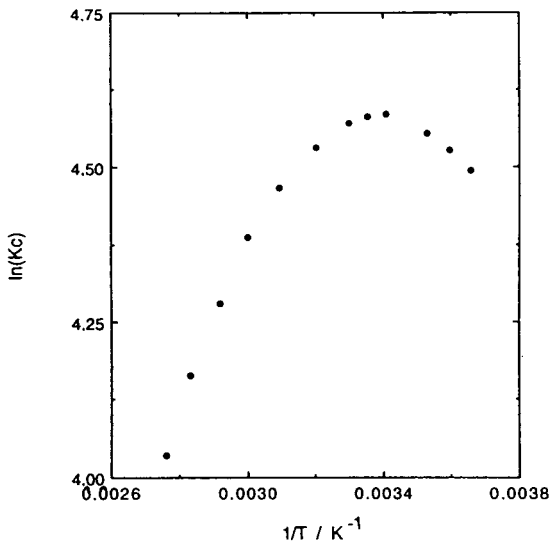

Fig. 2. Van 't Hoff plot for the partition coefficient, K_c, as obtained from the chromatographic retention of benzene.

mum corresponding to a point where the enthalpy of transfer is zero and where the solubility of the probe in water is at a minimum. We also note that the slope is not constant at any temperature, in contrast to what is normally found is reversed-phase systems with hydrocarbon-bonded silica as the stationary phase and water with organic modifier as the mobile phase. The unusual temperature behaviour in Fig. 2 has previously been successfully analysed in terms of a solute-induced solvent interaction, often described as water structuring, around the hydrophobic solute surface [8,16]. Hence we conclude that the difference in our results from those normally obtained with reversed-phase chromatography is that (i) the commonly used organic modifier affects the water in such a way that it does not structure on coming into contact with a hydrophobic surface and/or (ii) the hydrocarbon-bonded silica may not be a good reference in the sense that it may not act as a hydrophobic reference liquid for the transfer of the probe (solute) molecules [17]. We would also like to comment on the general consensus that a linear Van 't Hoff plot indicates an invariant separation mechanism [18,19]. Analysis of the curve in Fig. 2 for the four probes shows that in order to understand, or predict the behaviour in the figure only one mechanism need be assumed for the whole temperature range [8,16], despite the fact that $\Delta_L^W H'_\varphi$, *i.e.*, the slope of the plot, is not constant with temperature (see Fig. 3).

We return to Table II in order to discuss the thermodynamic quantities of the probe transfer from the pure probe liquid to water. Table II reveals that the free energy of transfer is large and positive and increases only slightly with temperature, whereas the enthalpy and entropy of transfer are both negative at low temperature and more strongly temperature dependent, increasing with temperature. The enthalpy of transfer crosses zero at about room temperature, having positive values at higher temperatures. The heat capacity is typical of aqueous solutions of non-polar molecules, *i.e.*, abnormally large and positive and decreasing with temperature [13].

Analysis of the results over small temperature intervals around room temperature is misleading, since this is where the $\Delta_L^W H'_\varphi$ is around zero. This observation forms the basis for the common misinterpretation that the hydrophobic effect is entropy driven. It can be seen from Table III that the enthalpy is in fact strongly temperature dependent and gives a large contribution to the free energy at temperatures other than around room temperature. An analysis of the results in Table III has been published previously [8] and an in-depth analysis of the hydrophobic effect will be presented elsewhere [16]. Further, we note that the data given in Table III shows an enthalpy–entropy compensation, a fact that is closely related with the creation, or destruction, of order in a system [8,20].

The values of the enthalpy and the temperature dependence, listed in Table III, compare very well with literature values [21] at 25°C, as shown in Fig. 3. The data in Fig. 3 afford an accurate estimate of the magnitude and temperature dependence of the heat of transfer. Further, the heat capacity of transfer at 25°C also compares reasonably well with literature values [13,21]: 244 *vs.* 238 or 225 ± 5 J/mol K for benzene, 256 *vs.* 305 or 236 ± 13 J/mol K for toluene, 262 *vs.* 318 ± 13 J/mol K for ethylbenzene and 413 *vs.* 391 ± 25 J/mol K for propylbenzene. The closeness in magnitude of the heat capacity data

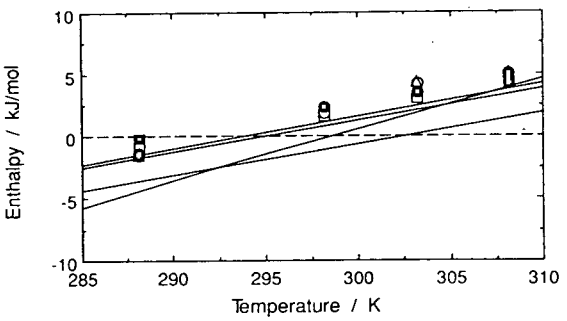

Fig. 3. Enthalpy for the transfer of probe molecules from the pure liquid to water, symbols as in Fig. 4, together with literature data from ref. 21.

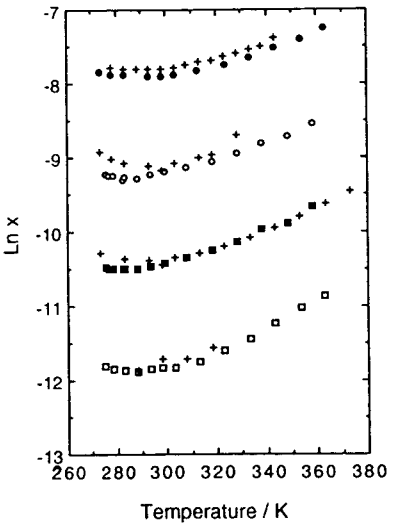

Fig. 4. Calculated values of the solubilities according to eqn. 22 as a function of the temperature. ● = Benzene; ○ = toluene; ■ = ethylbenzene; □ = propylbenzene; + = Literature data from ref. 22.

is remarkable considering that it is a second derivative with respect to temperature of the free energy, which has a rather low curvature. Hence the data clearly show that liquid–liquid chromatography is indeed a very powerful method for obtaining thermodynamic data for non-polar molecules in water. We note that the values for toluene and ethylbenzene in Table II differ from those previously published [8] for two reasons. The first is that in the previous paper we published $\Delta_L^W G_\varphi$ and not $\Delta_L^W G'_\varphi$ values as are shown here; the second is that this work involved a much more reliable analysis of the absolute amount of PDMS deposited on the column glass beads.

Solubilities

As seen in eqn. 22, it is possible to use the chromatographic data to calculate the solubilities of the probe molecules in water, or in any other suitable mobile phase. This is very interesting especially for strongly hydrophobic molecules where accurate and direct determinations are experimentally difficult owing to their extremely low solubility. Fig. 4 displays the calculated solubility, using eqn. 22, for the benzene to propylbenzene series together with literature values [22] as a function of temperature. It is apparent from Fig. 4 that the liquid–liquid chromatographic method accurately predicts both the absolute solubility and its temperature dependence for hydrocarbons in water.

We also note that in predicting the solubilities it is essential to report on what correction terms are taken into account. For example, omitting the χ_1^P term, *i.e.*, only studying the transfer from the stationary polymer phase to water instead of the transfer from pure probe liquid to water, will shift the predicted solubility curves by *ca.* 0.8 units, but the temperature dependence will not be altered. Such a shift would be dramatic if the solubilities are compared on a linear, instead of a logarithmic, scale.

We also emphasize the importance of choosing a realistic model in order to obtain the interactional free energy of transfer from solubility measurements. Unfortunately, the most common way to obtain $\Delta_L^W G$ from solubility measurements is through the equation

$$\Delta_L^W G_x = -RT \ln x_1(\text{sat}) \tag{23}$$

Using eqn. 23 implies the adoption of the regular solution model, *i.e.*, a model where it is assumed that the solute and solvent molecular sizes are the same. The entropy is further obtained from

$$\Delta_L^W S_x = \frac{\Delta_L^W H - \Delta_L^W G_x}{T} = \frac{\Delta_L^W H + RT \ln x_1(\text{sat})}{T} \tag{24}$$

We calculated $\Delta_L^W G_x$ from the following equation:

$$\frac{\Delta_L^W G_x}{RT} = \frac{\Delta_L^W G'_\varphi}{RT} + \ln\left[\frac{\bar{V}_1^W(\infty)}{\bar{V}_W}\right] + 1 - \frac{\bar{V}_1^W(\infty)}{\bar{V}_W} \quad (25)$$

which is obtained from eqns. 23 and 21b. The entropy of transfer was obtained from the first derivative of $\Delta_L^W G_x$ with respect to temperature. Values of $\Delta_L^W G_x$ and $\Delta_L^W S_x$ thus obtained are also given in Table III. We note that $\Delta_L^W S_x$ is larger than $\Delta_L^W S'_\varphi$. Further, plots of $\Delta_L^W S_x$ *versus* temperature reveal that $\Delta_L^W S_x$ is zero at temperatures around 130–160°C and becomes positive at higher temperatures. This temperature, T_s, where $\Delta_L^W S_x$ is zero, has been used in the analysis of the hydrophobic effect [23]. Such treatments should be used with caution as they are based on the assumption of equal-sized molecules and, hence, $\Delta_L^W S_x$ necessarily contains both intermolecular information and contributions from the combinatorial entropy of mixing [24]. We therefore strongly advocate the use of eqn. 20 instead of eqn. 23 in order to obtain meaningful thermodynamic information.

CONCLUSIONS

The agreement with literature data, in Fig. 4, shows that the primary retention data are of excellent quality. Liquid–liquid chromatography is indeed a method worth further exploiting in order to obtain high-quality thermodynamic and solubility data. Not only is the experimental set-up composed of readily available and relatively inexpensive equipment, it is also extremely flexible. The experimental parameters, temperature, mobile phase, stationary phase and probe molecules, can all be easily and quickly altered, affording a wide range of potential applications. This has been demonstrated using formamide as the mobile phase [25]. The success of this particular HPLC set-up lies in the balance between having a small enough thickness of the deposited polymer layer, such that it maintains equilibrium conditions, and large enough so as to ensure a liquid behaviour of the polymer, and in the use of a non-porous support material so that the effect of probe adsorption is negligible.

The availability of a phase ratio, as a result of an independent and exact determination of the volume of polymer in the column, is the cornerstone of the method. It is through the phase ratio, which appears in the equilibrium partition coefficient, that we are able easily to calculate absolute values for the probe transfer free energy, entropy and enthalpy and the solubility in water.

Finally, we emphasize the use of non-combinatorial quantities in $\Delta_L^W G'_\varphi$ and $\Delta_L^W S'_\varphi$ instead of the commonly accepted $\Delta_L^W G_x$ and $\Delta_L^W S_x$ quantities. This treatment gives meaningful interactional parts of the free energy that can be used in further analysis of the hydrophobic effect [16].

SYMBOLS

1	Probe
a_1^i	Activity of the probe in solvent phase i
$[1]^i$	Molar concentration of the probe in solvent i
A^P	Interfacial area of the polymer stationary phase
i	Solvent phase
K_c	Equilibrium partition coefficient on a molar concentration basis
K_φ	Equilibrium partition coefficient on a volume fraction basis
K_{ads}	Adsorption partition coefficient
k'	Capacity factor
MK	Unretained marker for the column dead volume
n_1^i	Moles of probe in solvent phase i
P	Polymer (PDMS) stationary phase
P	Pressure
P^*	Standard pressure = 1 atm
R	Retained probe
V^i	Volume of the solvent phase
$\bar{V}_1$, $\bar{V}_i$	Molar volume of the probe and solvent phase, respectively
$\bar{V}_1^i$	Partial molar volume of probe in solvent phase i
$\bar{V}_1^i(\infty)$	Partial molar volume of the probe at infinite dilution in phase i
W	Water mobile phase

χ_1^i Flory–Huggins interaction parameter of the probe in solvent phase i

$\Delta_P^W X$ Transfer quantity, where $X = G$ = free energy, H = enthalpy, S = entropy, C_p = heat capacity at constant pressure

$\Delta_P^W X'_\varphi$ Flory–Huggins non-combinatorial transfer quantities, where X is as above

$\Delta_P^W X_x$ Regular solution, mole fraction quantities, where X is as above

φ_1^i Volume fraction of the probe in solvent phase i

γ_1^i Activity coefficient of the probe in solvent phase i

ϕ Phase ratio

μ_1^i Chemical potential of the probe in solvent phase i

μ_1^0 Chemical potential of the pure probe

$x_1(\text{sat})$ Solubility limit of the probe, expressed in mole fraction

REFERENCES

1 D.C. Locke, *Adv. Chromatogr.*, 14 (1976) 87.
2 Cs. Horváth and W.R. Melander, in E. Heftmann (Editor), *Chromatography: Fundamentals and Applications of Chromatographic and Electrophoretic Methods*, Part A, Elsevier, Amsterdam, 1983, Ch. 3, p. A27.
3 P. Alessi, *Cron. Chim.*, 62 (1980) 3.
4 D.C. Locke, *Adv. Chromatogr.*, 8 (1969) 47.
5 D.R. Lloyd, T.C. Ward, H.P. Schreiber and C.C. Tizana, *Inverse Gas Chromatography—Characterization of Polymers and Other Materials* (*ACS Symposium Series*, No. 391), American Chemical Society, Washington, DC, 1989.
6 W.R. Summers, Y.B. Tewari and H.P. Schreiber, *Macromolecules*, 5 (1972) 12.
7 F. Franks, in F. Franks (Editor), *Water—A Comprehensive Treatise*, Vol. 4, Plenum Press, New York, 1975, p. 6.
8 R. Silveston and B. Kronberg, *J. Phys. Chem.*, 93 (1989) 6241.
9 J.Å. Jönsson, *Chromatographic Theory and Basic Principles*, Marcel Dekker, New York, 1987, p. 6.
10 D. Patterson, Y.B. Tewari, H.P. Schreiber and J.E. Guillet, *Macromolecules*, 4 (1971) 356.
11 L.R. DeYoung and K.A. Dill, *J. Phys. Chem.*, 94 (1990) 801.
12 D.C. Locke and D.E. Martire, *Anal. Chem.*, 39 (1967) 921.
13 G.I. Makhatadze and P.L. Privalov, *J. Chem. Thermodyn.*, 20 (1988) 405.
14 M. Galin, *Macromolecules*, 10 (1977) 1239.
15 R.S. Chahal, W.P. Kao and D. Patterson, *J. Chem. Soc., Faraday Trans. 1*, 69 (1973) 1834.
16 M. Costas, B. Kronberg and R. Silveston, submitted for publication.
17 K.A. Dill, *J. Phys. Chem.*, 91 (1987) 1980.
18 W. Melander, D.E. Campbell and Cs. Horváth, *J. Chromatogr.*, 158 (1978) 215.
19 R.J. Laub and S.J. Madden, *J. Liq. Chromatogr.*, 8 (1985) 187.
20 D. Patterson and M. Barbe, *J. Phys. Chem.*, 80 (1976) 2345.
21 S.J. Gill, N.F. Nichols and I. Wadsö, *J. Chem. Thermodyn.*, 8 (1976) 445.
22 D.G. Shaw (Editor), *IUPAC Solubility Data Series*, Analytical Chemistry Division Commission on Solubility Data, Pergamon Press, Oxford, 1989, Vol. 37, pp. 63–183 and 369–442, and Vol. 38, pp. 59–89 and 201–210.
23 P.L. Privalov and S.J. Gill, *Adv. Protein Chem.*, 39 (1988) 191.
24 B. Kronberg, M. Costas and R. Silveston, in preparation.
25 M. Sjöberg, R. Silveston and B. Kronberg, *Langmuir*, 9 (1993) 973.

Journal of Chromatography A, 659 (1994) 57–68
Elsevier Science B.V., Amsterdam

CHROM. 25 598

Development of chiral stationary phases for the enantiomeric resolution of dihydrodiols of polycyclic aromatic hydrocarbons by π-donor–acceptor interactions

M. Funk, H. Frank, F. Oesch and K.L. Platt*

Institute of Toxicology, University of Mainz, Obere Zahlbacher Strasse 67, D-55131 Mainz (Germany)

(First received July 27th, 1993; revised manuscript received September 28th, 1993)

ABSTRACT

Chiral stationary phases (CSPs) derived from (*R*)-(−)-2-(2,4,5,7-tetranitrofluoren-9-ylideneaminooxy)propionic acid (TAPA) covalently bound to silica gel have been developed by altering the alkyl group at the chiral centre or the number of aromatic rings and their degree of nitration. The chromatographic properties of the CSPs were characterized by use of a racemic model solute. Depending on the solvent strength of the mobile phase, the CSPs exhibit the quality of a normal or a reversed phase. The chromatographic behaviour of 30 racemic hydroxylated derivatives of polycyclic aromatic hydrocarbons (PAHs) on (*R*)-(−)-TAPA CSP revealed the structural requirements for chiral recognition. The applicability of the CSPs for the enantiomeric separation of *trans*-dihydrodiols of PAHs on an analytical as well as preparative scale and for investigating the enantioselectivity of the biotransformation and genotoxicity of PAHs is demonstrated.

INTRODUCTION

The class of polycyclic aromatic hydrocarbons (PAHs) contains some of the most powerful chemical carcinogens [1]. PAHs have to be enzymatically transformed to biologically reactive metabolites in order to exert their carcinogenic properties [2]. The sequential attack of cytochrome P-450 dependent monooxygenase(s) and of microsomal epoxide hydrolase leads to the regio- and stereoselective formation of *trans*-dihydrodiols [3]. The positional isomers as well as the enantiomers of the *trans*-dihydrodiols of PAHs possess widely varying biological activities [4]. Studies concerned with this aspect of chemical carcinogenesis, therefore, require efficient separation methods for the isomers of *trans*-dihydrodiols. Reversed-phase high-performance liquid chromatography (HPLC) is unsurpassed for the separation of positional isomers of *trans*-dihydrodiols [5]. For their enantiomeric resolution *trans*-dihydrodiols are in most cases converted with a suitable chiral acid to diastereomeric esters, which can be separated by normal-phase HPLC; ester cleavage then yields the enantiomerically pure *trans*-dihydrodiols [6]. For a long time attempts have been made to replace this rather cumbersome technique by direct enantiomeric separation of *trans*-dihydrodiols via chiral stationary phases (CSPs) [7]. Recently CSPs on the basis of (*R*)-N-(3,5-dinitrobenzoyl)phenylglycine or -leucine bonded to γ-aminopropylsilanized silica have become commercially available and were successfully used for the chromatographic resolution of racemic dihydrodiols of phenanthrene [8], chrysene [8], benz[*a*]anthracene [8–11] and benzo[*a*]pyrene [11].

* Corresponding author.

0021-9673/94/$07.00
SSDI 0021-9673(93)E1035-X

Since we have been interested in the stereoselective biotransformation of dibenz[*a*,*h*]anthracene [12] and picene [13], we tried to apply the direct chromatographic separation on CSPs to the enantiomeric resolution of *trans*-dihydrodiols of these PAHs. Unfortunately, a wide variety of commercial CSPs employing donor–acceptor interactions as well as CSPs based on chiral polymers, γ-cyclodextrin or cellulose triacetate were not suited to solve our separation problem; this failure was later independently confirmed [14]. Therefore we developed CSPs starting with 2-(2,4,5,7-tetranitrofluoren-9-ylideneaminooxy)carboxylic acids covalently bound to silica gel [15]. These CSPs could successfully be applied for the enantiomeric resolution of 18 *trans*-dihydrodiols of pyrene, chrysene, benz[*a*]anthracene, dibenz[*a*,*h*]anthracene, dibenz[*a*,*j*]anthracene, picene, benzo[*a*]pyrene and benzo[*e*]pyrene.

EXPERIMENTAL

Chemicals

The majority of the racemic *trans*-dihydrodiols used in this study (*cf.* Fig. 1) was prepared by reduction of suitable *o*-quinones with sodium borohydride in the presence of oxygen, *e.g.* **5**, **7**, **12**, **17**, **24** and **25** [16], **1–4**, **6**, **15**, **22** and **23** [17], **8** and **10** [18], **11**, **13** and **14** [19], **9**, **19** and **20** [20], **22c** and **22d** [21], **18** [22], **21** [23]. The syntheses of **16** [24] as well as of **7a**, **22a** and **22b** [25] were performed as described in the literature.

(−)-(1*R*,2*S*)-Ephedrine was purchased from Janssen Chimica (Brüggen, Germany). Fluoren-9-one, 2-nitro-, 2,7-dinitro-, 2,4,7-trinitro- and 2,4,5,7-tetranitrofluoren-9-one were obtained from Aldrich (Steinheim, Germany).

(*R*) - (−) - Isopropylideneaminooxypropionic acid (R_1 = methyl, Fig. 2) and its enantiomerical-

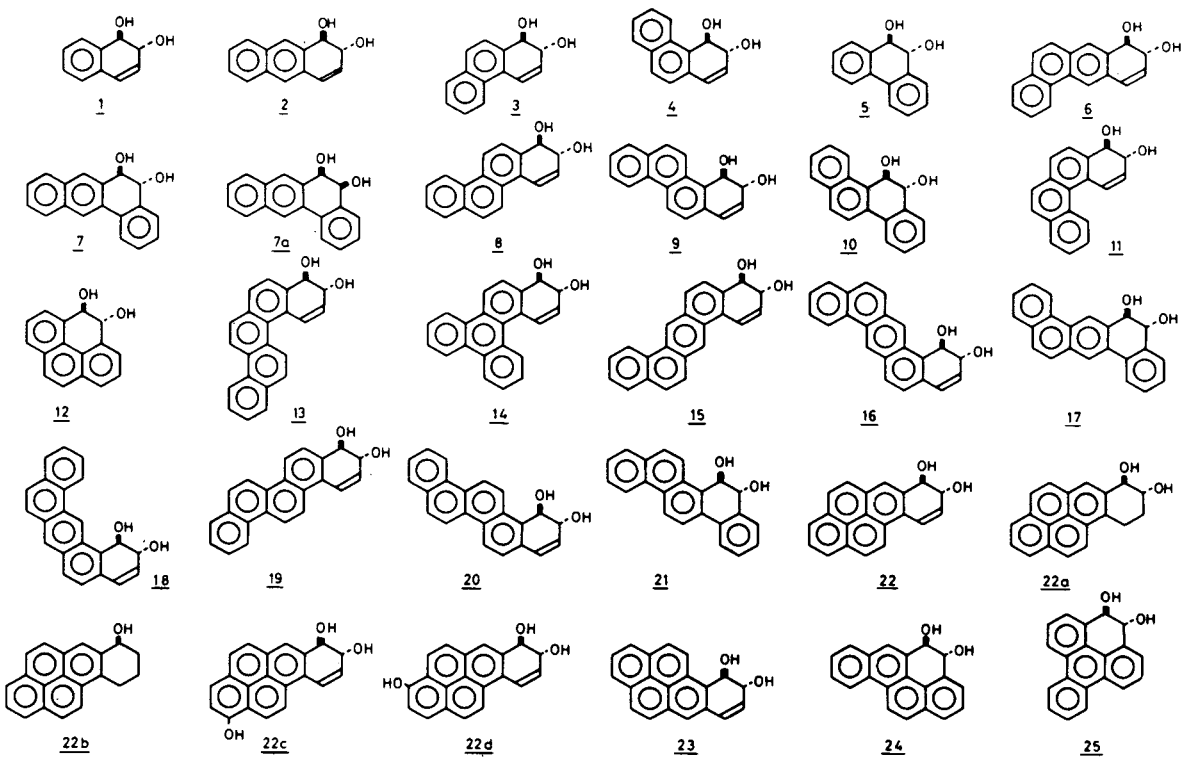

Fig. 1. Structure of dihydrodiols and related derivatives of polycyclic aromatic hydrocarbons (in the case of the *trans*-dihydrodiols only the enantiomer with *R*,*R* absolute configuration is shown in a position where the benzylic hydroxyl group points upward).

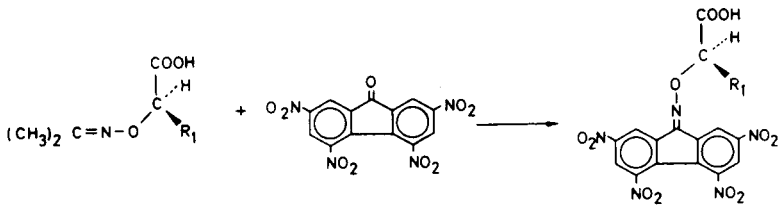

Fig. 2. Synthesis of chiral ligands by transoximation of (+)-2-isopropylideneaminooxy carboxylic acids with nitrated fluorenones.

ly pure homologues with R_1 = ethyl, propyl, isopropyl and butyl were synthesized analogously to Block and Newman [26] and characterized by elemental analysis, electron impact mass spectrometry (EI-MS), NMR, melting point (m.p.) determination and polarimetry (data not shown).

2,6,8 - Trinitro - 4*H* - cyclopenta[*def*]phenanthren - 4 - one (precursor for CSP 6) was prepared as described by Minabe *et al.* [27]. 1,3,5,8 - Tetranitro - 10*H* - benzo[*b*]fluoren - 10 - one (precursor for CSP 7) and 2,5,9,11 - tetranitro - 7*H*-benzo[*c*]fluoren - 7 - one (precursor for CSP 8) were obtained according to Ishikawa and Masubuchi [28] by nitration of 10*H*-benzo[*b*]-fluoren-10-one [29] and 7*H*-benzo[*c*]fluoren-7-one [30]. Purity and structural identity of the nitrofluorenones were confirmed by elemental analysis, EI-MS, NMR and m.p. determination (data not shown).

Methanol and dichloromethane for HPLC were supplied by Baker (Gross-Gerau, Germany), all other chemicals of analytical grade were from different commercial sources.

Preparation of CSPs

The synthesis of the chiral ligands was carried out according to Block and Newman [26]. A 14-mmol amount of the (+)-2-isopropylideneaminooxy carboxylic acid and 9 mmol of the corresponding fluorenone were dissolved in 30 ml glacial acetic acid and 0.12 ml concentrated sulphuric acid and heated under reflux for 2 h. Recrystallization from water–glacial acetic acid yielded pale yellow crystals, which were characterized by elemental analysis, EI-MS, NMR (data not shown), m.p. determination and polarimetry (Table I).

The coupling of the chiral ligands to LiChrosorb Si 100 (Merck, Darmstadt, Germany) was carried out by modifying the method described by Mikes *et al.* [15]. In a first step 8.34 mmol 3-aminopropyltriethoxysilane, 8.34 mmol of the chiral fluorenylideneaminooxy carboxylic acid and 9.16 mmol N,N′-dicyclohexylcarbodiimide were stirred at room temperature in 240 ml chloroform for 20 h. After filtration of the solution for separating the dicyclohexylurea and removing the solvent under reduced pressure the residue was dissolved in a suspension of 6.4 g LiChrosorb Si 100 (5 μm) in 100 ml *p*-xylene. The mixture was kept under an argon atmosphere and heated to 120°C for 8 h without stirring. After cooling to room temperature the modified silica was filtered through a glass diaphragm (porosity D5) and washed with 800 ml chloroform, acetone and methanol, respectively, with yields averaging 8 g of CSP. The CSPs were characterized by elemental analysis, which was used for calculating the amount of bound ligand (Table I).

Stainless-steel columns (250 × 4 mm) were filled with the CSPs by application of the balanced-density slurry packing method [31] by Knauer (Berlin, Germany). When the CSP columns were stored at room temperature with methanol and/or dichloromethane, their chromatographic performance deteriorated considerably within several months, probably due to partial cleavage of the covalent linkage of the chiral ligand to silica. Yet storage of the CSP columns at 4°C with *n*-hexane as eluent improved their stability considerably; these columns have retained their chromatographic properties for several years now.

Chromatographic conditions

For liquid chromatography a modular chromatographic system was used consisting of a

TABLE I

CHARACTERIZATION OF CHIRAL LIGANDS AND CSPs DERIVED THEREOF

All chiral ligands possess (*R*) absolute configuration.

Chiral ligand leading to CSP	Formula	Elemental analysis (%)			m/z^a (M^+ – COOH)	Melting point (°C)[b]	Specific rotation[c,d] $[\alpha]_D^{20}$	Elemental analysis (%) of the CSPs			Bound chiral ligand (mmol/g)
		C calc./ found	H calc./ found	N calc./ found				C	H	N	
1	$C_{16}H_{13}NO_3$	71.90/72.06	4.90/4.89	5.24/5.27	222 (32)	165–166	– 41.1	12.53	1.84	2.38	0.41
2	$C_{16}H_{12}N_2O_5$	61.54/61.55	3.87/3.76	8.97/8.90	267 (41)	210–211	– 52.1	12.05	1.68	2.48	0.56
3	$C_{16}H_{11}N_3O_7$	53.79/53.34	3.10/2.97	11.76/11.62	312 (19)	234–235	– 50.0	12.91	1.70	3.00	0.55
4	$C_{16}H_{10}N_4O_9$	47.77/47.73	2.51/2.47	13.92/13.83	357 (45)	200–202	– 81.4	11.55	1.93	2.92	0.46
5	$C_{16}H_9N_5O_{11}$	42.97/42.17	2.03/2.18	15.66/15.20	402 (27)	189–191 (200–201)	– 100.2 (– 90)	9.80	1.48	3.13	0.40
5a	$C_{17}H_{11}N_5O_{11}$	44.26/44.18	2.40/2.59	15.18/14.84	416 (73)	172–173 (184–185)	– 79.4 (– 88)	9.36	1.49	2.90	0.37
5b	$C_{18}H_{13}N_5O_{11}$	45.48/45.49	2.76/2.95	14.73/14.52	430 (100)	168–169	– 85.0	12.05	1.84	3.40	0.44
5c	$C_{18}H_{13}N_5O_{11}$	45.48/45.39	2.76/2.88	14.73/14.63	430 (100)	215–217 (200–202)	– 129.7 (– 103)	13.10	2.13	3.45	0.46
5d	$C_{19}H_{15}N_5O_{11}$	46.63/46.21	3.09/2.99	14.31/14.03	444 (100)	183–185 (207–209)	– 69.9 (– 22)	12.64	1.89	3.67	0.46
6	$C_{18}H_{10}N_4O_9$	50.72/49.90	2.36/2.74	13.14/12.58	380 (24)	207–209	– 75.5	12.71	1.68	2.90	0.45
7	$C_{20}H_{11}N_5O_{11}$	48.30/47.48	2.23/2.45	14.08/13.72	451[e] (13)	215–216	– 56.8	12.02	1.62	3.03	0.40
8	$C_{20}H_{11}N_5O_{11}$	48.30/48.11	2.23/2.54	14.08/13.50	451[e] (7)	230–232	– 94.3	12.41	1.64	2.93	0.40

[a] Given is *m/z* of a diagnostic fragment ion and its relative intensity (in parentheses).
[b] Melting points from the literature [15] are given in parentheses.
[c] Specific rotation values [°]; Concentration 1.5 mg/ml in chloroform.
[d] Specific rotation values measured at 633 nm [15] are given in parentheses.
[e] Fragment ion resulting from $M^+ - NO_2$.

solvent-delivery system SP 8700 (Spectra-Physics, Darmstadt, Germany), a sample injection valve (Model C6U, Valco, Schenkon, Switzerland) with a 25-μl sample loop, an UV detector (254 nm; Model D, LDC Analytical, Gelnhausen, Germany) and an integrator–plotter (Model CI-10, LDC Analytical). The mobile phase consisted of mixtures of dichloromethane and methanol. The standard operating conditions were a flow-rate of 0.8 ml/min and room temperature. The dead time t_0 was determined as the retention time of tetrachloromethane. The solutes were dissolved in dichloromethane, methanol or acetone depending on their solubility; 1–3 μg per 25 μl were injected onto the column.

RESULTS AND DISCUSSION

(*R*) - (−) - 2 - (2,4,5,7 - Tetranitrofluoren - 9 - ylideneaminooxy)propionic acid (TAPA) coupled to 3-aminopropyltriethoxysilane and then bonded to silica gel has first been used for the enantiomeric separation of *trans*-dihydrodiols of benz[*a*]anthracene and benzo[*a*]pyrene by Kim *et al.* in 1981 [7]. In order to explore scope and limitations of this type of chiral stationary phases for the separation of enantiomers, especially of dihydrodiols of PAHs, and to determine the electronic and structural parameters which govern this separation process, we developed stationary phases based on (*R*)-(−)-TAPA by altering (i) the π-electron density in the fluorenylidene moiety by the degree of nitration, (ii) the spatial requirement at the center of chirality by modifying the substituent R_1 (*cf.* Fig. 2), and (iii) the dimensions of the aromatic ring system (*cf.* Fig. 3; CSPs 6–8).

Preparation of chiral stationary phases

The CSPs 1–5, 5a–d, 6–8 used in this study (*cf.* Fig. 3) were prepared by covalent coupling of suitable chiral ligands to silica via an aminopropyl spacer.

For constructing the chiral ligand the oxime derivative bearing the chiral center and the nitrofluorenone were synthesized separately and coupled by transoximation as described by Block and Newman [26] (Fig. 2). The characteristic data of elemental analysis, m.p. determinations, mass spectra and specific rotation values are shown in Table I. In some cases differences as compared to data published earlier [15] have been encountered (Table I).

The covalent binding of the chiral ligand to silica was carried out via an aminopropyl spacer by modifying the method of Mikes *et al.* [15]. First the spacer was bound to the chiral ligand catalyzed by N,N′-dicyclohexylcarbodiimide. Then the resulting triethoxysilane amide was tempered with the silica to achieve covalent binding. The binding of the organic material to the silica was verified by elemental analysis (Table I). The amount of bound ligand was calculated to be in the range of 0.37 to 0.56 mmol/g modified silica, which compares well to other CSPs [32].

Reaction of residual silanol groups in CSP 5 with trimethylsilylimidazole yielded a CSP which did not exhibit a significant improvement of selectivity determined with the model solute **16** ($\alpha = 1.50$ in the case of CSP 5 *versus* $\alpha = 1.54$ in the case of "end-capped" CSP 5).

Influence of the structure of chiral stationary phases on the enantiomeric separation of a model solute

In order to characterize the interactions between solute and CSP leading to chiral recognition and thus to enantiomeric resolution, the capacity factor k' and the selectivity α of dibenz[*a*,*h*]anthracene (DBA) 1,2-diol **16** (*cf.* Fig. 1) on model CSPs based on TAPA (Fig. 2, R_1 = methyl) were determined (Table II). Dihydrodiol **16** was chosen as solute on the basis of its optimal enantiomeric separation by TAPA (CSP 5) thus being potentially a good indicator of alterations in the interaction between solute and CSP.

According to the chiral recognition model described by Pirkle and Pochapsky [33] one π-donor–acceptor interaction is required and additionally one stereochemically dependent interaction, in our case between the chiral center of the ligand and (at least) one of the hydroxyl groups of the dihydrodiol.

When the nitro groups in CSP 5 were stepwise

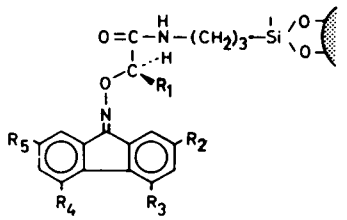

CSP	1	2	3	4	5	5a	5b	5c	5d
R_1	CH_3	CH_3	CH_3	CH_3	CH_3	C_2H_5	nC_3H_7	iC_3H_7	nC_4H_9
R_2	H	NO_2	NO_2	NO_2	NO_2	NO_2	NO_2	NO_2	NO_2
R_3	H	H	H	NO_2	NO_2	NO_2	NO_2	NO_2	NO_2
R_4	H	H	H	H	NO_2	NO_2	NO_2	NO_2	NO_2
R_5	H	H	NO_2	NO_2	NO_2	NO_2	NO_2	NO_2	NO_2

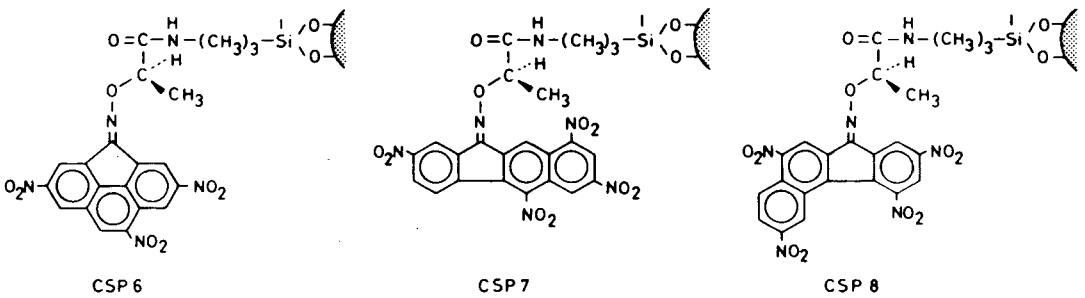

Fig. 3. Structures of chiral stationary phases (CSPs).

removed leading to CSP 4, 3, 2 and 1, the strength of the charge-transfer interaction weakened and consequently the capacity factors of **16** decreased; concomitantly the chiral discrimination deteriorated as indicated by the declining selectivity (Table II).

Variation of the alkyl group at the chiral center (R_1 in Fig. 3) demonstrates the influence of a weaker stereochemically dependent interaction, expressed as capacity factor, on the retention of **16**. CSP 5a is a good example of this effect. While the retention time has increased as compared to TAPA the selectivity is smaller; thus probably the less effective stereochemical interaction leads to an arrangement of the planar aromatic system which allows a stronger charge-transfer interaction.

The more bulky ligands in CSP 5b, 5c, 5d exhibit decreasing k' and α values indicating that both interactions are diminished.

The linearly annellated CSP 7 is the optimized system for the resolution of **16**. In addition to the strong chiral interaction the more effective charge-transfer interaction expressed by the large capacity factor, $k_1' = 12.00$, causes an increase of selectivity from $\alpha = 1.61$ (TAPA) to 2.01 (CSP 7). CSP 6 exhibits a weak $\pi-\pi$ interaction ($k_1' = 4.82$) which is too small for an efficient chiral recognition. CSP 8 and **16** obviously form a strong charge-transfer complex as shown by the large capacity factor, $k_1' = 10.9$, but the lack of enantiomeric resolution indicates that this arrangement might not allow any chiral interaction.

TABLE II

CHROMATOGRAPHIC BEHAVIOUR OF *trans*-1,2-DIHYDROXY-1,2-DIHYDRODIBENZ[*a*,*h*]ANTHRACENE (**16**) ON CHIRAL STATIONARY PHASES (*cf.* FIG. 3)

k_1' is the capacity factor of the first-eluted enantiomer, $k_1' = (t_{R1}/t_0) - 1$, where t_{R1} is the retention time of the first-eluted enantiomer and t_0 the retention time of a non-retained solute. The selectivity, α, between two enantiomers is the ratio of their respective capacity factors (k_1'/k_2'). Operating conditions: flow-rate, F, 2 ml/min; room temperature; column dimensions, 250 × 4 mm; $V_0 = 2.0$–2.3 ml, where $V_0 = Ft_0$; mobile phase: methanol–dichloromethane 30:70, v/v); UV detection at 280 nm.

CSP	k_1'	α
1	0	NR[a]
2	0.09	NR
3	2.11	1.09
4	3.12	1.38
5	9.74	1.61
5a	16.80	1.34
5b	5.02	1.36
5c	2.05	NR
5d	3.27	1.15
6	4.82	1.10
7	12.00	2.01
8	10.90	NR

[a] NR = No resolution, $\alpha = 1$

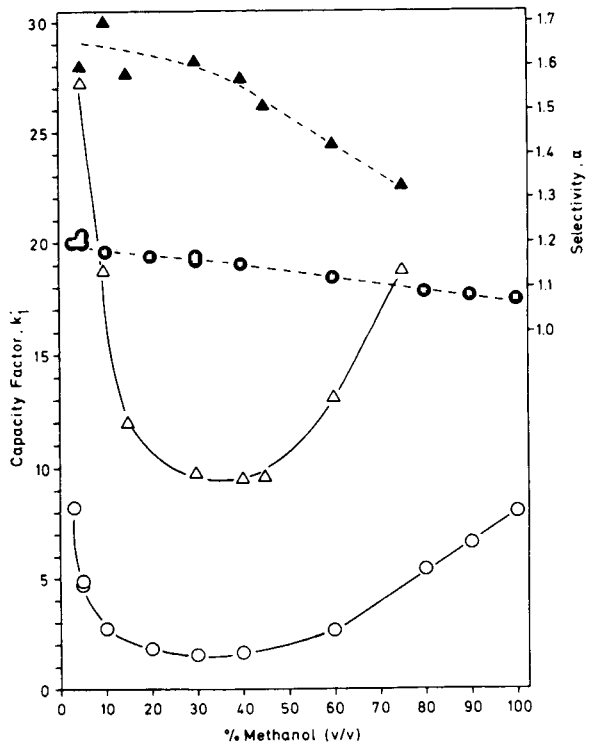

Fig. 4. Dependence of the capacity factor, k_1' (solid lines), of the first eluted enantiomer and of the selectivity, α (dotted lines), between the two enantiomers from the composition of the mobile phase consisting of methanol and dichloromethane; solutes: **16** = △, ▲(CSP 5); **22** = ○, ●(CSP 5a).

Influence of the composition of the mobile phase on the enantiomeric separation

Mixtures of methanol and dichloromethane proved to be suitable mobile phases for the enantiomeric resolution of *trans*-dihydrodiols on chiral stationary phases based on (*R*)-(−)-2-(2,4,5,7-tetranitrofluoren-9-ylideneaminooxy)-carboxylic acids. Variation of the composition of the binary mobile phase from pure dichloromethane to pure methanol resulted in a marked bimodal change of the capacity factor which reached its minimum at 30–35% (v/v) methanol in the binary mixture (Fig. 4). This behaviour is a general phenomenon as it is observed with different solutes as well as with different CSPs (Fig. 4) [32,34]. Similar results have also been obtained with diol and cyano phases applying mobile phases of different solvent strength [35]. This retention property indicates that the stationary phase exhibits an intermediate polarity, *i.e.* a polarity which is in between the polar unmodified silica (normal phase) and the non-polar, aliphatic hydrocarbon-modified silica (reversed phase). In pure dichloromethane, a rather non-polar solvent with a solvent strength parameter of $P' = 3.4$ [36], strong interaction with the CSP is shown by a high capacity factor k'; this interaction is of polar nature since it is weakened by an increase in the content of methanol, a polar solvent with a solvent strength parameter of $P' = 6.6$ [36]. In pure methanol, on the other hand, a strong non-polar interaction between solute and CSP is observed, which is weakened by increasing the dichloromethane content leading to a decrease in the value of the capacity factor k'. The lowest k' value is obtained at a methanol content in the binary mixture which represents a solvent strength of $P' = 4.36$–4.52 [37].

The hydrophobic interaction between solutes and CSP at high methanol content is furthermore confirmed by the observed differences in the capacity factors between solutes **16** and **22** (*cf.* Fig. 4). Thus the larger k' values and their stronger increase with increasing methanol content ($>40\%$) in the case of **16** as compared to **22** is a consequence of the different hydrophobic nature of the two *trans*-dihydrodiols. Using the partition coefficient P, which is a quantitative description of the lipophilicity of a compound, and estimating log P by summation of the hydrophobic fragmental constants according to Rekker [38] leads to the conclusion that **16** is more lipophilic with log $P \approx 4.56$ as compared to **22** with log $P \approx 3.84$. This results in stronger hydrophobic interactions of **16** with the CSP and consequently larger k' values in comparison to **22**.

Not only the retention of the solute but also the degree of chiral discrimination demonstrated by the selectivity α is influenced by the change in the composition of the mobile phase (Fig. 4) [32,34]. Polar interactions between the CSP and at least one of the chiral hydroxyl groups of the solute clearly play a more important role for chiral recognition than the non-polar interactions dominating at high methanol content. Additionally the *trans*-dihydrodiol and methanol could compete for hydrogen bonding sites in the CSP thereby impairing the chiral interactions. Furthermore, it should be emphasized that the chiral discrimination is only slightly influenced by the change in the composition of the mobile phase as compared to the marked alteration of the capacity factor.

Structural requirements for the enantiomeric separation of trans-dihydrodiols on chiral stationary phases based on (R)-(−)-2-(2,4,5,7-tetranitrofluoren-9-ylideneaminooxy)carboxylic acids

In order to account for the structural features of chiral compounds governing their chromatographic separation into enantiomers 30 hydroxylated derivatives (Fig. 1) of PAHs were applied to CSP 5; 27 of these solutes were metabolically relevant *trans*-dihydrodiols which exist as just two optical isomers, the *R,R*- and the *S,S*-enantiomer, in spite of their two centres of chirality.

Interaction between the dihydrodiols and the CSP leading to retention of the solute can take place between the aromatic ring system of the former and the nitrated fluorenylidene moiety of the latter (π-donor–acceptor interactions) as well as between the hydroxyl group(s) of the dihydrodiol and the amide carbonyl or the aminooxy moiety of the stationary phase (hydrogen bonds).

The $\pi-\pi$ interaction seems to play the most important role since an increase in the number of aromatic rings in the solute leads to stronger retention, expressed as capacity factor, k' (Table III): while compounds with one (**1**) or two isolated aromatic rings (**5**) are very weakly retained, the capacity factor increases with the number of annellated rings, *e.g.* **5**→**10**→**21**. The strongest retention is observed in the case of compounds with four annellated rings, *e.g.* **15**, **16**, **18–20** whereas the interaction of solutes with four unsubstituted condensed rings, *e.g.* **22**, **22a**, **22b**, **23**, is somewhat weaker. Increasing the basicity of the aromatic ring system by the +M effect of a phenolic hydroxyl group leads to stronger π-donor–acceptor interactions thus raising the retention considerably as in the case of **22c** and **22d** compared to **22**. Additionally, hydrogen bonds between the phenolic hydroxyl groups and the CSP could add to the retention of **22c** and **22d**. An olefinic double bond in the ring containing the diol moiety (**22**) leads to a higher capacity factor as in the case of the saturated ring system (**22a**) probably caused by the larger number of π-electrons or by the greater planarity of the ring system thus improving the interaction between solute and stationary phase.

For the enantiomeric recognition of a chiral compound by a CSP a three-dimensional interaction is necessary. π-Donor–acceptor interactions provide in principle two of the three interactions requiring just a single addition interaction for chiral discrimination [33]. For optimal chiral resolution the $\pi-\pi$ interaction between the nitrated fluorenylidene moiety and the aromatic ring system has to fix the chiral solute in a position allowing maximal interaction between one of the hydroxyl groups and the CSP. There-

TABLE III

CHROMATOGRAPHIC BEHAVIOUR OF DIHYDRODIOLS AND RELATED DERIVATIVES OF POLYCYCLIC AROMATIC HYDROCARBONS (*cf.* FIG. 1) ON CHIRAL STATIONARY PHASE CSP 5 (*cf.* FIG. 3)

For the meaning of k_1' and α see Table II. Operating conditions: flow-rate, 0.8–2.0 ml/min; room temperature; column dimensions, 250 × 4 mm; V_0 = 2.35 ml; mobile phase: the percentage (v/v) of methanol in dichloromethane is given; UV detection at 280 nm.

Dihydrodiol	Methanol (%)	k_1'	α
1	30	0.51	NR[a]
	0	0.09	NR
2	30	0.34	NR
	1	13.57[b]	1.05
3	30	0.25	NR
	1	5.46[b]	1.04
4	30	0.22	NR
	1	2.31	NR
5	30	0.23	NR
	5	0.44	NR
6	30	1.88	1.08
	5	5.91	1.10
7	30	0.92	1.07
	1	8.95	1.08
7a	30	0.53	NR
	1	3.58	NR
8	30	1.59	1.08
	1	10.09	1.20
9	30	0.77	NR
	1	5.61[b]	1.05
10	30	0.16	NR
	1	1.90	1.12
11	30	0.62	NR
	1	9.95	NR
12	30	0.74	NR
	1	5.48	1.11
13	30	3.50	NR
14	30	2.13	NR
	5	5.50	NR
15	30	14.03	1.09
	10	20.90	1.09
16	30	9.74	1.61
	5	27.25	1.65
17	30	4.23	1.06
	10	6.39	1.06
18	30	7.66	1.27
	10	13.48	1.27
19	30	10.98	1.07
	5	31.45	1.10
20	30	4.18	1.09
	5	15.05	1.08
21	30	0.75	1.20
	1	8.11	1.20
22	30	4.31	1.14
	10	7.42	1.16
22a	30	3.02	1.09
	10	4.57	1.11
	5	7.61	1.11
22b	30	2.85	1.12
	1	5.32	1.13
22c	30	16.10	1.09
	10	43.22	1.10
22d	30	17.39	1.12
23	30	1.79[b]	1.05
	5	6.48	1.06
24	30	3.66	1.20
	5	10.24	1.19
25	30	1.98	1.21
	5	6.02	1.24

[a] NR = No resolution, α = 1.
[b] Eluted as shoulder.

fore a marked π-donor–acceptor interaction is a necessary but not a sufficient requirement for chiral separation. This is demonstrated by the behaviour of **11**, **13**, **14** which exhibit a high capacity factor but lack any enantiomeric resolution. It is interesting to note that not only the enantiomers of **11**, **13**, **14** but also those of other *trans*-dihydrodiols possessing the structural element of a fjord-region[a] could not be separated by the CSPs depicted in Fig. 3. Obviously the helicity of fjord-region PAHs prevents the formation of the diastereomeric complex required for chiral discrimination.

In general the increase in the number of aromatic rings leads to an improvement in stereoselectivity exemplified by **5**, **10** and **21** (Table III). Two or three aromatic rings in the dihydrodiol are the minimum for chiral recognition by CSP 5 as shown by the partial separation of **2**, **3** and **9** into the enantiomers. The separation could not further be improved by modification of the mobile phase as was expected from the results of Fig. 4. In the case of *trans*-dihydrodiols **6**, **7**, **10**, **12**, **15**, **17**, **19**, **20**, **22**, **22c**, **22d**, **23** a more favourable chiral interaction leads to an improvement of enantiomeric separation (α = 1.06–1.19) which is further enhanced (α = 1.20–1.27) in the case of **8**, **16**, **18**, **21**, **24**, **25**. It should be noted that neither an olefinic double bond, *e.g.* **22a** as compared to **22**, nor two hydroxyl groups, *e.g.* **22b** as compared to **22a**, are required for chiral resolution. In the case of vicinal hydroxyl groups in the solute the *trans*-orientation seems to allow better chiral interactions with the CSP than the *cis*-orientation as in **7** *versus* **7a**. A similar observation has already been reported [7]. Apparently the two hydroxyl groups mutually compete for hydrogen bonds with the chiral center of the CSP.

The successful enantiomeric separation of a large number of metabolically relevant and biologically active *trans*-dihydrodiols of PAHs can now be applied to studies concerned with the

[a] The term fjord-region denotes a sterically crowded molecular region in a PAH, *e.g.* the region between C-1 and C-12 in benzo[*c*]phenanthrene; thus the fjord-region is a special case of a bay-region, *e.g.* the region between C-4 and C-5 in phenanthrene.

stereoselective formation of these metabolites [13,39] or with the biological activity of the enantiomers [12] and their covalent binding to DNA [40].

Applicability of the chiral stationary phases for the enantiomeric separation of metabolites of PAHs and of drugs

Although many of the *trans*-dihydrodiols depicted in Fig. 1 could be resolved into their enantiomers by application of CSP 5, in some cases this separation was not fully satisfactory. Thus in the case of the two non-bay-region *trans*-dihydrodiols of DBA the enantiomers of the 1,2-isomer, **16**, are well separated ($k_1' = 9.74$, $\alpha = 1.61$; *cf.* Table II) while those of the biologically very important 3,4-isomer **15** [12,39,40] were only poorly resolved ($\alpha = 1.09$, $R_s = 0.35$; Fig. 5A) despite of the stronger π-donor–acceptor interactions as expressed by a capacity factor of $k_1' = 14.03$ (Table III).

Assuming that the aromatic ring system of both *trans*-dihydrodiols is fixed in a similar manner to the tetranitrofluorenylidene system of CSP 5 the 3,4-substitution pattern obviously does not allow a similar effective chiral interaction as in the case of the 1,2-isomer.

An attempt to improve the chiral recognition by replacing the methyl group (R_1 in Fig. 3) in the center of chirality of CSP 5 by more bulky alkyl groups leading to CSP 5a, 5b, 5c, 5d did not succeed (data not shown). Therefore another strategy was pursued by modifying the geometry of the π-acceptor moiety in the CSP by annellating the original tetranitrofluorenylidene system with additional nitroaromatic rings in different positions leading to CSP 6, 7, 8. Indeed this approach finally yielded an almost base-line separation of the enantiomers of **15** with CSP 8 ($\alpha = 1.20$, $R_s = 1.07$; Fig. 5B) although at the expense of a rather long separation time; this CSP could also be employed for the separation of (+)- and (−)-**15** on a preparative scale [12]. As an example of the application of CSP 8 in the investigation of the biotransformation of tumorigenic DBA Fig. 5C demonstrates the stereoselective formation of (−)-(3*R*,4*R*)-dihydrodiol by hepatic microsomes of Sprague–Dawley rats pretreated with 3,4,3′,4′-tetrachlorobiphenyl.

The applicability of the CSPs described in this study is not restricted to the enantiomeric separation of *trans*-dihydrodiol but can also be expanded to other metabolically relevant deriva-

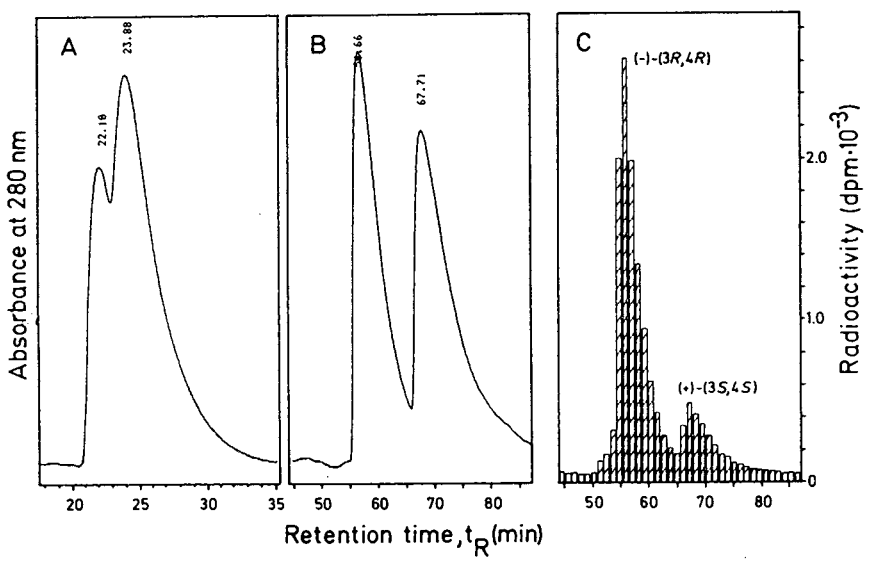

Fig. 5. Chromatographic separation of the enantiomers of synthetic (A, B) and metabolically formed (C) *trans*-3,4-dihydroxy-3,4-dihydrodibenz[*a*,*h*]anthracene on CSP 5 (A) and CSP 8 (B, C). Mobile phase: methanol–dichloromethane (30:70, v/v); flow-rate: 1.6 ml/min; $t_0 = 1.48$ min.

tives of PAHs like arene oxides [39], tetrahydrotetraols [39] phenoldihydrodiols (Fig. 1, Table III) and dihydrodiol oxides [7]. The enantiomeric separation of (±)-DBA 5,6-oxide on CSP 5b [39] indicates that not only hydroxyl groups but also an oxiranyl oxygen is able to form stereoselective interactions with the chiral center of the CSP. Finally these CSPs could successfully be applied to the preparation of enantiomeric pure intermediates for the synthesis of metabolically relevant derivatives of PAH [22].

However, attempts to employ these CSPs for the separation of racemic drugs, *e.g.* β-blockers, antiinflammatory agents, calcium-channel antagonists, anaesthetics and anticoagulants, failed in spite of marked charge-transfer interactions expressed by capacity factors in the range of $k' = 3–7$. Apparently the interactions between the substituents at the asymmetric carbon atom of the drug and the chiral center of the CSP or the distance between them did not permit any chiral discrimination.

CONCLUSIONS

Nitrated fluorenylideneaminooxy carboxylic acids covalently bound to silica gel via an aminopropyl spacer yielded CSPs suitable for the chromatographic separation of *trans*-dihydrodiols and related derivatives of PAHs thus avoiding the cumbersome separation of the enantiomers as their diastereomeric esters. Charge-transfer interactions between the π-acceptor of the CSP and the aromatic ring system of the solute in combination with chiral interactions via hydrogen bonds provide the basis for chiral discrimination. The retention of the solutes on the CSPs is strongly influenced by the composition of the mobile phase consisting of methanol–dichloromethane mixtures while the selectivity of the enantiomeric separation is only weakly affected. A minimum of two annellated aromatic rings in the solute were required for stereochemically discriminating interactions while an enlargement of the π-donor system to four aromatic rings resulted in an increase in stereoselectivity. The chiral interaction could furthermore be improved by modifications of the geometry of the π-acceptor part of the chiral ligand.

ACKNOWLEDGEMENTS

The authors express their appreciation to M. Bauer for her excellent technical assistance as well as to Drs. S. Reichert, I. Reischmann and M. Schollmeier for their contributions to this work.

Thanks are also due to Dr. G. Jennings for proof reading the rough draft and to I. Böhm for skilful help in the preparation of the manuscript.

We are grateful for financial support by the Deutsche Forschungsgemeinschaft (Grant SFB 302).

REFERENCES

1 A. Dipple, in C.E. Searle (Editor), *Chemical Carcinogens (ACS Monographs*, No. 173), American Chemical Society, Washington, DC, 1976, Ch. 5, p. 245.
2 H.V. Gelboin, *Physiol. Rev.*, 60 (1980) 1107.
3 S.K. Yang, *Biochem. Pharmacol.*, 37 (1988) 61.
4 D.R. Thakker, H. Yagi, W. Levin, A.W. Wood, A.H. Conney and D.M. Jerina, in M.W. Anders (Editor), *Bioactivation of Foreign Compounds*, Academic Press, Orlando, FL, 1985, Ch. 7, p. 177.
5 D.R. Thakker, H. Yagi and D.M. Jerina, *Methods Enzymol.*, 52 (1978) 279.
6 S.K. Yang, H.V. Gelboin, J.D. Weber, V. Sankaran, D.L. Fischer and J.F. Engel, *Anal. Biochem.*, 78 (1977) 520.
7 Y.H. Kim, A. Tishbee and E. Gil-Av, *J. Chem. Soc., Chem. Commun.*, (1981) 75.
8 H.B. Weems, M. Mushtaq, P.P. Fu and S.K. Yang, *J. Chromatogr.*, 371 (1986) 211.
9 S.K. Yang, M. Mushtaq and P.P. Fu, *J. Chromatogr.*, 371 (1986) 195.
10 S.K. Yang and H.B. Weems, *Anal. Chem.*, 56 (1984) 2658.
11 S.K. Yang, H.B. Weems, M. Mushtaq and P.P. Fu, *J. Chromatogr.*, 316 (1984) 569.
12 K.L. Platt, M. Schollmeier, H. Frank and F. Oesch, *Environm. Health Persp.*, 88 (1990) 37.
13 S. Reichert, J. Doehmer, H. Frank, F. Oesch and K.L. Platt, *Polycyclic Aromatic Comp.*, 3 (Suppl.) (1993) 895.
14 M. Mushtaq, H.B Weems and S.K. Yang, *Chem. Res. Toxicol.*, 2 (1989) 84.
15 F. Mikes, G. Boshart and E. Gil-Av, *J. Chromatogr.*, 122 (1976) 205.
16 K.L. Platt and F. Oesch, *Synthesis*, (1982) 459.
17 K.L. Platt and F. Oesch, *J. Org. Chem.*, 48 (1983) 265.
18 J. Klein, A. Seidel, H. Frank, F. Oesch and K.L. Platt, *Chem.-Biol. Interact.*, 79 (1991) 287.
19 H. Glatt, A. Piée, K. Pauly, T. Steinbrecher, R. Schrode, F. Oesch and A. Seidel, *Cancer Res.*, 51 (1991) 1659.
20 A. Seidel, *Ph.D. Thesis*, University of Mainz, Mainz, 1989.

21 R. Schrode, *Ph.D. Thesis*, University of Mainz, Mainz, 1990.
22 H. Frank, *Ph.D. Thesis*, University of Mainz, Mainz, 1986.
23 P. Petrovic, *Diploma Thesis*, University of Mainz, Mainz, 1979.
24 F. Oesch, G. Stillger, H. Frank and K.L. Platt, *J. Org. Chem.*, 47 (1982) 568.
25 D.J. McCaustland, D.L. Fischer, K.C. Kolwyck, W.P. Duncan, J.C. Wiley, C.S. Menon, J.F. Engel, J.K. Selkirk and P.P. Roller, in R.I. Freudenthal and P.W. Jones (Editors), *Carcinogenesis, Vol. 1, Polynuclear Aromatic Hydrocarbons: Chemistry, Metabolism, and Carcinogenesis*, Raven Press, New York, 1976, p. 349.
26 P. Block and M.S. Newman, *Org. Synth.*, 48 (1968) 120; *Org. Synth., Coll. Vol.*, V (1973) 1029.
27 M. Minabe, M. Yoshida and O. Kumuru, *Bull. Chem. Soc. Jpn.*, 58 (1985) 385.
28 S. Ishikawa and M. Masubuchi, *Japan. Kokai*, 77 131 570 (April 23, 1976/November 4, 1977); *C.A.*, 88 (1978) 144330x.
29 J. Thiele and J. Scheider, *Liebigs Ann. Chem.*, 369 (1909) 287.
30 A. Schaarschmidt, *Chem. Ber.*, 49 (1916) 1444.
31 J.J. Kirkland, *J. Chromatogr. Sci.*, 9 (1971) 206.
32 P. Pescher, M. Caude, R. Rosset and A. Tambuté, *J. Chromatogr.*, 371 (1986) 159.
33 W.H. Pirkle and T.C. Pochapsky, *Chem. Rev.* 89 (1989) 347.
34 L. Siret, A. Tambuté, M. Caude and R. Rosset, *J. Chromatogr.*, 498 (1990) 67.
35 W. Jost, G. Schwinn and M.Tüylü, *Labor Praxis*, 11 (1987) 168.
36 L.R. Snyder, *J. Chromatogr.*, 92 (1974) 223.
37 J.G. Stewart and P.A. Williams, *J. Chromatogr.*, 198 (1980) 489.
38 R.F. Rekker, *The Hydrophobic Fragmental Constant*, Elsevier, Amsterdam, 1977.
39 K.L. Platt and I. Reischmann, *Mol. Pharmacol.*, 32 (1987) 710.
40 J. Fuchs, J. Mlcoch, K.-L. Platt and F. Oesch, *Carcinogenesis*, 14 (1993) 863.

Journal of Chromatography A, 659 (1994) 69–74
Elsevier Science B.V., Amsterdam

CHROM. 25 627

Doubly tethered tertiary amide selectors

Modified version of Doyle *et al.*'s naproxen chiral stationary phase

William H. Pirkle*, Patrick L. Spence, Bo Lamm[☆] and Christopher J. Welch[☆☆]

School of Chemical Sciences, University of Illinois, Urbana, IL 61801 (USA)

(First received August 2nd, 1993; revised manuscript received October 5th, 1993)

ABSTRACT

The synthesis of an (*S*)-naproxen-derived chiral stationary phase (CSP) that differs from those of Doyle *et al.* [T.D. Doyle, C.A. Brunner and E. Smith, *US Pat.*, 4919 803 (1990) and T.D. Doyle, in W.J. Lough (Editor), *Chiral Liquid Chromatography*, Chapman & Hall, New York, 1989, pp. 102–128] and of Oliveros *et al.* [L. Oliveros, C. Minguillón, B. Desmazières and P. Desbène, *J. Chromatogr.*, 589 (1992) 53 and 606 (1992) 9] is reported. Instead of linking naproxen to a primary amino group in the tether, linkage is to a secondary amino group. This avoids the presence of an amide hydrogen which often serves to increase retention, attenuate enantioselectivity and diminish the efficiency of the CSP. The presently described CSP 2 typically shows improved performance relative to those described by the Doyle *et al.* and Oliveros *et al.*

INTRODUCTION

A naproxen-derived chiral stationary phase, CSP 1 (Fig. 1), initially developed by Doyle *et al.* [1,2], was later described [3] and then modified by Oliveros *et al.* [4]. Like other π-basic CSPs, CSP 1 typically requires that analytes contain π-acidic functionality if it is to afford more than trivial levels of enantioselectivity. Because we often have occasion to separate the enantiomers of π-acidic compounds on a preparative scale, the ease of preparation and the commercial availability of (*S*)-naproxen made CSP 1 attractive even though it typically affords less enantioselectivity than several other π-basic CSPs [5,6].

From our studies of chiral recognition mechanisms, we suspected that several structural features of Doyle *et al.*'s CSP were potentially detrimental to its performance, although they contribute to its ease of preparation. Doyle *et al.* passed (*S*)-carboxyl-activated naproxen through an aminopropyl column to perform an *in situ* modification, a procedure which fails to functionalize all of the amino groups. The presence of residual amino groups was early recognized as undesirable [7]. By joining the chiral selector to the silane tether prior to bonding to silica, one avoids the presence of free amino groups in the CSP. This approach has been used by at least one manufacturer of CSPs for some time, and while less convenient, affords a better CSP. This "pre-assembly" technique was applied by Oliveros *et al.* [4] to Doyle *et al.*'s CSP and found to improve its performance. We had independently prepared a "pre-assembled" naproxen CSP with similar results.

* Corresponding author.
☆ Present address: Astra Hässle AB, Mölndal, Sweden.
☆☆ Present address: Regis Technologies, Inc., Morton Grove, IL 60053, USA.

0021-9673/94/$07.00
SSDI 0021-9673(93)E1064-7

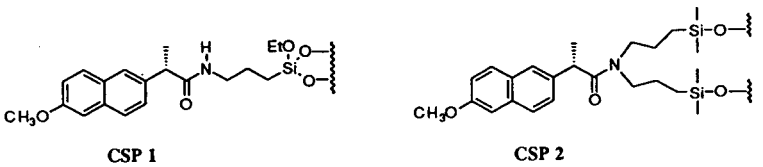

CSP 1 CSP 2

Fig. 1. Structures of the CSPs used in this study.

Experience gained from the chromatography of various naproxen derivatives led us to suspect that the amide N–H in this CSP is unnecessary for chiral recognition and likely to be deleterious to the performance of the CSP. Accordingly, we prepared CSP 2 in which the selector is a tertiary amide of (*S*)-naproxen, thus avoiding the supposedly superfluous N–H. This paper describes the preparation of this CSP and provides some comparative data concerning its performance relative to the naproxen-derived CSPs previously described. To better enable comparisons to be made, all of the CSPs described herein are bonded to the same spherical silica, 5 μm, 100 Å Rexchrom. The comparisons are of mechanistic interest and relevant to the design of other CSPs.

EXPERIMENTAL

General

The analytes used in this comparative study were either available from prior studies or were prepared in the manner described by the original workers [1–3].

^{1}H NMR spectrum was recorded on a Varian XL-200 Fourier transform NMR instrument operating at 200 MHz in the ^{2}H lock mode. Chemical shifts are reported in parts per million (ppm) relative to tetramethylsilane as the internal standard. Elemental analyses were performed by T. McCarthy and associates at the University of Illinois Microanalytical Service Facility. High- and low-resolution mass spectrum analyses were performed by R. Milberg and associates at the University of Illinois Mass Spectrometry Laboratory using fast atom bombardment on either a VG ZAB-SE (low resolution) or a VG 70-SE-4F (high resolution). HPLC analyses were performed using either a Rheodyne injector, Rainin Rabbit Model HPX pump and a Linear UVIS 200 variable-wavelength detector or a Rheodyne injector, Anspec pump and a Milton-Roy UV detector system (254, 280 nm)]. Rotations were measured on a Rudolph Autopol III digital polarimeter, equipped with a 1 dm flow cell operating at 589 nm.

Preparation of CSP 1A

The procedure used was that reported by Doyle *et al.* [1,2], without modifications.

Preparation of CSP 1B

(*S*)-Naproxen (2.30 g, 10 mmol) was suspended in 50 ml of CH_2Cl_2 and 2 ml of oxalyl chloride were added. After 3 h, the solution was evaporated to dryness and the remaining crystalline solid was dried under vacuum for 3 h. The solid was dissolved in dry diethyl ether–CH_2Cl_2 (1:1) and added dropwise to a solution of 1.2 g of triethylamine and 2 g of triethoxyaminopropylsilane in CH_2Cl_2. After 15 min, the reaction mixture was filtered through a sintered glass funnel and the filtrate was added to 5 g of Rexchrom 5 μm 100 Å silica which had been azetropically dried over benzene. The solvents were carefully evaporated, the residue was slurried in CH_2Cl_2, and 1 ml of dry N,N-dimethylformamide was added. The silane–silica mixture was then placed in an evacuated Kugelrohr apparatus at 45–50°C overnight. The resulting bonded phase was slurry packed into a 250 × 4.6 mm stainless-steel column. Elemental analysis of the dried silica remaining after packing showed a loading of 0.20 mmol selector per gram silica (by carbon) and 0.16 mmol selector per gram silica (by nitrogen). Chiral silane recovered from the bonding process had undergone no loss of enantiomeric purity (HPLC analysis on a π-acidic CSP).

PREPARATION OF CSP 2

(S)-Naproxen diallyl amide

(*S*)-Naproxen acid chloride (2.7 g, 10.86 mmol), prepared in a manner similar to that used by Doyle *et al.* [1,2], was placed in a 250-ml round-bottom flask with 100 ml of dry CH_2Cl_2 and cooled in an ice–water bath. Diallylamine (10.55 g, 108.6 mmol) was added slowly with stirring, and the reaction mixture was allowed to stand at room temperature for 2 h. The reaction mixture was washed twice with 100-ml portions of 1 *M* HCl, dried over $MgSO_4$, and the solvent removed by vacuum to afford 3.4 g (100%) of (*S*)-naproxen diallyl amide. The enantiomeric purity of the amide [evaluated using an (*S,S*)-Whelk-O 1 CSP (Regis)] was greater than 98%. ^{1}H NMR: δ 1.5 (d, 3H), 3.55–3.75 (m, 2H), 3.9–4.0 (m, 5H), 4.3–4.4 (dd, 1H), 4.9–5.2 (m, 4H), 5.5–7.5 (m, 2H), 7.1–7.2 (m, 2H), 7.4 (dd, 1H), 7.6–7.7 (m, 3H). Elemental analysis: theory: 77.64% C, 7.49% H, 4.53% N; found: 77.50% C, 7.52% H, 4.49% N.

Hydrosilylation of (S)-naproxen diallyl amide. (*S*)-Naproxen diallyl amide (2.9 g, 9.4 mmol) was placed in a 50-ml round-bottom flask with 15 ml of dry CH_2Cl_2. Dimethylchlorosilane (8.5 g, 89.9 mmol) was added to the reaction mixture in one portion, then followed by addition of *ca.* 5 mg of H_2PtCl_6. The reaction was heated to reflux and checked periodically by TLC. After 8 h, the solvent was evaporated and 15 ml of a solution of diethyl ether–ethanol–triethylamine (1:1:1) was added. The precipitated amine hydrochloride was removed by filtration and the filter cake was washed with diethyl ether. The combined filtrates were evaporated to near dryness and purified by flash chromatography on silica to afford 1.6 g (33%) of the bis-ethoxysilane. Low-resolution mass spectrum (M^+ = 518.4 a.m.u.); high-resolution mass spectrum; [$M^+_{exp.}$] was within 0.0002 a.m.u. of the calculated value.

Bonding the selector to silica to afford CSP 2. The bis-ethoxysilane (1.6 g, 3.09 mmol) was dissolved in 15 ml of dry CH_2Cl_2 and added to 5.0 g of azeotropically dried silica in a 50-ml round-bottom flask. The slurry was then evaporated to near dryness, another 15 ml of dry CH_2Cl_2 were added, and the slurry was again evaporated to near dryness. This was repeated once more with 1.0 ml of dry N,N-dimethylformamide added to the CH_2Cl_2. Following evaporation to near dryness, the silane–silica mixture was placed in a Kugelrohr apparatus and heated to 90–95°C for 24 h under reduced pressure (2 mmHg; 1 mmHg = 133.322 Pa) with gentle mixing. The bonded phase was then slurry packed into a 250 × 4.6 mm stainless-steel HPLC column. Elemental analysis of the thoroughly washed and dried silica packing material showed a loading of 0.22 mmol selector per gram silica (by carbon) and 0.21 mmol selector per gram silica (by nitrogen).

RESULTS AND DISCUSSION

Doyle *et al.* [1,2] prepared CSP 1 by recirculating a mixture of (*S*)-naproxen and a carboxyl activating agent through a commercial aminopropyl column. Any attempt to derivatize γ-aminopropyl silanized silica with a carboxyl-activated carboxylic acid will leave many aminopropyl strands underivatized. Since amino groups interact strongly with many π-acidic groups, any residual amino groups would be expected to increase retention, diminish enantioselectivity, and adversely affect the resolution afforded by any CSP so prepared. The presence of residual amino groups might well account for the addition of acetonitrile to the mobile phase by the original workers [1,2].

From chromatography of the tertiary amide derivatives of chiral acids on CSPs, we knew that they often exhibit greater enantioselectivity than do the corresponding secondary amide derivatives. Derivatives of naproxen and other α-arylpropionic acids fall into this category. Additionally, we have made several tertiary amide CSPs which afford greater enantioselectivities than do the corresponding secondary amide CSPs. Because one need not invoke the carboxamide N–H as an interaction site essential to the chiral recognition *of* naproxen, we suspected that the carboxamide N–H in CSP 1 is not essential for chiral recognition *by* naproxen. Hence, this N–H might lead to interactions with

analytes which increase their retention without distinguishing between enantiomers, thereby reducing enantioselectivity. By coupling carboxyl-activated naproxen to a secondary amine prior to immobilizing this selector on silica, several undesirable features of the original design can be eliminated. Additionally, use of diallylamine as the secondary amine potentially allows the selector to be doubly tethered to silica, thus increasing the robustness of the CSP.

CSP 1A was prepared by pumping an excess of carboxyl-activated (*S*)-naproxen through a commercial (Regis) aminopropyl column as described [1,2]. This column should be similar, but not necessarily identical, to those used by Doyle *et al.* and Oliveros *et al.* owing to differences in the silicas used and in the aminopropyl surface coverage. CSP 1B was prepared by acylation of γ-aminopropyltriethoxysilane with (*S*)-naproxen acid chloride *prior* to bonding the chiral silane to silica. This was done to avoid the presence of residual aminopropyl strands. Again, this CSP should be similar, but not necessarily identical, to the modified CSP of Oliveros *et al.* [4] for the reasons just stated. CSP 2 was made by acylating diallylamine with naproxen acid chloride, followed by hydrosilylation of the resulting olefinic amide precursor of CSP 2 with dimethylchlorosilane. Conversion of the enantiomerically pure bis-chlorosilane to the bis-ethoxysilane (to facilitate purification and characterization) led to the selector which was bonded to silica. The variously modified silicas were each slurry packed into 250 × 4.6 mm stainless-steel columns. The performance of these CSPs (see Table I) was compared with that reported by Doyle *et al.* [1,2] and by Oliveros *et al.* [3] for CSP 1 (first column, Table I).

The data reported (Table I) for CSP 1 by Oliveros *et al.* [3] (the first three entries), and by Doyle *et al.* [1,2] (the fourth entry) make it evident that the prior versions of CSP 1 generally afford longer retention and less enantioselectivity than is presently observed for CSP 1A. This possibly results from differences in the three types of aminopropyl silica used (J.T. Baker [1,2], Nucleosil [3] and Rexchrom). Consistent with the observations of the Oliveros *et al.* [4], CSP 1B affords less retention and greater enantioselectivity than does CSP 1A. The retention and enantioselectivities afforded by our CSP 1B correspond almost exactly to these reported by Oliveros *et al.* for their CSP 1B. The expectation that elimination of the amide N–H would be beneficial is borne out by the reduced retention, the increased enantioselectivity, and the greater resolution usually afforded by CSP 2 relative to those afforded by the other CSPs (see Table II).

For the last two entries in Table II, the levels of enantioselectivity afforded by CSP 2 are substantially greater than those afforded by the other CSPs, thus making it an attractive phase for the preparative resolution of these and related analytes. These greater enantioselectivities arise, to some extent, from the elimination of interactions which increase retention without distinguishing between enantiomers. Moreover, the extent of solvation of the selectors and their conformational preferences will be influenced by the manner of tethering. These factors also affect enantioselectivity and will influence the kinetics of adsorption and desorption in ways neither yet fully understood nor utilized to best advantage.

Oliveros *et al.* note that endcapping a CSP sometimes significantly improves enantioselectivity and sometimes has little effect. They speculate that this may be related to differences in the silicas used [4]. In our experience, endcapping leads to the greatest gains in enantioselectivity for those CSPs having low surface coverages by the chiral silane. High surface coverages reduce the number of silanol groups which remain to be endcapped. Consequently, endcapping causes only a modest change in the performance of a CSP having a high initial level of surface coverage.

CONCLUSIONS

There are doubtless other π-basic carboxylic acids which, when immobilized, will afford CSPs of greater enantioselectivity than does naproxen. Even so, naproxen is conveniently available and can be incorporated into a CSP which affords levels of enantioselectivity adequate for many applications, including preparative separations. By omitting an unnecessary polar site from the selector, one can often improve the performance

TABLE I

COMPARISON OF NAPROXEN-DERIVED CSPs

The same chromatographic conditions were used for all CSPs. For the first three analytes, the conditions were: chloroform–(0.5% methanol in heptane) (70:30) at 1.0 ml/min flow-rate, as reported [3]. For the last analyte, the conditions were: hexane–2-propanol (60:40) at 0.5 ml/min flow-rate [1,2] ($T = 20 \pm 2$°C). Void volumes were measured using 1,3,5-tri-*tert.*-butylbenzene (TTBB).

	CSP 1		CSP 1A		CSP 1B[a]		CSP 2		Ref.
	k_1' [b]	α	k_1' [b]	α	k_1' [b]	α	k_1' [b]	α	
3,5-Dinitrobenzamide of:									
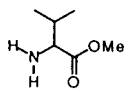	1.37 (*S*)	1.51	1.09 (*S*)	1.66	0.91 [1.00] (*S*)	1.84 [1.84]	0.56 (*S*)	3.11	3
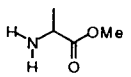	5.53 (*S*)	1.34	3.84 (*S*)	1.50	2.61 [3.00] (*S*)	1.69 [1.76]	1.60 (*S*)	2.47	3
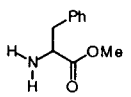	2.37 (*S*)	1.51	1.65 (*S*)	1.67	1.21 [1.29] (*S*)	1.83 [1.89]	0.74 (*S*)	2.30	3
3,5-Dinitroanilide of:									
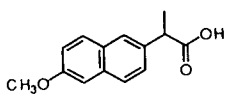	5.4 (*R*)	1.21	3.44 (*R*)	1.14	2.23 (*R*)	1.24	2.88 (*R*)	1.19	1, 2

[a] Values in brackets correspond to data reported in ref. 4.
[b] Absolute configuration of the least retained enantiomer.

of a CSP. This is the case for the present naproxen-derived CSP 2. Additional differences in the behavior of CSPs 1B and 2 and the mechanistic origins of these differences will be addressed subsequently.

In response to one reviewer's question regarding the origin of the much increased enantioselectivity afforded by CSP 2 for the last two entries in Table II, we can but *speculate*. Similar but less dramatic reductions of retention and enhancement of enantioselectivity are observed when these analytes are chromatographed on another naproxen-derived tertiary amide CSP (*i.e.* N–CH_3 instead of N–H). NMR studies of analyte–selector combinations are underway in the hope that a better understanding of the details of these recognition processes can be so attained.

It is known that the mode of attachment to silica can play an important role in determining retention and enantioselectivity. It is not unreasonable to think that, by virtue of the fact that the selector is doubly tethered, the spacing between the selector strands are altered. This could affect enantioselectivity in a manner expected to be rather analyte dependent.

ACKNOWLEDGEMENT

This work has been supported by grants from the National Science Foundation and from Eli Lilly and Company. Chromatographic solvents

TABLE II

SEPARATION OF SOME π-ACIDIC ENANTIOMERS ON NAPROXEN-DERIVED CSPs

Conditions: 2-propanol–hexane (20:80) at 2.0 ml/min flow-rate. Void volumes measured with TTBB.

3,5-Dinitrobenzamide of:	CSP 1A			CSP 1B			CSP 2		
	k'_1	k'_2	α	k'_1	k'_2	α	k'_1	k'_2	α
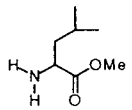	5.57	9.93	1.78	5.17	10.78	2.09	4.06	7.26	1.79
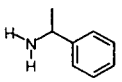	9.50 (*S*)	10.83	1.14	8.44 (*S*)	10.51	1.25	8.99 (*S*)	11.09	1.23
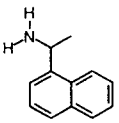	14.20 (*S*)	16.90	1.19	11.20 (*S*)	15.31	1.37	10.67 (*S*)	19.87	1.86
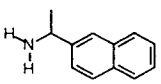	11.77 (*S*)	13.97	1.19	9.58 (*S*)	12.73	1.33	11.83 (*S*)	14.81	1.25
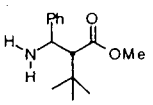	9.87	20.93	2.12	8.68	21.27	2.45	4.12	27.49	6.67
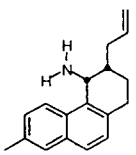	15.53	25.40	1.64	14.46	24.03	1.66	7.95	46.55	5.86

were generously provided by EM Science. C.J.W. received support in the form of a Graduate Fellowship from the Department of Education Advanced Opportunities in Chemistry Program.

REFERENCES

1 T.D. Doyle, C.A. Brunner and E. Smith, *US Pat.*, 4 919 803 (April 1990).
2 T.D. Doyle, in W.J. Lough (Editor), *Chiral Liquid Chromatography*, Chapman & Hall, New York, 1989, pp. 102–128.
3 L. Oliveros, C. Minguillón, B. Desmazières and P. Desbène, *J. Chromatogr.*, 589 (1992) 53.
4 L. Oliveros, C. Minguillón, B. Desmazières and P. Desbène, *J. Chromatogr.*, 606 (1992) 9.
5 W.H. Pirkle, K.C. Deming and J.A. Burke III, *Chirality*, 3 (1991) 183.
6 W.H. Pirkle, T.C. Pochapsky, G.S. Mahler, D.E. Corey, D.S. Reno and D.M. Alessi, *J. Org. Chem.*, 51 (1986) 4991.
7 W.H. Pirkle, D.W. House and J.M. Finn, *J. Chromatogr.*, 192 (1980) 143.

Journal of Chromatography A, 659 (1994) 75–86
Elsevier Science B.V., Amsterdam

CHROM. 25 566

Investigation on the chiral discrimination mechanism using an axially asymmetric binaphthalene-based stationary phase for high-performance liquid chromatography

Shuichi Oi, Hiroyuki Ono, Hideyuki Tanaka, Yutaka Matsuzaka and Sotaro Miyano*

Department of Biochemistry and Engineering, Faculty of Engineering, Tohoku University, Aramaki-Aoba, Aoba-ku, Sendai 980 (Japan)

(First received July 13th, 1993; revised manuscript received September 9th, 1993)

ABSTRACT

The chiral discrimination mechanism of 3,5-dinitrophenyl-derivatized enantiomeric alcohols, amines and carboxylic acids using a chiral stationary phase (CSP) prepared by bonding (*aS*)-1,1′-binaphthyl-2,2′-dicarboxylic acid to 3-aminopropylsilanized silica gel was investigated. Studies of the elution behaviour of a series of structurally related analytes on the CSP and ^{1}H NMR measurements of a solubilized model compound of the CSP and analytes indicated that a π-donor–acceptor interaction between one of the naphthalene planes of the CSP and the 3,5-dinitrophenyl ring of the analyte cooperates with the dipole stacking interaction between two sets of amide linkages of the CSP and the analytes to determine the stability of the diastereomeric adsorbates.

INTRODUCTION

The direct separation of enantiomers by high-performance liquid chromatography (HPLC) on chiral stationary phases (CSPs) has been the subject of intense investigations and a wide variety of CSPs have been developed [1–4]. Although many of the exact mechanisms of the chiral recognition by such CSPs still remain to be elucidated, so-called "brush-type" CSPs, which are based on chiral molecules bonded to silica gel, are known to be most amenable to rationalization by the use of chiral recognition models [3] and hence theoretical treatments [5,6]. Among such models, those based on the π-donor–acceptor interactions between CSPs and analytes, as proposed by Pirkle and co-workers [7–9], have been the most successful, giving a good guide for the design of novel CSPs of predictable performance.

In a previous paper, we described the preparation and performance of CSPs derived from axially asymmetric 2′-substituted-1,1′-binaphthyl-2-carboxylic acids bonded to aminoalkylsilanized silica gels through an amide linkage by use of the 2-carboxylic function [10]. The 2′-substituents tested included –CN, –COOH, $-CONH_2$, –CONHEt, $-CONEt_2$ and $-OCH_3$. At first, we suspected that incorporation of highly polar substituents such as –COOH and $-CONH_2$ might be disadvantageous owing to non-stereoselective, excessive selector–analyte interactions via strong hydrogen bonding causing

* Corresponding author.

0021-9673/94/$07.00
SSDI 0021-9673(93)E0996-8

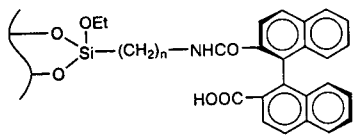

Fig. 1. Structure of CSP 1.

too much retention and peak tailing [11,12]. On the contrary, however, it has been found that a CSP with a 2′-carboxy substituent (CSP 1) is the best among those tested (Fig. 1); CSP 1 discriminates a wide range of enantiomeric amino acids, amines and alcohols as their 3,5-dinitrophenyl derivatives and biaryls bearing 2,2′-polar substituents in normal-phase HPLC [10]. Effective chiral discrimination of enantiomeric alcohols as the 3,5-dinitrophenylcarbamates is the most characteristic feature of CSP 1, and a tentative chiral discrimination model of such analytes has also been presented, in which simultaneous π-donor–acceptor interactions and dipole stacking interactions between the selector and the analyte play a critical role (Fig. 2). This paper presents the results of related investigations performed to shed more light on the mechanism by studying the HPLC behaviour of a series of structurally related analytes on CSP 1 and ^{1}H NMR measurements of a model compound of the CSP and analytes.

EXPERIMENTAL

General

Liquid chromatography was performed using a Shimadzu LC-6A apparatus equipped with a Shimadzu SPD-6A ultraviolet detector set at 254 nm.

IR spectra were measured on a Shimadzu IR-460 grating spectrophotometer. ^{1}H NMR spectra were recorded on a JEOL JNM-FX 60 instrument at 60 MHz or a Bruker AC-250T instrument at 250 MHz in the ^{2}H lock mode with tetramethylsilane as an internal standard.

Optical rotations were recorded on a Union PM-101 automatic digital polarimeter in a 1-cm cell.

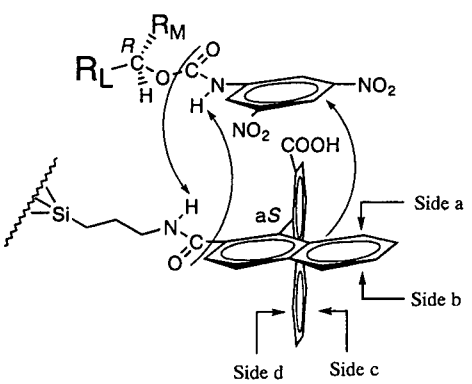

Fig. 2. Schematic representation of the more stable adsorbates formed from CSP 1 and derivatized (*R*)-alcohols.

Materials

Commercial materials were used as received unless stated otherwise. Solvents used for HPLC were distilled before use. Diethyl ether, tetrahydrofuran (THF) and dioxane were distilled from sodium diphenylketyl. Dimethylformanide (DMF), hexamethylphosphoric triamide (HMPA) and octylamine were distilled from calcium hydride under reduced pressure. Other amines and dichloromethane were distilled from calcium hydride. These materials were stored under nitrogen. Water-sensitive reactions were routinely carried out in a nitrogen atmosphere. Merck silica gel 60GF$_{254}$ was used for analytical and preparative thin-layer chromatography (TLC). Column chromatography was performed using Nacalai Tesque silica gel 60.

Acyl azides used for the derivatization of 1-phenylethanol were prepared as described [13].

Chiral stationary phase

CSP 1 was as used in a previous study [10], prepared by bonding (*aS*)-1,1′-binaphthyl-2,2′-dicarboxylic acid (**5**) to 3-aminopropylsilanized silica gel (spherical 5-μm particles, microsphere diameter 100 Å); 0.47 mmol binaphthyl unit/g gel.

Preparation of phenyl-substituted homologous alcohols and carboxylic acids

Enantiomeric (*R*)-(+)-1-phenylethanol (**2a**), (*R*)-(−)-2-phenylpropionic acid (**4a**) and (*R*)-(−)-3-phenylbutanoic acid (**4b**) were commercially available, and were used for the preparation of the phenyl-substituted homologous alcohols and carboxylic acids of known enantio-

meric composition. Typical preparations are as follows.

3-Phenyl-1-butanol (2c). To a stirred suspension of $LiAlH_4$ (1.26 g, 33.2 mmol) in dry diethyl ether (10 ml) was added a solution of 3-phenylbutanoic acid (**4b**) (1.86 g, 11.3 mmol) in diethyl ether (40 ml) under a nitrogen atmosphere and the mixture was refluxed for 1.5 h. After the reaction had cooled to 0°C, 2 *M* HCl (50 ml) was added slowly to the mixture. The organic layer was separated and the aqueous layer was extracted with diethyl ether (2 × 20 ml). The combined organic layer was washed with 2 *M* Na_2CO_3 (30 ml) and saturated aqueous NaCl solution (2 × 30 ml) and dried over $MgSO_4$. After filtration, the solvent was removed *in vacuo* to give 1.60 g of **2c** (94% yield). ^1H NMR (C^2HCl_3), δ (ppm) 1.28 (3H, d, CH_3), 1.34 (1H, s, OH), 1.82 (2H, m, CH_2), 2.86 (1H, m, CH), 3.60 (2H, t, CH_2), 7.20 (5H, s, Ar-H); IR (liquid film) (cm^{-1}), 3330, 3055, 2950, 1601, 1493, 1450, 1374, 1047, 762, 700.

1-Bromo-3-phenylbutane. To a mixture of **2c** (1.40 g, 9.32 mmol) and pyridine (0.81 g, 10.2 mmol) was added tribromophosphine (3.28 g, 12.1 mmol) slowly at −10°C. The mixture was then heated to 100°C and kept at this temperature for 15 h. After 2 *M* HCl (30 ml) and diethyl ether (30 ml) had been added to the mixture, it was stirred for 15 min and the precipitate was filtered off, then the solids were rinsed with diethyl ether. The organic layer was separated and the aqueous layer was extracted with diethyl ether (2 × 20 ml). The combined organic layer was washed with 1 *M* Na_2SO_3 (30 ml), 2 *M* Na_2CO_3 (2 × 30 ml) and with saturated aqueous NaCl solution (2 × 30 ml) and dried over $MgSO_4$. After filtration, the solvent was evaporated *in vacuo* and the residue was distilled by the Kugelrohr method under reduced pressure to give 1.70 g of 1-bromo-3-phenylbutane (86% yield). ^1H NMR (C^2CHl_3), δ (ppm) 1.27 (3H, d, CH_3), 2.08 (2H, m, CH_2), 2.65–3.51 (3H, m, CH_2, CH), 7.20 (5H, s, Ar-H); IR (liquid film) (cm^{-1}), 3055, 2950, 1601, 1491, 1453, 1375, 1258, 762, 700.

4-Phenylpentanoic acid (4c). To magnesium turnings (1.56 g, 64.1 mmol) in dry diethyl ether (25 ml) was added 1,2-dibromoethane (1.20 g, 6.41 mmol) under a nitrogen atmosphere and the mixture was irradiated with ultrasound (35 W, 41 kHz) for 30 min. To the activated magnesium was added dropwise a solution of 1-bromo-3-phenylbutane (1.37 g, 6.41 mmol) in diethyl ether (30 ml) over 1 h under ultrasound irradiation and the mixture was irradiated under reflux for 1 h to give a solution of 3-phenylbutylmagnesium bromide. The solution of the Grignard reagent was then added to crushed dry-ice (50 g) and the mixture was allowed to warm to room temperature. The mixture was extracted with 2 *M* NaOH (3 × 50 ml) and combined aqueous layer was washed with diethyl ether (2 × 30 ml). After the aqueous layer had been acidified with concentrated HCl and saturated with NaCl, the liberated carboxylic acid was extracted with diethyl ether (5 × 50 ml) and the combined organic layer was washed with saturated aqueous NaCl solution (2 × 50 ml) and dried over $MgSO_4$. After filtration, the solvent was removed *in vacuo* to give 0.89 g of **4c** (78% yield). ^1H NMR (C^2HCl_3), δ (ppm) 1.27 (3H, d, CH_3), 1.92 (2H, m, CH_2), 2.23 (2H, t, CH_2), 2.73 (1H, m, CH), 7.16–7.32 (5H, m, Ar-H), 11.0 (1H, br, COOH); IR (liquid film) (cm^{-1}), 3500–2500, 3025, 2950, 1710, 1450, 1283, 1221, 938, 762, 700.

Other compounds. 2-Phenyl-1-propanol (**2b**), 4-phenyl-1-pentanol (**2d**) and 5-phenylhexanoic acid (**4d**) were prepared similarly as above.

2b: ^1H NMR (C^2HCl_3), δ (ppm) 1.23 (3H, d, CH_3), 1.36 (1H, s, OH), 2.90 (1H, m, CH), 3.66 (2H, d, CH_2), 7.20 (5H, s, Ar-H); IR (liquid film) (cm^{-1}), 3350, 3030, 2960, 1605, 1500, 1455, 1040, 1020, 760, 700.

2d: ^1H NMR (C^2HCl_3), δ (ppm) 1.26 (3H, d, CH_3), 1.34–1.68 (5H, m, CH_2 and OH), 2.69 (1H, m, CH), 3.56 (2H, t, CH_2), 7.14–7.31 (5H, m, Ar-H); IR (liquid film) (cm^{-1}), 3330, 3025, 2950, 1600, 1491, 1448, 1058, 760, 700.

4d: ^1H NMR (C^2HCl_3), δ (ppm) 1.24 (3H, d, CH_3), 1.47–1.63 (4H, m, CH_2), 2.30 (2H, t, CH_2), 2.69 (1H, m, CH), 7.15–7.32 (5H, m, Ar-H), 10.9 (1H, br, COOH); IR (liquid film) (cm^{-1}), 3500–2500, 3025, 2950, 1709, 1453, 1287, 1221, 938, 762, 700.

Preparation of derivatized enantiomeric analytes [14]

Derivatization of alcohols. Carbamates of 1-

phenylethanol were prepared by treating an excess amount of isocyanates or acyl azides (the azides were thermally converted *in situ* into the isocyanates [14]) with 1-phenylethanol (**2a**) in dioxane in the presence of triethylamine as described before for the preparation of 1′-phenylethyl 3,5-dinitrophenylcarbamate (**2**α) [10]. 3,5-Dinitrophenylcarbamates (**2**β–δ) of phenylalkanols (**2b–d**) were similarly prepared.

Derivatization of amines. The preparation of N′-(1′-phenylethyl) - N - (3,5-dinitrophenyl)urea (**3a**) is representative. 1-Phenylethylamine (20 mg, 0.17 mmol) was added to a solution of 3,5-dinitrophenyl isocyanate (50 mg, 0.24 mmol) in dioxane (1 ml) (the azide could not be used because it reacted with amines to give the corresponding amides) and stirred at room temperature for 30 min. After 3-dimethylaminopropylamine (20 μl) had been added to the mixture to remove excess isocyanate, it was subjected to TLC to give a sample of **3a**.

Derivatization of carboxylic acids. The preparation of 2′-phenylpropion-3,5-dinitroanilide (**4**α) is representative. A mixture of 2-phenylpropionic acid (**4a**) (20 mg, 0.13 mmol), 3,5-dinitroaniline (24 mg, 0.13 mmol), 1,3-dicyclohexylcarbodiimide (DCC) (54 mg, 0.26 mmol) and pyridine (10 μl) in dichloromethane (1 ml) was stirred at room temperature for 24 h and then subjected to TLC to give a sample of **4**α.

Although the reaction was much accelerated by the use of 4-dimethylaminopyridine in place of pyridine as the base, the derivatization of enantiomerically pure carboxylic acids resulted in the formation of the racemic anilides.

Preparation of model compounds for NMR analysis

The preparation of atropisomerically pure 1,1′-binaphthyl-2,2′-dicarboxylic acid (**5**) has been previously reported [15–17].

*(aS)-2′-Octylcarbamoyl-1, 1′-binaphthyl-2-carboxylic acid [(aS)-**1**].* To a stirred solution of (*aS*)-**5** (1.00 g, 2.92 mmol) in THF (30 ml) was added a solution of DCC (0.602 g, 2.92 mmol) in THF (20 ml) at room temperature for 1 h under a nitrogen atmosphere. The mixture was stirred for another 2 h at that temperature and then heated at reflux for 4 h. After cooling to room temperature, triethylamine (0.5 ml) and octylamine (0.453 g, 3.50 mmol) were added, and the mixture was heated at reflux for 3 h. The mixture was allowed to cool to room temperature, precipitated N,N′-dicyclohexylurea was filtered off and the solids were rinsed with small portions of THF. The solvent was distilled from the filtrate under reduced pressure and the residue was dissolved in chloroform (50 ml). The solution was washed with concentrated HCl (2 × 50 ml) and then with water (4 × 50 ml) and dried over $MgSO_4$. After filtration, the solvent was evaporated *in vacuo* to give 1.29 g of a mixture of unchanged (*aS*)-**5**, (*aS*)-**1** and (*aS*)-2,2′-bis(octylcarbamoyl)-1,1′-binaphthyl.

As the separation of the mixture as such into each component was difficult, the desired (*aS*)-**1** was purified via the methyl ester as follows. The mixture was dissolved in HMPA (10 ml) and then a 25% (w/w) aqueous solution of NaOH (1.1 ml) was added. After stirring for 1 h at room temperature, methyl iodide (1.2 ml) was added to the solution and stirring was continued for another 1 h. Then, was added 2 *M* HCl (20 ml) to the mixture, which was then extracted with diethyl ether (3 × 20 ml). The combined organic layer was washed with 2 *M* HCl (2 × 20 ml) and water (2 × 20 ml) and dried over $MgSO_4$. After filtration, the solvent was evaporated *in vacuo* to give 1.14 g of the residue, which was chromatographed on a silica gel column (100 g) with hexane–ethyl acetate (2.5:1) as eluent to give 0.66 g of the methyl ester of (*aS*)-**1**. This was then dissolved in ethanol (10 ml) with warming, and a solution of KOH (1.0 g) in water (3 ml) was added. After the mixture had been heated at reflux for 3 h, volatiles were removed under reduced pressure. The residue was dissolved in water (40 ml) and washed with diethyl ether (2 × 10 ml) to remove non-acidic compounds. The aqueous layer was acidified with concentrated HCl and the resulting precipitate was extracted with ethyl acetate (3 × 20 ml). The combined organic layer was washed with water (3 × 20 ml) and dried over $MgSO_4$. After filtration, the solvent was removed *in vacuo* to give 0.53 g of (*aS*)-**1** as a colourless glass [40% yield based on the starting (*aS*)-**5**].

$[\alpha]_D^{20}$ −106° (*c* 1.00, acetone); ^{1}H NMR (C^2HCl_3), δ (ppm) 0.75–1.29 (15H, m, CH_2, CH_3), 3.00 (2H, m, CH_2), 6.62 (1H, m, NH), 6.90–8.01 (12H, m, Ar-H); IR (KBr) (cm^{-1}), 3750–2600, 3390, 2915, 1696, 1591, 1552, 822, 760.

(S)-1'-Phenylethyl 3,5-dinitrophenylcarbamate [(S)-2α]. A solution of (*S*)-1-phenylethanol (**2a**) {0.28 g, 2.3 mmol; $[\alpha]_D^{23} = -41.3°$ (neat)}, 3,5-dinitrobenzoylazide (0.82 g, 3.5 mmol) and one drop of triethylamine in dioxane (10 ml) was stirred at 100°C for 1 h; the azide was converted into the isocyanate *in situ* and allowed to react with the alcohol. To the solution was added 3-dimethylaminopropylamine (0.5 ml) to remove excess isocyanate and the solvent was removed *in vacuo*. The residue was purified by silica gel column chromatography (100 g) with hexane–ethyl acetate (6:1) as eluent to give 0.76 g of (*S*)-**2α** as a pale yellow solid (94% yield). ^{1}H NMR (C^2HCl_3), δ (ppm) 1.65 (3H, d, CH_3), 5.94 (1H, q, CH), 7.28 (1H, br, NH), 7.26–7.41 (5H, m, Ar-H), 8.62 [2H, d, *o*-H of 3,5-$(NO_2)_2C_6H_3$], 8.68 [1H, t, *p*-H of 3,5-$(NO_2)_2C_6H_3$].

By using (*R*)-1-phenylethanol {$[\alpha]_D^{23} = +42°$ (neat)}, (*R*)-**2α** was similarly prepared as above.

^{1}H NMR chemical shift measurements

Samples for ^{1}H NMR measurements were prepared by diluting measured amounts of (*aS*)-**1** and (*S*)- or (*R*)-**2α** to 0.1 mol dm^{-3} with C^2HCl_3. All measurements were carried out at 250 MHz at 20°C.

RESULTS AND DISCUSSION

As is generally recognized, enantiomer separation on a CSP requires that the analyte should contain properly arranged functionalities, which may be either steric or electronic in nature, for interaction with complementary sites in the CSP [3]. Fig. 2 shows the proposed model for the more stable adsorbates of enantiomeric alcohols as the 3,5-dinitrophenylcarbamates on CSP 1 [10]. The plane which contains the CSP amide linkage, –CO–NH–CH–, is twisted *ca.* 50° downward from the connected naphthalene plane, and hence the lower side of the amide plane is shielded by the lower half of the vertical naphthalene (side d). This in turn means that side d of the said naphthalene plane is blocked by the amide hydrogen and the connecting arm of the CSP, allowing the dipole stacking interaction between the two sets of the amide linkages of the selector and analyte only from upper side of the horizontal naphthalene plane (side a). Thus, only the overlap of the 3,5-dinitrophenyl ring with the horizontal naphthalene plane on side a can cooperate with the dipole stacking interaction between two sets of the properly arranged amide linkages of the selector and analyte, resulting in the *R* enantiomer of the carbamate analyte being more retained by the chiral selector bearing the (*aS*)-binaphthyl axis. The conformation of the analyte in Fig. 2 is different from that postulated by Pirkle and House [18,19] to be the most heavily populated in solution, in that the carbinyl hydrogen is not eclipsed with the carbonyl oxygen. The latter conformational arrangement, however, has frequently been precedented. For example, Lipkowitz *et al.* [5] showed an example where a model carbamate has torsion angle defined by the carbonyl C=O and carbinyl C–H bonds is 60°, as suggested by MM2C and MM2D force-field calculations and MNDO semi-empirical molecular orbital methods (a similar *gauche* disposition of the carbonyl oxygen and the carbinyl hydrogen was also postulated by Uccelo-Barretta *et al.* [20]). Further, it is known that the energy barriers separating minima of conformational isomers are usually between 2 and 5 kcal mol^{-1} (1 kcal = 4.184 kJ), ensuring rapid interconversion between the conformational states. Therefore, it may not be unreasonable to assume that the balance between the steric repulsion and lipophilic interaction on approach of the analyte to the CSP allows a slight conformational change of the analyte to be approximated as suggested [10]. It has also been suggested that the π-donor–acceptor interactions may be possible between the CSP and analyte on both sides b and c, but seemingly they are non-stereoselective as space-filling Corey–Pauling–Koltun (CPK) model inspections indicate [10]. The following data support the soundness of the proposed

chiral discrimination mechanism of the 3,5-dinitrophenyl-derivatized analytes by CSP 1.

Importance of π-accepting site in the analyte

In order to assess the contribution of π-acidic sites of the analyte for chiral separation [18], ten carbamates were prepared from 1-phenylethanol (**2a**) and analysed on CSP 1. The data in Table I exhibit a large, although not monotonous, decrease in retention (k') and selectivity (α) with decrease in the electron-withdrawing ability of the aryl carbamate moiety. As expected, the retention and selectivity decrease considerably with the phenylcarbamates bearing an *ortho*-substituent, indicating that the vicinity of the amide nitrogen is vital for chiral recognition and the presence of a superfluous substituent in this region imposes severe steric repulsion between the selector and analyte. These results show that cooperation of the π-donor–acceptor interaction with the dipole stacking interaction between the selector and analyte plays the dominant role in the retention and chiral recognition by CSP 1, the highest retention and separation being obtained with the 3,5-dinitrophenylcarbamate. The longer retention of the 4-methoxyphenylcarbamate compared with the 4-methylphenyl counterpart, which is inconsistent with the order of the electronic effects of the substituents, may be indicative of the contribution of non-stereoselective hydrogen bonding interactions between the methoxyl oxygen and the 2′-carboxylic proton of the CSP. The isopropylcarbamate results in no separation with little retention, showing the critical importance of a π-accepting site in the analyte.

Table I also contains the results of the separation of enantiomeric 2-phenylpropionic acid (**4a**) as the various amides and will be discussed later.

^{1}H NMR studies of a model compound of CSP 1 and enantiomeric analytes

Although diastereomeric complexes formed from a working CSP and enantiomeric analytes may be significantly different from those of a solubilized model CSP analogue and analytes, it has been well demonstrated that NMR studies on rationally designed CSP model compounds and analytes can be a great aid in the elucidation of the chiral discrimination mechanism by CSPs [20,21].

In a previous paper [10], we reported a good separation of the 3,5-dinitrophenylcarbamates derived from enantiomeric alcohols by CSP 1; a separation factor (α) of 1.59 was obtained from the carbamate (**2α**) of 1-phenylethanol (**2a**) using

TABLE I

SEPARATION OF CARBAMATES OF 1-PHENYLETHANOL (**2a**) AND AMIDES OF 2-PHENYLPROPIONIC ACID (**4a**)

Mobile phases: hexane–2-propanol, (A) 95:5 and (B) 90:10. Flow-rate: 1 ml/min. k' = Capacity factor for the first-eluted enantiomer. The configuration of the first-eluted enantiomer is indicated in parentheses. The separation factor, α, is the ratio of the capacity factors of the enantiomers.

R	$PhCH(CH_3)OCONH$-R			$PhCH(CH_3)CONH$-R		
	Eluent	k'_1	α	Eluent	k'_1	α
$3,5\text{-}(NO_2)_2C_6H_3$	A	18.20(*S*)	1.59	B	14.18(*R*)	1.59
$2,4\text{-}(NO_2)_2C_6H_3$	A	1.44	1.00	B	2.10(*R*)	1.07
$p\text{-}NO_2C_6H_4$	A	10.89(*S*)	1.20	B	10.73(*S*)	1.32
$3,5\text{-}Cl_2C_6H_3$	A	3.21(*S*)	1.23	B	3.28(*R*)	1.40
$2,4\text{-}Cl_2C_6H_3$	A	0.34	1.00	B	0.71(*R*)	1.05
$p\text{-}ClC_6H_4$	A	3.10(*S*)	1.12	B	5.45(*R*)	1.22
C_6H_5	A	2.37(*S*)	1.06	B	3.77(*R*)	1.14
$p\text{-}CH_3C_6H_4$	A	1.98(*S*)	1.05	B	3.33(*R*)	1.14
$p\text{-}CH_3OC_6H_4$	A	4.04(*S*)	1.03	B	6.37(*R*)	1.11
$i\text{-}C_3H_7$	A	0.86	1.00	B	1.74(*R*)	1.06

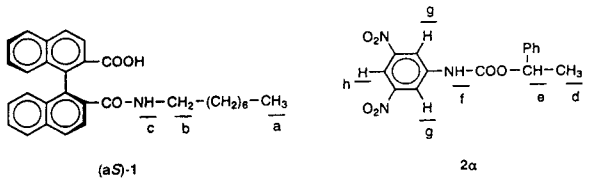

Fig. 3. Structures of model compounds of CSP 1 and analytes.

5% 2-propanol in hexane as the eluent (Table I). As chiral separation by the axially asymmetric binaphthalene-based CSPs seemed almost independent on the length of the arms connecting to the solid support [10], we chose (*aS*)-2′-octylcarbamoyl-1,1′-binaphthyl-2-carboxylic acid [(*aS*)-**1**] as the solubilized model compound for CSP 1 (Fig. 3). Taking into account of the results of Pirkle and Pochapsky [21] and of Uccelo-Barretta *et al.* [20], NMR studies in chloroform may be reasonably used to interpret normal-phase chromatographic separations by CSP 1. Thus, deuterochloroform (C^2HCl_3) was used as a solvent of low polarity to amplify the induced shift differences caused by mixing of the two pertinent components. Table II summarizes the results of the ^1H NMR measurements, and shows the chemical shifts of the selected protons in (*aS*)-**1**, (*S*)- and (*R*)-**2α** in the free, *aS*, *S* and *aS*, *R* mixtures. Although the induced shifts on mixing are small, they are generally in accordance with the expected shielding effect by the naphthalene plane and the deshielding effect by dipole stacking interactions and/or hydrogen bonding.

A larger upfield shift of aromatic H_g protons ($\Delta\delta H_g = +0.053$) of the *aS*, *R* complex compared with that ($\Delta\delta H_g = +0.015$) of the *aS*, *S* complex should be noted. This indicates that H_g protons of the *aS*, *R* complex are more closely disposed over the naphthalene plane via π-donor–acceptor interactions than those of the *aS*, *S* complex. Similarly, a downfield shift of the amide H_c proton ($\Delta\delta H_c = -0.020$) of the *aS*, *R* complex compared with a very small upfield shift ($\Delta\delta H_c = +0.006$) of the *aS*, *S* complex indicates that the H_c proton of the former complex is more deshielded than the latter, presumably via dipole stacking interaction with the urethane amide bond of **2α**. Induced shifts of the other protons are similar in both the *aS*, *S* and *aS*, *R* complexes, which may be the result of the non-stereoselective interactions of (*aS*)-**1** and the enantiomeric **2α** on mixing. These ^1H NMR observations may indicate that the attractive interaction of (*aS*)-**1** is stronger with (*R*)-**2α** than with (*S*)-**2α**, which is consistent with the chromatographic behaviour of enantiomeric **2α** in that (*R*)-**2α** is more retained than (*S*)-**2α** by CSP 1 bearing an (*aS*)-binaphthyl axis.

Here again, from the stereospecificity of the induced shifts of the H_g and H_c protons, it may be said that a π-donor–acceptor interaction between the 3,5-dinitrophenyl ring of **2α** and the naphthalene ring of CSP 1 and a dipole stacking

TABLE II

^1H NMR CHEMICAL SHIFTS OF SELECTED PROTONS IN (*aS*)-**1** AND (*S*)- OR (*R*)-**2α** IN THE FREE, *aS*, *R* AND *aS*, *S* MIXTURES

All shifts measured at 250 MHz relative to tetramethylsilane in C^2HCl_3 at 20°C. Concentration 0.1 *M* for components. Shifts are reported for the centre of multiplets.

Proton	Free (δ, ppm)	*aS*, *R* (δ, ppm)	Δδ (ppm)	*aS*, *S* (δ, ppm)	Δδ (ppm)	$\Delta\lvert\delta(aS, S) - \delta(aS, R)\rvert$
H_a	0.873	0.870	+0.003	0.870	+0.003	0.000
H_b	3.024	3.062	−0.038	3.051	−0.027	0.011
H_c	6.627	6.647	−0.020	6.621	+0.006	0.026
H_d	1.648	1.574	+0.074	1.560	+0.088	0.014
H_e	5.933	5.875	+0.058	5.876	+0.059	0.001
H_f	7.279	8.180	−0.901	8.193	−0.909	0.008
H_g	8.621	8.568	+0.053	8.607	+0.015	0.038
H_h	8.681	8.602	+0.079	8.607	+0.073	0.006

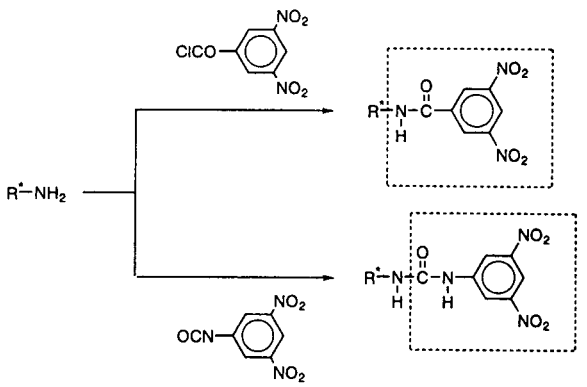

Fig. 4. Derivatization of enantiomeric amines.

interaction between the urethane bond of **2**α and the amide bond of CSP 1 act cooperatively in chiral recognition by CSP 1.

Improvement of the chiral separation of amines by conversion into 3,5-dinitrophenylureas

The chiral discrimination model for enantiomeric alcohols as the 3,5-dinitrophenylcarbamates (Fig. 2) emphasizes that the direction of the –CO–NH– linkage connecting to the 3,5-dinitrophenyl nucleus, *i.e.*, –CO–NH–Ar (Ar = 3,5-dinitrophenyl), also plays an important role in attractive interactions with the CSP by dipole stacking interactions. Previously [10], however, chiral separation of amines was carried out as their 3,5-dinitrobenzoyl derivatives. This seemingly resulted in an inferior separation of the derivatized amines by CSP 1 because of the mismatched direction of the amide linkage, *i.e.*, –NH–CO–Ar, for the dipole stacking interaction to cooperate effectively with the π-donor–acceptor interaction. This reasoning led us to adjust the mode of the attachment of the π-accepting moiety by converting amines into the 3,5-dinitrophenylurea derivatives. This could be accomplished by using 3,5-dinitrophenyl isocyanate (Fig. 4). The chromatographic data in Table III and Fig. 5 clearly show the increased retention as judged from the composition of the eluent used and the significant improvement in the chiral separation.

Chiral separation of enantiomeric carboxylic acids as the 3,5-dinitroanilides

Derivatization of carboxylic acids into the 3,5-dinitroanilides builds up a structure that is closely related to the 3,5-dinitrophenylcarbamates from the corresponding alcohols in that both have the –CO–NH–Ar linkage as indicated in Fig. 6. Further, the chiral centre of the acid derivative is α to the carbonyl centre, whereas that of the alcohol derivative is β, separated by the intervening ester oxygen. This situation strongly suggests that carboxylic acids as the 3,5-dinitroanilides should be better separated by CSP 1 than the corresponding alcohols as the 3,5-dinitrophenylcarbamates based on the proposed chiral discrimination model (Fig. 2). Table IV gives several examples of such separations of

TABLE III

COMPARISON OF THE SEPARATION OF AMINES AS THE 3,5-DINITROPHENYLUREAS (**3a–c**) WITH THAT AS THE 3,5-DINITROBENZAMIDES (**3′a–c**)

Mobile phases: hexane–2-propanol, (B) 90:10 and (D) 80:20, and hexane–ethanol, (E) 90:10 and (F) 80:20. See Table I for HPLC conditions.

R^1	R^2	$R^1CHR^2NHCONH$-3,5-$(NO_2)_2C_6H_3$ (**3**)				R^1CHR^2NHCO-3,5-$(NO_2)_2C_6H_3$ (**3′**)			
		3	Eluent	k'_1	α	**3′**	Eluent	k'_1	α
CH_3	Ph	**3a**	F	4.48(*S*)	1.30	**3′a**	D	6.55(*S*)	1.17[a]
CH_3	1-Naphth	**3b**	F	5.47(*S*)	1.24	**3′b**	D	7.90	1.07[a]
CH_3	n-C_6H_{13}	**3c**	E	4.45	1.16	**3′c**	B	5.34	1.00[a]

[a] Data from ref. 10.

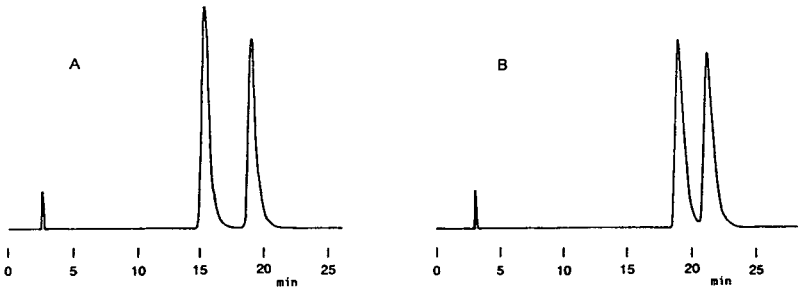

Fig. 5. Chromatographic separation of enantiomers on CSP 1. (A) N′-(1′-Phenylethyl)-N-(3,5-dinitrophenyl)urea (**3a**); (B) N-(3′,5′-dinitrobenzoyl)-1-phenylethylamine (**3′a**). Chromatographic conditions as in Table III.

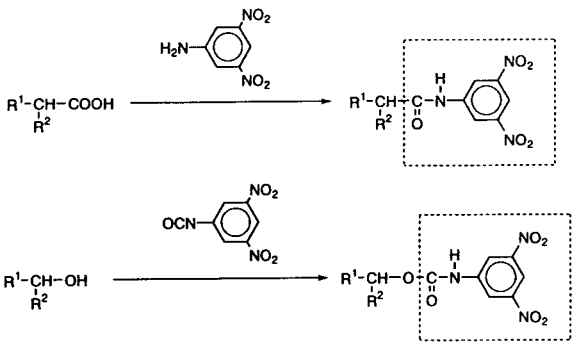

Fig. 6. Appropriate derivatization of enantiomeric carboxylic acids compared with that of alcohols.

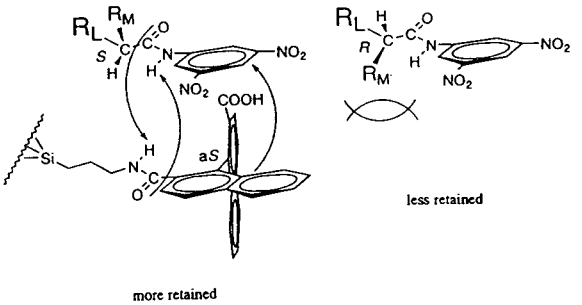

Fig. 7. Chiral discrimination model for enantiomeric carboxylic acids as the 3,5-dinitroanilides.

carboxylic acid derivatives compared with those of the alcohol counterparts. Interestingly, the anilides of (*R*)-carboxylic acids elute first on the (*aS*)-binaphthyl chiral selector. This is in good accord with the chiral discrimination model depicted in Fig. 7, which is a rational outcome of the model shown in Fig. 2.

The right-hand side of Table I clearly shows

TABLE IV

COMPARISON OF THE SEPARATION OF CARBOXYLIC ACIDS AS THE 3,5-DINITROANILIDES WITH THAT OF ALCOHOLS AS THE 3,5-DINITROPHENYLCARBAMATES

Mobile phases: hexane–2-propanol, (B) 90:10 and (C) 85:15. See Table I for HPLC conditions.

R^1	R^2	R^1CHR^2CONH-3,5-$(NO_2)_2C_6H_3$			R^1CHR^2OCONH-3,5-$(NO_2)_2C_6H_3$		
		Eluent	k'_1	α	Eluent	k'_1	α
CH_3	C_2H_5	B	12.33	1.08	B	5.36	1.00
CH_3	n-C_4H_9	B	8.97(*R*)	1.27	B	4.38	1.15
CH_3	n-C_6H_{13}	B	7.93	1.37	B	3.93(*S*)	1.21
CH_3	Ph	C	7.57(*R*)	1.63	C	3.86(*S*)	1.54[a]
C_2H_5	Ph	C	7.26(*R*)	1.46	C	3.44	1.53[a]
n-C_3H_7	Ph	C	7.02	1.47	C	3.33	1.43[a]

[a] Data from ref. 10.

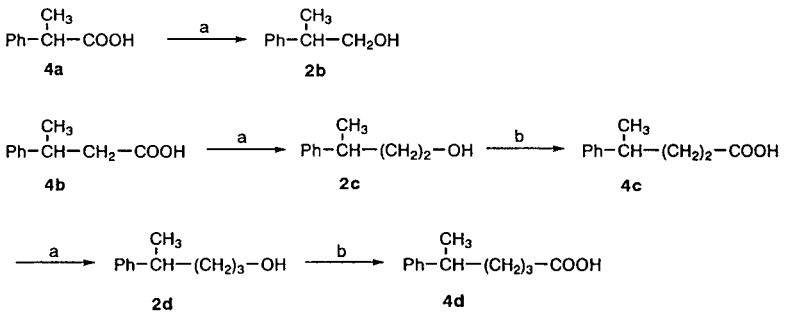

Fig. 8. Preparation of phenyl-substituted homologous alcohols and carboxylic acids. (a) $LiAlH_4$–Et_2O; (b) (1) PBr_3–pyridine, (2) Mg–Et_2O, (3) CO_2, (4) H^+–H_2O.

the importance of a π-acidic site for the derivatized carboxylic acid analytes. Table I also shows the better separation, in general, of the carboxylic acid derivatives than the corresponding alcohol counterparts.

Separation of homologous α- to δ-chiral alcohols and carboxylic acids as the 3,5-dinitrophenyl derivatives

Studies of the HPLC elution behaviour of suitable homologous series of compounds, in which stereochemistry and performance can be correlated, are of great help in elucidating the arrangement of the diastereomeric complexes formed from a chiral selector and analytes.

Enantiomerically pure 1-phenylethanol (**2a**), 2-phenylpropionic acid (**4a**) and 3-phenylbutyric acid (**4b**) are readily available, and were utilized for the preparation of a series of samples of phenyl-substituted homologous alcohols (**2a–d**) and carboxylic acids (**4a–d**) of known enantiomeric compositions (Fig. 8). Table V summarizes the separation of the derivatized homologous alcohols (**2α–δ**) and carboxylic acids (**4α–δ**) bearing a phenyl substituent on the α- to δ-carbon atom from the hydroxyl oxygen and carboxyl carbon, respectively.

CSP 1 can discriminate the α- and β-chiral alcohols as the 3,5-dinitrophenylcarbamates (**2α** and **2β**), but not the derivatized γ-chiral alcohol (**2γ**). As will be discussed later, the stereochemistry of the first eluting enantiomer of **2α** is *S*, whereas that of **2β** alters to *R* by intervention of one methylene unit between the chiral centre and the hydroxyl oxygen.

In the series of the carboxylic acid derivatives, an increase in the distance of the chiral centre from the carbonyl group by intervention of methylene unit(s) also results in a significant decrease in selectivity (α). However, the derivat-

TABLE V

SEPARATION OF HOMOLOGOUS α- TO δ-CHIRAL ALCOHOLS AND CARBOXYLIC ACIDS AS THE 3,5-DINITROPHENYL DERIVATIVES

Mobile phase: hexane–2-propanol (85:15). See Table I for HPLC conditions.

n	$PhCH(CH_3)(CH_2)_nOCONH$-3,5-$(NO_2)_2C_6H_3$ (**2**)			$PhCH(CH_3)(CH_2)_nCONH$-3,5-$(NO_2)_2C_6H_3$ (**4**)		
	2	k'_1	α	**4**	k'_1	α
0	**2α**	3.86(*S*)	1.54[a]	**4α**	7.57(*R*)	1.63
1	**2β**	5.05(*R*)	1.09	**4β**	7.82(*R*)	1.50
2	**2γ**	5.23	1.00	**4γ**	8.14(*S*)	1.07
3	**2δ**	4.99	1.00	**4δ**	9.79	1.00

[a] Data from ref. 10.

ized γ-chiral carboxylic acid (**4γ**) can still be discriminated by CSP 1. Here again, alternation of the absolute configuration of the first-eluting enantiomers of the homologous acid derivatives, $PhCH(CH_3)(CH_2)_nCONHAr$, with the intervening methylene unit number ($n = 0$, 1 and 2) should be noted.

Table V indicates that the separability of **2α** is similar to that of **4β**. The chiral centre of these analytes is located β from the carbonyl carbon, and the absolute stereochemistry of the first-eluting enantiomers is the same as illustrated in Fig. 9B. A similar situation holds for the chromatographic behaviour of **2β** and **4γ**, except that the chiral centre is located γ from the carbonyl carbon and the stereochemistry of the first-eluting enantiomers is altered (Fig. 9C). Hence it may be concluded that CSP 1 discriminates the chiral centre of $PhCH(CH_3)(CH_2)_n$–X–CONHAr ($n = 0$ and 1) irrespective of whether the intervening X group is O or CH_2. On the other hand, shorter retentions of the derivatized alcohols (**2α** and **2β**) compared with those of the corresponding carboxylic acid derivatives (**4β** and **4γ**), respectively, may be ascribed to the electron-donating resonance effect of the ester oxygen lone pair in the amide system reducing the dipole stacking interaction. It should be noted that 1-phenylethylamine as the 3,5-dinitrophenylurea (**3a**) falls in the same category as **2α** and **4β** (Fig. 9B), although the presence of a superfluous, mismatched amide linkage seemingly reduces the separability to some extent.

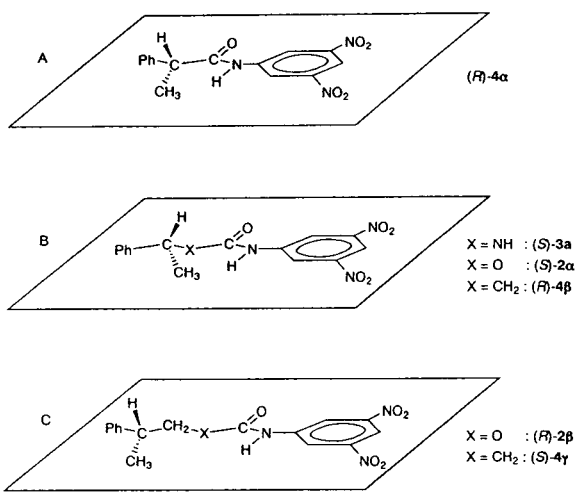

Fig. 9. Configuration of the first-eluting 3,5-dinitrophenyl-derivatized analytes.

For convenience, Fig. 9 schematically presents selected examples of the first-eluting analytes bearing a –CO–NH–Ar linkage when eluted on CSP 1. This kind of illustrative presentation is of great help in grasping the absolute stereochemistry of the chiral centre of these molecules, because the *R* and *S* designation (*e.g.*, Table V) varies with the substituent priority sequence. The molecular planes in Fig. 9 are defined by disposing pertinent atoms or groups of the analytes according to the proposed chiral discrimination model by CSP 1 (Fig. 2) [10]. It should be noted that the molecular arrangement is not inconsistent with Prelog's generalization to predict the stereochemistry of the addition of a nucleophile to chiral alkyl esters of benzoylformic acid [22]. It can be seen that those enantiomeric analytes which have the methyl substituent disposed on the underside of the molecular plane always elute faster than the enantiomeric counterparts which have the hydrogen disposed on the underside, irrespective of whether the intervening X functionality is O, CH_2 or NH.

CONCLUSIONS

The chiral discrimination mechanism of enantiomeric analytes by CSP 1 has been investigated. Generally, the model depicted in Fig. 2 explains well the HPLC behaviour of the 3,5-dinitrophenyl derivatized alcohols, and the model can be applied to the corresponding amine and carboxylic acid derivatives. The π-donor–acceptor interaction between one of the naphthalene planes of the CSP and the 3,5-dinitrophenyl ring of the analyte cooperates with the steric fit of the amide linkages for dipole stacking between the two species mainly to determine the magnitude of the resolution and retention. Because of this, the elution order of the enantiomers shows a high degree of regularity, which may permit the assignment of the absolute configurations of properly derivatized analytes based on the elution order with considerable confidence.

ACKNOWLEDGEMENTS

We are grateful to the Ministry of Education, Science and Culture, Japan (Grant-in-Aid No. 02555177), and to Tosoh for financial support.

REFERENCES

1 S.G. Allenmark, *Chromatographic Enantioseparation, Methods and Applications*, Ellis Horwood, Chichester, 1988.
2 A.M. Krstulović (Editor), *Chiral Separations by HPLC*, Ellis Horwood, Chichester, 1989.
3 W.H. Pirkle and T.C. Pochapsky, *Chem. Rev.*, 89 (1989) 347.
4 E. Francotte and A. Junker-Buchheit, *J. Chromatogr.*, 576 (1992) 1.
5 K.B. Lipkowitz, D.A. Demeter, R. Zegarra, R. Larter and T. Darden, *J. Am. Chem. Soc.*, 110 (1988) 3446.
6 S. Topiol, M. Sabio, J. Moroz and W.B. Caldwell, *J. Am. Chem. Soc.*, 110 (1988) 8367.
7 W.H. Pirkle and M.H. Hyun, *J. Chromatogr.*, 322 (1985) 309.
8 W.H. Pirkle, C.J. Welch and B. Lamm, *J. Org. Chem.*, 57 (1992) 3854.
9 W.H. Pirkle and M.H. Hyun, *J. Org. Chem.*, 49 (1984) 3043.
10 S. Oi, M. Shijo, H. Tanaka, S. Miyano and J. Yamashita, *J. Chromatogr.*, 645 (1993) 17.
11 W.H. Pirkle and C.J. Welch, *J. Chromatogr.*, 589 (1992) 45.
12 L. Oliveros, C. Minguillón, B. Desmazières and P.-L. Desbène, *J. Chromatogr.*, 606 (1992) 9.
13 J. Munch-Petersen, *Org. Synth., Coll. Vol.*, 4 (1963) 715.
14 W.H. Pirkle, T.C. Pochapsky, G.S. Mahler, D.E. Corey, D.S. Reno and D.M. Alessi, *J. Org. Chem.*, 51 (1986) 4991.
15 S. Oi, Y. Matsuzaka, J. Yamashita and S. Miyano, *Bull. Chem. Soc. Jpn.*, 62 (1989) 956.
16 S. Oi, K. Matsunaga, T. Hattori and S. Miyano, *Synthesis*, (1992) 895.
17 T. Ohta, M. Ito, K. Inagaki and H. Takaya, *Tetrahedron Lett.*, 34 (1993) 1615.
18 W.H. Pirkle and D.W. House, *J. Org. Chem.*, 44 (1979) 1957.
19 See, *e.g.*, J.A. Dale and H.S. Mosher, *J. Am. Chem. Soc.*, 95 (1973) 512.
20 G. Uccelo-Barretta, C. Rosini, D. Pini and P. Salvadori, *J. Am. Chem. Soc.*, 112 (1990) 2707.
21 W.H. Pirkle and T.C. Pochapsky, *J. Am. Chem. Soc.*, 109 (1987) 5975.
22 J.D. Morrison and H.S. Mosher, *Asymmetric Organic Reactions*, Prentice-Hall, Englewood Cliffs, NJ, 1971, pp. 55–83.

Journal of Chromatography A, 659 (1994) 87–93
Elsevier Science B.V., Amsterdam

CHROM. 25 558

High-performance liquid chromatographic separations of naphthoquinones and their derivatives

Effect of hydrogen bonding on retention

Wenche Stensen and Einar Jensen*

Department of Plant Physiology and Microbiology, IBG, University of Tromsø, N-9037 Tromsø (Norway)

(First received May 17th, 1993; revised manuscript received September 14th, 1993)

ABSTRACT

A method for the separation and determination of fifteen naphthoquinone derivatives was developed, based on reversed-phase high-performance liquid chromatography and ultraviolet–visible detection. The effect on the selectivity of different mobile phase compositions (*e.g.*, methanol–water and acetonitrile–water binary mixtures and methanol–acetonitrile–water ternary mixture) was investigated. The retention order of the compounds with methanol–water as eluent is interpreted on the basis of intramolecular hydrogen bonding in the solute *versus* intermolecular hydrogen bonding between the solute and the solvent. The hydrogen bonding pattern was studied using quantum chemical calculations.

INTRODUCTION

It is well documented that many 1,4-naphthoquinone derivatives show antimicrobial activity, especially if a hydroxy group is present at the C-5 position [1]. A chlorine substituent in the quinone ring also increases the activity of 1,4-naphthoquinones [2,3], and dichlone (2,3-dichloro-1,4-naphthoquinone) is a well known agricultural fungicide [4].

We have recently tested the effects of several naphthoquinones on some common fish pathogenic bacteria, *Aeromonas salmonicida*, *Vibrio salmonicida* and *V. anguillarum*, and also *Escherichia coli*. The results indicated that very low concentrations (<1 μg/ml) of some of the tested compounds inhibit the growth of the pathogenic bacteria, but have no effect on *E. coli* in the tested concentration range [5]. In order to evaluate the potential use of these naphthoquinones as antibacterial compounds in problems related to fish farming, chromatographic methods for the determination of different naphthoquinones had to be established.

There are few reports describing chromatographic separations and determinations of non-isoprenoid naphthoquinones. In a study of the metabolism of plumbagin in rats, a method based on thin-layer chromatography has been used [6]. Marston and Hostettmann [7] demonstrated the separation of six different naturally occurring naphthoquinones using a μBondapak CN column, and Rittich and Krska [8] used Micro Pak Si-10 and CN-10 columns in an attempt to separate a mixture of quinones.

We wanted to find analytical methods for a subsequent study of some of the naphthoquinones and their metabolites in a biological matrix. However, none of the above-mentioned methods seemed to be appropriate in this respect. We therefore found it necessary to

* Corresponding author.

0021-9673/94/$07.00
SSDI 0021-9673(93)E0999-B

develop methods for the separation and determination of a wide range of natural and synthetic naphthoquinone derivatives (Fig. 1). In general, a metabolite is more polar than its parent substance [9], so on a reversed-phase column metabolites are expected to elute before the substrate as retention time decreases with increasing polarity. With this in mind, we decided to use a reversed-phase C_{18} column.

During the work we observed that the retention order of some of the compounds was the opposite of what was expected from a superficial understanding of retention mechanisms in reversed-phase systems. In order to explain the observed results, we used semi-empirical molecular orbital calculations to derive the hydrogen bonding patterns for some typical naphthoquinones.

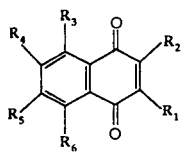

Compound	R1	R2	R3	R4	R5	R6
1	H	H	H	H	H	H
2	H	H	OH	H	H	H
3	H	H	OH	H	H	OH
4	CH_3	H	OH	H	H	H
5	CH_3	H	OH	H	CH_3	H
6	CH_3	H	OCH_3	H	CH_3	H
7	CH_3	CH_3	OH	H	CH_3	H
8	CH_3	CH_2CH_3	OH	H	CH_3	H
9	CH_3	H	OH	CH_2CH_3	CH_3	H
10	CH_3	H	OH	CH_3CO	CH_3	H
11	CH_3	H	OH	H	CH_3	CH_3CO
12	CH_3	H	OCH_3	CH_3CO	CH_3	H

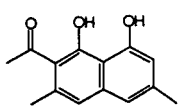

13

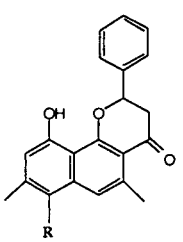

Compound	R
14	H
15	Cl

Fig. 1. Structures of naphthoquinone derivatives.

EXPERIMENTAL

Methanol and acetonitrile, obtained from Lab-Scan and Fluka, respectively, were of HPLC grade. Water was distilled and filtered through a 0.45-μm Millipore filter.

5-Hydroxy-1,4-naphthoquinone (juglone) (**2**) and 5-hydroxy-2-methyl-1,4-naphthoquinone (plumbagin) (**4**) were purchased from Aldrich. 1,4-Naphthoquinone (**1**), 5,8-dihydroxy-1,4-naphthoquinone (naphtazarin) (**3**), 5-hydroxy-2,7-dimethyl-1,4-naphthoquinone (**5**), 5-methoxy-2,7-dimethyl-1,4-naphthoquinone (**6**), 5-hydroxy-2,3,7-trimethyl-1,4-naphthoquinone (**7**), 3-ethyl-5-hydroxy-2, 7-dimethyl-1,4-naphthoquinone (**8**), 6-ethyl-5-hydroxy-2,7-dimethyl-1,4-naphthoquinone (**9**), 6-acetyl-5-hydroxy-2,7-dimethyl-1,4-naphthoquinone (**10**), 8-acetyl-5-hydroxy-2,7-dimethyl-1,4-naphthoquinone (**11**), 6-acetyl-5-methoxy-2, 7-dimethyl-1, 4-naphthoquinone (**12**), 2-acetyl-3,6-dimethyl-1,8-naphthalenediol (**13**), 10-hydroxy-5,8-dimethyl-2-phenyl- 2,3- dihydronaphtho[1,2-*b*]pyran- 4 -one (**14**), and 7-chloro-10-hydroxy-5,8-dimethyl-2-phenyl -2,3- dihydronaphtho[1,2-*b*]pyran- 4 -one (**15**) were generously donated by Dr. J.C. Overeem, TNO Research Institute, Zeist, Netherlands.

Solutions of naphthoquinones in methanol for HPLC analysis were in the concentration range 0.05–0.10 μg/μl, and 10–15 μl were injected on to the column. The mobile phase was a combination of the following solutions: (a) methanol with 30 m*M* acetic acid, (b) water with 30 m*M* acetic acid and (c) acetonitrile with 30 m*M* acetic acid.

Separations were performed on a Waters HPLC system consisting of a Model 600 E multisolvent delivery system, a column heater, a Model 712 Wisp autoinjector, a Model 486 absorbance detector operated at 415 nm and a Model 746 integrator. A Waters Nova-Pak 4-μm C_{18} reversed-phase column (150 × 3.9 mm, I.D.) operated at 30°C was used. The flow-rate was 1 ml/min. UV–Vis spectra were recorded on a Shimadzu UV 160 spectrophotometer.

Semi-empirical molecular orbital calculations were performed on a Silicon Graphics Personal Iris 4D/30 EG computer using the programs Quanta 3.3/CHARMm 22 [10] and MOPAC v

5.00 [11]. Starting conformations for the quantum mechanical calculations were obtained from CHARMm-optimized structures. The semi-empirical calculations were performed using the AM1 Hamiltonian with full geometry optimization.

RESULTS AND DISCUSSION

All the naphthoquinones and their derivatives were yellow to reddish powders or crystalline needles. They absorbed visible light relatively strongly and by studying their UV–Vis spectra (Table I), 415 nm was found to be a suitable wavelength for chromatographic detection. This wavelength was convenient because our experience indicated that with a biological sample, less interference from other substances in the matrix can be expected the longer is the wavelength used.

TABLE I

UV–VIS SPECTROSCOPIC DATA

The compounds were dissolved in 96% ethanol.

Compound	λ (nm)	Log ε	Compound	λ (nm)	Log ε
1	274	3.46	**9**	277	3.92
	333	3.50		415[a]	3.65
	415[a]	2.26		434	3.68
2	271	3.55	**10**	278	4.02
	415[a]	3.56		415[a]	3.88
	423	3.57			
3	280	3.92	**11**	277	4.01
	415[a]	3.37		415[a]	3.66
	488	3.88		425	3.68
4	276	3.87	**12**	273	3.91
	415[a]	3.77		357	3.60
				415[a]	2.71
5	276	3.90	**13**	275	3.89
	415[a]	3.62		347	3.73
	423	3.63		415[a]	3.32
6	274	3.99	**14**	276	3.89
	400	3.77		389	3.93
	415[a]	3.71		415[a]	3.46
7	282	4.06	**15**	275	4.11
	415[a]	3.70		393	3.83
	422	3.71		415[a]	3.49
8	281	4.04			
	415[a]	3.61			
	422	3.62			

[a] Wavelength used for chromatographic detection.

Isocratic elution

First, a study of the chromatographic behaviour of the naphthoquinones and their derivatives was carried out with different isocratic methanol–water compositions as mobile phase. Table II gives the retention times of the compounds listed in order of elution. With the system used, *i.e.*, a reversed-phase column and an aqueous mobile phase, the most polar solutes are least retained. The observed order of elution was as expected for some of the compounds; naphthoquinones **2**, **4**, **5** and **7** with no, one, two and three methyl groups, respectively, eluted in order of increasing lipophilicity. However, the elution order was unexpected in some series. For

TABLE II

CAPACITY FACTORS (k') IN DIFFERENT ISOCRATIC ELUTIONS WITH METHANOL–WATER AS MOBILE PHASE

Compound	k'						
	Methanol concentration (%)						
	40	50	55	60	65	70	80
1	4.0	1.9	1.4	1.0	0.7	0.5	–
2	5.9	2.8	2.0	1.1	1.1	0.8	–
11	10.4	4.1	2.7	1.8	1.2	0.9	–
3	–	4.0	2.9	2.3	1.6	1.2	–
6	12.5	4.6	3.0	2.0	1.3	0.9	–
12	13.2	4.8	3.0	2.0	1.3	0.9	–
4	15.3	6.6	4.5	3.1	2.1	1.5	–
10	–	9.2	5.7	3.6	2.4	1.6	–
5	–	–	9.0	5.9	3.9	2.6	–
13	–	–	16.3	9.1	5.4	3.2	1.6
7	–	–	21.5	13.0	8.2	5.2	2.3
9	–	–	–	–	12.7	7.7	3.0
8	–	–	–	–	13.8	8.3	3.2
14	–	–	–	–	19.0	13.5	4.0
15	–	–	–	–	–	28.2	8.2

instance, compounds **1**, **2** and **3** with no, one and two hydroxyl groups, respectively, would be expected on the basis of the number of polar functional groups to elute in the opposite order. In addition, the regioisomers **10** and **11** separated unexpectedly well, in contrast to **8** and **9**, which eluted with similar retentions.

The precise mechanism of retention is difficult to describe owing to the complexity of the possible mechanisms, and various theories have been put forward pointing out which interactions are important in reversed-phase chromatography [12–14]. The general opinion appears to be that interactions between solute and mobile phase are of great importance. For polar molecules in a polar solvent the most powerful interaction is hydrogen bonding. The mobile phase in our system consisted of polar protic solvents that are able to form strong hydrogen bonds. The solutes are all hydrogen bond acceptors (carbonyl and hydroxyl groups) and in addition some are hydrogen bond donors (hydroxyl groups), hence all the compounds are able to form hydrogen bonds with the solvents. However, naphthoquinones with hydroxyl groups in *peri* positions to the carbonyl functions are able to form strong intramolecular hydrogen bonds, creating a six-membered ring. It is well known that most intramolecular hydrogen bonding occurs when six-membered rings can be formed [15]. There will then be a competition between intramolecular (solute–solute) and intermolecular (solute–solvent) hydrogen bonding, where in general the intramolecular interaction will win. A classical example of this relationship is seen in nitrophenols: *o*-nitrophenol, which forms an intramolecular hydrogen bond, is eight times less soluble in water than the *para* isomer [16]. The effect of intramolecular solute hydrogen bonding on retention on silica and alumina stationary phases has been discussed previously [17].

Theoretical energy calculations of the naphthoquinones with a hydroxyl group in a *peri* position show an internal hydrogen bond that is approximately three times stronger than the binding energy between two water molecules [18]. Experimental evidence for the presence of a strong hydrogen bond in similar systems has also been reported using NMR and IR spectroscopy [19,20], adsorption chromatography [21] and liquid–liquid chromatography [22].

On the basis of the theory that the intermolecular solute–solvent hydrogen bonding interaction is the most important retention mechanism, the order of elution is easier to explain. For the naphthoquinone series **1**, **2** and **3**, **1** has two free carbonyl groups that can act as hydrogen bond acceptors for water and methanol. The interaction is consequently large and the compound distributes easily in the mobile phase and will thus be very little retained. Naphthoquinone **3**, on the other hand, has two strong intramolecular hydrogen bonds, rendering the two quinonoid carbonyls much less efficient hydrogen bond acceptors, and hence it dissolves less efficiently in the mobile phase and is more retained than **1**. Naphthoquinone **2**, with one intramolecular hydrogen bond and one free carbonyl group, shows intermediate retention.

The same argument can be used to explain the relative retention between **10** and **12** and between **5** and **6**. Naphthoquinones **10** and **12** have the same structure except that the hydroxyl group in **10** is replaced by a methoxy group in **12**. The expected effect of this should be that **12** is less polar than **10** and would therefore be more retained, which is the opposite of what is observed. The reason for this is again found in intramolecular hydrogen bonding. Naphthoquinone **10** forms an intramolecular hydrogen bond which is precluded by the methoxy group in **12**. The result is that **12** has two free hydrogen bond acceptor carbonyls whereas **10** has only one. Consequently, **12** dissolves more easily in the mobile phase and is less retained than **10**. The effect of breaking the intramolecular hydrogen bond by a methoxy group is likewise seen in the retentions of **5** and **6**.

Isomeric compounds often show similar retentions in reversed-phase chromatography [23], as we observed for **8** and **9**. In this context, the retention difference between **10** and **11** is striking; **11** is much less retained than **10**. Although a hydrogen bond between the hydroxyl group and the acetyl function can be envisaged for **10**, calculations show this to be of minor importance.

TABLE III

CAPACITY FACTORS (k') AND RESOLUTION (R_s) FOR NON-BASELINE-SEPARATED PEAKS WITH GRADIENT ELUTION

Gradient A, methanol–water: linear gradient from 40% to 80% methanol in 40 min followed by isocratic elution with 80% methanol for 10 min. Gradient B, acetonitrile–water: linear gradient from 25% to 75% acetonitrile in 55 min. Gradient C, methanol–acetonitrile–water: linear gradient from 37% to 80% methanol–acetonitrile (93:7) in 43 min followed by isocratic elution with 80% methanol–acetonitrile (93:7) for 10 min.

Compound	k' (R_s)		
	Gradient A	Gradient B	Gradient C
1	4.1	5.8	4.5
2	5.8	7.3	6.3
11	9.2	11.8	10.1
3	7.8	8.8 (1.3)	8.1
6	10.2 (0.5)	9.7 (1.3)	11.1 (1.2)
12	10.6 (0.5)	13.1 (0.4)	11.6 (1.2)
4	11.9	13.5 (0.4)	12.5
10	15.1	17.4	16.0
5	18.2	19.3	18.7
13	23.3	24.6	24.0
7	25.4	25.9	25.7
9	29.5 (1.0)	30.9 (0.6)	30.0 (0.7)
8	30.0 (1.0)	31.2 (0.6)	30.4 (0.7)
14	34.5	37.2	34.9
15	39.9	43.8	39.9

Consequently, the intramolecular hydrogen bonding pattern is expected to be similar for both compounds. One quinonoid carbonyl is occupied in intramolecular hydrogen bonding, leaving the other quinonoid carbonyl and the acetyl free for intermolecular hydrogen bonding in both compounds. The difference in elution order can be explained by their different accessibilities for intermolecular hydrogen bonding. Geometry optimisation of **11** placed the carbonyl in the acetyl group perpendicular to the ring plane, whereas for **10** the carbonyl formed an angle of approximately 40° to ring plane pointing towards the methyl group. The acetyl group is therefore less sterically hindered for hydrogen bonding towards the solvent in **11** than in **10**.

Gradient elution

None of the isocratic methanol–water elutions separated all fifteen compounds (Table II). The pairs of compounds **6**–**12** and **11**–**3** eluted nearly simultaneously with methanol–water (1:1). On lowering the methanol content in the mobile phase, **6** and **12** were partly resolved but **3** showed very poor chromatographic properties. Based on Table II, a methanol–water gradient (gradient A in Table III) was defined that separated all the components except **6** and **12** and the regioisomers **8** and **9** (Fig. 2).

It has been demonstrated that replacing meth-

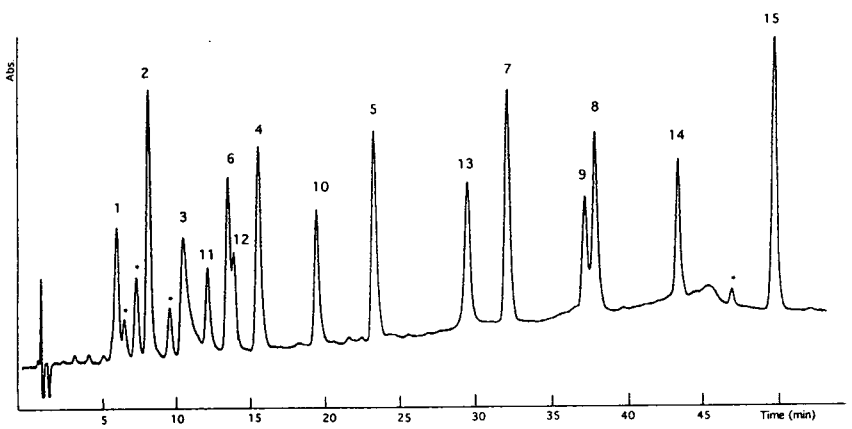

Fig. 2. HPLC separation of naphthoquinones with a linear methanol–water gradient (gradient A in Table III). The relative concentrations are not identical in the chromatograms. Asterisks indicate impurities.

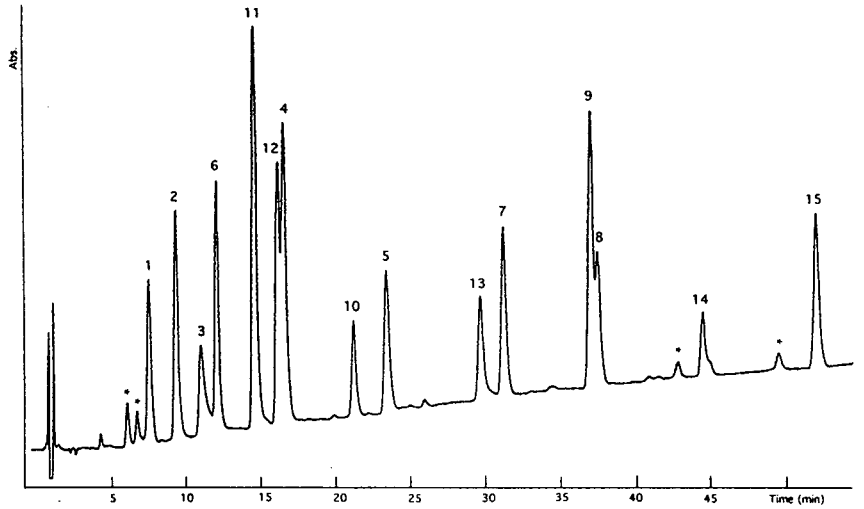

Fig. 3. HPLC separation of naphthoquinones with a linear acetonitrile–water gradient (gradient B in Table III). The relative concentrations are not identical in the chromatograms. Asterisks indicate impurities.

anol with acetronitrile in the mobile phase gives a slightly different selectivity towards compounds that are difficult to separate in methanol–water systems [24]. Employing this principle, a linear acetonitrile–water gradient (gradient B in Table III) was applied and baseline separated compounds **6** and **12**. However, the separation between the regioisomers **9** and **8** and between **12** and **4** decreased (Fig. 3).

Therefore, a ternary gradient composed of methanol, acetonitrile and water was constructed (gradient C in Table III). This system gave an acceptable solution to the separation problem, although **6** and **12** were not baseline separated

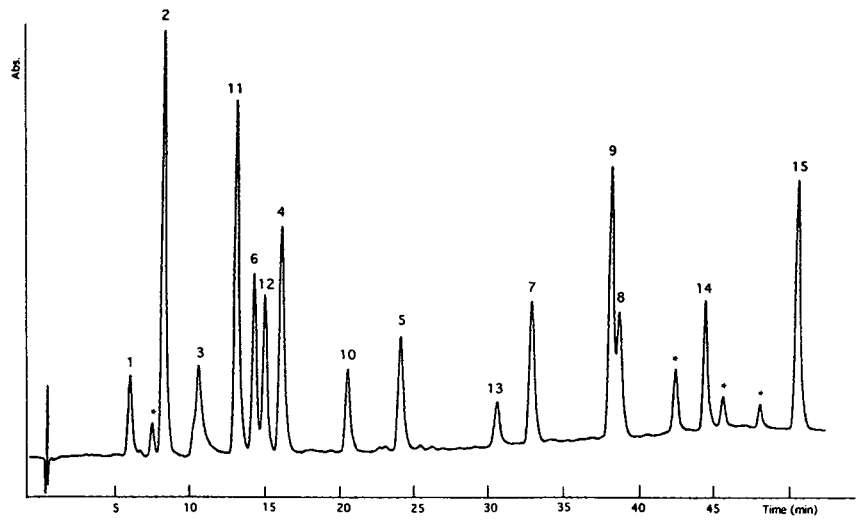

Fig. 4. HPLC separation of naphthoquinones with a ternary gradient composed of methanol–acetonitrile–water (gradient C in Table III). The relative concentrations are not identical in the chromatograms. Asterisks indicate impurities.

(resolution 1.2) (Fig. 4). In addition, the regioisomers **9** and **8** were not adequately resolved, but this pair could be separated in an additional isocratic analysis with methanol–water (65:35) (Table II).

CONCLUSIONS

Chromatographic methods employing a ternary gradient were developed that separated thirteen of fifteen naphthoquinones and naphthoquinone derivatives; the two remaining compounds had to be separated in an additional step. Hydrogen bonding between the solute and the solvent can explain the observed retention with methanol–water eluents. Intramolecular hydrogen bonding in the solute led to less solubility in the eluent resulting in an increase in the retention. Consequently, compounds with polar substituents will not necessarily be less retained on a reversed-phase column. This result indicates that the assumption that the metabolites of the naphthoquinones will have decreased retention compared with the parent substance will not always be true.

ACKNOWLEDGEMENTS

Financial support from the Norwegian Research Council (NFR) is gratefully acknowledged. Thanks are also due to Dr. Jan Raa for introducing us to the field of marine antibiotics, to Dr. Jan C. Overeem for providing the different naphthoquinones and to Dr. John S. Svendsen for performing the calculations.

REFERENCES

1 B.A. Kulkarni, V.D. Kelkar and P.L. Kulkarni, *Indian J. Pharm. Sci.*, 45 (1983) 21.
2 A.V.B. Sankaram, T.N. Srinivasan and A.S. Indulkar, *Pestic. Sci.*, 6 (1975) 165.
3 V. Ambrogi, D. Artini, I. De Carneri, S. Castellino, E. Dradi, W. Logemann, G. Meinardi, M. Di Somma, G. Tosolini and E. Vecchi, *Br. J. Pharmacol.*, 40 (1970) 871.
4 S. Budavari (Editor), *The Merck Index*, Merck, Rahway, NJ, 11th ed., 1989, p. 3032.
5 J. Raa, personal communication.
6 B. Chandrasekaran and B. Nagarajan, *J. Biosci.*, 3 (1981) 395.
7 A. Marston and K. Hostettmann, *J. Chromatogr.*, 295 (1984) 526.
8 B. Rittich and M. Krska, *J. Chromatogr.*, 130 (1977) 189.
9 H.P. Rang and M.M. Dale, *Pharmacology*, Churchill Livingstone, New York, 2nd ed., 1991, p. 91.
10 B.R. Brooks, R.E. Bruccoleri, B.D. Olafson, D.J. States, S. Swaminathan and M. Karplus, *J. Comput. Chem.*, 4 (1983) 187.
11 J.J.P. Stewart and F.J. Seiler, *MOPAC: A General Molecular Orbital Package*, QCPE 455, Department of Chemistry, Indiana University, Bloomington, IN.
12 S.R. Bakalyar, R. McIlwrick and E. Roggendorf, *J. Chromatogr.*, 142 (1977) 353.
13 P.E. Antle, A.P. Goldberg and L.R. Snyder, *J. Chromatogr.*, 321 (1985) 1.
14 J.G. Dorsey and K.A. Dill, *Chem. Rev.*, 89 (1989) 331.
15 J. March, *Advanced Organic Chemistry*, Wiley, New York, 4th ed., 1992, p. 76.
16 R.T. Morrison and R.N. Boyd, *Organic Chemistry*, Allyn and Bacon, Newton, MA, 5th ed., 1987, p. 998.
17 L.R. Snyder, *Principles of Adsorption Chromatography*, Marcel Dekker, New York, 1968, p. 315.
18 L.A. Curtiss and M. Blander, *Chem. Rev.*, 88 (1988) 827.
19 W.-I. Shiau, E.N. Duesler, I.C. Paul, D.Y. Curtin, W.G. Blann and C.A. Fyfe, *J. Am. Chem. Soc.*, 102 (1980) 4546; and references cited herein.
20 G. Wurm and B. Goessler, *Arch. Pharm. (Weinheim, Ger.)*, 322 (1989) 489.
21 S.B. Padhye and B.A. Kulkarni, *Chromatographia*, 8 (1975) 352.
22 J. Franc and J. Sechovec, *J. Chromatogr.*, 212 (1981) 139.
23 L.R. Snyder and J.J. Kirkland, *Introduction to Modern Liquid Chromatography*, Wiley, New York, 2nd ed., 1979, p. 356.
24 E. Jensen, *J. Chromatogr.*, 246 (1982) 126.

Journal of Chromatography A, 659 (1994) 95–99
Elsevier Science B.V., Amsterdam

CHROM. 25 620

Separation of *cis* and *trans* unsaturated fatty acid methyl esters by silver ion high-performance liquid chromatography

Richard O. Adlof

US Department of Agriculture, Agricultural Research Service, National Center for Agricultural Utilization Research, 1815 N. University, Peoria, IL 61614 (USA)

(First received August 23rd, 1993; revised manuscript received October 4th, 1993)

ABSTRACT

A variety of isomeric fatty acid methyl esters were separated on a commercially available silver ion chromatography column utilizing a versatile, isocratic solvent system composed of acetonitrile in hexane and utilizing UV detection. Samples containing all possible *cis* and *trans* isomers derived from methyl oleate (*cis*-9-octadecenoate; 18:1), methyl linoleate (*cis*-9, *cis*-12-octadecadienoate; 18:2), methyl linolenate (*cis*-9, *cis*-12, *cis*-15-octadecatrienoate; 18:3) and methyl arachidonate (*cis*-5, *cis*-8, *cis*-11, *cis*-14-eicosatetraenoate; 20:4) were analyzed. The *cis* and *trans* isomers from methyl oleate, methyl linoleate and methyl linolenate were resolved, as were 15 of the 16 isomers from methyl arachidonate. The separation of the 20:4 isomers exceeded the capability of capillary gas and liquid chromatographic methodologies.

INTRODUCTION

While silver ion liquid chromatography has been utilized to separate fatty acid methyl esters (FAMEs) by number of double bonds and by the configuration (*cis*/*trans*) of the double bonds [1–3], lack of commercial HPLC silver ion columns has limited the impact of this technology. Christie and co-workers [4–7] utilized a commercially available Nucleosil 5SA HPLC column and, by adding silver ions, were able to fractionate a variety of fatty acid isomers.

A commercially available column containing silver ions has recently been developed by Chrompack (ChromSpher Lipids HPLC column). A solvent system (developed by Christie and co-workers [5,6]) composed of dichloromethane, dichloroethane and small amounts (0.01 to 0.025%) of acetonitrile (ACN) is used with both the Nucleosil and Chrompack HPLC columns. Because chlorinated solvents are opaque at the wavelengths (200–210 nm) used for FAME analyses, the use of UV detectors is precluded unless the phenacyl derivatives of the fatty acids are first prepared [6]. We developed a UV-compatible solvent system (acetonitrile in hexane) for the separation of polyunsaturated *cis*- and *trans*-FAMEs.

EXPERIMENTAL

Materials and reagents

Hexane (Allied Fisher Scientific, Orangeburg, NY, USA), isooctane, light petroleum (b.p. 35–60°C) and ACN (all E. Merck, Darmstadt, Germany) were, except for the isooctane, HPLC grade and used as received. The *cis* and *trans* isomer mixtures were prepared from the all-*cis* precursors by *p*-toluenesulfinic acid-catalyzed isomerization [8]. This procedure results in less than 0.5% double bond migration [8,9]. Methyl oleate (*cis*-9-18:1), linoleate (*cis*-9, *cis*-12-18:2), linolenate (*cis*-9, *cis*-12, *cis*-15-18:3) and arachidonate (*cis*-5, *cis*-8, *cis*-11, *cis*-14-20:4) were

SSDI 0021-9673(93)E1050-A

isomerized in this manner. The 50:50 safflower (SFO)–linseed oil (LSO) methyl ester (7.1% 16:0, 3.6% 18:0, 19.9% 18:1, 35.9% 18:2 and 33.1% 18:3) mixture was prepared from commercial samples. All samples were eluted with light petroleum through a silica gel Sep-Pak (Waters, Milford, MA, USA) and dissolved in isooctane.

High-performance liquid chromatography

The HPLC equipment consisted of a Spectra-Physics (Freemont, CA, USA) P2000 solvent-delivery system, a Rheodyne (Cotati, CA, USA) 7125 injector with a 20-μl injection loop and an ISCO (Lincoln, NE, USA) V^4 absorbance detector. The ChromSpher Lipids column (250 mm × 4.6 mm I.D. stainless steel; 5 μm) was purchased from Chrompack (Middelburg, Netherlands) and used as received. Solvent flow was standardized at 1.0 ml/min and run temperatures at 22–23°C. A small cooling fan was used to minimize temperature fluctuations and bubble formation at the solvent pump mixing solenoid.

Analysis

The FAME samples were collected in scintillation vials and the solvents were evaporated. The fractions were analyzed on a Varian (Palo Alto, CA, USA) 3400 gas chromatograph equipped with a 30 m × 0.32 mm SP2380 (Supelco, Bellefonte, PA, USA) capillary column, flame ionization detector and utilizing helium as carrier gas. Thin-layer chromatography (TLC) was done on 3 × 1 in. (1 in. = 2.54 cm) silica gel 60A plates (Whatman, Maidstone, UK) impregnated with 10% silver nitrate. Ag-TLC was necessary for analysis of the eluted *cis/trans* fractions from methyl linolenate and arachidonate, since GC analysis of the former is difficult and has not been done for the latter. TLC solvent systems used were benzene for *cis/trans*-methyl linolenate and chloroform–acetone–acetic acid (96:4:0.5; v/v/v) for *cis/trans*-methyl arachidonate fractionation. TLC plates were sprayed with 2′,7′-dichlorofluorescein, dried and the spots were visualized by UV at 254 nm. TLC R_F values (5 cm solvent front migration) for isomerized methyl linolenate were 0.70 (three *trans*), 0.60 (two *trans*, one *cis*), 0.56 (one *trans*, two *cis*) and 0.44 (three *cis*). For isomerized methyl arachidonate, the values were 0.70 (four *trans*), 0.58 (three *trans*, one *cis*), 0.50 (two *trans*, two *cis*), 0.40 (one *trans*, three *cis*) and 0.38 (four *cis*). The FAMEs were separated only by the total number of *cis* and *trans* double bonds, not by the specific location of the *cis* and *trans* double bonds.

RESULTS AND DISCUSSION

Acetonitrile, the cosolvent of choice for increasing the eluting capability of solvents in silver ion chromatography [2], is soluble in hexane to *ca.* 1.5% (v/v) at 23°C. A binary system composed of hexane and 0.5% ACN in hexane was found to provide a wide range of solvent strengths and excellent baseline stability. However, elution times for methyl linoleate differed when we used a binary system [A–B (50:50) where A = hexane and B = 1.0% ACN in hexane] *vs.* a single solvent reservoir containing 0.5% ACN in hexane. Whether this was due to the HPLC pump, the solvent reservoirs or the solvent mixing solenoid was not investigated. Thus, an isocratic system with a single reservoir containing the appropriate % ACN in hexane mixture was more suitable for column characterization and reproducible FAME separations.

The separation of SFO–LSO methyl esters is shown in Fig. 1. FAME elution reproducibility, resolution and baseline stability were maintained at sample sizes of 17 to 170 μg, although capacity factors (k) decreased approximately 25% between the 17 and 170 μg sample sizes. The trend of longer retention times with smaller sample sizes was consistent throughout our studies. Peak distortion, such as observed when gas chromatographic columns are overloaded, was not observed in our system. Perhaps larger FAME samples compete for silver ion sites the same way the ACN cosolvent competes for those sites. Excellent peak shapes were obtained even with sample elution times of 1.5 to 2.0 h.

Separation of the *cis/trans* isomers of methyl 18:2 (4 isomers; Fig. 2), 18:3 (8 isomers; Fig. 3) and 20:4 (16 isomers; Fig. 4) are illustrated in Figs. 2–4. Baseline separation of the 9-*trans* and 9-*cis*-18:1 isomers was also achieved within 8 min

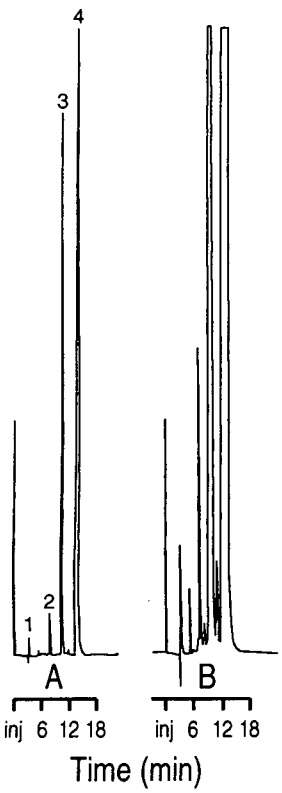

Fig. 1. Separation of SFO–LSO methyl ester standard. Flow-rate: 1.0 ml/min 0.2% ACN in hexane. UV detection at 210 nm. Sample size: A = 17 μg; B = 170 μg. Peaks: 1 = 16:0 and 18:0; 2 = 18:1; 3 = 18:2; 4 = 18:3.

of injection (0.2% ACN in hexane; chromatogram not shown). The order of elution for the methyl linoleate isomers (Fig. 2) was *trans*-9,*trans*-12-; *trans*-9,*cis*-12-; *cis*-9,*trans*-12- and *cis*-9,*cis*-12-18:2. The observed elution order differs from that obtained with capillary GC (SP 2330, SP 2340 or SP 2560 stationary phases) in which *cis*-9,*trans*-12-18:2 elutes before *trans*-9, *cis*-12-18:2.

The separation of all eight *cis*/*trans* isomers of methyl 18:3 (Fig. 3) was similar to, but with better resolution than, the separation obtained on a 50 m CP Sil 88 capillary GC column [10] or by packed capillary supercritical fluid chromatography [11]. The FAMEs eluted in four peaks or sets of peaks corresponding to the total number of *cis* and *trans* double bonds. These are marked as A (three *trans*), B (two *trans*, one *cis*), C (one *trans*, two *cis*) and D (three *cis*).

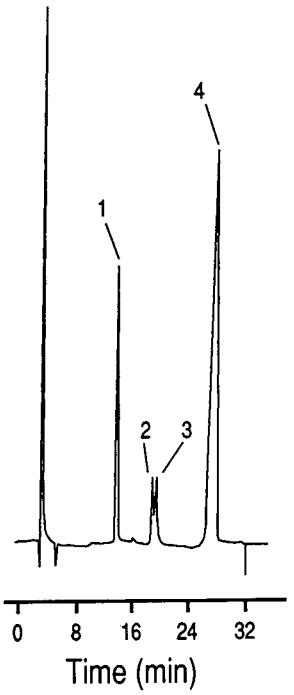

Fig. 2. Separation of isomerized methyl linoleate. Sample size: 20 μg. Flow-rate: 1.0 ml/min 0.125% ACN in hexane. UV detection at 210 nm. Peaks: 1 = *trans*-9, *trans*-12; 2 = *trans*-9, *cis*-12; 3 = *cis*-9, *trans*-12; 4 = *cis*-9, *cis*-12.

The resolution of 15 of the 16 possible *cis*/*trans* isomers of methyl 20:4 (Fig. 4) far exceeded the capabilities of current GC, other HPLC or other analytical methodology. Again, the eluted isomers are grouped by total *cis* and *trans* double bonds, with an elution pattern of A (four *trans*), B (three *trans*, one *cis*), C (two *trans*, two *cis*), D (one *trans*, three *cis*) and E (four *cis*). At 0.15% ACN in hexane, the 20:4 isomers could be separated within 25 min; with this solvent system, all four (three *trans*, one *cis*) isomers can be separated, but one (two *trans*, two *cis*?) of the other isomers is unresolved. These results may be compared to the work by Lanser and Emken [12], who separated isomerized methyl arachidonate into only five fractions on an XE254 silver ion column. As in silver ion TLC, separation was based on total number but not on specific location of the *cis* and *trans* double bonds. Work is currently underway to further identify the 18:3 and 20:4 isomers and to develop solvent systems to minimize *cis*/*trans*

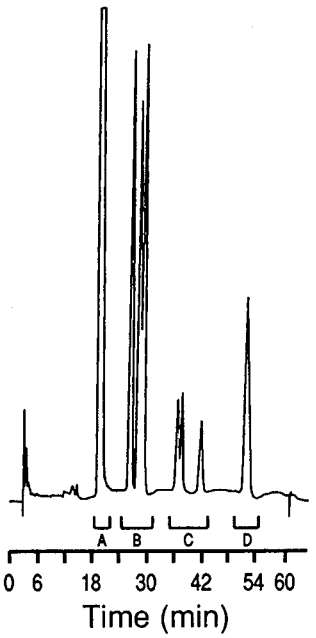

Fig. 3. Separation of isomerized methyl linolenate. Sample size: 20 μg. Flow-rate: 1.0 ml/min 0.125% ACN in hexane. UV detection at 210 nm. Groups: A = three *trans*); B = two *trans*, one *cis*; C = one *trans*, two *cis*); D = three *cis*.

isomer overlap during the analysis of mixtures of 18:2, 18:3, and 20:4 isomers.

Christie and Breckenridge [5], reported a gradual loss in resolution after sometimes only six months of column use. Whether this loss of resolution is due to silver ion removal by the ACN [5,13] or is due to the use of chlorinated solvents (silver salt formation?) is unclear. Another point of interest was the time required to equilibrate the system after changes were made in solvent composition. While the ChromSpher Lipids column had a column volume of *ca.* 3 ml, an increase in ACN concentration was not noted until the introduction of 7 to 8 ml of solvent (determined with refractive index detector). The problem of ACN–silver ion interaction and subsequent ACN retention is not new and may be noted in all forms of chromatography employing silver ions in the stationary phase. In our isocratic system, the column was equilibrated with the appropriate solvent mix for at least 0.5 h before sample injection. Since ACN dissolves very slowly into hexane, the ACN–hexane solvent mix was thoroughly stirred

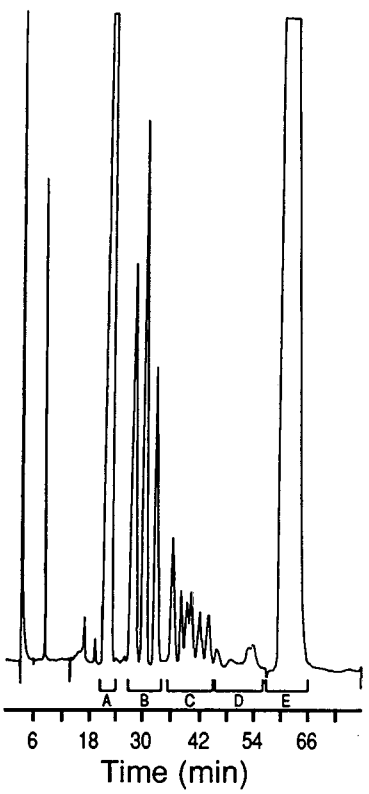

Fig. 4. Separation of isomerized methyl arachidonate. Sample size: 100 μg. Flow-rate: 1.0 ml/min 0.125% ACN in hexane. UV detection at 210 nm. Groups: A = four *trans*; B = three *trans*, one *cis*; C = two *trans*, two *cis*; D = one *trans*, three *cis*; E = four *cis*.

for 5 min before use. To obtain reproducible retention times, thorough mixing of the ACN and hexane is essential.

A solvent system containing 0.125 to 0.15% ACN in hexane can provide good resolution in reasonable time for FAMEs containing up to four double bonds (15–30 min for mono- and dienoic fatty acids, 40–60 min for tri- and tetraenoic fatty acids). Up to 200 μg of sample can be applied to the column without severe peak distortion or significant (>25%) loss of retention with resolutions often exceeding the capabilities of capillary GC. Development of this and other solvent systems and utilizing commercially available silver ion HPLC columns should enhance the importance of this technology in the analysis of triacylglycerides, phospholipids and other unsaturated molecules.

REFERENCES

1 R.O. Adlof and E.A. Emken, *J. Am. Oil Chem. Soc.*, 58 (1981) 99.
2 W.J. DeJarlais and R.O. Adlof, *J. Am. Oil Chem. Soc.*, 60 (1983) 975.
3 R.O. Adlof and E.A. Emken, *J. Am. Oil Chem. Soc.*, 62 (1985) 1592.
4 W.W. Christie, *J. High Resolut. Chromatogr. Chromatogr. Commun.*, 10 (1987) 148.
5 W.W. Christie and G.H. McG. Breckenridge, *J. Chromatogr.*, 469 (1989) 261.
6 B. Nikolova-Damyanova, B.G. Herslof and W.W. Christie, *J. Chromatogr.*, 609 (1992) 133.
7 W.W. Christie, E.Y. Brechany and K. Stefanov, *Chem. Phys. Lipids*, 46 (1988) 127.
8 J.M. Snyder and C.R. Scholfield, *J. Am. Oil Chem. Soc.*, 59 (1982) 469.
9 T.W. Gibson and P. Strassburger, *J. Org. Chem.*, 41 (1976) 791.
10 R.L. Wolf, *J. Chromatogr. Sci.*, 30 (1992) 17.
11 M. Demirbüker, I. Hägglund and L.G. Blomberg, *J. Chromatogr.*, 605 (1992) 263.
12 A.C. Lanser and E.A. Emken, *J. Chromatogr.*, 256 (1983) 460.
13 W.W. Christie, personal communication.

Journal of Chromatography A, 659 (1994) 101–109
Elsevier Science B.V., Amsterdam

CHROM. 25 582

Utilization of high-performance liquid chromatography as an enrichment step for the determination of cyclic fatty acid monomers in heated fats and biological samples

J.L. Sebedio*, J. Prevost, E. Ribot and A. Grandgirard

INRA, Station de Recherches sur la Qualité des Aliments de l'Homme, Unité de Nutrition Lipidique, 17 Rue Sully, 21034 Dijon Cedex (France)

(First received March 29th, 1993; revised manuscript received August 30th, 1993)

ABSTRACT

A method was developed to determine traces of cyclic fatty acid monomers (CFAM) in oils and animal tissues. This method is a combination of some techniques developed earlier but with the enrichment step being achieved by high-performance liquid chromatography (HPLC) instead of urea inclusion. After transformation of the lipids into methyl esters, the latter were hydrogenated after addition of an internal standard (methyl heptadecanoate or ethyl hexadecanoate). The mixture was enriched in CFAM by HPLC on a semi-preparative C_{18} reversed-phase column using acetonitrile–acetone (90:10, v/v) at 4 ml/min. The enriched fraction containing the CFAM and the internal standard was then analysed by gas chromatography on a polar column (cyanosilicone phase). This method was developed using known mixtures of CFAM isolated from both heated sunflower and linseed oils. Small amounts of CFAM (50 μg/g of sample) were determined with good reproducibility without any loss during the HPLC enrichment step and with no modification of the relative proportions of the CFAM in the mixture. This method can be applied to either heated fats and oils or biological samples (heart cell culture) that contain only traces of CFAM. Ethyl hexadecanoate (16:0 ethyl ester) can be used as an internal standard for samples containing small amounts of 17:0.

INTRODUCTION

Among the components of oils that are formed during deep-fat frying [1,2] are cyclic fatty acid monomers (CFAM), which have shown potential toxicity in some cases [3–7]. The structures of these cyclic fatty acids are different if they are formed from linoleic rather than linolenic acids [8–10]. Those formed from linoleic acid are mainly C_{18} monounsaturated acids having a five-carbon α-disubstituted ring, whereas those arising from linolenic acid are a mixture of C_{18} diunsaturated fatty acids having a five- or a six-carbon α-disubsituted ring. The rat has been widely used as a model to study the potential toxicity of heated fats, and we have recently shown that heart cell in culture is a good model to follow the incorporation of CFAM in phospholipids [11]. However, the amounts incorporated into the phospholipids of tissues are small, and it has been very difficult to determine the CFAM very precisely with existing analytical methods [7]. All the methods are based on gas chromatography of the totally hydrogenated fatty acid methyl esters [7,12]. After hydrogenation, the sample to be analysed usually consists of a mixture of straight-chain saturates (mainly 16:0, 18:0, 20:0 and 22:0) and the hydrogenated CFAM. There are basically two methods for their determination. One is a direct GC analysis of the hydrogenated sample [12,13] and the other is the use of an enrichment step prior to

* Corresponding author.

0021-9673/94/$07.00
SSDI 0021-9673(93)E1011-N

GC analysis. This enrichment step is usually carried out by low-temperature crystallization [14] or by urea adduction [15]. Both methods (with or without enrichment steps) present major drawbacks, and Gere *et al.* [16] have shown that discrepancies exist when determining CFAM using the different methods.

Methods using an enrichment step are frequently used [7]. However, urea adduction or low-temperature crystallization does not completely eliminate 18:0 so that some CFAM are eluted in the tailing 18:0 peak and, further, the utilization of urea for enrichment in CFAM results in a loss of about 20% of the cyclic fatty acid during complexation [7]. The problem could be partly resolved by using phenanthrene as an internal standard instead of methyl heptadecanoate (17:0). Phenanthrene would behave in a similar way to cyclic monomers [16]. Further, we have found that the utilization of urea for small sample size brings out many impurities which can be detected during GC analyses. A clean-up procedure was developed by Rojo and Perkins [17] in order to remove interfering substances that co-elute with the CFAM during GC analysis.

We have therefore developed a method to determine small amounts of CFAM in oils and biological samples using a different enrichment step. This method is a combination of hydrogenation of the total methyl esters on PtO_2, enrichment in CFAM using high-performance liquid chromatography (HPLC) on a C_{18} reversed-phase column followed by analysis by gas chromatography coupled with mass spectrometry (GC–MS). This method is very reproducible for amounts of CFAM as low as 50 μg/g of lipid sample.

EXPERIMENTAL

Standards

Methyl octadecanoate and heptadecanoate and ethyl hexadecanoate were purchased from Sigma Chimie (La Verpillère, France).

Isolation of cyclic fatty acid monomers

Two types of CFAM were isolated using methods described elsewhere [8]. Those arising from linoleic acid were isolated from sunflower oil heated at 275°C for 12 h under nitrogen, whereas those arising from linolenic acid were prepared from linseed oil heated under the same conditions. Briefly, the heated oils were saponified and converted into fatty acid methyl esters using sulphuric acid as catalyst. The total fatty acid methyl esters were fractionated by column chromatography and the non-polar fraction was submitted to urea fractionation as described previously [18]. For CFAM isolated from the heated sunflower oil, the non-adduct fraction which contained a mixture of CFAM and 18:2 $n-6$ ($n-6$ represents the position of ethylenic bonds on the carbon chain) was further purified by preparative liquid chromatography as described previously [8] using a reversed-phase column (Waters, Milford, MA, USA) (30 cm × 5.7 cm I.D.) and acetonitrile–water (90:10) as the eluent at a flow-rate of 150 ml/min.

Hydrogenation of CFAM

Hydrogenation was affected using PtO_2 (Merck, Darmstadt, Germany) as catalyst [12] in 10 ml of chloroform–methanol (2:1, v/v) as solvent and with a hydrogen pressure of 3–4 bar. The reaction was allowed to proceed for 4 h. The catalyst was removed by filtration.

High-performance liquid chromatography

HPLC analyses were carried out on a C_{18} reversed-phase column (Merck, LiChrosorb) (25 cm × 7 mm I.D., particle size 5 μm) using a Waters R 410 refractive index detector. The sample (up to 40 mg) was dissolved in acetone. The solvent systems used were either acetonitrile–acetone (90:10, v/v), pure acetonitrile or pure methanol at 4 ml/min, depending on the separation tested. A Nova Pak C_{18} column (Waters) (10 cm × 8 mm I.D., particle size 4 μm) was used for smaller amounts (up to 1 mg) with the same solvent systems tested at 1.6 ml/min.

Gas chromatography

GC analyses were effected on a Intersmat IGC 120 FL chromatograph (Delsi, Argenteuil, France) fitted with a flame ionization detector and a Ross injector. The analyses were performed on capillary columns coated with CP-Sil

84 at 180°C (Chrompack, Middelburg, Netherlands) (50 m × 0.25 mm I.D., film thickness 0.2 μm). All quantitative analyses were carried out using a Spectra-Physics (San Jose, CA, USA) Chromjet integrator.

Gas chromatography–mass spectrometry

All GC–MS analyses were performed using a DB-Wax column (J&W Scientific, Folsom, CA, USA) (30 m × 0.25 mm I.D., film thickness 0.5 μm) and a Hewlett-Packard (Palo Alto, CA, USA) HP-5970 mass-selective detector. The chromatographic conditions were similar to those already published for the analyses of CFAM [10]. The temperature was programmed from 50 to 200°C at 20°C/min, held at 200°C for 25 min, then programmed from 200 to 220°C and held at 220°C until completion of the analyses. Splitless injection was used in all instances, and the injection port was maintained at 240°C.

Reproducibility of the method

The reproducibility of the method was checked by preparing a solution that contained 30 mg of 18:0, 1.5 μg of CFAM isolated from a heated linseed oil and 1.5 μg of 17:0 as internal standard. A similar mixture containing the CFAM isolated from a heated sunflower oil was also studied. Each sample was run five times through the HPLC system, followed by GC analysis, using 17:0 as an internal standard, to determine the reproducibility of the method.

Determination of CFAM in spiked rat liver lipids

Liver lipids of Wistar rats were extracted according to the method Folch *et al.* [19] and converted into the methyl esters [20]. Two identical mixtures were then prepared. CFAM (2.5 μg) isolated from heated linseed oil and 16:0 EE (EE = ethyl ester) (2.5 μg) were added to the liver lipid methyl esters (50 mg). The mixtures were totally hydrogenated. One hydrogenated mixture was submitted to HPLC fractionation and the other to urea adduction [18], and the non-urea adduct fraction which contained the CFAM was analysed by GC on a CP-Sil 84 column (see above).

Heart cell culture

The culture medium was Ham's F10 basal medium supplemented with 10% foetal bovine serum (Seromed, Munich, Germany) and 10% human serum (CTS, Dijon, France). CFAM in ethanol was added to the medium using lipid-free bovine serum albumin (fraction V) (Sigma, St. Louis, MO, USA) at 37°C, at a CFAM-to-albumin molar ratio of 6:1 [21]. The medium containing the CFAM was then sterilized by filtration (Millex GS, 0.22 μm; Millipore, Milford, MA, USA).

Primary cultures of rat ventricular cells were prepared as described previously [22]. The hearts from 2–4-day-old rats were aseptically removed, minced and washed three times in a cold Saline G solution and once again in the same solution for 10 min at 30°C in a shaking water-bath. The fragments were then submitted to a seven-step trypsinization process. The supernatants of the last six proteolytic treatments were pooled and diluted in culture medium. The muscle to non-muscle cell ratio was increased by a two-step (30- and 150-min) selective adhesion procedure. The final cell suspension was diluted to $4 \cdot 10^5$ cells/ml in culture medium and seeded in 60-mm plastic Petri dishes (5 ml per dish). Cultures were maintained at 37°C in a humidified atmosphere (5% CO_2, 19% O_2, 76% N_2). The culture medium was renewed 24 h after seeding and thereafter every 48 h.

Cells were incubated in the CFAM-containing solutions (2.5, 5 or 10 mg/l) for 2 days. Cells were then harvested by scraping with a rubber "policeman" and pelleted by centrifugation.

Total lipids were extracted from the medium according to the method of Folch *et al.* [19] slightly modified [11].

Phospholipids were separated from non-phosphorus lipids using a Sep-Pak silica cartridge (Waters) as described by Juaneda and Rocquelin [23]. The lipids were converted into methyl esters using BF_3–MeOH according to Morrison and Smith [20].

RESULTS AND DISCUSSION

An ideal method should permit the CFAM to be determined after total elimination of the 18:0

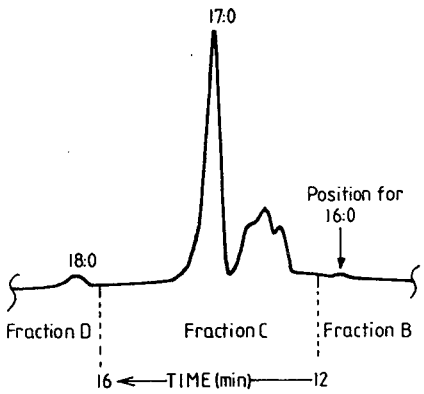

Fig. 1. HPLC fractionation of a mixture of 17:0 and hydrogenated CFAM isolated from a heated linseed oil. Eluent: acetonitrile–acetone (90:10, v/v) at 4 ml/min.

as some CFAM have retention times close to that of 18:0 on either polar or non-polar phases [15,24]. Unfortunately, this is not the case when using urea adduction as the enrichment step [24,25]. This elimination of 18:0 should also be done without any selective loss of CFAM and the method should allow verification of the compounds detected as CFAM and not artefacts having similar retention times. The present method is a combination of esterification, total hydrogenation, isolation of the CFAM by HPLC and GC or GC–MS analyses of the isolated fraction.

The HPLC procedure was developed in order first to isolate in the same fraction both the internal standard and the CFAM, and second to separate them from the major straight-chain saturated fatty acid methyl esters formed after hydrogenation such as methyl hexadecanoate

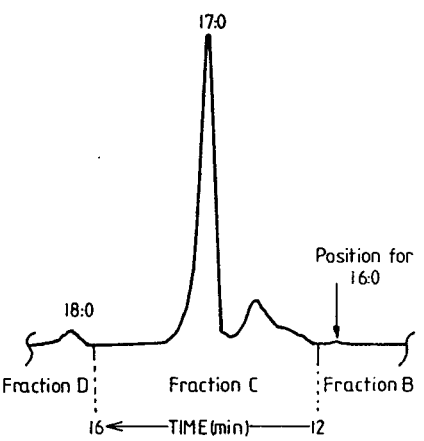

Fig. 2. HPLC fractionation of a mixture of 17:0 and hydrogenated CFAM isolated from a heated sunflower oil. Eluent: acetonitrile–acetone (90:10, v/v) at 4 ml/min.

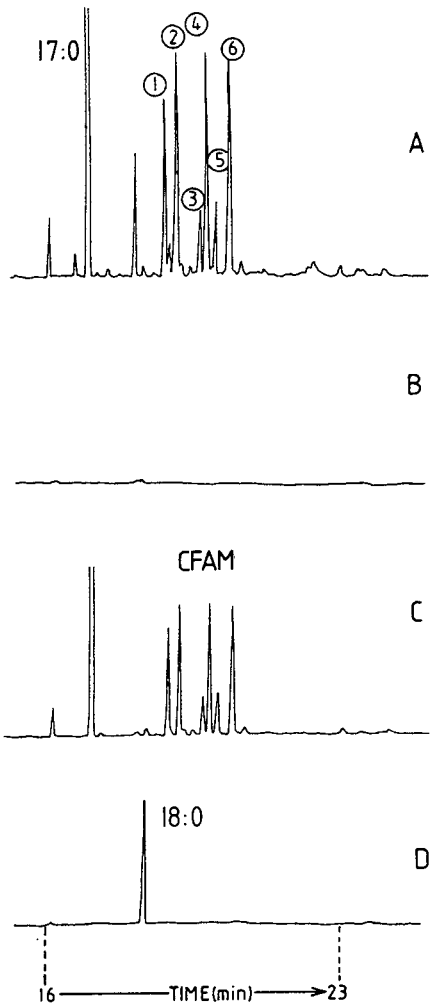

Fig. 3. GC analyses (CP-Sil 84) of (A) a mixture of 17:0 and hydrogenated CFAM isolated from a heated linseed oil and (B, C and D) of the fraction collected by HPLC (Fig. 1). For peak identification (1–6) see CFAM from linseed oil in Table I.

(16:0) and 18:0. This was possible (Figs. 1 and 2) using a C_{18} reversed-phase (semi-preparative) column and acetonitrile–acetone (90:10, v/v) as eluent at 4 ml/min. Both the CFAM isolated from linseed and sunflower oils [8] have the same retention volume under these experimental conditions. This is very important as these are representative of CFAM formed from the two major polyunsaturated fatty acids of vegetable oils, *i.e.*, linolenic and linoleic acids. The fraction collected between 16:0 and 18:0 would therefore contain both the internal standard and the CFAM. Of all the solvents tested, acetonitrile–acetone (90:10, v/v) gave a good compromise between total separation and a short analysis time. The separation can also be effected using analytical columns using the same solvent mixture at 1.6 ml/min; 1 mg would be the maximum amount injected. However, for GC–MS studies it is often necessary to have appreciable amounts of CFAM, so it is better to carry out the separation on a semi-preparative column where the maximum amount of sample injected would be between 25 and 30 mg.

In this method, the internal standard (17:0) is added to the sample before esterification and hydrogenation. Any loss of material during these steps would not affect the determination. It is also possible to use a triglyceride as an internal standard (triheptadecanoin). For samples that may contain appreciable amounts of 17:0, it is possible to use ethyl hexadecanoate (16:0 EE). It is necessary to add it after esterification and just prior to hydrogenation in order to avoid its conversion into the methyl ester. For the HPLC fractionation, 16:0 EE has a retention volume between those of CFAM and 17:0.

In order to verify that the GC profile of CFAM was not modified after the HPLC step, a mixture of CFAM isolated from a heated linseed oil and of 17:0 as internal standard was fractionated by HPLC. The mixture was first analysed by GC (Fig. 3A) and by GC–MS (Table I). Peak identifications were made by comparison of their mass spectra and GC retention times on CP-Sil 84 and DB-Wax columns with those of authentic standards synthesized previously [26]. This sample was submitted to HPLC and three fractions (B, C and D, Fig. 1) were collected and further analysed by GC (Fig. 3). The first fraction was collected from the solvent peak to the end of the retention volume of 16:0 (fraction B). The second fraction was collected from the end of the retention volume of 16:0 to the beginning of the elution of 18:0 (fraction C), and the third fraction (D) corresponded to the elution of 18:0. Fraction B (Fig. 3) did not contain appreciable amounts of any known fatty acids, whereas fraction C (Fig. 3) contained the CFAM and the internal standard and fraction D (Fig. 3)

TABLE I

MAJOR HYDROGENATED CFAM IDENTIFIED BY GC–MS IN HEATED SUNFLOWER AND LINSEED OILS (275°C, 12 h)

Sample	Peak No.	Component	Configuration
Heated linseed oil (Fig. 3)	1	Methyl 9-(2′-butylcyclopentyl)nonanoate	*trans*
	2	Methyl 10-(2′-propylcyclopentyl)decanoate	*trans*
	3	Methyl 9-(2′-butylcyclopentyl)nonanoate	*cis*
	4	Methyl 9-(2′-propylcyclohexyl)nonanoate	*trans*
	5	Methyl 10-(2′-propylcyclopentyl)decanoate	*cis*
	6	Methyl 9-(2′-propylcyclohexyl)nonanoate	*cis*
Heated sunflower oil (Fig. 4)	1	Methyl 7-(2′-hexylcyclopentyl)heptanoate + methyl 4-(2′-nonylcyclopentyl)butanoate	*trans* *trans*
	2	Methyl 9-(2′-butylcyclopentyl)nonanoate	*trans*
	3	Methyl 7-(2′-hexylcyclopentyl)heptanoate	*cis*
	5	Methyl 9-(2′-butylcyclopentyl)nonanoate + ?	*cis*

contained the 18:0 without any detectable amount of CFAM.

A similar experiment was carried out with the CFAM isolated from a heated sunflower oil (Table I, Fig. 2). The determination of the structures of CFAM 4, 6, 7 and 8 for sunflower oil are still under investigation. The GC analyses of the total CFAM mixture and the internal standard and also the three fractions collected are shown in Fig. 4. Fraction D contained only 18:0 and fraction C contained the CFAM and

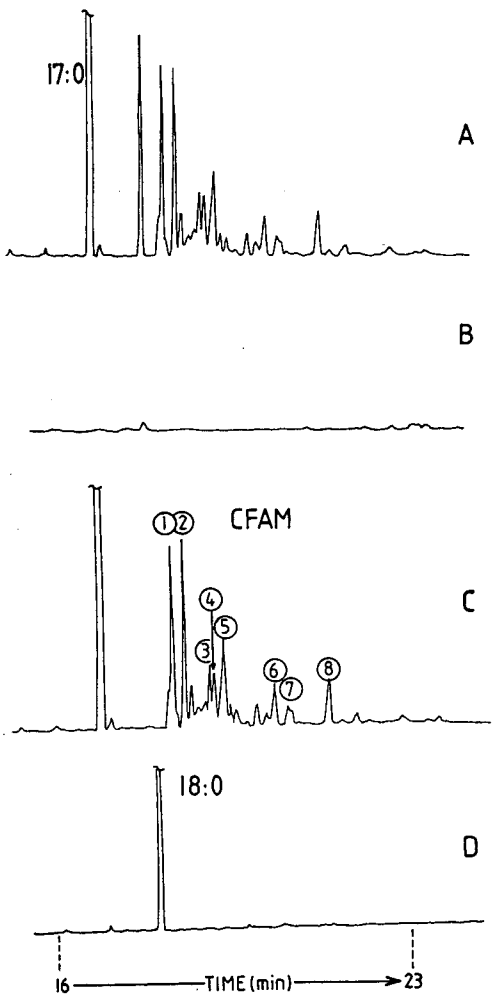

Fig. 4. GC analyses (CP-Sil 84) of (A) a mixture of 17:0 and hydrogenated CFAM isolated from a heated sunflower oil and (B, C and D) of the fraction collected by HPLC (Fig. 2). For peak identification (1–8) see CFAM from sunflower oil in Table I.

17:0. Fraction B showed only trace amounts of components that did not seem to be any known fatty acids. Each fraction was also analysed by GC–MS in order to confirm the structures of the different fatty acids. The relative proportions of the major CFAM obtained while collecting the CFAM fractions were not modified by HPLC (Table II). The data in Table II represent an average of two HPLC runs. Only very small differences were observed.

The results of the reproducibility tests described under Experimental are reported in Table III. Before HPLC, the CFAM represented 50 μg/g of the total sample. After HPLC the values ranged from 43 to 51 μg/g for the CFAM isolated from linseed oil and from 46 to 57 μg/g for those isolated from sunflower oil. The mean values were 49.2 ± 4.4 and 50.0 ± 3.6 μg/g, respectively, which indicated that the method was very reproducible at this low CFAM level. The reason why the reproducibility of the method was checked on a sample containing 50 μg of a mixture of CFAM per gram of sample is that this value seems to be much lower (5–10 times) than the level usually detected in refined commercial oils [15,27,28]. An attempt was made to determine lower concentrations of CFAM in oils. For CFAM isolated from a heated linseed oil (four major and two minor peaks, Fig. 3), one can determine levels as low as 10 μg/g of oil. However, at this level, the relative proportions of the different isomers changed slightly from one quantification to another, and 50 μg/g of such a mixture (six components) should be considered as the minimum optimum level of total CFAM mixture that can be analysed with good reproducibility.

The purpose of this study was to compare the results obtained using HPLC as the enrichment step with those obtained using urea inclusion and to apply this method to biological samples. Fig. 5 shows parts of the GC analyses of the CFAM fraction which was used to spike the sample of rat liver lipids (Fig. 5A), the isolated HPLC fraction (Fig. 5B) and the non-urea adduct fraction (NUAF) (Fig. 5C). The same CFAM profile was obtained when HPLC was used, whereas the GC analysis of the NUAF showed a different profile. GC–MS analysis of this fraction

TABLE II

RELATIVE PROPORTIONS OF CFAM ISOLATED FROM HEATED LINSEED OIL (FIG. 3) AND SUNFLOWER OIL (FIG. 4) BEFORE AND AFTER HPLC RECOVERY

Average of two determinations (HPLC followed by GC).

Sample	Stage	Peak No. (Figs. 3 and 4)							
		1	2	3	4	5	6	7	8
Heated linseed oil	Before HPLC	15.8	22.4	7.0	22.3	9.4	23.1		
	After HPLC	15.8	22.3	6.5	22.5	9.3	23.6		
Heated sunflower oil	Before HPLC	25.5	19.8	7.7	9.2	17.4	7.6	5.1	7.7
	After HPLC	25.9	20.5	8.2	8.5	16.7	7.7	5.1	7.4

also showed the presence of impurities. Further, one could speculate whether preferential urea inclusion of some CFAM could occur when dealing with such small amounts of CFAM (2.5 μg). GC quantitative analysis of the HPLC fraction using 16:0 EE as an internal standard gave 52.6 μg of CFAM per gram of sample, compared with 50.0 μg/g in the mixture prior to fractionation. The HPLC fractionation method was far superior to urea adduction, especially for samples that may contain only traces of CFAM. GC–MS analysis of the fraction collected by HPLC gave spectra similar to those published previously [10].

This method was applied to the determination of CFAM in heart cell cultures. Heart cell cultures have been used in our laboratory to study the biological effects of CFAM [29]. In order to compare the effects of CFAM arising from linoleic acid with those arising from linolenic acid, cultured rat cardiomyocytes were treated with solutions containing CFAM at concentrations of 2.5, 5 and 10 mg/l as described under Experimental. After separation of the non-phosphorus lipids and the phospholipids, the amount of CFAM was determined using the described method. Each result (Table IV) represents the average of three separate cultures (about 100 Petri dishes each). These data show that small amounts of CFAM can be determined in this type of biological sample and that these CFAM can be incorporated into the membrane lipids. Our continuing research will permit the effects of such an incorporation to be investigated [29].

The major advantages of this method over those published previously are the purity of the CFAM fraction, the rapidity and the sensitivity. Also, there is no loss of product during the isolation step (HPLC) and no modification of the ratio of the different types of cyclic fatty acids. We should also emphasize that the analysis of the isolated CFAM fractions should be carried out by GC–MS instead of GC to verify that there are no contaminants in the isolated sample, as already mentioned by Rojo and Perkins [30].

TABLE III

DETERMINATION OF CFAM (μg/g OF SAMPLE) ISOLATED FROM HEATED SUNFLOWER AND LINSEED OILS BEFORE AND AFTER HPLC FRACTIONATION (FIVE INDEPENDENT DETERMINATIONS)

Stage	Heated linseed oil	Heated sunflower oil
Before HPLC	50	50
After HPLC	44, 58, 50, 43, 51 (mean ±S.D. = 49.3 ± 5.4)	46, 46, 49, 52, 57 (mean ±S.D. = 50.0 ± 4.6)

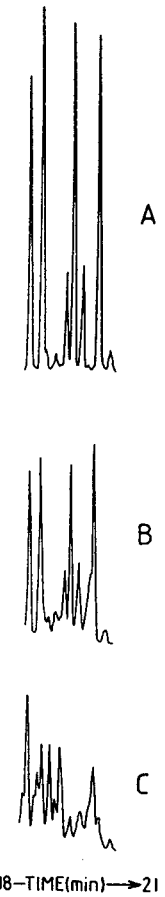

Fig. 5. Parts of the GC analyses (CP-Sil 84) of (A) a mixture of 17:0 and hydrogenated CFAM isolated from a heated linseed oil, (B) the CFAM fraction collected by HPLC of the methyl esters of a spiked lipid extract of rat liver and (C) the non-urea adduct fraction of the same sample.

In the biological field, this method is applicable to animal tissues where the amounts of CFAM incorporated are small.

REFERENCES

1 N.R. Artman, *Adv. Lipid Res.*, 7 (1969) 245.
2 E.G. Perkins, *Rev. Fr. Corps Gras*, 23 (1976) 257.
3 E.W. Crampton, R.H. Common, F.A. Farmer, A.F. Wells and D. Crawford, *J. Nutr.*, 49 (1953) 333.
4 E.W. Crampton, R.H. Common, E.T. Pritchard and F.A. Farmer, *J. Nutr.*, 60 (1956) 13.
5 F.A. Farmer, E.W. Crampton and M. Siddall, *Science*, 113 (1951) 408.
6 B. Potteau, *Ann. Nutr. Alim.*, 30 (1976) 67.
7 J.L. Sebedio and A. Grandgirard, *Prog. Lipid Res.*, 28 (1989) 303.
8 J.L. Sebedio, J. Prevost and A. Grandgirard, *J. Am. Oil Chem. Soc.*, 64 (1987) 1026.
9 J.L. Sebedio, J.L. Le Quere, E. Semon, O. Morin, J. Prevost and A. Grandgirard, *J. Am. Oil. Chem. Soc.*, 64 (1987) 1324.
10 J.L. Sebedio, J.L. Le Queré, O. Morin, J.M. Vatele and A. Grandgirard, *J. Am. Oil Chem. Soc.*, 66 (1989) 704.
11 E. Ribot, A. Grandgirard, J.L. Sebedio, A. Grynberg and P. Athias, *Lipids*, 27 (1992) 79.
12 L.T. Black and R.A. Eisenhauer, *J. Am. Oil Chem. Soc.*, 40 (1963) 272.
13 M. Gente and R. Guillaumin, *Rev. Fr. Corps Gras*, 24 (1977) 211.
14 J.B. Meltzer, E.N. Frankel, T.R. Bessler and E.G. Perkins, *J. Am. Oil Chem. Soc.*, 53 (1981) 779.
15 A. Grandgirard and F. Julliard, *Rev. Fr. Corps Gras*, 30 (1983) 123.
16 A. Gere, C. Gertz and O. Morin, *Rev. Fr. Corps Gras*, 31 (1984) 341.
17 J.A. Rojo and E.G. Perkins, *J. Am. Oil Chem. Soc.*, 66 (1989) 1593.

TABLE IV

DETERMINATION OF CFAM IN PHOSPHOLIPIDS (PL) AND NON-PHOSPHORUS LIPIDS (NPL) OF CARDIOMYOCYTES INCUBATED IN CFAM-CONTAINING MEDIUM

Results are expressed as μg esters/mg proteins. Average of three separate cultures.

Sample	Concentration of CFAM medium (mg/l)	PL	NPL
Heated linseed oil	2.5	0.5 ± 0.08	0.6 ± 0.05
	5	0.8 ± 0.01	1.1 ± 0.17
	10	1.7 ± 0.14	2.3 ± 0.44
Heated sunflower oil	2.5	1.0 ± 0.07	1.5 ± 0.10
	5	1.5 ± 0.18	3.2 ± 0.11
	10	2.8 ± 0.19	702 ± 1.04

18 D. Firestone, S. Nesheim and W. Horwitz, *J. Assoc. Off. Anal. Chem.*, 44 (1961) 465.
19 J. Folch, M. Lees and G.H. Sloane-Stanley, *J. Biol. Chem.*, 226 (1957) 497.
20 W.R. Morrison and L.M. Smith, *J. Lipid Res.*, 5 (1964) 600.
21 D.G. Wenzel and J.W. Kleoppel, *Toxicology*, 15 (1979) 105.
22 A. Grynberg, P. Athias and M. Degois, *In Vitro*, 22 (1986) 44.
23 P. Juaneda and G. Rocquelin, *Lipids*, 20 (1984) 40.
24 J.A. Rojo and E.G. Perkins, *J. Am. Oil Chem. Soc.*, 64 (1987) 414.
25 B. Potteau, P. Dubois and J. Rigaud, *Ann. Technol. Agric.*, 27 (1978) 655.
26 J.M. Vatele, J.L. Sebedio and J.L. Le Queré, *Chem. Phys. Lipids*, 48 (1988) 119.
27 A. Grandgirard and F. Julliard, *Rev. Fr. Corps Gras*, 34 (1987) 213.
28 E.N. Frankel, L.M. Smith, C.L. Hamblin, R.K. Creveling and A.J. Clifford, *J. Am. Oil Chem. Soc.*, 61 (1984) 87.
29 A. Grynberg, P. Athias, E. Ribot, A. Fournier, J.L. Sebedio and A. Grandgirard, in *Proceedings of the 1st International Congress of the ISSFAL, Lugano, June 30–July 3, 1993*, in press.
30 J.A. Rojo and E.G. Perkins, *Lipids*, 24 (1989) 467.

Journal of Chromatography A, 659 (1994) 111–118
Elsevier Science B.V., Amsterdam

CHROM. 25 599

Determination of dansyl amino acids using tris(2,2′-bipyridyl)ruthenium(II) chemiluminescence for post-column reaction detection in high-performance liquid chromatography

Won-Yong Lee and Timothy A. Nieman *

Department of Chemistry, University of Illinois at Urbana-Champaign, 600 South Mathews Avenue, Urbana, IL 61801-3792 (USA)

(First received June 15th, 1993; revised manuscript received September 28th, 1993)

ABSTRACT

Dansyl amino acids are determined using a tris(2,2′-bipyridyl)ruthenium(II) [$Ru(bpy)_3^{2+}$] chemiluminescence (CL) post-column reaction. The derivatized amino acids are separated on a reversed-phase column (Zorbax ODS) using a mobile phase containing 15% acetonitrile in 25 m*M* trifluoroacetate at pH 7.5. The eluted dansyl amino acids are combined at a mixing tee with 2.0 m*M* $Ru(bpy)_3^{2+}$ CL reagent. The combined solution passes through a flow cell, which has a dual platinum electrode at a potential of 1250 mV. On the surface of the electrode $Ru(bpy)_3^{2+}$ is oxidized to $Ru(bpy)_3^{3+}$ which reacts with dansyl amino acids to emit light. CL intensities vary only slightly with CL reagent or with mobile phase flow-rates. CL intensities increase significantly with an increase in pH over the pH 6–8 region. A slight increase in CL intensity is obtained with increasing acetonitrile in the mobile phase. The working curve for dansyl-derivatized glutamate covers three orders of magnitude with a detection limit of 0.1 μM (2 pmol injected).

INTRODUCTION

1 - Dimethylaminonaphthalene - 5 - sulphonyl chloride (dansyl chloride, Dns-Cl) is a well known derivatizing agent for amino acid analysis and peptide sequencing. The derivatization method is well established [1]. The reaction scheme is shown in Fig. 1. In general, dansyl derivatives of amino acids can be detected either by absorbance at 254 nm or by fluorescence (excitation maximum 385 nm, emission maximum 460–495 nm).

In recent years chemiluminescence (CL) has become an attractive detection method for liquid chromatography due to very low detection limits and wide linear working ranges which can be obtained while using relatively simple instrumentation [2]. 5-Amino-2,3-dihydro-1,4-phthalazinedione (luminol) CL has been applied to the detection of various organic species separated by

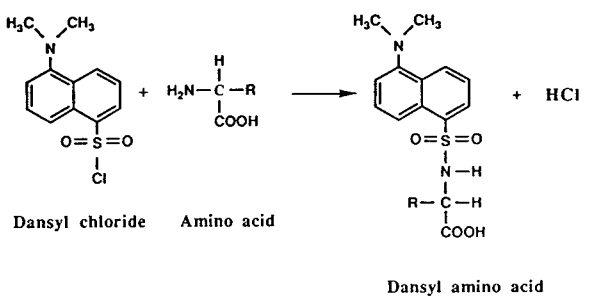

Fig. 1. Reaction scheme for the dansyl derivation of amino acids.

* Corresponding author.

0021-9673/94/$07.00
SSDI 0021-9673(93)E1028-X

HPLC [3–7] and for the detection of metal ions separated by ion exchange [8]. N,N′-Dimethyl-9,9′-diacridinium nitrate (lucigenin) has been used to detect corticosteroids separated by reversed-phase chromatography [9]. Peroxyoxalate CL has been widely used for HPLC detection of fluorescent analytes (*e.g.* polycyclic aromatic hydrocarbons) and fluorescent derivatives (*e.g.* dansyl and *o*-phthalaldehyde derivatives of amino acids and amines) [10,11]. The CL reaction with tris(2,2′-bipyridyl)ruthenium(III), $Ru(bpy)_3^{3+}$, has been used for the detection of aliphatic amines [12], amino acids [13–15] and clindamicin antibiotics [16] separated by HPLC.

The CL system of interest in this study is $Ru(bpy)_3^{3+}$. This CL reaction has been applied for the determination of oxalate [17,18], aliphatic and alicyclic amines [15,19,20], amino acids and proteins [13–15,21,22], NADH and species coupled to NADH production [18,23], and tris(2,2′-bipyridyl)ruthenium(II) [$Ru(bpy)_3^{2+}$] itself [24]. Since CL intensities for amines reacting with $Ru(bpy)_3^{3+}$ increase 10-fold going from primary to secondary amines and another 10–50-fold going from secondary to tertiary amines, dansyl derivatives should give rise to intense emission with $Ru(bpy)_3^{3+}$ due to the secondary and tertiary amine groups. The oxidative–reduction reaction scheme for chemiluminescence from $Ru(bpy)_3^{2+}$ has been postulated by Rubinstein *et al.* [25].

$$Ru(bpy)_3^{2+} \rightarrow Ru(bpy)_3^{3+} + e^-$$

$$Ru(bpy)_3^{3+} + \text{reductant} \rightarrow \text{product} + [Ru(bpy)_3^{2+}]^*$$

$$[Ru(bpy)_3^{2+}]^* \rightarrow Ru(bpy)_3^{2+} + h\nu$$

The initial oxidation of $Ru(bpy)_3^{2+}$ to $Ru(bpy)_3^{3+}$ is performed at an electrode surface. The electrogenerated chemiluminescence (ECL) intensity is directly proportional to the amount of reductant, which is the dansyl derivative in this case.

In this paper, we report a method for the determination of dansyl amino acids using $Ru(bpy)_3^{2+}$ CL reaction after HPLC separation on a reversed-phase column. The effects on CL intensity for dansyl derivatives determined in a flow injection system will be described for flow-rates of CL reagent and mobile phase, pH of mobile phase and organic modifier composition of mobile phase.

EXPERIMENTAL

Instrumentation

Flow injection analysis and HPLC experiments were done with the chemiluminescence detection system shown in Fig. 2. For flow injection analysis a Rainin Rabbit peristaltic pump (Woburn, MA, USA) was used to deliver the $Ru(bpy)_3^{2+}$ CL reagent. An Altex Model 110 A HPLC pump (Berkeley, CA, USA) was used to deliver the buffered mobile phase through an Altex Model 210 injector equipped with a 20-μl injector loop. The sample in the buffer stream then combined with the $Ru(bpy)_3^{2+}$ CL reagent at a mixing tee.

The HPLC system was composed of a silica pre-column, a Partisil ODS guard-column (70 mm × 2.0 mm I.D.) and a DuPont Zorbax ODS

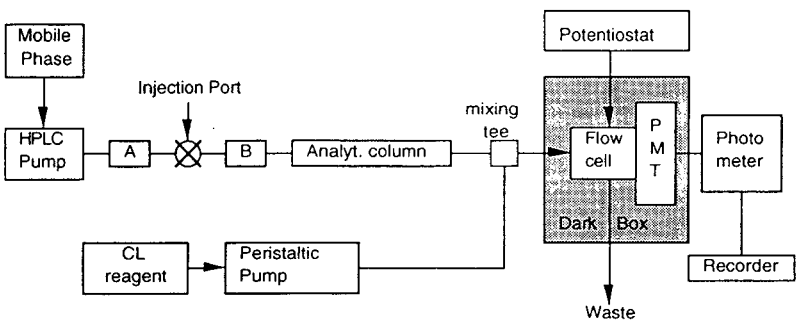

Fig. 2. Schematic diagram for chemiluminescence detection in flow injection and HPLC system (guard and analytical columns are not present in flow injection system). A = Silica pre-column; B = guard column.

column (5 μm, 250 mm × 4.6 mm I.D.). The mobile phase [25 m*M* trifluoroacetic acid (TFA), pH 7.5 with 15% (v/v) acetonitrile] was delivered at a flow-rate of 1.0 ml/min. After passing through the HPLC system the column effluent was combined at a mixing-tee with the $Ru(bpy)_3^{2+}$ solution [2 m*M* $Ru(bpy)_3^{2+}$ in 2.5 m*M* TFA with no organic modifier] which was delivered with a peristaltic pump at a flow-rate of 1.0 ml/min. The combined solution then passed through the flow cell.

In both the flow injection and HPLC systems described above, the flow cell was assembled from a conventional LC–electrochemical detection dual platinum electrode (Bioanalytical Systems, West Lafayette, IN, USA) and a Plexiglas window for detection of CL emission. A PTFE spacer was inserted between the electrode and the Plexiglas to create a 10-μl flow cell volume. In addition to the dual working electrode, a stainless-steel counter electrode at the cell exit and a screw-in Ag/AgCl reference electrode (Bioanalytical Systems) were employed. The cell employed here contained a platinum working electrode, but glassy carbon working electrodes yield equivalent results. Cyclic voltammograms of $Ru(bpy)_3^{2+}$ solutions show the same peak potentials with both electrodes. ECL emission intensities are about 20–30% higher with platinum electrodes.

The flow cell was mounted directly across from the photomultiplier tube (PMT) window. A collimating lens was placed between the flow cell and the PMT window in order to improve the collection efficiency. The entire flow cell was enclosed in a dark box. During all experiments, the working electrode was held at a potential of +1.25 V (*vs.* Ag/AgCl) in order to oxidize $Ru(bpy)_3^{2+}$ to $Ru(bpy)_3^{3+}$. The potential was maintained using a Bioanalytical Systems BAS 100A electrochemical analyzer. The photomultiplier used was a Hamamatsu R928 photomultiplier (Middlesex, NJ, USA) biased at 900 V. The PMT currents were measured using a Pacific Instruments Model 124 photometer (Concord, CA, USA) followed by a Curken Instrument Corp. 250 series strip chart recorder (Hawleyville, CT, USA). Optimization of separation conditions was carried out with the HPLC system using an Altex Model 153 UV–Vis detector to monitor the column effluent.

Reagents

Dansyl chloride, dansyl alanine and free amino acids were purchased from Sigma (St. Louis, MO, USA). Tris(2,2′-bipyridyl)ruthenium(II) chloride hexahydrate and TFA were purchased from Aldrich (Milwaukee, WI, USA). Acetonitrile was HPLC grade and distilled over dansyl chloride in order to remove potential interferences. The remaining sample solutions were prepared from reagent-grade or better chemicals and purchased from commercial sources. Water for all solutions was purified using a Milli-Q water purification system (Millipore, Bedford, MA, USA). The HPLC mobile phase, 25 m*M* TFA adjusted to pH 7.5 with 1.0 *M* sodium hydroxide solution and mixed with acetonitrile (85:15, v/v), was prepared and then degassed prior to use. A stock dansyl chloride solution (5.0 m*M*) was prepared with distilled acetonitrile.

Dansylation

Dansylation was carried out according to the modified procedure of Tapuhi *et al.* [1]. Dansyl chloride was dissolved in distilled acetonitrile (5.0 m*M*). The various amino acids were dissolved in 40 m*M* lithium carbonate buffer (pH 9.5 adjusted with HCl). A 1-ml volume of the dansyl chloride solution was rapidly added to 2 ml of the amino acid solution; this resulted in a 10-fold or greater excess of dansyl chloride reagent. The mixture was sonicated for 10 min and then allowed to stand at room temperature. During derivatization the reaction ampoule was wrapped in aluminum foil since dansyl derivatives are known to be photosensitive. A 20-μl aliquot was removed from the ampoule after 50 min and analyzed by the HPLC–CL detection system. Tapuhi *et al.* [1] have reported dansyl chloride derivatization for the amino acids we used here to be greater than 90% complete under these conditions.

pH Studies

Solutions of each analyte were prepared in 100 m*M* potassium phosphate buffered at different pH values covering the range from pH 6 to 8. CL

reagent solutions of 2.0 m*M* $Ru(bpy)_3^{2+}$ were also prepared in 100 m*M* potassium phosphate buffered at different pH values. Concentrations used for each analyte were 5.0 μM for dansyl alanine and 50 μM for dansyl chloride. The carrier stream was changed for each pH tested, and the carrier stream and CL reagent were at the same pH.

Organic modifier studies

A 50 μM concentration of Dns-Ala was prepared in 25 m*M* TFA (pH 7.5). The amount of acetonitrile was varied from 0 to 50% in the 25 m*M* TFA mobile phase. The carrier stream was changed for each percentage acetonitrile tested. The CL reagent solution was always 2 m*M* $Ru(bpy)_3^{2+}$ in 25 m*M* TFA, pH 7.5 with no organic modifier. Diffusion coefficients were measured in each mobile phase having a different percentage of acetonitrile. Electrochemical experiments were performed in a three-electrode configuration consisting of a dual platinum electrode (area 0.16 cm^2), a platinum counter electrode and an Ag/AgCl reference electrode. A Bioanalytical Systems BAS 100A electrochemical analyzer was used to obtain cyclic voltammograms for 1.0 m*M* $Ru(bpy)_3^{2+}$ in buffers containing 0–40% (v/v) acetonitrile at scan rates of 25, 50, 75, 100 and 150 mV/s. Diffusion coefficients were calculated from the slopes of Randles–Sevcik plots for the cyclic voltammetric data in each buffer [26].

RESULTS AND DISCUSSION

Aliphatic amines have been known to be detected with $Ru(bpy)_3^{2+}$. Although aromatic amines such as aniline and N-methylaniline quench CL emission, N,N′-dimethylaniline is known to be quite reactive [19]. Since CL intensities for amines with $Ru(bpy)3^{2+}$ increase 10-fold going from primary to secondary amines and another 10–50-fold going from secondary to tertiary amines, it was the tertiary and secondary amine groups of dansyl amino acids that originally caught our attention. The tertiary amine group has a structure similar to N,N-dimethylaniline. The secondary amine group is adjacent to a SO_2 group. Generally little is known about how the substituent adjacent to the nitrogen atom affects the CL signal although an adjacent carbonyl leads to very low CL intensity. However, it was recently reported that certain sulfonamides (chlorothiazide, trichloromethiazide and hydrochlorothiazide) gave strong emission upon reaction with $Ru(bpy)_3^{3+}$ CL reagent [27].

Using the flow injection system shown in Fig. 2, detection limits (signal-to-noise ratio 2) for dansyl chloride and Dns-Ala were obtained with both 100 m*M* phosphate buffer (pH 7.5) and 25 m*M* trifluoroacetate (pH 7.5). The detection limits for dansyl chloride and Dns-Ala were 1.0 μM (20 pmol) and 0.1 μM (2 pmol), respectively, in both mobile phases. However, a two-fold higher slope in the working curves was obtained with phosphate buffer than with TFA. The lower detection limits for Dns-Ala relative to that of dansyl chloride may result from the fact that the dansyl amino acids contain both secondary and tertiary amine functionalities whereas the dansyl chloride contains only tertiary amine group. Because both tertiary and secondary amine groups react with $Ru(bpy)_3^{2+}$ to emit light, the combined emission intensity from both amine groups of Dns-Ala results in the lower detection limit.

Flow-rate effect

The effect of flow-rate on the CL signal was characterized using the flow injection system shown in Fig. 2. Fig. 3 shows the CL dependence on the flow-rates for 50 μM Dns-Ala in 25 m*M* TFA (pH 7.5). The HPLC carrier stream was maintained at a flow-rate of 1.0 ml/min, while the $Ru(bpy)_3^{2+}$ reagent flow-rate was varied. Increasing the flow-rate from 0.5 to 2.0 ml/min led to an almost constant CL signal. It might be anticipated that decreased residence times of the CL reagent and resulting decreased diffusion distances in the flow cell would lead to the CL intensities showing significant dependence on the flow-rate. However, since the amount of $Ru(bpy)_3^{2+}$ is in large excess with respect to the analyte and the electron transfer is so efficient in solution phase, the flow-rate of CL reagent is not a significant factor on the CL signal. When the CL reagent flow-rate was maintained at 1.0 ml/min, the CL signal was varied with the change of

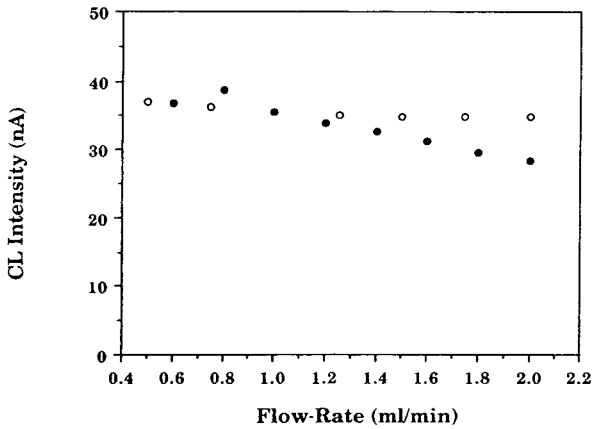

Fig. 3. Effect of flow-rates on CL for 50 μM Dns-Ala. ○ = Varying CL reagent flow-rate; ● = varying mobile phase flow-rate.

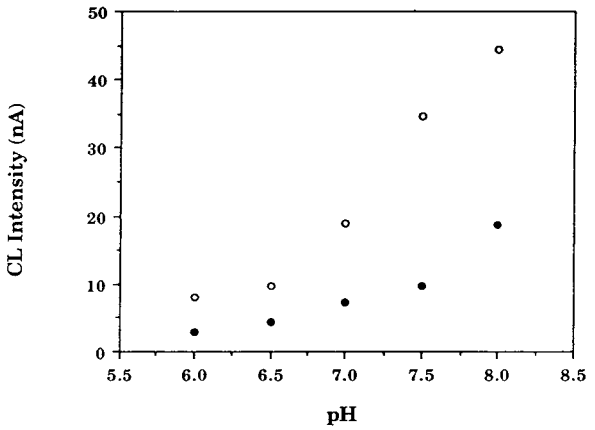

Fig. 4. Effect of pH on CL for 50 μM dansyl chloride (●) and 5.0 μM Dns-Ala (○).

flow-rate of mobile phase carrier stream. An increased CL was observed up to 0.8 ml/min and a continuous CL decrease was obtained after that range. Overall, the signal varied little with change of flow-rate for Dns-Ala.

pH Effect

In order to obtain the optimum condition for the separation of a mixture of dansyl amino acids via reversed-phase HPLC, the choice of optimal parameters (composition, molarity and pH of the mobile phase) should be made. Therefore the effect of mobile phase pH on the CL intensities for 50 μM dansyl chloride and 5.0 μM Dns-Ala was investigated. This work was centered around pH 7.5, since the optimum pH for the separation has been reported to be 7.6 for 25 mM TFA mobile phase [28]. Fig. 4 shows the results obtained. As the pH of mobile phase increases, the CL signal increases significantly for both species. The noise level remained constant, so higher CL intensities correspond to higher signal-to-noise ratios. This variation in CL intensity with pH is similar to the results for amino acids reported by Brune and Bobbitt [15,21]. Although the CL intensities increase for Dns-Ala and dansyl chloride at a higher pH, dissolution of the silica gel matrix of the column support starts at pH > 8. For that reason, we used a pH 7.5 mobile phase. The CL reagent was always at the same pH as the mobile phase in this work. Because the CL reagent was added after the separation, it would have been possible to buffer that reagent at a more alkaline pH to obtain higher CL intensities. Mixing must be very efficient then to avoid degradation in precision. Additionally, if immobilized $Ru(bpy)_3^{2+}$ was used for the detection step [18,23], then no post-separation solution additions are required at all if the separation pH and detection pH are the same.

Effect of organic modifier composition

In a reversed-phase separation, a significant amount of an organic solvent as modifier can be required in the mobile phase. Therefore, it was necessary to investigate the effects such an organic solvent would have on the CL reaction. Acetonitrile and methanol are commonly used as organic modifiers in reversed-phase HPLC. Acetonitrile was used as an organic modifier in this experiment because it was also used as the solvent for the dansyl derivatization reaction of amino acids. Increasing the acetonitrile content from 0 to 50% (v/v) in the 25 mM TFA carrier stream (pH 7.5) led to an slight increase in the observed CL intensities for 50 μM Dns-Ala. This result is represented in Fig. 5. The relative standard deviation was about 3% for all these measurements. Brune and Bobbitt [15] have reported slightly enhanced $Ru(bpy)_3^{2+}$ CL intensities with up to 20% acetonitrile in the mobile phase. Diffusion coefficients were measured for

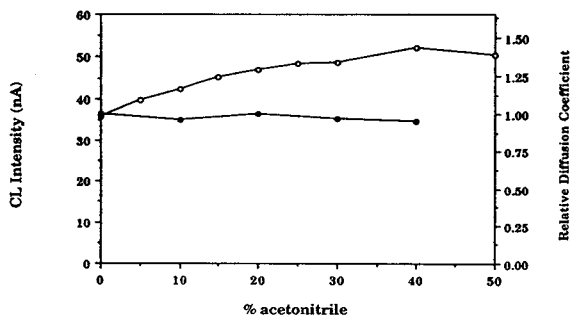

Fig. 5. Effect of acetonitrile composition on CL for 50 μM Dns-Ala. ○ = CL intensity; ● = relative diffusion coefficient.

each buffer having different compositions of acetonitrile in order to know whether or not a change in the mass transfer rate could be occurring and be responsible for the observed increase in the CL signal. The measured diffusion coefficients are almost constant over the 0–40% acetonitrile range (Fig. 5). This result shows that the presence of acetonitrile in the mobile phase buffer may not be affecting the mass transfer rate but instead may affect the quantum efficiencies of the CL process. Bard and co-workers [25,29] have reported that the ECL efficiency (photons emitted/$Ru(bpy)_3^{3+}$ generated) of this reaction is around 5% in acetonitrile and 2% in aqueous solution. Therefore the increased ECL efficiencies are responsible for the observed increase in CL intensity.

HPLC of dansyl-derivatized amino acids

TFA buffer is known to be highly selective for the separation of peptides [30–32] and phenylthiohydantoin derivatives of amino acids [33]. From the studies by Levina and Nazimov [28], optimum separation of dansyl amino acids was obtained with 25 mM TFA at pH 7.6. The HPLC system we used is shown in Fig. 2. In order to minimize resolution degradation all tubing used was 0.01 in. I.D. (1 in. = 2.54 cm) up to flow cell inlet. Separation of the dansyl-derivatized amino acids was performed with a Zorbax ODS (5 μm) column using a mobile phase containing 15% acetonitrile in 25 mM TFA at pH 7.5. Fig. 6 shows the separation of a mixture of six dansyl derivatized amino acids.

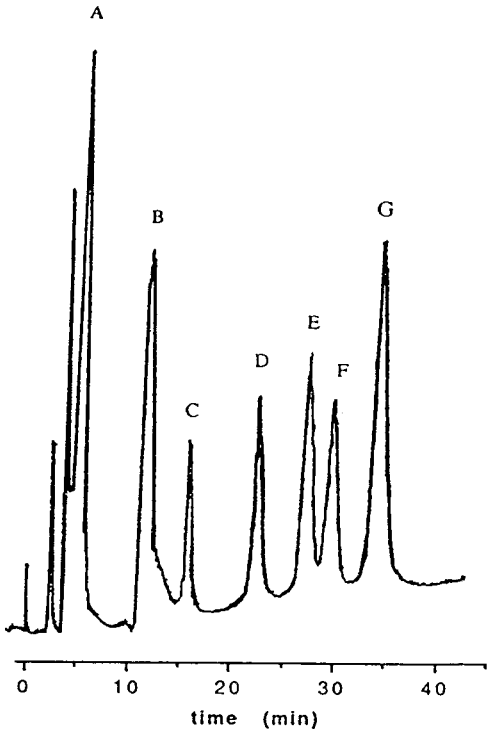

Fig. 6. Isocatic separation of six dansyl amino acids on Zorbax ODS column (5 μm) with a mobile phase containing 15% acetonitrile in 25 mM trifluoroacetate (pH 7.5). Flow-rate 1.0 ml/lmin. Each compound is 25 μM (500 pmol). Peaks: A = Dns-Glu; B = Dns-OH; C = Dns-Asn; D = Dns-Ser; E = Dns-Thr; F = Dns-Gly; G = Dns-Ala.

The six dansyl amino acids were well resolved from each other. The first two peaks are caused by the derivatization solvents. Li_2CO_3 (40 mM) at pH 9.5 was used to dissolve amino acids in the derivatization procedure; therefore, hydroxide ion in the sample resulted in CL response. A working curve for dansyl-derivatized glutamate has been obtained using the same separation conditions. Fig. 7 shows the CL signal for Dns-Glu concentrations from 0.1 to 250 μM. Each point is a mean of 3 or more injections of a sample. The relative standard deviations at 1 μM and above range from 1.5–4.5%. Least squares parameters for the 5 to 250 μM concentration range are given in Table I for both linear and logarithmic plots. The signals represented were based on peak heights instead of peak areas since the result based on peak areas was the same as that obtained based on peak heights.

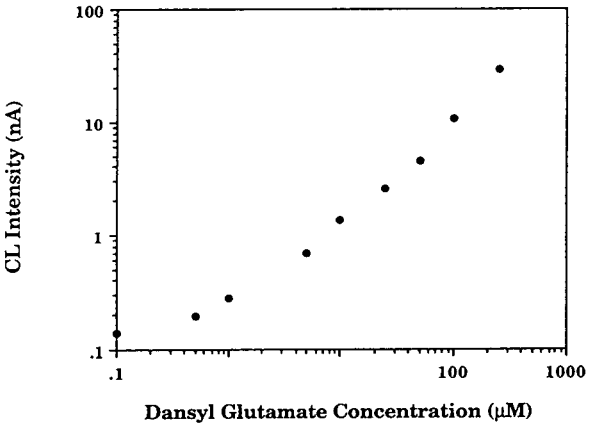

Fig. 7. Dns-Glu working curve using HPLC–CL system.

The chromatographic detection limit (signal-to-noise ratio 2) obtained was 0.1 μM (2 pmol) for Dns-Glu.

CONCLUSIONS

This detection method has a wide dynamic range and detection limits which are comparable to those reported using other methods. The detection limit obtained for Dns-Glu (2 pmol) is 25 times lower than that achieved with UV absorbance detection (50 pmol) and only slightly higher than that reported using fluorescence (sub-pmol) detection. Peroxyoxalate CL has considerably lower detection limits (10 fmol) for dansyl amino acids; however, $Ru(bpy)_3^{2+}$ CL has advantages of reagent stability, greater compatibility with common reversed-phase HPLC solvent systems, and the possibility to use the $Ru(bpy)_3^{2+}$ as an immobilized regenerable CL reagent [18]. Furthermore, it is likely that significantly improved $Ru(bpy)_3^{2+}$ detection limits could be achieved with a dansyl-like derivatization reagent designed specifically for $Ru(bpy)_3^{2+}$ CL. Although underivatized amino acids can be detected with $Ru(bpy)_3^{3+}$ CL, the dansyl derivatives have detection limits improved by three orders of magnitude. In our same flow system we observe detection limits of 2 nmol for underivatized glutamate and 1 nmol for underivatized alanine as compared to 2 pmol for Dns-Glu. The separations reported here were done with isocratic elution; however, gradient elution could be easily applied to our HPLC–CL method for the complete separation of all dansyl derivatives of the 20 common amino acids in a short time period since organic modifier in the mobile phase does not degrade the CL reaction.

TABLE I

LEAST-SQUARES PARAMETERS FOR WORKING CURVES (5–250 μM Dns-Glu)

	Linear	Logarithmic
Slope	0.117 nA/M	0.936
Slope standard error	0.003	0.049
Intercept	−0.397 nA	−4.23
Intercept standard error	0.372	0.223
Correlation coefficient	0.997	0.989
Standard error estimate	0.691	0.061

ACKNOWLEDGEMENT

This work was funded, in part, by a grant from the Biotechnology Research and Development Corporation.

REFERENCES

1 Y. Tapuhi, D.E. Schmidt, W. Lindner and B.L. Karger, *Anal. Biochem.*, 115 (1981) 123.
2 T.A. Nieman, in J.W. Birks (Editor), *Chemiluminescence and Photochemical Reactions and Detection in Chromatography*, VCH, New York, 1989, Ch. 4, pp. 99–123.
3 T. Hara, M. Toriyama and T. Ebuchi, *Bull. Chem. Soc. Jpn.*, 58 (1985) 109.
4 T. Kawasaki, M. Maeda and A. Tsuji, *J. Chromatogr.*, 328 (1985) 121.
5 S.R. Spurlin and M.M. Cooper, *Anal. Lett.*, 19 (1986) 2277.
6 P.J. Korner, Jr. and T.A. Nieman, *Mikrochim. Acta.*, II (1987) 79.
7 P.J. Korner, Jr. and T.A. Nieman, *J. Chromatogr.*, 449 (1988) 217.
8 M.P. Neary, W.R. Seitz and D.M. Hercules, *Anal. Lett.*, 7 (1974) 583.
9 M. Maeda and A. Tsuji, *J. Chromatogr.*, 352 (1986) 213.
10 S. Kobayashi and K. Imai, *Anal. Chem.*, 52 (1980) 424.
11 K. Miyaguchi, K. Honda and K. Imai, *J. Chromatogr.*, 303 (1984) 173.
12 J.B. Noffsinger and N.D. Danielson, *J. Chromatogr.*, 387 (1987) 520.
13 K. Uchikura and M. Kirisawa, *Anal. Sci.*, 7 (1991) 971.
14 L. He, K.A. Cox and N.D. Danielson, *Anal. Lett.*, 232 (1990) 195.

15 S.N. Brune and D.R. Bobbitt, *Anal. Chem.*, 64 (1992) 166.
16 M.A. Targove and N.D. Danielson, *J. Chromatogr. Sci.*, 28 (1990) 505.
17 I. Rubinstein, C.R. Martin and A.J. Bard, *Anal. Chem.*, 55 (1983) 1580.
18 T.M. Downey and T.A. Nieman, *Anal. Chem.*, 64 (1992) 261.
19 J.B. Noffsinger and N.D. Danielson, *Anal. Chem.*, 59 (1987) 865.
20 K. Uchikura and M. Kirisawa, *Anal. Sci.*, 7 (1991) 803.
21 S.N. Brune and D.R. Bobbitt, *Talanta*, 38 (1991) 419.
22 K. Uchikura and M. Kirisawa, *Chem. Lett.*, (1991) 1373.
23 A.F. Martin and T.A. Nieman, *Anal. Chim. Acta.*, 281 (1993) 475.
24 D. Ege, W.G. Becker and A.J. Bard, *Anal. Chem.*, 56 (1984) 2413.
25 I. Rubinstein, C.R. Martin and A.J. Bard, *Anal. Chem.*, 55 (1983) 1580.
26 P.T. Kissinger and W.R. Heineman, *Laboratory Techniques in Electroanalytical Chemistry*, Marcel Dekker, New York, 1984, p. 82.
27 J.A. Holeman and N.D. Danielson, *Anal. Chim. Acta*, 227 (1993) 55.
28 N.B. Levina and I.V. Nazimov, *J. Chromatogr.*, 286 (1984) 207.
29 N.E. Tokel-Takvoryan, R.E. Hemingway and A.J. Bard, *J. Am. Chem. Soc.*, 95 (1973) 6582.
30 W.C. Mahoney and M.A. Hermodson, *J. Biol. Chem.*, 255 (1980) 199.
31 H.P.J. Bennett, C.A. Browne and S. Solomon, *J. Liq. Chromatogr.*, 3 (1980) 1353.
32 P. Yuan, H. Pande, B.R. Clark and J.E. Shively, *Anal. Biochem.*, 120 (1982) 289.
33 D. Hawke, P. Yuan and J.E. Shively, *Anal. Biochem.*, 120 (1982) 302.

Journal of Chromatography A, 659 (1994) 119–126
Elsevier Science B.V., Amsterdam

CHROM. 25 512

Comparison of UV absorption and electrospray mass spectrometry for the high-performance liquid chromatographic determination of domoic acid in shellfish and biological samples

James F. Lawrence*, Benjamin P.-Y. Lau, Chantal Cleroux and David Lewis

Food Research Division, Bureau of Chemical Safety, Food Directorate, Health Protection Branch, Ottawa, Ontario K1A 0L2 (Canada)

(First received June 11th, 1993; revised manuscript received August 19th, 1993)

ABSTRACT

Domoic acid, a neurotoxic amino acid produced by the marine diatom *Nitchia pungens* multiseries, was determined in samples of anchovies, razor clams, mussels, crab, rat serum, urine and feces by HPLC with UV absorption and electrospray (ESI) mass spectrometric (MS) detection. Shellfish samples were extracted with methanol–water followed by clean-up of the extracts with solid-phase extraction cartridges (strong anion or strong cation exchange). An aliquot of the fraction containing the domoic acid was analysed by HPLC. HPLC column size, mobile phase composition and flow-rate were selected so that essentially the same conditions could be used for both HPLC–UV and HPLC–ESI-MS with selected ion monitoring (SIM) determinations. These included the use of acetonitrile–water–formic acid as the mobile phase, at a flow-rate of 0.2 ml/min (split 13:1 for HPLC–ESI-MS-SIM, 10 μl/min to the mass spectrometer). The results indicated that extracts found positive by the HPLC–UV method could be readily confirmed directly by HPLC–ESI-MS-SIM without additional sample treatment down to levels of 0.1 μg/g of domoic acid. This study demonstrates the use of HPLC–ESI-MS-SIM for the routine confirmation of domoic acid in a wide variety of samples.

INTRODUCTION

Domoic acid (Fig. 1) is a neurotoxic amino acid which was first isolated from the red alga *Chondria armata* [1,2]. It was identified as the toxic substance in mussels from eastern Canada that caused a poisoning episode resulting in several deaths [3]. Since then, several methods for the determination of domoic acid in shellfish and plankton have been reported [4–6], all involving HPLC with UV absorption detection. Several chemical confirmatory procedures have also been developed [7–9] based on the formation of either UV-absorbing or fluorescent derivatives.

The sample preparation procedure for domoic acid in shellfish is fairly simple, requiring minimal sample clean-up after the initial extraction [4,5,10,11]. This is more than adequate to enforce the guideline level of 20 μg/g (ppm) domoic acid in shellfish set by the Canadian Department of Health and Welfare. However, for certain applications these methods may not be adequate. For example, more sensitive methods might be useful for studying the uptake of domoic acid by bivalve molluscs, in toxicology feeding studies or for the prediction of potential accumulation of domoic acid in shellfish well in advance of any serious contamination. During the course of some research on the chemical

* Corresponding author.

0021-9673/94/$07.00
SSDI 0021-9673(93)E0916-I

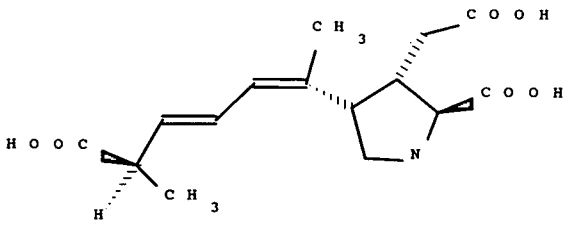

Domoic Acid

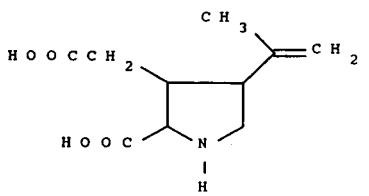

Kainic Acid

Fig. 1. Structures of domoic acid and kainic acid.

confirmation of domoic acid, we found that the use of two solid-phase extraction (SPE) cartridges (an anion-exchange followed by a reversed-phase cartridge) was very effective in removing co-extracted material which interfered in the derivatization reactions [7,9]. The strong anion-exchange clean-up procedure developed by Quilliam *et al.* [6] is even simpler and applicable to most shellfish samples for the direct determination of domoic acid at sub-μg/g levels. The chemical derivatization procedures, although useful, do not provide unequivocal proof that domoic acid is present in a sample. In this respect, HPLC–mass spectrometry (MS) has a significant advantage. Domoic acid and other seafood toxins have been studied by Quilliam and Pleasance's group [12–15] using HPLC–electrospray (ESI) MS. Their work clearly demonstrated the potential of the technique for the confirmation of domoic acid and other seafood toxins in shellfish extracts.

In this paper we describe investigations into the use of HPLC–ESI-MS for the routine confirmation of domoic acid in a variety of sample extracts. The aim was to determine how easily and quickly the confirmation could be made and to compare the results with values obtained by HPLC–UV analysis. The timeliness of HPLC–ESI-MS confirmation is particularly important in cases where regulatory guidelines are exceeded or human illness is involved so that appropriate action can be taken quickly.

EXPERIMENTAL

Reagents

Domoic acid standard solutions were prepared in doubly deionized water from a calibration solution (DACS, 0.89 μg/ml; National Research Council of Canada, Halifax, Canada). All solvents and chemicals were of HPLC or analytical-reagent grade. All solutions of standards and samples were refrigerated when not in use.

Liquid chromatography–UV detection

The HPLC system consisted of an Eldex Model 9600 ternary gradient pump, a Rheodyne Model 8125 injector with a 20-μl sample loop, a reversed-phase LC-18 (Supelco) column (150 × 2.1 mm I.D., 5 μm) and a diode array detector (Hewlett-Packard Model 1040A) set to monitor at 242 nm. The mobile phase consisted of 0.2% (v/v) formic acid plus 12% (v/v) acetonitrile in water (pH 3.0). The flow-rate was set at 0.5 ml/min.

Liquid chromatography–mass spectrometry

The HPLC system consisted of a Beckman Model 112 pump, a Rheodyne Model 8125 injector with a 20-μl (for seafood) or a 50-μl loop (for serum, urine and feces) and a reversed-phase Deltabond ODS (Keystone) column (200 × 2.1 mm I.D., 5 μm). The mobile phase consisted of 0.1% (v/v) formic acid + 12% (v/v) acetonitrile in water and was pumped isocratically at a flow-rate of 0.20 ml/min. In order to accommodate the low flow-rate of the electrospray interface, the LC effluent was split. A splitter was constructed by connecting two pieces of fused-silica tubing with different internal diameters (0.12 and 0.35 mm I.D.) to a tee-union (Valco). The length of each tube was adjusted to facilitate a suitable splitting ratio of between 5:1 and 13:1. The end of the larger diameter tubing was connected to a UV detector (Micromeritics Model 788) operating at a wavelength of 254 nm such that UV chromatograms

could be concurrently recorded. The smaller-diameter tubing carrying a flow-rate of 40–10 μl/min was directly connected to the pneumatic-assisted electrospray interface, which was constructed in our laboratory with a similar design to a commercial model (API 3; Sciex, Toronto, Canada). As shown in Fig. 2, a zero-dead-volume tee-union (Valco) was used to hold two pieces of coaxial stainless-steel tubing, the inner 27-gauge (0.205 mm I.D. × 0.406 mm O.D.) tubing was 45 mm long and the outer 21-gauge (0.406 mm I.D. × 0.813 mm O.D.) tubing was 37 mm long. The inner tubing protruded *ca.* 1 mm from the tip of the outer stainless-steel tubing. The 0.17 mm O.D. (0.12 mm I.D.) fused-silica tubing delivering the LC effluent passed through the inner stainless-steel tubing and protruded 0.5 mm from its tip. A nitrogen nebulizing gas [40 p.s.i. (275.8 kPa)] was delivered through the side-arm of the tee-union such that it flowed through the gap between the inner and outer stainless-steel tubing. The tee-union was connected to a high-voltage power supply (Bertan Series 125) with a limiting current of 50 μA. The optimum voltage was usually 5–6 kV. The splitter and the electrospray probe assembly were mounted on a solid PTFE block [or other electrical insulation material, about 1/4 in. (0.635 cm) thick] which in turn was mounted on a three-dimensional micro-manipulator (Brinkman) so that the position of the electrospray probe could be reproducibly adjusted in the x, y and z directions. The position of the electrospray probe tip was about 1–2 cm away from the counter electrode (*i.e.*, the atmospheric pressure ion source "interface plate") and was 0.5–1 cm off-axis from the ion-entrance orifice. It was found that the noise could be minimized by setting the angle of the probe to 30–45° with respect to the mass spectrometer axis.

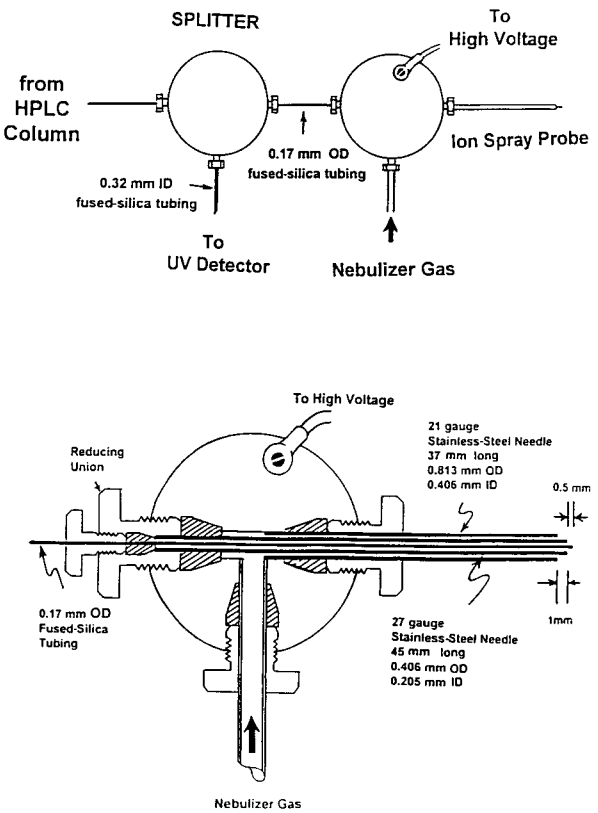

Fig. 2. Top: schematic diagram showing the construction of the electrospray interface. Bottom: details of the probe tip and nebulizer gas connection.

The mass spectrometer employed was a TAGA 6000E triple quadruple mass spectrometer (Sciex) equipped with an atmospheric pressure ionization ion source. It was operated in a single quadruple mode for maximum sensitivity. Daily operating parameters (including the position of the electrospray probe, voltages of focusing lens) were optimized by using arginine as a reference standard. Instrumentation control, data acquisition and data processing were software (Sciex) controlled by a DEC PDP-11 computer. All quantitative analyses were performed in the selected ion monitoring (SIM) mode. Three ions were simultaneously monitored, at m/z 312, 214 and 205, corresponding to the $[M + H]^+$ ion of domoic acid, kainic acid (as an internal standard) and tryptophan, respectively. The dwell time was set at 100 ms for seafood and 750 ms for the serum, feces and urine analyses.

Extraction of shellfish

The extraction procedure was similar to those described elsewhere [6,9] with combinations of methanol and water as the extraction solvent. A 10-g amount of homogenized tissue (Sorval homogenizer) was mixed with 10 ml of deionized water in a 50-ml centrifuge tube for 1 min using a

vortex mixer. A 20-ml volume of methanol was added and the contents were mixed again for 1 min on the vortex mixer. The mixture was centrifuged (5 min at 3000 rpm (700 *g*) or until a clear supernatant was obtained) and the supernatant removed to a clean tube. A 10-ml volume of methanol was added to the residue and the contents were mixed and centrifuged again as mentioned above. The clear supernatant was removed and combined with the first. The final volume was adjusted to 50 ml and represented a sample concentration of 0.2 g/ml.

Preparation of rat serum, urine and feces samples

Serum and urine samples were diluted ten-fold with 50% (v/v) methanol water before SPE clean-up. For each clean-up, 2.0 ml of serum extract (or 2.5 ml of urine extract) were passed through the SPE cartridges. Feces samples (2 g) were extracted using the same volumes of methanol–water (50:50, v/v) as used for the shellfish samples. A 2.0-ml aliquot of the supernatant was used for SPE clean-up.

Strong anion-exchange clean-up

The clean-up is essentially the same as that described elsewhere [6]. A 5-ml volume of shellfish extract (or 2.0 ml of serum extract, 2.5 ml of urine extract or 2.0 ml of feces extract) was passed through a 3-ml Supelclean LC-SAX SPE cartridge (Supelco, USA) [which was preconditioned with 6 ml of methanol followed by 3 ml of deionized water and 3 ml of methanol–water (50:50, v/v)]. The effluent was discarded and the cartridge washed with 5 ml of acetonitrile–water (10:90, v/v), which was also discarded. Domoic acid was eluted with 3 ml of acetonitrile–water–formic acid (10:88:2, v/v/v). A 20-μl volume of this solution was analysed by HPLC.

Strong cation-exchange clean-up

This clean-up procedure has been described elsewhere [7]. An aliquot of sample extract (acidified to pH 3–4) was added to a 3-ml phenylsulfonic acid strong cation-exchange (SCX) SPE cartridge (Bond Elut SCX, Baker, USA) (pre-conditioned with 6 ml of methanol followed by 6 ml of 0.1 *M* hydrochloric acid) and the effluent discarded. The cartridge was washed with 3 ml of deionized water and the effluent discarded. Domoic acid was eluted with 6 ml of 0.7 *M* hydrochloric acid directly on to a 3-ml reversed-phase C_{18} SPE cartridge (Baker) (preconditioned with 6 ml of methanol followed by 6 ml of 0.7 *M* hydrochloric acid). All acid passing through the reversed-phase SPE cartridge was discarded and the cartridge was then washed with 3 ml of deionized water which was discarded. Domoic acid was eluted with 4 ml of 20% (v/v) acetonitrile in 1% (v/v) aqueous acetic acid. A 20-μl volume of this solution was injected into the HPLC system.

RESULTS AND DISCUSSION

The methanol–water extraction worked well for all sample types examined. Some adjustments to the sample mass:extraction solvent ratios were required to obtain extracts suitable for clean-up with both the urine and feces samples. Recoveries from both spiked and naturally incurred shellfish samples were usually greater than 90% over a range of 0.2–40 μg/g domoic acid with good repeatability similar to that observed earlier for shellfish [12]. The recoveries at the 1.0 μg/g level from spiked urine (84%) and feces (86%) were lower. There were some differences in the effectiveness of the two SPE clean-up procedures employed for HPLC with UV detection. Both performed well for all seafood samples (mussels, razor clams, crab meat, anchovies) and the serum samples studied (detection limits were in the range 0.05–0.1 μg/g). The SAX SPE procedure was used for these samples on a regular basis as only one SPE cartridge was required as opposed to two cartridges for the SCX SPE clean-up. However, the SAX SPE clean-up was not as effective as the SCX SPE clean-up for urine and feces samples. Fig. 3 compares chromatographic results for extracts of rat feces spiked at 1 μg/g using the SCX clean-up. The extracts cleaned up with SAX SPE required a modification of the mobile phase (from 12 to 10% acetonitrile, see Experimental) to separate domoic acid from interfering co-extractives in both feces and urine samples. Detection limits for urine and feces

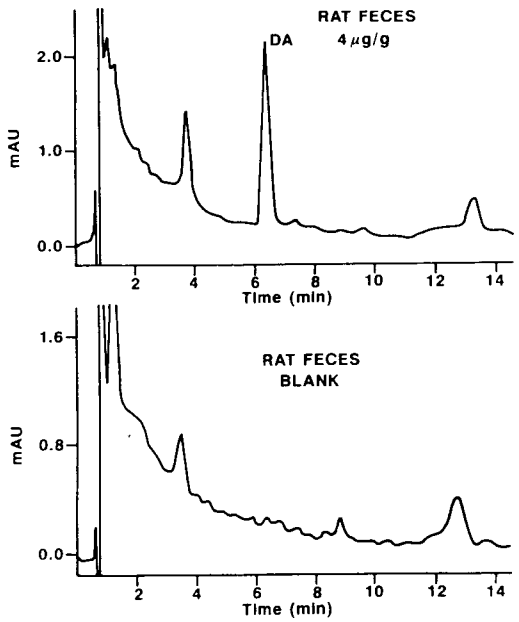

Fig. 3. Chromatograms of extracts of blank and spiked (1 μg/g domoic acid) rat feces samples cleaned up using SCX/C_{18} SPE cartridges. DA = Domoic acid.

samples were about 0.1–0.2 μg/g with the SCX cleanup.

Fig. 4 shows the electrospray mass spectrum of domoic acid in the positive-ion mode. Similar to that reported by Quilliam *et al.* [12], the electrospray mass spectrum displays a large peak at *m/z* 312 that arises from the protonated molecule and no significant fragmentation. Sodium attachment produces an ion at *m/z* 334. The dominant protonated molecule was chosen in the selected ion monitoring.

The use of kainic acid as an internal standard proved to be useful in providing more reliable quantitative results. Although it is not an ideal compound (the first choice would be a stable isotopically labeled domoic acid, but none is commercially available) and it does not share a common structure with domoic acid (compare the structures in Fig. 1). Its availability in our laboratory was the prime reason why we chose this compound as an internal standard to compensate for variations in the splitting ratio of the LC effluent. Fig. 5 shows the SIM responses from an injection containing 38.5 ng of domoic acid and 50 ng of kainic acid, using a dwell time of 100 ms for each ion. The minimum detection limit (MDL, based on an *S/N* ratio of 5:1) for the domoic acid under these conditions was estimated (by extrapolation) to be 1.5 ng per injection or equivalent to 0.1 μg/g in the samples. Extending the dwell time to 750 ms in later serum, urine and feces analyses improved the *S/N* ratio by a factor of 4–6 thus routinely attaining the MDL at 0.4–0.3-ng levels (some-

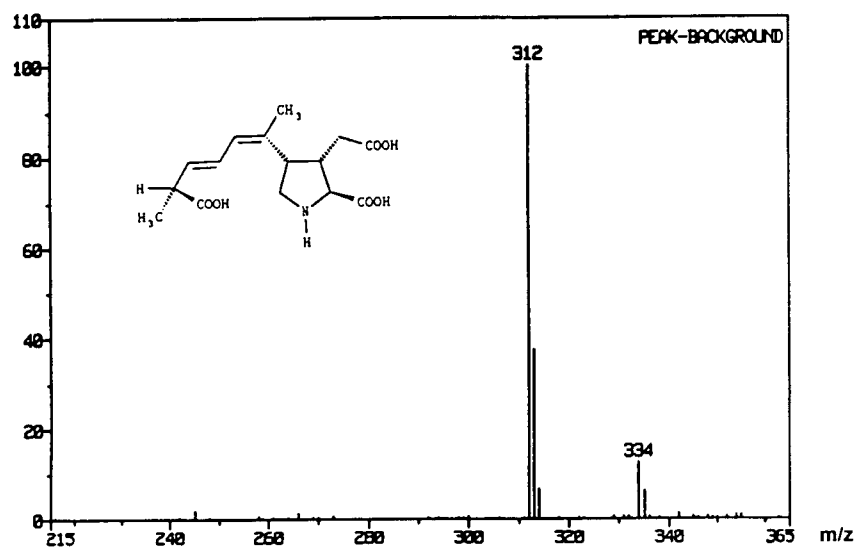

Fig. 4. Electrospray mass spectrum of domoic acid in the positive-ion mode. Scanning range: *m/z* 100–400. Y-axis, relative intensity, %.

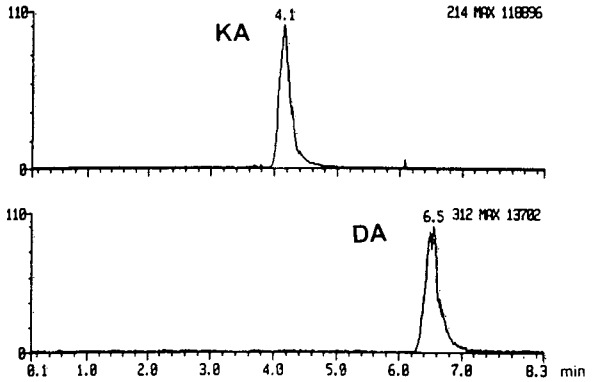

Fig. 5. SIM mass chromatograms of an injection containing 38.5 ng domoic acid (DA) and 50 ng kainic acid (KA) using a dwell time of 100 ms. Injecton volume, 20 μl. Y-axis, relative intensity, %.

times even down to 0.1 ng). When a splitting ratio of 10–15:1 was employed, absolute minimum detection limits at the low-picogram level could be achieved. This compares favorably with that reported by Quilliam *et al.* [12] using a commercial version of an electrospray interface and a newly improved mass spectrometer (Sciex Model API 3). The calibration graph showed linear responses within the working concentration range (1–140 ng). The same linear range was observed for the HPLC–UV analyses.

Table I compares results obtained by HPLC–UV detection with those obtained by HPLC–ESI-MS-SIM for a variety of sample extracts. As can be seen, the agreement between the two techniques is good over more than a 100-fold concentration range (0.4–41.2 μg/g of domoic acid). Also, the analyses were carried out over several days, indicating a good day-to-day correlation betweeen the two methods. The HPLC–ESI-MS-SIM results clearly confirm the findings obtained by HPLC–UV detection. Figs. 6 and 7 compare chromatograms for razor clams and crab meat obtained with the two detection methods. The first example shows a sample contaminated at the level of 16.5 μg/g near the Canadian guideline of 20 μg/g, whereas the second

TABLE I

COMPARISON OF RESULTS OBTAINED BY HPLC–UV AND HPLC–ESI-MS-SIM METHODS FOR DOMOIC ACID IN BIOLOGICAL SAMPLES

Sample	Domoic acid (μg/g)	
	HPLC–UV[a]	HPLC–ESI-MS-SIM[a]
Razor clam A[b]	41.2	43.1
Razor clam B[b]	16.6	16.5
Anchovy[b]	10.5	12.6
Crab meat[b]	0.4	0.5
Blank mussel (Prince Edward Island, Canada)	ND[c]	ND[c]
Blank mussel (Nova Scotia, Canada)	ND	ND
Spiked mussel (Prince Edward Island, Canada)	6.1	6.5
Spiked mussel (Nova Scotia, Canada)	5.1	6.2
Blank urine	ND	ND
Spiked urine A	3.7	2.7
Spiked urine B	0.4	0.3
Blank feces	ND	ND
Spiked feces A	2.7	3.4
Spiked feces B	0.6	0.7
Blank serum	ND	ND
Spiked serum A	8.5	12.5
Spiked serum B	0.4	0.5

[a] Single determinations.
[b] Naturally incurred residues.
[c] ND = Not detected.

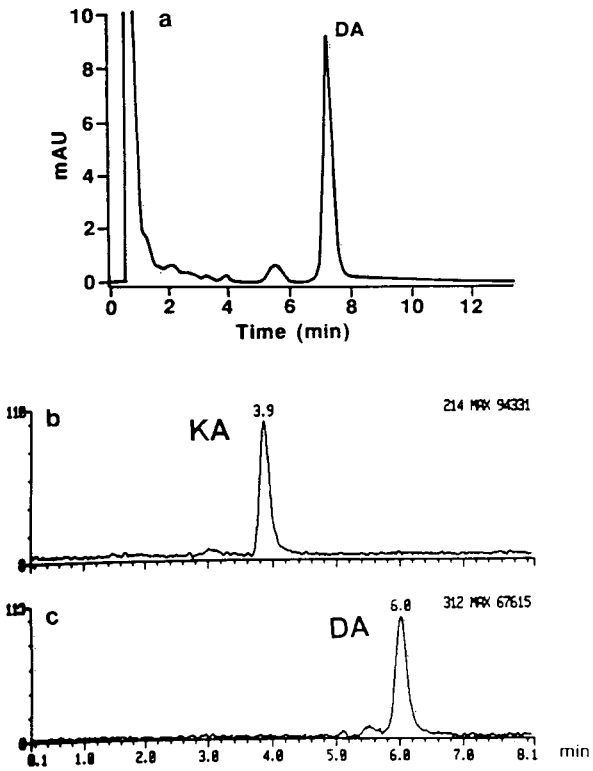

Fig. 6. Comparison of chromatograms from (a) HPLC–UV detection and (b, c) HPLC–ESI-MS-SIM analyses of a contaminated razor clam sample (16.5 μg/g). Injecton volume, 20 μl; dwell time, 100 ms. KA = Kainic acid; DA = domoic acid. Y-axis, relative intensity, % (b and c).

example (contaminated with 0.53 μg/g of domoic acid) shows that contamination even 40 times below the guideline can be easily detected and confirmed by the HPLC–ESI-MS-SIM method. Minor interferences become more apparent at low levels. It is not certain whether or not the small peaks (retention times 3.4 and 5.8 min in Fig. 7) that eluted before the domoic acid (retention time 6.3 min) are isomers of domoic acid, although several domoic acid isomers have been previously reported to be present in shellfish and plankton [12]. Perhaps MS–MS will be helpful in establishing the identity of these peaks.

Extending the analysis of domoic acid to biological samples is beneficial in the area of toxicological research but it is also more demanding in the development of analytical methodology. Both the sensitivity and selectivity

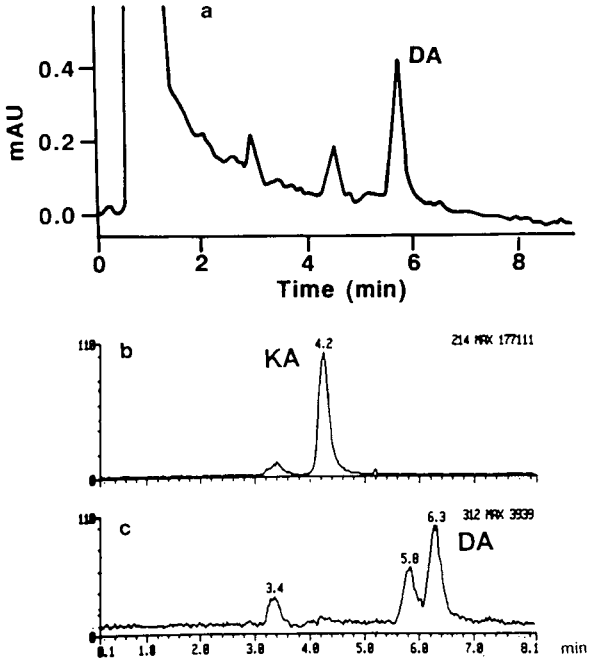

Fig. 7. Comparison of chromatograms from (a) HPLC–UV detection and (b, c) HPLC–ESI-MS-SIM analyses of a contaminated crab meat sample (0.53 μg/g). Injecton volume, 20 μl; dwell time, 100 ms. KA = Kainic acid; DA = domoic acid. Y-axis, relative intensity, % (b and c).

requirements are usually higher owing to the lower concentrations and the more complex nature of the sample matrix. In both respects, HPLC–ESI-MS-SIM proves to be a valuable tool in these applications. For example, tryptophan is known to be a potential interferent with UV detection especially if no SPE clean-up is employed. However, the compound is easily distinguished from domoic acid by MS because of their mass differences. Monitoring of this compound was added in the later analyses of monkey urine, serum and feces by HPLC–ESI-MS-SIM. It was found that the matrix from urine and feces imposed no particular problem during the MS determination. As shown in Fig. 8, ng/g levels can be easily detected. However, serum samples appear to contain a high concentration of some strong ionic compounds that eluted earlier than the kainic acid and domoic acid. The ion current was so strong that it exceeded the limiting current and automatically shut off the high-voltage power supply, as indicated by the negative

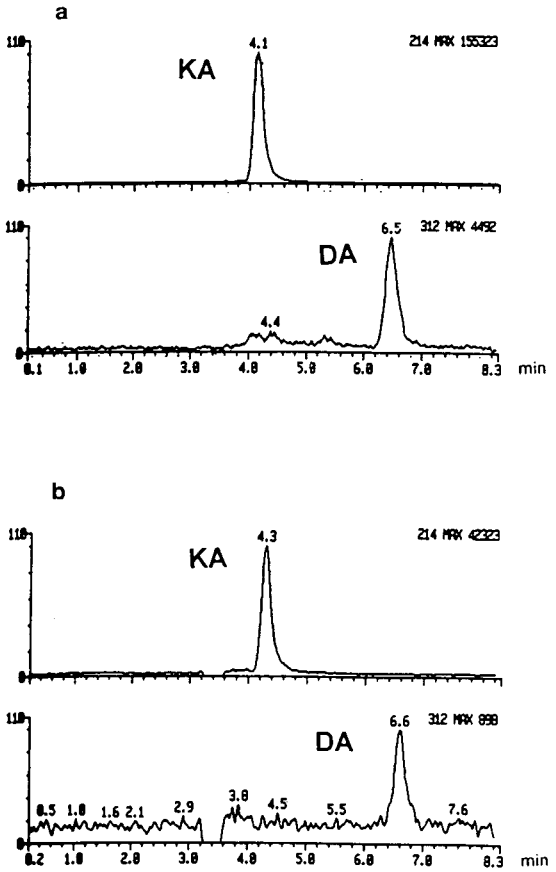

Fig. 8. SIM mass chromatograms from (a) a spiked rat urine sample (0.18 ppm) and (b) a spiked rat serum sample (0.14 ppm). Injection volume, 50 μl; dwell time, 750 ms. KA = Kainic acid; DA = domoic acid. Y-axis, relative intensity, %.

dip in the mass chromatogram in Fig. 8. A manual reset of the high-voltage power supply was required to restore the high voltage on the electrospray probe before the elution of the analytes of interest. It is not certain whether the tailing of these strong electrolytes has any effect on the ionization of the later-eluting kainic acid. If so, it may lower the response of the kainic acid and thus affect the domoic acid determination.

CONCLUSIONS

The results presented in Table I clearly demonstrate that MS confirmation is particularly useful at levels near the detection limit of the HPLC–UV method, as unambiguous results were obtained by the former owing to the substantially greater selectivity and somewhat better sensitivity. It has been successfully applied to the analysis of various seafood and biological samples.

REFERENCES

1 T. Takemoto, K. Daigo, Y. Kondo and K. Kondo, *Yakugaku Fasahi*, 86 (1966) 874.
2 M. Maeda, T. Kodama, T. Tanaka, H. Yoshizumi, T. Takemoto, K. Nomoto and T. Fujita, *Chem. Pharm. Bull.*, 34 (1986) 4892.
3 J.L.C. Wright, R.K. Boyd, A.S.W. de Freitas, M. Falk, R. Foxall, W.D. Jamieson, M.V. Laycock, A.W. McCulloch, A.G. McInnes, P. Odense, V. Pathak, M.A. Quilliam, M. Ragan, P.G. Sim, P. Thibault, J.A. Walter, M. Gilgan, D. Richard and D. Dewar, *Can. J. Chem.*, 67 (1989) 481.
4 M.A. Quilliam, P.G. Sim, A.W. McCulloch and A.G. McInnes, *Int. J. Environ. Anal. Chem.*, 36 (1989) 139.
5 J.F. Lawrence, C.F. Charbonneau, C. Ménard, M.A. Quilliam and P.G. Sim, *J. Chromatogr.*, 462 (1989) 349.
6 M.A. Quilliam, M. Xie and W.R. Hardstaff, *Technical Report No. 64, NRCC 33001*, National Research Council of Canada, Institute of Marine Biosciences, Halifax, 1991.
7 J.F. Lawrence, C.F. Charbonneau, B.D. Page and G.M.A. Lacroix, *J. Chromatogr.*, 462 (1989) 419.
8 R. Pocklington, J.E. Milley, S.S. Bates, C.J. Bird, A.S.W. de Freitas and M.A. Quilliam, *Int. J. Environ. Anal. Chem.*, 38 (1990) 351.
9 J.F. Lawrence and C. Ménard, *J. Chromatogr.*, 550 (1991) 595.
10 M.S. Nijjar, B. Grimmelt and J. Brown, *J. Chromatogr.*, 568 (1991) 393.
11 J.R.T. Blanchard and R.A.R. Tasker, *J. Chromatogr.*, 526 (1990) 546.
12 M.A. Quilliam, B.A. Thompson, G.J. Scott and K.W.M. Siu, *Rapid Commun. Mass Spectrom.*, 3 (1989) 145.
13 S. Pleasance, M.A. Quilliam, A.S.W. de Freitas, J.C. Marr and A.D. Cembella, *Rapid Commun. Mass Spectrom.*, 4 (1990) 206.
14 S. Pleasance, S.W. Ayer, M.V. Laycock and P. Thibault, *Rapid Commun. Mass Spectrom.*, 6 (1992) 14.
15 S. Pleasance, M.A. Quilliam and C. Julie, *Rapid Commun. Mass Spectrom.*, 6 (1992) 121.

Journal of Chromatography A, 659 (1994) 127–131
Elsevier Science B.V., Amsterdam

CHROM. 25 577

Determination of tomatine in foods by liquid chromatography after derivatization

Kayoko Takagi* and Masatake Toyoda

National Institute of Health Sciences, 1-18-1, Kamiyoga, Setagaya-ku, Tokyo 158 (Japan)

Megumi Shimizu and Tomomi Satoh

Kitasato University, 1-51-1, Kitasato, Sagamihara-shi, Kanagawa 228 (Japan)

Yukio Saito

National Institute of Health Sciences, 1-18-1, Kamiyoga, Setagaya-ku, Tokyo 158 (Japan)

(First received May 14th, 1993; revised manuscript received September 21st, 1993)

ABSTRACT

A liquid chromatographic method for measuring tomatine levels in tomatoes and tomato products was developed. Tomatine was extracted with 1% acetic acid and purified on a C_{18} cartridge. Tomatine in the eluate was acetylated with acetic anhydride and isolated on a C_{18} cartridge. The solvent in the eluate was evaporated and the residue was dissolved in acetonitrile. An aliquot was injected into an Inertsil ODS-2 HPLC column and the acetylated tomatine was measured at 205 nm using a UV detector. The limit of determination was 1 $\mu g\ g^{-1}$. Tomatine was detected in the green portions of tomatoes and in tomato ketchups and juices at levels below 7 $\mu g\ g^{-1}$.

INTRODUCTION

Tomatine is a steroidal glycoalkaloid which has anti-fungal activity [1] and appears to be restricted in its taxonomic distribution to the family Solanaceae and, in particular, to the genera *Solanum* and *Lycopersicon* [2].

The human toxicity of tomatine is twofold, that is, it inhibits cholinesterase [3] and cytostatic activities [3–5]. We previously showed the membrane-distruptive properties of tomatine, α-chaconine, α-solanine and solanidine, among which tomatine had the strongest effect [6].

Tomatine is contained in tomato leaves (2000–5000 $\mu g\ g^{-1}$) and in unripe fruits (300–900 $\mu g\ g^{-1}$) [2]. Food poisoning caused by tomatine however, has not been reported until recently, because tomatine disappears during the ripening process of tomatoes owing to enzymatic degradation [7].

Earlier methods used for determining tomatine levels were bioassays based on the degree of growth inhibition of cultured fungi. This was followed by spectrometric methods. However, as tomatine does not have any chromophoric groups, it has been determined photometrically after reaction with chromogenic reagents [8–11]. It can also be determined by thin-layer chromatography [12]. The separation and quantitation of *Solanum* steroidal alkaloids in potatoes by reversed-phase HPLC has been investigated [13]. However, these methods for measuring tomatine in foods were unsatisfactory

* Corresponding author.

0021-9673/94/$07.00
SSDI 0021-9673(93)E1009-O

as they were subject to interference from other tomato components.

In this paper, we describe a method for measuring residual tomatine levels in tomatoes and tomato products by extraction and high-performance liquid chromatography.

EXPERIMENTAL

Instrumentations

A mini-food processor (New Cooker SKC-03; Sogo-Giken, Tokyo, Japan) was used to homogenize the samples and a universal homogenizer (Nippon Seiki, Tokyo, Japan) was used for extraction. A Rheodyne Model 7125 injector, a Model 880-PU pump, a Model 870 UV detector (Japan Spectroscopic, Tokyo, Japan), an Inertsil ODS-2 column (25 cm × 4.6 mm I.D., particle size 5 μm) (GL Sciences, Tokyo, Japan) and a LiChrospher NH_2 column (25 cm × 4 mm I.D., particle size 5 μm) (Cica-Merck, Tokyo, Japan) constituted the HPLC system.

Mobile phase

Acetonitrile–water (90:10) was the solvent for Inertsil ODS column chromatography and acetonitrile–50 m*M* potassium dihydrogenphosphate (75:25) for LiChrospher NH_2 column chromatography.

Reagents

All chemicals were of special grade, with the exception of acetonitile, which was of analytical-reagent grade, and were obtained from Wako (Osaka, Japan). HiFlo Super-Cel, which is a kind of diatomaceous earth and helps rapid filtration, was also purchased from Wako. Sep-Pak C_{18} cartridges (volume 1 ml) were purchased from Waters (Milford, MA, USA). Tomatine was obtained from Sigma (St. Louis, MO, USA).

Materials

Commercial tomatoes and processed tomato foods were purchased in Tokyo and unripe tomatoes (*Lycopersicon esculentum*, Mill.) were supplied by the National Research Institute of Vegetables, Ornamental Plants and Tea (Aichi, Japan).

Extraction and purification of tomatine

One piece of tomato was homogenized using a mini-food processor. Five grams of the homogenate were mixed with 50 ml of 1% acetic acid and 2.5 g of HiFlo Super-Cel. The mixture was homogenized for 3 min using a universal homogenizer. The homogenate was filtered through Toyo filter-paper No. 5A (Toyo-roshi, Kyoto, Japan) and the residue was re-extracted with 40 ml of 1% acetic acid. The filtrates were combined and made up to 100 ml with 1% acetic acid. A 40-ml volume was applied to a Sep-Pak C_{18} cartridge previously washed with 10 ml of methanol and 10 ml of 1% acetic acid in that order. The sample on the column was washed with 5 ml of 1% acetic acid followed by 10 ml of 20% methanol, then tomatine was eluted with 5 ml of methanol. The methanol eluate was concentrated to dryness using a rotary evaporator in a 30-ml pear-shaped flask.

Acetylation of tomatine

To the residue, 0.2 ml of pyridine and 0.5 ml of acetic anhydride were added, then refluxed on a boiling water-bath for 1 h. After cooling to room temperature, 30 ml of 50% methanol were added to the flask. The mixture in the flask was applied to a Sep-Pak C_{18} cartridge that had previously been washed with 10 ml of methanol and 10 ml of 50% methanol, then the same flask was rinsed with 5 ml of 50% methanol, the rinsed solution was also applied to the cartridge and the cartridge was washed with 10 ml of 70% methanol. Acetylated tomatine was eluted with 5 ml of methanol. The methanol eluate was concentrated to dryness using a rotary evaporator, the residue was dissolved in 0.5 ml acetonitrile and the solution was analysed by HPLC.

HPLC conditions

Acetylated tomatine was separated on an Inertsil ODS-2 column at room temperature (25°C). The flow-rate was 1.0 ml min^{-1} and the eluate was monitored at 205 nm. The injection volume was 20 μl.

RESULTS AND DISCUSSION

Purification of tomatine on a Sep-Pak C_{18} cartridge

A 1-ml volume of tomatine standard (50 μg ml^{-1}) was applied to a Sep-Pak C_{18} cartridge and eluted with 5 ml each of 20, 30 and 100% methanol. Tomatine levels in the eluates were determined by HPLC with UV detection (205 nm) using an amino-bonded column. None of the applied tomatine was eluted with 5 ml of 20% methanol, 4.6% of it was eluted with 5 ml of 30% methanol and 100% of it was recovered with 5 ml of 100% methanol. We therefore decided to wash the column with 5 ml of 20% methanol before eluting tomatine with 5 ml of methanol.

Acetylation of tomatine

After passage through the C_{18} cartridge, numerous interfering compounds remained, as determined by HPLC (Fig. 1). To eliminate them, we derivatized tomatine with an acetylating agent and again passed it through the cartridge.

The methanol eluate from a Sep-Pak C_{18} cartridge was concentrated completely to dryness, then 0.2 ml of pyridine and 0.5 ml of acetic anhydride were added to the residue. The mixture was refluxed on a boiling water-bath for 120 min. Fig. 2 shows the time course of acetylation of tomatine. The maximum peak height was

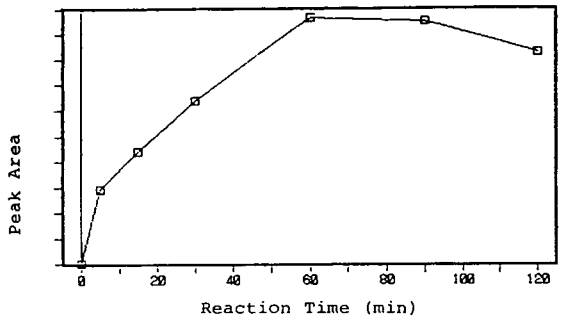

Fig. 2. Time course of tomatine acetylation. An 800-μg amount of tomatine was reacted with 0.2 ml of pyridine and 0.5 ml of acetic anhydride on a boiling water-bath for 5, 15, 30, 60, 90 or 120 min. The reaction mixtures were purified on a Sep-Pak C_{18} cartridge and analysed by HPLC.

obtained after 60 min. Methanol (50%) was added to the solution, then the mixture was loaded on a Sep-Pak C_{18} cartridge. As shown in Fig. 3, 70–100% methanol was passed through the column, and 100% of the acetylated tomatine was recovered with 100% methanol.

Acetylation made it easy to purify tomatine in the methanol eluate and to separate it from interfering components in tomato, as shown in Fig. 4. Acetylated tomatine was determined by HPLC using an ODS column, and the calibration graph was linear in the range 10–800 μg ml^{-1} of tomatine.

One mol of α-tomatine, a steroidal glycoalkaloid, possesses 2 mol of D-glucose and 1 mol each of D-galactose and D-xylose. The removal of the sugars by partial hydrolysis in dilute acid

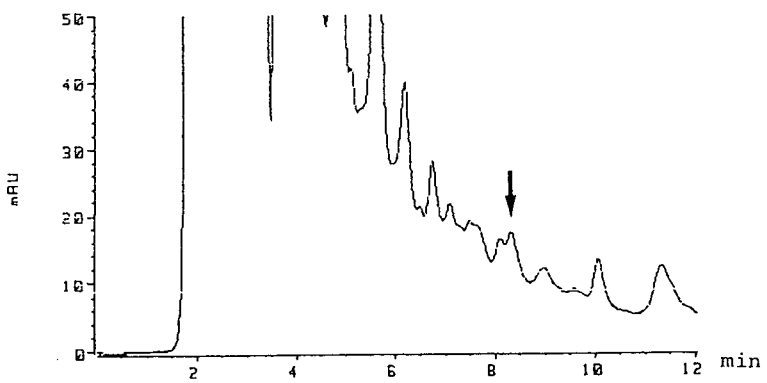

Fig. 1. HPLC of tomato extract after passage through a Sep-Pak C_{18} cartridge and before acetylation. Tomatine was added to the tomato homogenate at 50 μg g^{-1}. The arrow indicates the tomatine peak. HPLC conditions: column, LiChrospher NH_2 (250 mm × 4.6 mm I.D.); mobile phase, CH_3CN–50 m*M* KH_2PO_4 (75:25); detection wavelength, 205 nm.

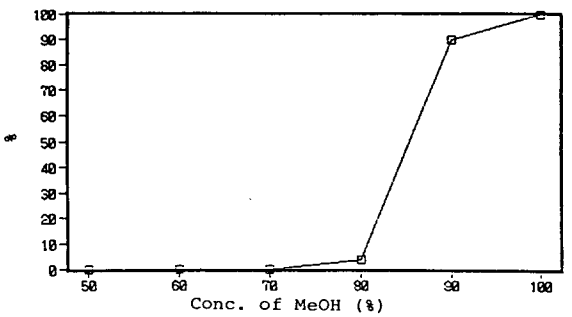

Fig. 3. Elution profile of acetylated tomatine from a Sep-Pak C_{18} cartridge using various concentrations of methanol. Acetylated tomatine (200 μg as tomatine) in 10 ml of 50% methanol was applied to a Sep-Pak C_{18} cartridge and eluted with 10 ml each of 50, 60, 70, 80, 90 and 100% methanol. Each eluate was concentrated to dryness, the residue dissolved in 0.5 ml of acetonitrile and the solution analysed by HPLC.

results in β_1-tomatine (minus D-xylose), β_2-tomatine (minus one D-glucose), γ-tomatine (minus D-xylose and one D-glucose) and the aglycone tomatidine [7]. We confirmed the presence of these sugar molecules in standard tomatine, which means that the main component of the tomatine used in this experiment was α-tomatine. Before and after derivatization the UV spectra did not change, but the polarities changed drastically. For this reason, the main peak on the chromatogram (Fig. 4) may correspond to acetylated α-tomatine, but elucidation of the structure is still under investigation.

Recovery of tomatine from ripe tomatoes

The recoveries of tomatine from commercial half-ripened fruit spiked at 200 and 20 μg g^{-1} were 89.3 ± 1.4% (n = 3) and 66.9 ± 1.2% (n = 3), respectively. The half-ripened fruit contained tomatine at 3.8 ± 0.4 μg g^{-1} (n = 3). Typical high-performance liquid chromatograms of a ripe fruit and a spiked extract are shown in Fig. 4. The limit of determination was 1.0 μg g^{-1} at a signal-to-noise ratio of 3 for raw samples. Fig. 5 shows a typical chromatogram of an extract from unripe tomato containing 3.0 μg ml^{-1} of tomatine.

Tomatine content in mini-tomato plants

Tomatine levels in leaves, green unripe fruit and red ripe fruits from two mini-tomato plants were analysed. Fairly large amounts of tomatine were detected in the leaves (493.4 and 616.3 μg g^{-1}), and green unripe fruits contained tomatine at levels of 154.4 and 196.7 μg g^{-1}, as reported previously [7]. On the other hand, all three red ripe fruits contained tomatine only at 1 μg g^{-1}.

Time course of disappearance of tomatine during storage of unripe tomatoes

Tomatoes were harvested before maturation, when their surfaces were almost all green. About twenty tomatoes were kept at 10°C in the dark and the tomatine levels in batches of three tomatoes were determined after 0, 4 and 9 days. On day 0, tomatine was detected at a level of 2.2–4.5 μg g^{-1} (average ± S.D. = 3.0 ± 1.3 μg g^{-1}), on day 4 at 1.0–2.6 μg g^{-1} (average ±

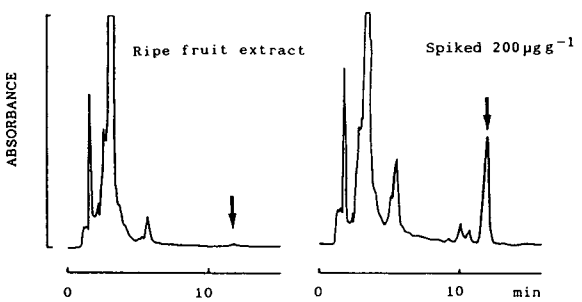

Fig. 4. Chromatograms of extracts from ripe tomatoes and from a spiked sample. Tomatine was added at 200 μg g^{-1} to the tomato homogenate. Arrows indicate acetylated tomatine peaks. The retention time was 12.3 min.

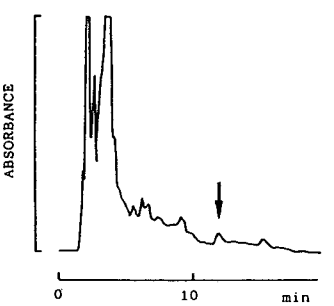

Fig. 5. Chromatogram of an extract from an unripe tomato containing 3.0 μg ml^{-1} of tomatine.

S.D. = 1.6 ± 0.7 μg g^{-1}) and on day 9 it was undetectable and all fruits were red ripe. On day 0, the green portion cut off from three tomatoes contained tomatine at an average level of 3.9 ± 1.6 μg g^{-1}. However, tomatine was not detected in the red portion removed from the same tomatoes. These results suggest that almost all the tomatine in the green portion of tomato disappears during ripening.

The tomatine contents in one commercial tomato purée, three ketchups and three juices were measured. Tomatine was detected in two of the ketchups at levels of 5.5 and 6.5 μg g^{-1} and in two of the juices at levels of 2.5 and 3.7 μg g^{-1}. The oral toxicity of α-tomatine has been examined only in mice and rats [7], and the lethal dose was 500 and 900–1000 mg kg^{-1}, respectively. The concentrations of tomatine detected in half-ripened fruits and tomato products were thus considerably lower than the lethal levels.

ACKNOWLEDGEMENT

The author thanks Mr. Yoshio Nonoyama (Ministry of Agriculture, Forestry and Fisheries) for the gift of unripe tomato samples.

REFERENCES

1 P.A. Arneson and R.D. Durbin, *Plant Physiol.*, 43 (1968) 683.
2 J.G. Roddick, *Phytochemistry*, 13 (1974) 9.
3 J.G. Roddick, *Phytochemistry*, 28 (1989) 2631.
4 J.G. Roddick, *Phytochemistry*, 18 (1979) 1467.
5 J.G. Roddick and A.L. Rijnenberg, *Phytochemistry*, 26 (1987) 1325.
6 M. Toyoda, W.D. Raush, K. Inoue, Y. Ohno, Y. Fujiyama, K. Takagi and Y. Saito, *Toxicol. in Vitro*, 5 (1991) 347.
7 S.T. Jadhav, R.P. Sharma and D.K. Salunkhe, *CRC Crit. Rev. Toxicol.*, 11 (1981) 21.
8 G. Diaz, A. Zaffaroni, G. Rozenkrantz and C. Djerassi, *J. Org. Chem.*, 26 (1952) 747.
9 H.A. Walens, A. Turner and M.E. Wall, *Anal. Chem.*, 26 (1954) 325.
10 H. Socic, *Planta Med.*, 19 (1971) 6.
11 J.G. Roddick and D.N. Butcher, *Phytochemistry*, 11 (1972) 2019.
12 M.B.E. Fayez and A.A. Saleh, *Fresenius' Z. Anal. Chem.*, 246 (1969) 380.
13 S.F. Osman and S.L. Sinden, *J. Chromatogr.*, 479 (1989) 189.

Journal of Chromatography A, 659 (1994) 133–141
Elsevier Science B.V., Amsterdam

CHROM. 25 488

Liquid chromatographic determination of copper speciation in jet fuel resulting from dissolved copper

Daniel B. Taylor and Robert E. Synovec*

Department of Chemistry, BG-10, University of Washington, Seattle, WA 98195 (USA)

(First received June 22nd, 1993; revised manuscript received August 3rd, 1993)

ABSTRACT

A method involving a dual normal-phase/ion-exchange mechanism, preconcentration and separation of copper cyclohexanebutyrate, copper tetramethylheptanedionate and N,N′-disalicylidene-1,2-propylenediaminocopper on the polymeric stationary phase poly(vinyl alcohol) using a ternary gradient of 2-propanol, acetonitrile and 10 m*M* KCF_3SO_3 in methanol was developed. Copper compounds with formation constants of 10^{20} or greater in water were retained via a normal-phase mechanism, whereas copper compounds with formation constants of 10^{15} or less were retained via an ion-exchange mechanism. The method was used to characterize and to determine copper compounds with a limit of detection of 10 μg/l. The developed method was used to monitor the five classes of copper complexes formed when jet fuel samples with and without DuPont Metal Deactivator (DMD), the active ingredient of which is N,N′-disalicylidene-1,2-propylenediamine, were placed in contact with a metallic copper surface.

INTRODUCTION

Scientists in a number of fields including marine chemistry [1–4], biochemistry [5], environmental chemistry [6], food chemistry [7] and medicinal chemistry [8] are interested in the development of methods capable of yielding information about the speciation of metals in solution. It is believed that methods capable of yielding information about metal speciation, where the speciation of a metal is defined by the ligands associated with the metal ion, will be useful in the study of properties such as catalytic activity, transport mechanisms, bioavailability and mobility of metals in systems [9–12]. Methods that determine the speciation of metals in solution will ultimately lead to a better understanding of the chemistries that involve those metals than is possible by methods that simply determine the bulk concentrations of those metals. The coupling of high-performance liquid chromatography (HPLC) with element-specific detection is one technique that has been used to gain information about the speciation of metals dissolved in aqueous [1,2,4] and non-aqueous systems [13,14].

The speciation of metals in petroleum is not generally determined; only the metal bulk concentrations are traditionally determined [15–17]. Metal complexes have been shown to poison catalysts [15] and act as catalysts in the autoxidation of finished petroleum products [18–23]. The ability to determine the speciation of a metal in solution will permit the investigation of not only metal ions, but also of the specific metal ligand complexes responsible for the degradation of fuel and gasoline. Specifically, a method is needed that can determine the concentrations of the copper compounds present in hydrocarbon matrices. Such a method would allow the determination of the identity of the specific copper ligand complex that decreases the thermal stability of finished petroleum products.

While striving to develop a method for determining the speciation of copper in jet fuel, it

* Corresponding author.

0021-9673/94/$07.00
SSDI 0021-9673(93)E0896-3

became evident that the chromatographic techniques periodically reported for determining the speciation of metals in aqueous systems could not be used [1,2,5,7]. Jet fuel is much less polar than water and is immiscible with the mobile phases traditionally used with reversed-phase separations. Because copper compounds are more polar than the petroleum matrix in which they are dissolved, one can reason that it should be possible to separate the copper compounds using normal-phase chromatography. A stationary phase that retains the copper compounds without inducing the dissociation of the ligands from the copper ion is needed if one is to gain information about copper speciation. The ideal stationary phase for the normal-phase separation of the copper complexes in jet fuel would be polar enough to retain the copper complexes, but the polar groups would have a very low affinity for copper ions. Every polar stationary phase has a threshold that is a function of its propensity to release H^+ ions and to complex with copper ions. Strongly bound copper complexes, those with formation constants, K_f, sufficiently greater than the threshold of the stationary phase, will be retained via a normal-phase mechanism and the copper complexes will be eluted intact by polar solvents. Copper complexes with formation constants below the threshold of the stationary phase will dissociate into copper ions and ligand ions as they interact with the stationary phase. The copper ions will be retained via an ion-exchange mechanism. The copper can then only be eluted by adding an ion-pairing agent or additional cations to the eluent.

The search for a suitable stationary phase revealed that copper could not be eluted from alumina, a stationary phase used in normal-phase liquid chromatography [24], unless acid was added to the mobile phase [14]. The addition of acid to the mobile phase caused all the copper species to co-elute. The alumina retained all the copper compounds injected via an ion-exchange mechanism [14,25], indicating that alumina had a threshold greater than the formation constants of all the copper compounds tested. The formation constant for the most stable copper compound injected, copper DuPont Metal Deactivator (CuDMD), was 10^{21} in water [26]. This is not to say that 10^{21} described the formation constant of CuDMD in 2-propanol or hexane, the solvents used, but that the relative relationship between the formation constants of different copper compounds should remain nearly constant when the compounds are in a solvent system other than water.

Although alumina was not satisfactory for preserving copper speciation, it does provide a useful reference point against which polar polymeric stationary phases can be evaluated. Polymeric stationary phases offer advantages in the realm of preserving metal speciation because they are more covalent than alumina. The feasibility of preserving metal speciation on a polymeric stationary phase was investigated by Mackey [2,27], who found that even poly(styrene–divinylbenzene) (PS–DVB), a stationary phase thought to possess negligible ion-exchange properties, retained metal cations. The metal cations could only be eluted by mobile phases modified with acids or ion-pairing agents.

In a previous report, an investigation with the polymeric stationary phase polyvinylpyrrolidone (PVP) for the separation of copper species was described [14]. A column was packed with PVP particles, a fairly novel stationary phase, that enabled two classes of copper compounds in a petroleum matrix to be separated. Unfortunately, the particles were not engineered for HPLC and were very sensitive to the amount of water in the eluent. The efficiency of the column packed with PVP was not as high as the efficiencies provided by most commercially available HPLC columns.

Recent investigations with the stationary phase poly(vinyl alcohol) (PVA) [28] have indicated significant improvements relative to the previously reported method using PVP [14]. The PVA stationary phase has been specifically "engineered" for chromatography, which has led to a higher efficiency column. PVA columns have been utilized in the micelle exclusion separation of heavy metals [29] and in the determination of the speciation of arsenic compounds in marine life [4], but no one has reported the suitability of PVA for the separation of copper compounds. The alcohol groups of the PVA polymer should make the stationary phase polar enough to retain the copper complexes when the mobile phase is

non-polar. The non-polar components in jet fuel should act as a non-polar mobile phase that is unretained by PVA when a jet fuel sample is injected. Given the observation by Mackey [2,27] that PS–DVB exhibited ion-exchange properties, one should carefully consider the likelihood that PVA will exhibit ion-exchange behavior. Further, alumina acts as a cation exchanger at pH 7.6 [30]. The cation-exchange behavior of PVA has not been evaluated. It is less likely that PVA will act as an ion exchanger and cause the copper complexes in the fuel to dissociate, as reversible proton exchange on PVA is not favored. PVA should be more suitable than alumina or PS–DVB for the separation of copper complexes in jet fuel.

A liquid chromatographic method, consisting of the preconcentration and separation of a group of standard copper compounds, was developed utilizing PVA as a stationary phase. Solutions of copper compounds with a range of formation constants were analyzed by the method to determine the speciation/ionization threshold of PVA for copper. The threshold determined the minimum formation constant value required to keep the native ligands associated with copper ion when copper compounds were exposed to PVA. The developed method was then used to determine the concentrations of the copper species formed when jet fuel samples, with and without DMD added, were exposed to copper metal. Grabel and Nowack [22] determined the bulk concentration of copper solvated by jet fuel exposed to metallic copper, but made no attempt to determine the copper complexes formed in the jet fuel. No one has addressed the issue of how a copper atom is transformed from the metallic state to a copper(II) complex in jet fuel. Assignments of the ligands associated with the solvated copper were made based on the retention times of the copper compounds used as standards.

EXPERIMENTAL

Reagents

N,N′-disalicylidene-1,2-propylenediamine, the active ingredient in DMD, potassium trifluoromethanesulphonate (KCF_3SO_3), copper cyclohexanebutyrate and copper dimethyldithiocarbamate were purchased from Pfaltz and Bauer (Waterbury, CT, USA), technical-grade copper naphthenate from Chem Service (West Chester, PA, USA), copper(II) tetramethylheptanedionate and analytical-reagent grade copper acetate from Aldrich (Milwaukee, WI, USA), copper powder from J.T. Baker (Phillipsburg, NJ, USA) and ACS reagent grade electrolytic copper foil from E.M. Science (Gibbstown, NJ, USA). No attempt was made to clean or modify the surface of either the copper foil or the copper powder. Copper organometallic standard (1000 μg/g) was purchased from SPEX Industries (Edison, NJ, USA). Because the copper naphthenate and cyclohexanebutyrate were of unknown purity, solutions of all three carboxylates were made and the copper content was determined by flame atomic absorption spectrometry (FAAS). Baker analyzed HPLC reagent grade 2-propanol, acetonitrile and hexane were purchased from J.T. Baker. The jet fuel analyzed was provided by the Fuels Research Branch at Wright-Patterson Air Force Base (Dayton, OH, USA).

Column

The column was a 100 mm × 7.5 mm I.D. Asahipak GS-510M column packed with 9-μm PVA particles made by Asahi Chemical Industry and purchased from Keystone Scientific (Bellefonte, PA, USA).

Apparatus

The HPLC system was a Dionex BioLC system with a variable-wavelength absorbance detector. The system provides a metal-free eluent flow path which ensured no sample contamination by the chromatographic system and a low baseline. The HPLC system was coupled to the FAA spectrometer by connecting the variable-wavelength absorbance detector outlet tubing to the FAA nebulizer with an 18-gauge blunt-tipped needle and 20-gauge Teflon tubing. A Perkin-Elmer (Norwalk, CT, USA) Model 403 FAA spectrometer with a manual controller, a spoiler nebulizer and a 10.5-cm three-slot burner was used as an element-specific detector. The operating conditions for FAAS are given in Table I.

TABLE I

FLAME ATOMIC ABSORPTION SPECTROMETRIC OPERATING CONDITIONS

Lamp current	15 mA
Slit	1 mm, 0.7 nm
Wavelength	326.4 nm
Flame	Air–acetylene
Air–acetylene flow-rate ratio	1.5/1.0
Nebulizer type	Spoiler
Burner type	10.5 cm, three-slot

Mobile phase program

The trace in Fig. 1a shows the mobile phase program delivered by the solvent programmer which was used to separate the copper complexes. The solvent programmer delivered 2-propanol for the first 10 min of the run with a 50-μl or 1.00-ml sample injection at 0.5 min. A linear gradient from 100% 2-propanol to 100% acetonitrile was delivered by the solvent programmer between 10 and 15 min. The solvent programmer delivered a linear gradient from 100% acetonitrile to 100% 10 m*M* KCF_3SO_3 in methanol from 15 to 20 min and then held the solvent composition at 100% 10 m*M* KCF_3SO_3 in methanol for the duration of the separation.

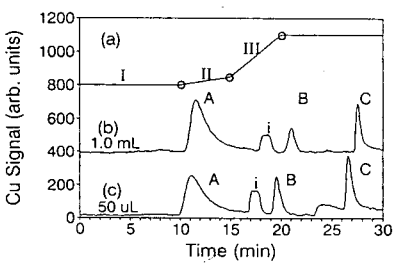

Fig. 1. (a) Solvent program: (I) 0 to 10 min, 2-propanol; (II) 10 to 15 min, gradient from 100% 2-propanol to 100% acetonitrile; (III) 15 to 20 min, gradient from 100% acetonitrile to 100% 10 m*M* KCF_3SO_3 in methanol; a mobile phase of 10 m*M* KCF_3SO_3 in methanol was delivered for the duration of the separation on PVA. After the separation was complete the mobile phase is switched directly to 2-propanol. The flow-rate was 1.0 ml/min. (b) Separation of a 1.00-ml injection volume containing (A) 200 ppb of Cu complexed with DMD. (B) 100 ppb of Cu complexed by dimethyldithiocarbamate and (C) 170 ppb of Cu complexed with cyclohexanebutyrate. (c) Separation of a 50-μl injection containing (A) 3750 ppb of Cu complexed with DMD, (B) 1840 ppb of Cu complexed with dimethyldithiocarbamate and (C) 3100 ppb Cu complexed with cyclohexanebutyrate. Peak i in both chromatograms is due to an impurity in the DMD. Detection was accomplished by FAAS; see Table I for details.

Data acquisition, control and quantitative analysis

The data acquisition and system control were done using an IBM (Boca Raton, FL, USA) AT computer with an IBM DACA board. The data acquisition and system control software was written in-house using Microsoft Quick Basic (Microsoft, Bellevue, WA, USA). Copper in jet fuel samples was determined using peak areas for known concentrations of CuDMD and copper cyclohexanebutyrate. For peaks eluting before 24 min CuDMD was used as the standard, and for those after 24 min copper cyclohexanebutyrate was used.

RESULTS AND DISCUSSION

A separation of standard copper compounds was developed using the PVA column and a solvent program. The standard copper compounds included CuDMD, copper dimethyldithiocarbamate and copper cyclohexanebutyrate. A separation of the standard copper compounds and the solvent program used to affect that separation are shown in Fig. 1. The mobile phase program used to separate the copper compounds was developed by injecting solutions of the individual copper compounds on to the column under isocratic conditions with the different mobile phases to determine which mobile phase most effectively eluted the individual copper compounds. Fig. 1b and c show the separation of mixtures of the standard copper compounds. The solvent programmer delivered 2-propanol for the first 10 min of the run. Initially, we shall consider the separation using a 50-μl injection volume (Fig. 1c). The 2-propanol eluted the peak labeled A, CuDMD, at 11 min. 2-Propanol was a suitable initial solvent because it eluted non-polar compounds such as CuDMD. 2-Propanol was miscible with non-polar solvents such as hexane and jet fuel and also polar solvents such as acetonitrile and methanol. When jet fuel samples were injected, the 2-propanol eluted all the non-polar components in the fuel.

The peak at 17.5 min is due to an impurity in the DMD. The peak labeled B in Fig. 1c, eluting at 20 min, was copper dimethyldithiocarbamate. The copper dimethyldithiocarbamate was eluted by the linear gradient from 100% 2-propanol to 100% acetonitrile delivered by the solvent programmer between 10 and 15 min. The 5-min difference in the elution time of 20 min and the linear gradient ending at 15 min was due to the combination of the dead volumes of the column and tubing connecting the solvent programmer, pump, injection valve, UV absorbance detector, FAAS detector, the gradient system delivery response rate and the pump flow-rate. The last peak in Fig. 1c, labeled C, was copper cyclohexanebutyrate, which was eluted by the linear gradient from 100% acetonitrile to 100% 10 m*M* potassium trifluoromethanesulphonate in methanol delivered by the solvent program between 15 and 20 min. The programmer delivered 100% 10 m*M* KCF_3SO_3 in methanol for the duration of the separation to be certain that any compounds retained by an ion-exchange mechanism on the PVA were eluted.

As the mobile phase program was being developed, the copper compounds were found to elute earlier as the mobile phase became more polar, suggesting that the copper compounds were indeed retained by a normal-phase mechanism. This was important because one does not want the non-polar components in the jet fuel to disrupt the separation of the polar copper compounds when a jet fuel sample was injected. The polarity of a copper compound is defined by the portion of the ligand that binds the copper ion. The region of the ligand that binds to the copper has a permanent dipole and is capable of hydrogen-bonding. Thus, the portion of the ligand that binds to the copper determines how strongly the copper compound is retained by the stationary phase. The separation in Fig. 1c of the three copper compounds used as standards is an indication the speciation of the copper compounds was being preserved. If the copper compounds had dissociated, all the copper compounds would have eluted at the same time. To determine whether the separation could be used to differentiate between copper compounds with similar binding groups, solutions of copper acetate and copper naphthenate were injected as well as a dilution of a SPEX organometallic copper standard containing a copper sulphonate and a solution of copper(II) tetramethylheptanedionate. All these copper compounds were strongly retained by the PVA stationary phase and required the addition of KCF_3SO_3, an ion-pairing reagent, to the mobile phase to elute the copper. The copper from solutions of all these compounds eluted at the same time as the copper cyclohexanebutyrate (27 min). The absorbance of the eluent at 300 nm was monitored for all the separations. The copper peak eluting at 27 min did not absorb at 300 nm while the solutions of the individual copper compounds did absorb at 300 nm, which led us to the conclusion that the more strongly retained copper compounds, the copper carboxylates, copper sulphonate and copper(II) tetramethylheptanedionate, were indeed dissociating as they were absorbed on the PVA and the copper was eluting as $Cu(CF_3SO_3)_2$.

One of the consequences of having a polar copper ligand bond is that as the bond becomes more ionic in character, the species become capable of existing as separate ions. This is evidenced by the small formation constant of copper cyclohexanebutyrate listed in Table II. The formation constants of the five copper compounds eluting at 27 min are less than or equal to 10^{15}. PVA appears to have a threshold for displacing ligands from copper compounds with K_f values in water between 10^{15} and 10^{20}. The ion-exchange retention of copper compounds by polymeric stationary phases is in agreement with the results reported by Mackey [2,27], who found that even PS–DVB stationary phases exhibit ion-exchange characteristics.

The limit of detection for the method was 160 ppb of copper as CuDMD when the volume injected was 50 μl. A detection limit of 20 ppb or less was needed if the technique was to be useful in the determination of the concentrations of the copper species that could cause fuel instability. One way to lower the detection limit was to use on-column preconcentration. With a normal-phase retention mechanism, on-column preconcentration involved injecting a large volume of non-polar sample, which acted as a non-polar mobile phase, causing the copper com-

TABLE II

FORMATION CONSTANTS IN WATER AND LIMITS OF DETECTION (LOD) FOR COPPER COMPOUNDS

Species	Log K_f [26]	Concentration LOD (μg/l Cu)		Mass LOD (ng CU)
		50 μl	1.0 ml	
CuDMD	21	162	10	10
Cu dimethyldithiocarbamate	29	198	16	16
Cu cyclohexanebutyrate	3	168	10	10
Cu tetramethylheptanedionate	15	–[a]	–[a]	–[a]

[a] Not measured.

pounds to be strongly retained by the stationary phase and focused on to a much smaller volume on the column. The copper compounds were then eluted by a polar mobile phase as narrowed peaks, and the limit of detection was improved by the ratio of the injection volumes as long as the peak widths did not substantially increase. The chromatograms in Fig. 1b and c show that the peak width was not substantially increased, but remained at approximately 1.5 ml for all the species except CuDMD, when the injection volume was increased by a factor of 20 from 50 μl to 1.00 ml. Table II shows the 3σ limits of detection for the technique were lowered by a factor of 16 from 160 to 10 ppb of copper as CuDMD with a 1.00-ml injection loop using on-column preconcentration [31]. The time shift between the two chromatograms in Fig. 1b and c was produced by the difference in injection volumes. An additional *ca.* 1 min was required for the solvent program to travel through the injection loop when the volume was increased from 50 μl to 1.00 ml.

Once the separation had been developed, the detection limit had been lowered to a suitable level using on-column preconcentration and the reproducibility of the separation had been demonstrated, the method was used to characterize the copper dissolved by a jet fuel sample exposed to copper metal. The observation that copper metal is solvated by jet fuel has been reported by Grabel and Nowack [22], who monitored the bulk concentration of copper solvated by jet fuel. The method described above was used both to monitor the concentrations of the copper species formed and to gain information about their speciation as a function of the number of days the jet fuel had been exposed to metallic copper. Fig. 2a shows a summary of the

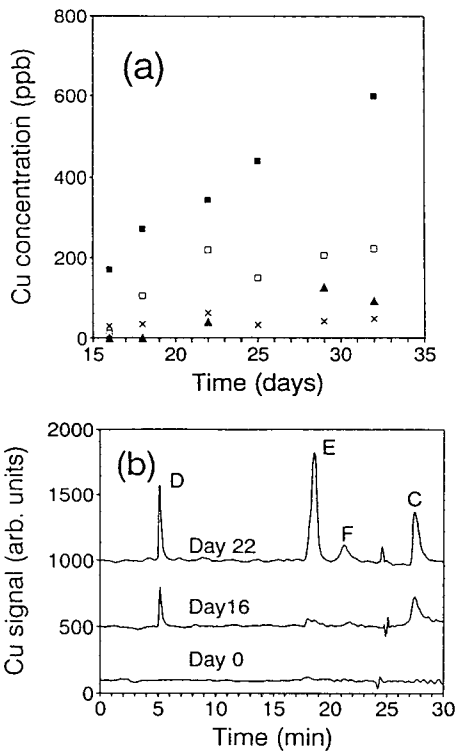

Fig. 2. (a) Concentrations of the copper complexes formed in 30 ml of JP8-S15 as a function of the number of days the fuel has been exposed to 0.2 g of copper powder. × = peak D in (b); □ = peak E in (b); ▲ = peak F in (b), ■ = peak C in (b). (b) Representative chromatograms of the same samples as in (a) for the number of days given. The disturbance between 24 and 25 min is explained in the text.

concentrations of the copper species in the jet fuel sample as a function of the time the fuel sample had been in contact with copper powder. The emergence of several classes of copper compounds in Fig. 2a indicates that more than one copper species is formed in the fuel. The presence of more than one peak also indicates the presence of several ligands native to the fuel capable of complexing the copper. The increasing concentrations of the classes of copper in Fig. 2a is an indication that the copper powder is being dissolved by the jet fuel.

Fig. 2b shows three representative chromatograms of a jet fuel sample that had been standing over copper powder for the number of days indicated. The chromatogram of the jet fuel before it had been exposed to metallic copper, day 0, does not show an appreciable amount of copper. This was confirmed when the fuel was analyzed by FAAS directly. After the jet fuel had been exposed to the metallic copper for 16 days, Fig. 2a shows the fuel had solvated 200 ppb copper as two different species. An amount of 170 ppb of copper was solvated as the complex eluting as the peak labeled C. Based on our copper standards we can speculate that this species had a binding group similar to a carboxylate or at least the K_f of the copper complex formed was less than 10^{15}. An amount of 28 ppb of copper was solvated as the peak labeled D eluting at 5 min. The early elution time of peak D is an indication that the copper compound is less polar than any of the standards. Peak E was just above the detection limit of the method on day 16. Fig. 2b indictes that after the fuel had been exposed to copper for 22 days, significant concentrations of all four of the copper species reported in Fig. 2a had been solvated by the fuel. The lack of a peak at 11 min, as in peak A in Fig. 1b, indicates that the jet fuel sample had not been treated with DMD. Based on the retention time of the copper dithiocarbamate standard, peak B in Fig. 1b, one can speculate that peak F in Fig. 2a is due to a copper complex with ligands with chemical functionalities similar to a dithiocarbamate, resulting in the formation of a copper complex with a polarity similar to that of copper dithiocarbamate. The very narrow disturbance at 24 min in the three chromatograms was an artifact of the solvent program. Between 24 and 25 min was the region when the potassium trifluoromethanesulphonate and methanol first reached the detector and were aspirated by the nebulizer. The flame characteristics changed owing to the transition from acetonitrile to methanol and the combustion of the potassium yielded an intensely orange flame. The binding functionalities of the ligands of the classes of copper compounds labeled D and E in Fig. 2 are unknown. The ligands attached to copper having these retention times would have to be determined by mass spectrometry or some other technique capable of yielding information about the ligands.

The data shown in Fig. 2 demonstrated the feasibility of using the developed method to differentiate between the copper complexes in jet fuel and monitor their concentrations. The method was then used to characterize the copper complexes formed when a jet fuel sample treated with DMD was exposed to copper foil. The active ingredient in DMD was added to an aliquot of the same fuel used in the study in Fig. 2 near the maximum concentration allowed by the US Air Force [32]. The fuel with added DMD was then placed in a polyethylene bottle with a strip of copper foil. Aliquots of the fuel were withdrawn and analyzed to monitor the solvation of copper by the fuel. Fig. 3 summarizes the results of the study of the fuel treated with DMD and exposed to copper foil. Fig. 3a shows chromatograms from injections of the aliquots of fuel treated with DMD and exposed to copper foil. The most prominent feature of the chromatograms in Fig. 3a is the peak labeled A, the peak due to the CuDMD complex. The peak due to the CuDMD complex increased with the time the fuel was exposed to copper until all the DMD was consumed, as shown in Fig. 3b. A comparison of the shape of peak i in Fig. 3a with the peak labeled i in Fig. 1b and c suggests the peak is due to an impurity in the DMD. The increase in the ratio of the height of the impurity peak to the height of the CuDMD peak in the chromatogram for day 17 compared with that for day 10 suggests the DMD has either a higher binding constant than the impurity, but not excessively higher, or a difference in the rate of

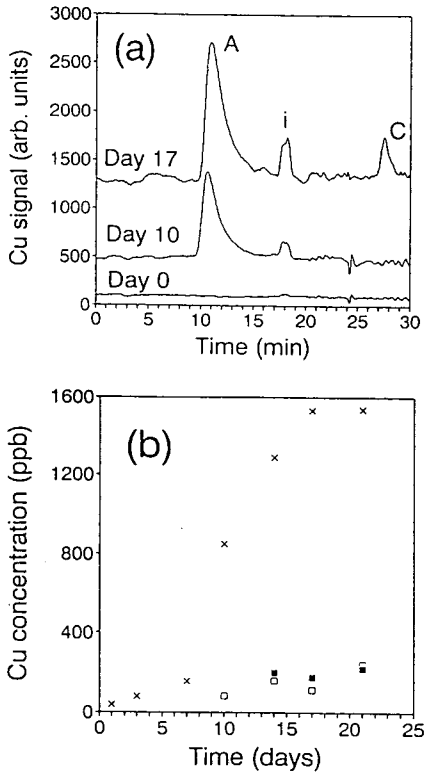

Fig. 3. (a) Representative chromatograms of 16 ml of JP8-S15 with 6.3 mg/l of DMD exposed to 0.3 g of copper foil for the number of days given. Peak A is CuDMD, peak i is a copper complex formed by copper and an impurity in DMD and peak C is due to copper with weakly bound ligands. (b) Concentrations of the copper species formed in the jet fuel as a function of the number of days the fuel was exposed to copper foil. × = peak A in (a); □ = peak i in (a); ■ = peak C in (a).

copper complex formation between DMD and the impurity. The binding constant of the CuDMD complex is given in Table II.

Fig. 3b indicates that peak C in Fig. 3a was only present once the DMD in the fuel sample had been consumed. Peak C was not present until the DMD had been consumed, indicating that DMD has a higher binding constant than the ligands native to the fuel; therefore, all the copper solvated by the jet fuel was complexed by the DMD ligand as long as there was uncomplexed DMD. Once all the DMD had been consumed, the additional copper solvated by the fuel was complexed by native ligands in the fuel. Based on the retention times of the standards used to develop the separation, one can speculate that peak C in Fig. 3a is due to a carboxylate or other potential native ligand in the fuel, forming a copper complex with a K_f value less than 10^{15}.

It is interesting to consider Figs. 2 and 3 and to compare the copper species formed when a jet fuel sample without DMD was exposed to copper with the copper species formed when the same fuel was treated with DMD and exposed to copper. The fuel not treated with DMD solvated four different classes of copper compounds, while most of the copper solvated by the fuel treated with DMD was complexed by the DMD or the impurity in the DMD. A comparison between the species formed and the concentrations of solvated copper in the two studies should not be attributed solely to the presence of DMD, because the physical forms of the copper used in the two studies were different. In the study summarized in Fig. 2 the jet fuel was standing over copper powder and in the study in Fig. 3 the jet fuel was standing over copper foil.

In order to gain a better understanding of how the physical form of the copper affected the concentration of copper solvated by the fuel and the copper species formed in the jet fuel, 140 ml of jet fuel were treated with 3.1 mg/l of DMD and placed over copper in two physical forms. Half of the treated jet fuel was placed over copper powder and the other half over an equivalent mass of copper foil. The DMD-treated fuel over copper foil solvated 700 ppb of copper as CuDMD in 12 days, which was sufficient copper to consume all the DMD added to the fuel, whereas the fuel over copper powder solvated only 160 ppb of copper as DMD in 17 days. The same species, CuDMD and the Cu peak due to the impurity in the DMD, were formed in both aliquots of jet fuel. This observation is contrary to what would be expected on the basis of the surface areas of the two physical forms of copper. One explanation for the difference in the concentrations of copper solvated by the fuels is the copper must be oxidized by the oxygen dissolved in the jet fuel to be solvated by the fuel. Only the copper atoms that jet fuel containing dissolved oxygen can circulate past are likely to be oxidized. The rigid structure of

the copper foil allowed the jet fuel to circulate past much of the copper, whereas the copper powder formed a pile in the bottom of the container and the jet fuel only circulated past the copper on the outer layer of the pile.

CONCLUSIONS

A method capable of distinguishing between several classes of copper compounds in jet fuel has been developed. The method offers significant improvements in chromatographic resolution over the previously reported method [14]. The increased chromatographic resolution facilitated the determination and characterization of five classes of copper compounds formed when jet fuel is exposed to metallic copper. The method is capable of determining copper at the concentrations that have reportedly caused fuel stability problems [18,19,22,23]. The method provides a valuable tool in the effort to determine the copper species responsible for catalyzing autoxidation in petroleum products and degrading fuel stability. The method could also be used to measure the effectiveness of potential metal deactivators by determining how well the active ingredients complex the metal ions.

ACKNOWLEDGEMENTS

The authors thank the US Air Force, specifically Steve Anderson at Wright-Patterson Air Force Base, for providing support and the jet fuel samples for this work.

REFERENCES

1 D.J. Mackey and H.W. Higgins, *J. Chromatogr.*, 436 (1988) 243.
2 D.J. Mackey, *J. Chromatogr.*, 236 (1982) 81.
3 A. Mazzucotelli, R. Frache, A. Viarengo and G. Martino, *Talanta*, 35 (1988) 693.
4 M. Morita and Y. Shibata, *Anal. Sci.*, 3 (1987) 575.
5 D. Behne, *Analyst*, 117 (1992) 555.
6 Y.K. Chau and P.T.S. Wong, *Fresenius' J. Anal. Chem.*, 339 (1991) 640.
7 G. Weber, *Anal. Chim. Acta*, 200 (1987) 79.
8 J.W. O'Laughlin, *J. Liq. Chromatogr.*, 7 (1984) 127.
9 Y.K. Chau, *Analyst*, 117 (1992) 571.
10 C.J. Cappon, *LC · GC*, 6 (1987) 584.
11 B.P. Karcher and I.S. Krull, *Trace Metal Analysis and Speciation (Journal of Chromatography Library*, Vol. 47), Elsevier, Amsterdam, 1991, p. 123.
12 E.M. Perdue, *Aquatic Humic Substances; Influence on Fate and Treatment of Pollutants*, American Chemical Society, Washington, DC, 1989, p. 281.
13 M.R. Danna, *Dissertation*, Michigan State University, East Lansing, MI, 1985.
14 D.B. Taylor and R.E. Synovec, *Talanta*, 40 (1993) 495.
15 A.J. Smith and C. Collins *At. Spectrosc.*, 8 (1987) 96.
16 J.H. Karchmer and E.L. Gunn, *Anal. Chem.*, 24 (1952) 1733.
17 J.L. Fabec, *Anal. Chem.*, 57 (1985) 208R.
18 C.J. Pederson, *Oil Soluble Complexing Agents as Metal Deactivators*, DuPont, Wilmington, DE, 1955.
19 *DMD and DMD-2 Petroleum Additives*, DuPont, Wilmington, DE, 1987.
20 R.H. Clark, in H.N. Giles (Editor), *Proceedings of the 3rd International Conference on Stability and Handling of Liquid Fuels*, 1988, p. 283.
21 Coordinating Research Council (Editor), *Literature Survey on the Thermal Oxidation Stability of Jet Fuel*, Vol. 509, CRC Inc., Atlanta, GA, 1979, p. 1, 53.
22 L. Grabel and C. Nowack, *CRC Jet Fuel Thermal Oxidation Stability Symposium, Los Angeles, CA*, CRC Inc., Atlanta, GA, 1977.
23 R.E. Morris and N.H. Turner, *Fuel Sci. Technol. Int.*, 8 (1990) 327.
24 G.L. Schmitt and D.J. Pietrzyk, *Anal. Chem.*, 57 (1985) 2247.
25 J. Michal, *Inorganic Chromatographic Analysis*, Van Nostrand Reinhold, New York, 1973, p. 75.
26 A.E. Martell and R.M. Smith, *Critical Stability Constants*, Vol. 3, Plenum Press, New York, 1977.
27 D.J. Mackey, *J. Chromatogr.*, 242 (1982) 275.
28 E.V. Hort, in *Kirk-Othmer, Encyclopedia of Chemical Technology*, Vol. 23, Wiley-Interscience, New York, 1978, p. 848.
29 T. Okada, *Anal. Chem.*, 60 (1988) 2116.
30 M. Tanaka, T. Ashizawa and M. Shikata, *Kagaku no kenkyo*, 5, *Inorg. Anal. Chem.*, (1949) 35.
31 B.F. Johnson, J. Bramlage and J.G. Dorsey, *Anal. Chim. Acta*, 255 (1991) 127.
32 *Military Specification Turbine Fuel, Aviation, Grades JP-4, JP-5 and JP-5/JP-8 ST*, MIL-T-5624N, 1989, ASD/ENES, Wright-Patterson Air Force Base, Dayton, OH.

Journal of Chromatography A, 659 (1994) 143–150
Elsevier Science B.V., Amsterdam

CHROM. 25 569

Effect of adsorption on the retention values in capillary columns coated with OV-225 and PEG 20M

A. Orav*, K. Kuningas, T. Kailas, E. Koplimets and S. Rang

Institute of Chemistry, Estonian Academy of Sciences, Akadeemia tee 15, EE0026 Tallinn (Estonia)

(First received July 7th, 1993; revised manuscript received September 16th, 1993)

ABSTRACT

The effect of adsorption of compounds of different homologous series (*n*-alkanes, *n*-alkenes, *n*-alkynes, *n*-alkylcyclohexenes, arenes, alkanones) on capillary columns with different contents of polycyanopropylphenylmethylsiloxane (OV-225) and polyethylene glycol (PEG 20M) on retention indices, relative retention and capacity factors was quantitatively studied. The relationships between the retention characteristics and the stationary phase film thickness or capacity factor of a standard solute were established. These correlations permit the prediction of retention data depending on film thickness. It has been shown that among the compounds studied, the adsorption of *n*-alkanes and *n*-alkenes is maximum and comprises up to one third of the relative retention on columns with a thin film of PEG 20M.

INTRODUCTION

Problems connected with the reproducibility of retention values in capillary gas chromatography (GC) are of great importance. The most important factor affecting the reproducibility of retention values is the adsorption phenomena on the gas–liquid and liquid–solid interfaces. A more polar stationary phase (SP) leads to more variation in the retention data caused by variations in the coating thickness of the SP. The influence of the thickness of the SP film on retention due to adsorption has been studied by several investigators [1–11]. In recent studies [12,13] we examined the effect of adsorption on retention indices and their temperature coefficients for *n*-tetradecenes in capillary columns coated with PEG 20M.

This work was aimed at elucidating the influence of the thickness of polycyanopropylphenylmethylsiloxane (OV-225) and polyethylene glycol (PEG 20M) films coated on stainless-steel surfaces on the retention indices, relative retentions and capacity factors of compounds of different homologous series (*n*-alkanes, *n*-alkenes, *n*-alkynes, *n*-alkylcyclohexenes, arenes and alkanones). On this basis, adsorption parameters were evaluated for these solutes.

EXPERIMENTAL

An unmodified stainless-steel tube (50 m × 0.25 mm I.D.) was used for preparation of capillary columns. The columns were cleaned by rinsing with 20 ml of different solvents (chloroform, methanol, 2-propanol, 10% nitric acid, water, methanol, chloroform). Coating with the liquid phases (OV-225 and PEG 20M) was carried out by the dynamic method using chloroform solutions of different concentrations. The film thickness (d_f) of the SP was calculated by using the amount of the liquid phase present in the column. The precision of d_f values was about 0.01 μm.

Experiments were performed on Chrom-4 and Chrom-5 chromatographs (Laboratórní Přístro-

* Corresponding author.

0021-9673/94/$07.00
SSDI 0021-9673(93)E0993-5

je, Prague, Czech Republic) equipped with a flame-ionization detector. The splitting ratio was about 1:150 and helium was used as the carrier gas. The oven temperature was 70–100°C at 10°C intervals calibrated with an accuracy of 0.2°C. The injector temperature was 200–250°C. Retention times were measured with an accuracy of 0.1 s. The column hold-up time was determined by extrapolation from the retention times of *n*-alkanes. *m*-Xylene was used as a reference standard owing to its weak adsorption in the chromatographed system used, controlled as in ref. 5.

The reproducibility of the retention indices, *I*,

TABLE I

CHARACTERIZATION AND WORKING CONDITIONS OF CAPILLARY COLUMNS AT 80°C

Parameter	Stationary phase					
	OV-225			PEG 20M		
Column No.	1	2	3	4	5	6
Stationary phase film thickness, d_f (μm)	0.30	0.58	0.65	0.13	0.19	0.22
No. of theoretical plates for *n*-dodecane	79 000	70 000	64 000	86 000	72 000	70 000
Capacity factor *k* for *m*-xylene	1.37 ± 0.02	2.60 ± 0.03	3.09 ± 0.01	0.869 ± 0.003	0.899 ± 0.002	1.40 ± 0.02
Helium flow-rate (ml/min)	0.46	0.40	0.57	0.51	0.51	0.67
Hold-up time (min)	5.34 ± 0.06	6.07 ± 0.13	4.31 ± 0.46	4.95 ± 0.03	4.96 ± 0.02	3.81 ± 0.01

TABLE II

RETENTION INDICES *I* AT 80°C AND TEMPERATURE INCREMENTS $10(\delta I/\delta T)$ OF SELECTED COMPOUNDS ON OV-225

Peak No.	Compound	Column 1		Column 2		Column 3	
		I	$10(\delta I/\delta T)$	*I*	$10(\delta I/\delta T)$	*I*	$10(\delta I/\delta T)$
1	*trans*-2-Decene	1036.8	0.5	1037.7	−0.1	1037.8	0.1
2	*cis*-2-Decene	1053.1	0.9	1054.2	0.8	1054.3	1.0
3	*trans*-5-Decene	1020.9	0.2	1021.4	0.2	1021.5	0.2
4	*cis*-5-Decene	1028.7	0.9	1029.3	0.8	1029.5	1.0
5	*trans*-2-Dodecene	1237.1	0.0	1238.3	−0.6	1237.7	0.0
6	*cis*-2-Dodecene	1252.4	0.8	1253.6	0.8	1253.3	0.8
7	*trans*-5-Dodecene	1217.8	0.3	1217.3	0.6	1217.8	0.4
8	*cis*-5-Dodecene	1222.4	0.9	1222.2	1.2	1222.9	1.0
9	1-Decyne	1139.3	0.6	1140.0	0.6	1140.6	0.5
10	3-Decyne	1147.7	−0.1	1149.0	0.2	1149.4	−0.1
11	1-Ethyl-1-cyclohexene	954.3	4.2	955.4	4.3	956.8	4.6
12	1-Butyl-1-cyclohexene	1135.1	4.9	1136.1	4.6	1137.9	4.7
13	3-Butyl-1-cyclohexene	1130.2	4.8	1131.4	5.0	1133.2	5.1
14	Benzene	853.1	5.3	854.1	5.0	856.1	5.5
15	Toluene	956.6	5.5	957.9	5.2	959.8	5.6
16	*m*-Xylene	1056.4	5.5	1057.8	5.4	1059.4	5.6
17	*o*-Xylene	1095.7	6.5	1097.5	6.3	1099.5	6.6
18	2-Pentanone	–	–	944.0	4.0	945.1	4.4
19	3-Hexanone	1029.3	4.0	1030.5	3.9	1030.9	4.1
20	4-Heptanone	1109.4	4.1	1111.3	3.9	1111.5	4.0

TABLE III

RETENTION INDICES I AT 80°C AND TEMPERATURE INCREMENTS $10(\delta I/\delta T)$ OF SELECTED COMPOUNDS ON PEG 20M

Peak No.	Compound	Column 4		Column 5		Column 6	
		I	$10(\delta I/\delta T)$	I	$10(\delta I/\delta T)$	I	$10(\delta I/\delta T)$
1	1-Dodecene	1238.4	1.7	1240.6	1.5	1241.9	1.4
2	*trans*-2-Dodecene	1251.8	1.6	1254.4	1.4	1255.7	1.3
3	*cis*-2-Dodecene	1262.3	2.5	1265.7	2.3	1267.2	2.3
4	1-Tridecene	1337.2	1.8	1339.4	1.7	1340.9	1.7
5	*trans*-2-Tridecene	1350.4	1.8	1353.1	1.5	1354.9	1.4
6	*cis*-2-Tridecene	1360.5	2.7	1363.7	2.5	1365.6	2.5
7	1-Decyne	1215.6	1.4	1221.9	1.3	1226.3	1.0
8	2-Decyne	1240.7	2.9	1248.0	2.8	1251.7	2.4
9	3-Decyne	1190.3	1.7	1196.2	1.7	1199.2	1.0
10	1-Dodecyne	1410.3	2.4	1416.4	2.2	1421.8	2.2
11	2-Dodecyne	1434.0	3.9	1441.2	3.6	1445.9	3.6
12	3-Dodecyne	1382.5	2.9	1388.6	2.4	1392.5	2.4
13	1-Butyl-1-cyclohexene	1156.1	7.3	1163.5	7.2	1166.9	6.6
14	3-Butyl-1-cyclohexene	1151.5	7.3	1158.8	7.2	1161.8	7.2
15	1-Hexyl-1-cyclohexene	1342.4	8.1	1350.0	7.7	1354.6	7.3
16	3-Hexyl-1-cyclohexene	1344.3	8.3	1352.0	7.8	1355.7	7.8
17	Benzene	945.2	6.3	958.2	6.2	959.5	6.0
18	Toluene	1039.5	7.2	1052.3	6.9	1054.2	6.8
19	*m*-Xylene	1134.6	7.7	1147.3	7.7	1149.9	7.4
20	*o*-Xylene	1174.6	8.6	1188.7	8.6	1191.4	8.3
21	2-Pentanone	979.4	4.6	992.6	–	994.6	4.0
22	3-Hexanone	1050.0	4.7	–	–	1065.0	4.4
23	4-Heptanone	1120.8	5.2	1131.9	5.2	1135.5	4.9
24	5-Nonanone	1309.9	6.1	1321.0	6.0	1325.6	6.0
25	2-Nonanone	1367.9	6.6	1380.0	6.5	1385.7	6.5

expressed in terms of the standard deviation (S.D.) was 0.1–0.2 index unit (i.u.). The accuracy of the capacity factors k and relative retentions r in terms of the relative standard deviation (R.S.D.) was below 2%.

The characterization and working conditions of capillary columns 1–6 are given in Table I and the retention indices I and their temperature increments, $10(\delta I/\delta T)$, for the compounds studied on OV-225 and PEG 20M columns are given in Tables II and III.

The contribution of adsorption and dissolution to retention was investigated using known linear equations [5,9,10,12]:

$$I = I_0 + a/k_{st} \quad (1)$$

$$I = I_0 + b/d_f \quad (2)$$

$$k = A + r_0 k_{st} \quad (3)$$

$$r = r_0 + r_0(\Delta f/d_f) \quad (4)$$

where I_0 and r_0 are an invariant retention index and an invariant relative retention, respectively, d_f is the film thickness of the stationary phase, a, b, A and Δf are adsorption coefficients and the subscript st represents the reference standard (*m*-xylene).

RESULTS AND DISCUSSION

It can be seen from the experimental data (Tables II and III) that the I values increase differently with increasing film thickness d_f for different homologous series (ΔI, i.u.), as shown in Table IV.

TABLE IV

DIFFERENCE IN I VALUES (ΔI, i.u.) FOR THE DIFFERENT HOMOLOGOUS SERIES

Homologous series	OV-225 (0.30–0.65 μm)	PEG 20M (0.13–0.22 μm)
n-Alkenes	<1.2	4–5
n-Alkynes	1–2	9–12
n-Alkylcyclohexenes	2.5–3.0	10–12
Arenes	3–4	14–17
Alkanones	1.5–2.0	15–18

The lower I values on the column with a thin film of PEG 20M are connected with the higher adsorption of *n*-alkanes in comparison with the other solutes studied. On the column with silicone OV-225 the dependence of I on d_f is less significant. At a sufficiently large film thickness the values of I do not depend markedly on d_f. As found previously [13], the temperature increments of I for *n*-alkenes on PEG 20M decrease with increasing d_f. A similar decrease in $10(\delta I/\delta T)$ values is observed for the other homologous series (*n*-alkynes, *n*-alkylcyclohexenes, arenes, alkanones) on PEG 20M, but not on OV-225. In order to minimize ΔI and $10(\delta I/\delta I)$, one should use a column of large d_f at high temperature [7].

The retention index I, relative retention r (standard compound *m*-xylene) and capacity factor k calculated from the experimental data for the solutes studied are described satisfactorily by the linear eqns. 1–4. By means of the least-squares linear regression, the slope and intercept for each linear plot were calculated (Tables V and VI). From the intercept of eqns. 1 and 2 we can calculate the values of invariant retention indices I_0 which are determined only by dissolution of a solute in the stationary phase, but not by secondary retention forces [5,6,12,13]. The invariant retention indices for the solutes studied on OV-225 determined by eqns. 1 and 2 were in good agreement, the differences not exceeding 0.1 i.u. The intercept of eqn. 3, A, characterizes the contribution of the adsorption of the solutes to the capacity factor k. The A values are negative when the adsorption of the carrier gas–SP interface for the solutes studied (arenes, alkanones) is less significant than for the standard solute (*m*-xylene) [11]. The A values for more polar solutes (arenes, alkanones) are markedly lower than those for less polar (alkenes, alkynes, *n*-alkylcyclohexenes) or non-polar (alkanes) solutes on both liquid phases. It has been found that a linear relationship can be observed between log A and carbon atom number n in a homologous series (Fig. 1). This linear relation-

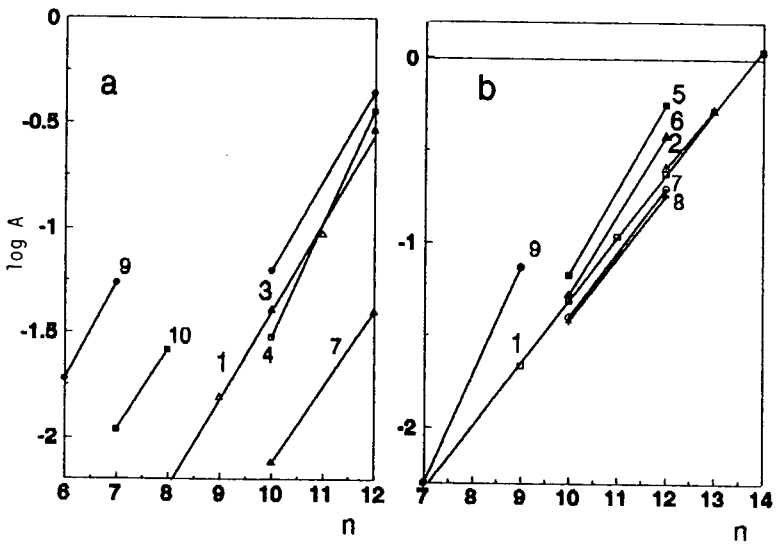

Fig. 1. Dependence of log A on the number of carbon atoms, n, in the solute molecule on (a) OV-225 and (b) PEG 20M at 80°C. 1 = *n*-Alkanes; 2 = 1-alkenes; 3 = *trans*-2-alkenes; 4 = *cis*-2-alkenes; 5 = 1-alkynes; 6 = 3-alkynes; 7 = 1-alkyl-1-cyclohexenes; 8 = 3-alkyl-1-cyclohexenes; 9 = alkanones; 10 = arenes.

TABLE V

PARAMETERS OF EQNS. 1–4 AND S.D. VALUES FOR SELECTED COMPOUNDS ON OV-225 AT 80°C

Compound	Eqn. 1			Eqn. 2			Eqn. 3			Eqn. 4			
	I_0	a	S.D.	I_0	b	S.D.	A	r_0	S.D. $\cdot 10^{-2}$	r_0	$(r_0\Delta f)\cdot 10^{-2}$	$\Delta f \cdot 10^{-2}$	S.D. $\cdot 10^{-3}$
n-Octane	–	–	–	–	–	–	−0.001	0.18	0.1	0.18	0.10	0.56	2.2
n-Nonane	–	–	–	–	–	–	0.015	0.35	0.5	0.35	0.27	0.78	1.9
n-Decane	–	–	–	–	–	–	0.041	0.66	1.9	0.67	0.59	0.89	0.2
n-Undecane	–	–	–	–	–	–	0.093	1.3	4.5	1.3	1.4	1.1	5.6
n-Dodecane	–	–	–	–	–	–	0.29	2.4	10	2.5	4.0	1.6	17
trans-2-Decene	1038.7	−2.5	0.01	1038.7	−0.56	0.0	0.030	0.87	3.3	0.86	0.69	0.80	2.6
cis-2-Decene	1055.3	−3.0	0.0	1055.4	−0.67	0.01	0.063	0.95	5.0	0.96	0.57	0.59	1.4
trans-5-Decene	1022.0	−1.5	0.2	1022.0	−0.33	0.02	0.026	0.78	2.8	0.77	0.58	0.75	1.3
cis-5-Decene	1030.1	−1.9	0.0	1030.1	−0.42	0.1	0.055	0.81	4.2	0.82	0.54	0.66	0.8
trans-2-Dodecene	1238.8	−2.1	0.4	1238.8	−0.50	0.2	0.36	3.1	14	3.1	5.6	1.8	8.1
cis-2-Dodecene	1254.4	−2.6	0.2	1254.4	−0.60	0.2	0.45	3.4	17	3.5	6.2	1.8	6.2
trans-5-Dodecene	1217.4	0.49	0.1	1217.4	0.12	0.3	0.34	2.7	10	2.7	5.6	2.1	1.3
cis-5-Dodecane	1222.8	−0.61	0.3	1222.8	−0.12	0.2	0.33	2.8	9.9	2.8	5.5	1.3	0.6
1-Decyne	1141.3	−2.8	0.1	1141.3	−0.61	0.2	0.068	1.7	7.8	1.7	0.88	0.52	4.3
3-Decyne	1150.7	−4.0	0.2	1150.7	−0.89	0.1	0.084	1.8	7.5	1.8	1.7	0.93	6.4
1-Ethyl-1-cyclohexene	958.0	−5.1	0.5	958.0	−1.1	0.5	−0.008	0.52	1.1	0.51	0.005	0.01	1.9
1-Butyl-1-cyclohexene	1139.0	−5.5	0.7	1139.0	−1.2	0.7	0.040	1.7	6.9	1.7	0.17	0.10	1.2
3-Butyl-1-cyclohexene	1134.5	−6.0	0.6	1134.5	−1.3	0.4	0.048	1.6	5.7	1.6	0.94	0.59	0.8
Benzene	857.2	−5.8	0.7	857.2	−1.3	0.7	−0.010	0.27	0.2	0.26	−0.16	−0.61	2.7
Toluene	961.2	−6.4	0.7	961.2	−1.4	0.7	0.011	0.51	1.6	0.52	−0.08	−0.15	3.1
m-Xylene	1060.9	−6.2	0.6	1060.9	−1.4	0.5	–	–	–	–	–	–	–
o-Xylene	1101.4	−9.7	0.6	1101.4	−1.7	0.7	0.026	1.3	14	1.3	0.43	0.33	0.0
3-Hexanone	1032.1	−3.7	0.2	1032.1	−0.83	0.1	0.019	0.83	0.3	0.83	0.22	0.27	0.0
4-Heptanone	1113.3	−5.2	0.0	1113.2	−1.2	0.1	0.055	1.4	5.7	1.4	0.79	0.56	5.9

TABLE VI

PARAMETERS OF EQNS. 2–4 AND S.D. VALUES FOR SELECTED COMPOUNDS ON PEG 20M AT 80°C; $n = 3$

Compound	Eqn. 2			Eqn. 3			Eqn. 4			
	I_0	b	S.D.	A	r_0	S.D. $\cdot 10^{-2}$	r_0	$(r_0\Delta f)\cdot 10^{-2}$	$\Delta f \cdot 10^{-2}$	S.D. $\cdot 10^{-3}$
n-Octane	–	–	–	0.005	0.10	0.4	0.09	0.29	3.3	1.7
n-Nonane	–	–	–	0.022	0.18	0.6	0.17	0.59	3.5	1.0
n-Decane	–	–	–	0.049	0.34	1.1	0.32	1.2	3.6	2.2
n-Undecane	–	–	–	0.11	0.64	2.1	0.62	2.4	3.9	1.7
n-Dodecane	–	–	–	0.24	1.2	4.4	1.2	5.0	4.3	3.8
*n*Tridecane	–	–	–	0.52	2.3	9.4	2.2	10.7	4.9	4.9
n-Tetradecane	–	–	–	1.09	4.3	18	4.1	22.2	5.4	0.6
1-Dodecene	1246.5	−1.1	0.1	0.26	1.6	4.7	1.6	5.6	3.6	7.1
trans-2-Dodecene	1260.9	−1.2	0.0	0.31	1.8	5.2	1.7	6.2	3.6	4.4
cis-2-Dodecene	1273.9	−1.5	0.2	0.40	1.8	5.1	1.9	6.1	3.3	7.5
1-Tridecene	1345.6	−1.1	0.3	0.52	3.1	9.8	2.9	12.0	4.1	10
trans-2-Tridecene	1360.7	−1.4	0.3	0.41	3.5	11	3.3	12.0	3.6	17
cis-2-Tridecene	1372.3	−1.5	0.4	0.57	3.7	11	3.6	11.6	3.2	5.1
1-Decyne	1239.9	−3.2	0.8	0.068	1.6	2.7	1.5	2.4	1.6	13
2-Decyne	1266.5	−3.4	0.6	0.039	1.9	2.9	1.8	2.5	1.4	9.2
3-Decyne	1211.1	−2.7	0.5	0.053	1.4	2.1	1.3	2.1	1.7	6.8
1-Dodecyne	1435.9	−3.4	1.2	0.56	5.4	11	5.3	12.0	2.3	33
2-Dodecyne	1461.2	−3.6	1.0	0.70	6.4	11	6.3	13.3	2.1	20
3-Dodecyne	1405.4	−3.0	0.8	0.38	4.6	9.6	4.4	10.7	2.5	21
1-Butyl-1-cyclohexene	1181.6	−3.3	0.4	0.040	1.1	1.7	1.1	1.3	1.2	5.5
3-Butyl-1-cyclohexene	1176.1	−3.2	0.3	0.038	1.1	2.0	1.0	1.4	1.3	4.9
1-Hexyl-1-cyclohexene	1370.5	−3.7	0.8	0.20	3.7	6.6	3.5	6.5	1.9	7.8
3-Hexyl-1-cyclohexene	1371.1	−3.5	0.4	0.18	3.8	6.3	3.6	6.2	1.7	16
Benzene	982.0	−4.8	0.9	−0.002	0.29	0.06	0.29	−0.08	−0.28	0.6
Toluene	1076.8	−4.8	0.6	−0.001	0.53	0.12	0.54	−0.13	−0.23	0.08
m-Xylene	1172.8	−5.0	0.4	–	–	–	–	–	–	–
o-Xylene	1216.7	−5.5	0.4	−0.001	1.3	2.3	1.3	−0.21	−0.16	0.7
2-Pentanone	1017.9	−5.0	0.7	−0.011	0.37	0.04	0.36	−0.06	−0.16	0.3
3-Hexanone	1086.7	−4.8	0.9	−0.010	0.59	0.01	0.58	−0.09	−0.16	53
4-Heptanone	1156.5	−4.7	0.04	0.005	0.90	0.37	0.90	0.14	0.16	2.1
5-Nonanone	1347.3	−4.9	0.5	0.074	3.1	2.5	3.1	2.0	0.66	11
2-Nonanone	1409.9	−5.5	0.7	0.077	4.6	4.2	4.6	2.0	0.44	20

ship can be used to predict the A values for the higher members of the homologous series studied. The values of the invariant relative retention r calculated by eqns. 3 and 4 are in good agreement (<0.02), but the mean values of the errors are lower for eqn. 4.

The values of the adsorption coefficient, Δf, increase with increasing carbon number n in the solute molecule for the homologous series of *n*-alkanes, *n*-alkenes, *n*-alkynes and *n*-alkylcyclohexenes. For arenes and alkanones this relationship between Δf and n is less pronounced (Fig. 2). The Δf values are the highest for *n*-alkanes and *n*-alkenes on PEG 20M and the lowest for arenes and alkanones on both phases. The value of Δf may be used to express the percentage adsorption contribution to the relative retention, Δr (Table VII):

$$\Delta r\ (\%) = \frac{\Delta f}{d_f} \cdot 100$$

The maximum contribution of adsorption to the relative retention of the compounds studied was 33% for *n*-dodecane on PEG 20M and 6% for *trans*-2-dodecene on OV-225 (Fig. 3). On columns with a thin film of PEG 20M the adsorption represents a significant contribution to the retention data for *n*-alkanes and *n*-alkenes.

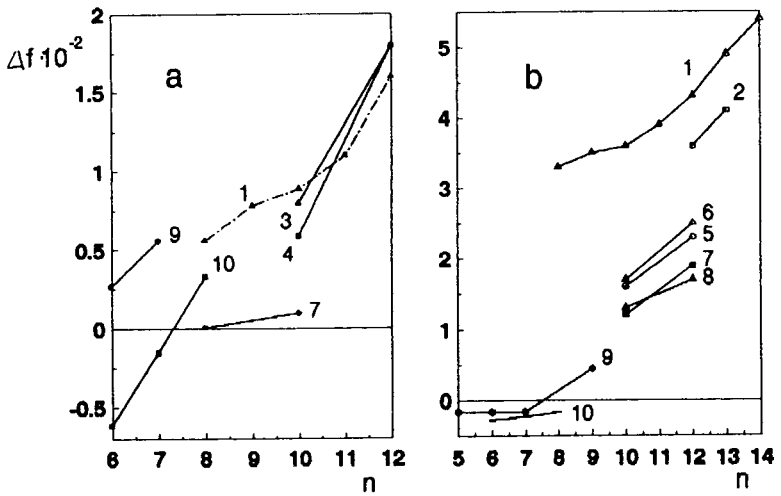

Fig. 2. Dependence of Δf on the number of carbon atoms, n, in the solute molecule on (a) OV-225 and (b) PEG 20M at 80°C. Symbols as in Fig. 1.

The effect of adsorption is lower for *n*-alkynes or *n*-alkylcyclohexenes, and lowest for arenes and alkanones. On OV-225 the Δr values differ from those obtained on the more polar PEG 20M. On OV-225 the adsorption of *n*-alkanes and 2-alkenes with the same carbon number is similar, being more pronounced than that for the other compounds studied.

TABLE VII

CONTRIBUTION OF ADSORPTION TO THE RELATIVE RETENTION (Δr, %) OF SELECTED COMPOUNDS ON OV-225 AND PEG 20M COLUMNS 1–6 AT 80°C

Compound	OV-225			PEG 20M		
	1	2	3	4	5	6
n-Nonane	2.6	1.4	1.2	27	19	16
n-Decane	3.0	1.5	1.4	28	19	16
n-Undecane	3.5	1.8	1.6	30	21	18
n-Dodecane	5.4	2.8	2.5	33	23	20
trans-2-Dodecene	6.0	3.1	2.8	28	19	16
cis-2-Dodecene	5.9	3.1	2.7	25	17	15
1-Decyne	1.7	0.9	0.8	12	8.2	7.0
3-Decyne	3.1	1.6	1.4	13	8.7	7.5
1-Butyl-1-cyclohexene	0.3	0.2	0.2	9.2	6.3	5.5
3-Butyl-1-cyclohexene	2.0	1.0	0.9	10	7.0	6.0
Benzene	2.0	1.1	0.9	2.2	1.5	1.3
Toluene	0.5	0.3	0.2	1.8	1.2	1.1
o-Xylene	1.1	0.6	0.5	1.2	0.8	0.7
2-Pentanone	–	–	–	1.2	0.8	0.7
3-Hexanone	0.9	0.5	0.4	1.3	0.9	0.8
4-Heptanone	1.9	1.0	0.9	1.2	0.8	0.7

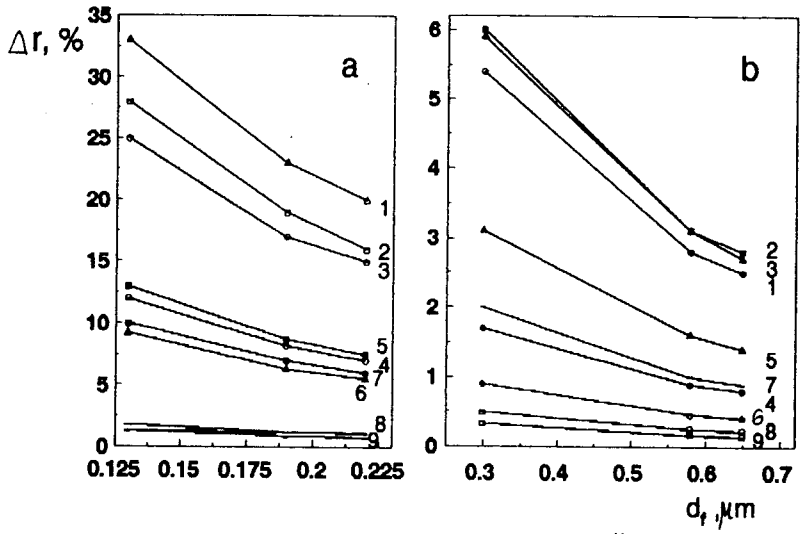

Fig. 3. Dependence of Δr on the film thickness of the SP, d_f, on (a) PEG 20M and (b) OV-225 at 80°C. 1 = *n*-Dodecane; 2 = *trans*-2-dodecene; 3 = *cis*-2-dodecene; 4 = 1-decyne; 5 = 3-decyne; 6 = 1-butyl-1-cyclohexene; 7 = 3-butyl-1-cyclohexene; 8 = toluene; 9 = 3-hexanone.

CONCLUSIONS

The experimental data for some *n*-alkanes, *n*-alkenes, *n*-alkynes, *n*-alkyl-1-cyclohexenes, arenes and alkanones (38 compounds) on OV-225 and PEG 20M capillary columns with different thicknesses of the SP film appear to be in agreement with the linear relationships of I *versus* $1/k_{st}$ or $1/d_f$, k *vs.* k_{st} and r *vs.* $1/d_f$. These equations were used to demonstrate the adsorption effects of compounds of different homologous series when using a polar column. Among the compounds studied, *n*-alkanes make the maximum contribution of adsorption to the relative retention (up to 30%) on PEG 20M with a thin SP film. On the less polar silicone phase (OV-225) the effect of adsorption of *n*-alkanes and alkenes is lower than on PEG 20M.

The results obtained can be used to predict the variation of retention data (I, k, r) with film thickness and also for the identification of and physico-chemical calculations on the compounds studied.

REFERENCES

1 R.L. Martin, *Anal. Chem.*, 35 (1963) 116.
2 R.N. Nikolov, *J. Chromatogr.*, 241 (1982) 237.
3 J.J. Dowling, M.B. Evans and J.K. Haken, *J. Chromatogr.*, 500 (1990) 355.
4 L. Soják, J. Krupčík and J. Janák, *J. Chromatogr.*, 195 (1980) 43.
5 V.G. Berezkin and A.A. Korolev, *Chromatographia*, 20 (1985) 482.
6 V.G. Berezkin and A.A. Korolev, *J. High Resolut. Chromatogr.*, 12 (1989) 617.
7 T. Shibamoto, K. Harada, K. Yamagushi and A. Aitoku, *J. Chromatogr.*, 194 (1980) 277.
8 A. Bemgård and L. Blomberg, *J. Chromatogr.*, 502 (1990) 1.
9 G.L. Zhao and R.X. Chi, *Chromatographia*, 29 (1990) 575.
10 G.L. Zhao and G.Y. Wang, *Chromatographia*, 30 (1990) 635.
11 A.R. Jumaev and V.G. Berezkin, *Zh. Anal. Khim.*, 46 (1990) 1960.
12 G. Gusev, S. Rang, V. Berezkin and A. Orav, *Izv. Akad. Nauk ESSR, ser. Khim., Proc. Est. Acad. Sci., Chem.*, 35 (1986) 205.
13 G. Gusev, S. Rang and A. Orav, *Izv. Akad. Nauk ESSR, ser. Khim., Proc. Est. Acad. Sci., Chem.*, 37 (1988) 285.

Journal of Chromatography A, 659 (1994) 151–161
Elsevier Science B.V., Amsterdam

CHROM. 25 587

Gas chromatographic determination of polycyclic aromatic compounds with fluorinated analogues as internal standards

Jan T. Andersson* and Uwe Weis

Department of Analytical and Environmental Chemistry, University of Ulm, D-89069 Ulm (Germany)

(Received March 29th, 1993)

ABSTRACT

In the gas chromatographic determination of polycyclic aromatic compounds (PACs), internal standards (I.S.s) are frequently used in order to correct for losses and fluctuating experimental variables. It is shown that fluorinated PACs exhibit many advantages as I.S.s. Thus, for each parent compound, several standards can be obtained, which means that the optimum I.S. can be selected for each sample so as to avoid co-elution with other sample components. Another advantage is the possibility of adding I.S.s to the sample during different stages of the work-up with the result that the associated losses in each step can be measured in one determination. This work centred on fluorinated naphthalenes, biphenyls and phenanthrenes. Samples included a coal tar (SRM 1597) and a chimney ash.

INTRODUCTION

Owing to the widespread occurrence and well documented carcinogenic properties of many polycyclic aromatic compounds (PACs), this class of compounds has been the focus of much analytical work. Since sixteen polycyclic aromatic hydrocarbons (PAHs), a sub-group of the PACs, have been classified by the US Environmental Protection Agency (EPA) as priority pollutants, efficient and reliable analytical procedures are required for their determination. The complexity of most environmental samples frequently makes sample pretreatment necessary in order to remove matrix and interfering compounds before the analysis can be carried out. Liquid–liquid or solid-phase extractions and adsorption chromatography are typical first steps which can be followed by further clean-up steps if necessary. All such steps possess the inherent risk of leading to losses of all or some of the analytes and should be monitored for this possibility.

Chromatographic techniques are usually employed for the determination of PACs [1] as the large number of parent and substituted PACs present in most real samples makes an efficient separation imperative. Gas chromatography (GC) with highly efficient capillary columns, often coupled with selective detectors, and high-performance liquid chromatography (HPLC), which can be made considerably more powerful with a time-programmed fluorescence detector, are in routine use. Columns which separate all the EPA priority PAHs are commercially available for both techniques. For such determinations, standards must be used, either internal (I.S.) or external, depending on whether the standard compound is added to the sample or not.

Several demands must be fulfilled by com-

* Corresponding author. Present address: Department of Analytical Chemistry, University of Münster, Wilhelm-Klemm-Strasse 8, D-48149 Münster, Germany.

0021-9673/94/$07.00
SSDI 0021-9673(93)E1012-O

pounds used as I.S.s in chromatography [2,3]: the I.S. and the analytes should have matching chemical and physical properties; the compound used as an I.S. must not be present in the sample; the I.S. should elute close to the analytes in question but resolved from them; the I.S. must not co-elute with any other detectable compound in the sample; the I.S. and analyte should show similar behaviour in the detector; and the I.S. should be obtainable in high purity and be chemically stable.

In many instances, aromatics which are not present in the sample have been used as the I.S. Isotopically labelled PACs have also become popular as I.S.s; several such compounds are commercially available. If a mass-selective detector is used, a PAC containing ^{13}C-labelled atoms can be used with advantage as it makes it possible to use a compound that is present in the sample, thus in an ideal manner fulfilling the criterion that the I.S. should resemble the analytes as closely as possible. The chromatographic separation of the I.S. from the analyte is not of importance as the detector will record the I.S. and the analyte at two different m/z values.

Perdeuterated PACs have gained prominence for other GC detectors; however, the separation efficiency of the column must be high enough to separate the deuterated and the non-labelled compounds. An example where this is not the case is given in Fig. 1, from the area of polycyclic aromatic sulphur heterocycles (PASHs), which we have extensively investigated [4,5]. PASHs are frequently oxidized to the dioxides in order to separate them from the PAHs. Although perdeuterodibenzothiophene is sufficiently well

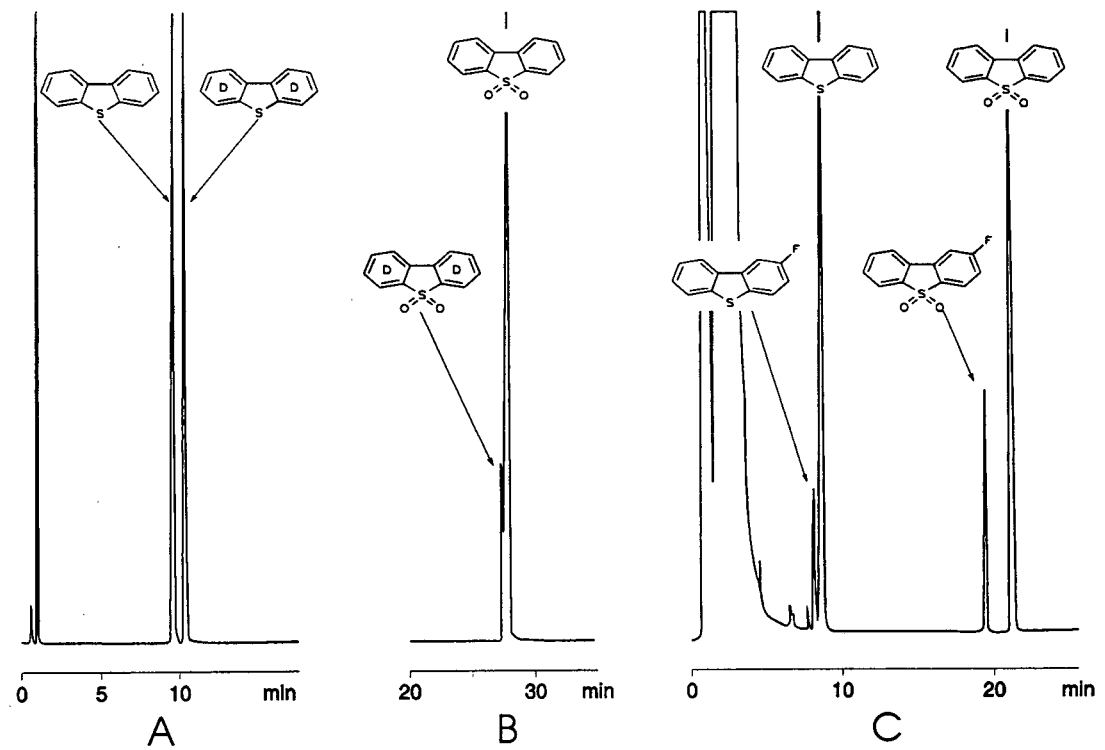

Fig. 1. Gas chromatographic separation of perdeuterodibenzothiophene, perdeuterodibenzothiophene dioxide, 2-fluorodibenzothiophene and 2-fluorodibenzothiophene dioxide from their parent compounds. GC conditions: (A) column, SB-Biphenyl-30, 25 m × 0.32 mm I.D., film thickness 0.25 μm; initial temperature, 100°C for 2 min, increased at 4°C/min; (B) same column as in (A) initial temperature 140°C for 2 min, increased at 4°C/min; (C) column, OV-1701, 25 m × 0.34 mm I.D., film thickness 0.10 μm; initial temperature, 150°C for 2 min, increased at 4°C/min.

separated from dibenzothiophene to be used as an I.S. (Fig. 1A), perdeuterodibenzothiophene dioxide is shown not to be sufficiently resolved from the non-labelled analogue (Fig. 1B). One solution to this separation problem might be to choose a different stationary phase, but this could lead to overlapping peaks in other areas of the chromatogram.

Despite the importance of I.S.s, the number of commercially available compounds suitable for such use is fairly limited. We speculated [6] that a series of benefits would be realizable if the number of potential I.S. could be increased considerably: for each parent compound several I.S.s can be made available; co-elution problems can be minimized, as a suitable I.S. can be chosen that elutes in an area of the chromatogram which is free of sample peaks; for recovery studies during work-up procedures, a different I.S. can be added to the sample before each step and all of them determined together at one time; and if the synthesis and the purification of the I.S. are simple enough, I.S.s for analytes that do not have isotopic analogues available commercially can be easily prepared.

Our first choice was fluorinated PACs, which to a first approximation fulfil the criteria listed earlier. The synthesis of fluorinated PACs has been extensively explored in recent years in connection with studies on the carcinogenicity of PACs and consequently suitable synthetic methods are available. As PACs possess several different carbon atoms that can be substituted, several fluorinated derivatives are possible for each parent. Further, it is conceivable to use di- and higher fluorinated compounds also, provided that they fulfil the other criteria.

The first example studied was that of 2-fluorodibenzothiophene (2-F-DBT) and its sulphone in order to see whether it might be a better choice than the deuterated analogues. As can be seen in Fig. 1C, 2-F-DBT shows about the same resolution from DBT as does perdeutero-DBT, but the resolution between the sulphones of 2-F-DBT and of DBT is much superior to that between the sulphones of perdeutero-DBT and DBT. This observation led to the following study which was undertaken in order to explore the gas chromatographic properties of fluorinated PACs (F-PACs) and their use as I.S.s for the gas chromatographic determination of PACs.

EXPERIMENTAL

Chemicals were purchased from Fluka or Aldrich and Nanograde solvents from Promochem. The F-PACs were synthesized in a Wittig reaction from appropriately substituted fluorobenzylphosphonic acid diethyl esters with a fluorinated benzaldehyde [7]. The resulting stilbene was photocyclized to a phenanthrene [8]. As most of the compounds synthesized have not been described before, they were fully characterized by spectroscopic techniques. Those data will be published elsewhere. The compounds synthesized are listed in Table I and are denoted G–P.

Table II shows the GC conditions used for the various measurements. The columns are listed in Table III. In all instances hydrogen was used as the carrier gas. The temperature programme was as follows: 80°C for 2 min, increased at 4°C/min to 270°C and held at the final temperature for 5 min. Reference solutions were prepared in toluene at a concentration of 50 ng/μl. The retention indices were calculated according to ref. 9. As some F-PACs co-eluted with phenanthrene, their retention indices were measured using benzothiophene and dibenzothiophene as retention standards and then calculated with the equation

$$I(x) = \frac{t(x) - t(\mathrm{BT})}{t(\mathrm{DBT}) - t(\mathrm{BT})} \cdot [i(\mathrm{DBT}) - i(\mathrm{BT})] + I(\mathrm{BT}) \quad (1)$$

where I = retention index, t = retention time, x = investigated compound, BT = benzothiophene and DBT = dibenzothiophene. The means of at least three injections are given in Table II. The standard deviations are given in the last column in Table II.

SRM 1597

An aliquot of a freshly opened ampoule of the National Institute of Standards and Technology (NIST) standard reference material SRM 1597 Coal Tar was weighed and a known amount of a

TABLE I

RETENTION INDICES OF SOME PACs AND F-PAHs ON VARIOUS STATIONARY PHASES

Columns as in Table III.

Peak	Compound	Formula	Retention index					Molar response[a]
			Column 1	Column 2	Column 3	Column 4	Column 5	
A	1-Fluoronaphthalene	$C_{10}H_7F$	200.11	200.19	199.50	197.62	198.43	1.03
B	Octafluoronaphthalene	$C_{10}F_8$	186.73	189.20	193.65	174.01	162.99	0.96
C	2-Fluorobiphenyl	$C_{12}H_9F$	232.03	231.69	227.97	228.76	226.44	1.24
D	4-Fluorobiphenyl	$C_{12}H_9F$	233.89	233.59	230.29	229.16	230.04	n.d.[b]
E	2,2′-Difluorobiphenyl	$C_{12}H_8F_2$	229.19	229.47	226.89	226.93	226.78	1.22
F	4,4′-Difluorobiphenyl	$C_{12}H_8F_2$	233.78	234.08	231.82	227.52	233.87	n.d.
G	1-Fluorophenanthrene	$C_{14}H_9F$	298.36	298.47	297.48	295.26	294.92	1.36
H	3-Fluorophenanthrene	$C_{14}H_9F$	297.01	297.18	297.45	293.84	296.87	1.41
I	1,2-Difluorophenanthrene	$C_{14}H_8F_2$	298.53	299.09	298.93	293.11	293.78	n.d.
K	1,3-Difluorophenanthrene	$C_{14}H_8F_2$	290.35	290.06	287.95	281.59	283.25	n.d.
L	1,6-Difluorophenanthrene	$C_{14}H_8F_2$	294.59	295.04	294.41	288.99	291.80	n.d.
M	2,4-Difluorophenanthrene	$C_{14}H_8F_2$	290.51	290.23	287.72	282.81	282.97	n.d.
N	3,6-Difluorophenanthrene	$C_{14}H_8F_2$	298.87	294.34	295.42	287.08	294.92	n.d.
O	2,4,6-Trifluorophenanthrene	$C_{14}H_7F_3$	288.88	288.87	287.38	277.79	280.76	1.37
P	1,3-Difluorobenzo[*c*]-phenanthrene	$C_{18}H_{10}F_2$	n.d.	n.d.	n.d.	370.67	n.d.	1.79
1	Naphthalene	$C_{10}H_8$	200.00	200.00	200.00	200.00	200.00	1.00
2	Benzothiophene (BT)	C_8H_6S	200.92	201.34	201.97	204.10	207.63	0.79
3	2-Methylnaphthalene	$C_{11}H_{10}$	n.d.	n.d.	n.d.	215.87	n.d.	1.10
4	1-Methylnaphthalene	$C_{11}H_{10}$	n.d.	n.d.	n.d.	220.67	n.d.	1.06
5	Biphenyl	$C_{12}H_{10}$	233.78	233.46	229.87	231.80	228.73	1.20
6	Acenaphthylene	$C_{12}H_8$	n.d.	249.19	n.d.	247.46	249.77	n.d.
7	Dibenzofuran (DBF)	$C_{12}H_8O$	n.d.	257.02	n.d.	254.77	256.99	1.12
8	Fluorene	$C_{13}H_{10}$	n.d.	268.37	n.d.	266.28	264.34	1.28
9	Dibenzothiophene	$C_{12}H_8S$	295.77	295.78	295.09	296.29	295.17	1.21
10	Phenanthrene	$C_{14}H_{10}$	300.00	300.00	300.00	300.00	300.00	1.32
11	Anthracene	$C_{14}H_{10}$	301.61	301.54	301.48	300.61	300.41	1.38
12	2-Methylphenanthrene	$C_{15}H_{12}$	n.d.	n.d.	n.d.	314.65	n.d.	1.52
13	4,5-Methylenephen-anthrene	$C_{15}H_{10}$	n.d.	n.d.	n.d.	320.88	n.d.	n.d.
14	1-Methylphenanthrene	$C_{15}H_{12}$	n.d.	n.d.	n.d.	319.96	n.d.	n.d.
15	Fluoranthene	$C_{16}H_{10}$	n.d.	n.d.	n.d.	341.58	n.d.	1.57
16	Pyrene	$C_{16}H_{10}$	n.d.	n.d.	n.d.	351.05	n.d.	n.d.
17	Benz[*a*]anthracene	$C_{18}H_{12}$	n.d.	n.d.	n.d.	395.63	n.d.	n.d.
18	Chrysene	$C_{18}H_{12}$	400.00	400.00	400.00	400.00	400.00	1.73

[a] Determined on column 4 (see Table III).
[b] n.d. = Not determined.

solution of the I.S. was added. Following dilution with toluene the solution was injected into the gas chromatograph five times. The analytes were quantified by comparison of the peak areas with that of the nearest eluting I.S. and final calculation by means of the following equation, using response factors determined previously:

$$w(x) = \frac{m(x)}{m(\mathrm{SRM})} = \frac{ar(x)}{ar(\mathrm{I.S.})} \cdot \frac{rf(\mathrm{I.S.})}{rf(x)} \cdot \frac{m(\mathrm{I.S.})}{m(\mathrm{SRM})} \quad (2)$$

where w = concentration, m = mass, ar = peak

TABLE II

EXPERIMENTAL CONDITIONS FOR GC MEASUREMENTS AND STANDARD DEVIATIONS OF THE PARAMETERS MEASURED

Parameter	Apparatus	Injection technique	Column	Number of injections	Standard deviation
Retention index	Delsi Di200	Splitless	1[a]	3–6	≤0.08 i.u.
	Delsi Di200	Splitless	2[a]	3–6	≤0.12 i.u.
	HP 5890 II	On-column	3[a]	4–8	≤0.05 i.u.
	HP 5890 II	On-column	4[a]	4–8	≤0.05 i.u.
	Delsi Di200	Splitless	5[a]	3–6	≤0.12 i.u.
Response	HP 5890	On-column	4[a]	3	≤3%
	Carlo Erba FV 2300 AC	Splitless	BP-5, 25 m × 0.22 mm I.D., 0.25 μm	5	≤4%
Quantification, SRM	Carlo Erba FV 2300 AC	Splitless	BP-5, 25 m × 0.22 mm I.D., 0.25 μm	5	See Table IV
Quantification; chimney ash	Carlo Erba FV 2300 AC	Splitless	BP-5, 25 m × 0.22 mm I.D., 0.25 μm	3	See Table IV

[a] See Table III.

area, rf = response factor, x = analyte, I.S. = internal standard and SRM = SRM 1597.

Chimney ash

A flow-chart of the work-up procedure is shown in Fig. 2. A sample of 100 g of chimney ash from a paper- and wood-burning home furnace was ground in a mortar and known amounts of three I.S.s were added (see Fig. 2). After Soxhlet extraction with benzene (48 h) and volume reduction by rotary evaporation, two additional I.S.s were added. After separation of the long-chain aliphatics and the PACs from polar compounds on an alumina column with benzene as the eluent, separation of the aliphatics and PACs was done by normal-phase HPLC on an aminopropyl-bonded 5-μm LiChrosorb NH_2 column (250 mm × 20 mm I.D.) with hexane as the eluent for the aliphatics and hexane–methylene chloride (96:4, v/v) for

TABLE III

PROPERTIES OF THE COLUMNS USED

Column No.	Stationary phase	Polarity[a]	Length (m)	Inner diameter (mm)	Film thickness (μm)	Phase ratio, β
1	PB-1, polydimethylsiloxane	222	50	0.32	0.20	400
2	DB-5, methyl–phenylsilicone (95:5)	334	30	0.32	0.25	320
3	OV-1701, cyanopropyl–phenyl–methylsilicone (5:7:88)	789	30	0.20	0.15	330
4	DB-17, methyl–phenylsilicone (50:50)	884	30	0.32	0.25	320
5	DB-WAX 20M, polyethylene glycol	2308	30	0.32	0.25	320

[a] Sum of McReynolds constants.

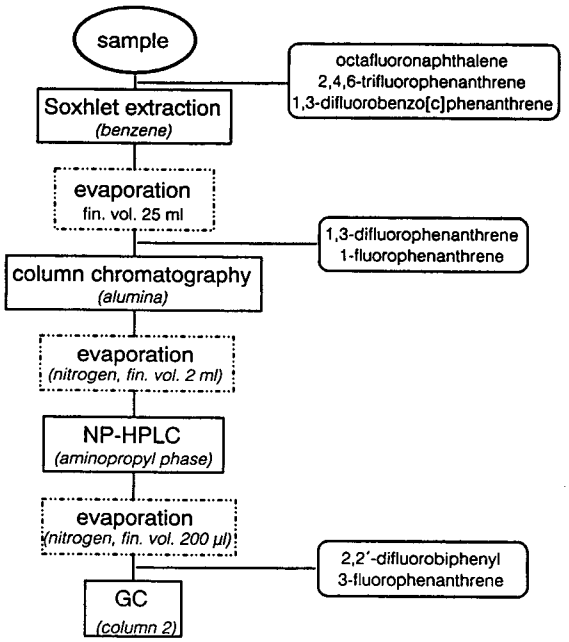

Fig. 2. Flow chart of the work-up procedure for chimney ash.

the PACs. After the final addition of two I.S.s, quantification was done by GC on a 0.25-μm DB-5 column (25 m × 0.22 mm I.D.).

RESULTS AND DISCUSSION

Several aromatic compounds containing two to four rings and one to three fluoro substituents were synthesized and investigated as potential I.S.s in the gas chromatographic determination of PACs in two samples. The F-PACs are listed in Table I together with the molar response factors (flame ionization detection) and the retention indices on five different stationary phases. Phases of different polarity were used so that the tabulated retention indices can serve as a guide to the selection of suitable fluorinated standards in other laboratories. The data in Table I show that many F-PACs are well resolved from the parent compounds.

As the fluorine atom is nearly as small as the hydrogen atom it does not cause much of a steric effect and therefore the causes responsible for the differences in retention behaviour between the fluoroaromatics and their parent compounds must be electrostatic in nature. These interactions in gas chromatography with liquid stationary phases are known as Van der Waals interactions and include the interactions between permanent dipoles (Keesom forces), interactions between molecules with permanent dipoles and with induced dipoles (inductive interactions) and dispersive interactions between molecules without any dipole (London forces). In addition to these physical forces, chemical forces (donor–acceptor interactions, hydrogen bonding) also exist [10,11]. Fluorine substitution in general leads to a weaker interaction between a solute and the stationary phase and therefore to shorter retention times for the fluorinated aromatics, so that they elute ahead of their parent compounds. We therefore prefer to refer to retention decrements (not increments) when discussing the influence of the fluorine atom on the retention index. This effect is known for perfluorinated alkanes and alkenes also [12].

The strongly electron-withdrawing effect of fluorine, on the other hand, has consequences for the elution pattern of the F-PACs in that the changes in retention are particularly pronounced the more polar is the stationary phase.

As not all isomers of the mono- and disubstituted phenanthrenes were available, no attempt has so far been made towards an empirical correlation of the structure with retention. Some general conclusions can be drawn, however, from the results for the eight fluorophenanthrenes studied here. It is obvious that the position of the fluoro substituent has a strong effect on the retention, as can be seen by comparison of the data in Table I. The retention decrements are illustrated in Fig. 3.

As expected, the higher fluorinated derivatives show a larger decrement except for 1,2-difluorophenanthrene, which on some phases displays a surprisingly small decrement. This may be attributed to the so-called *ortho* effect, which is known to contribute to a longer retention time for *ortho*-substituted alkyl aromatics [13] and chlorobenzenes [14]. *Meta* substitution means a larger decrement than a simple addition of the decrements for the corresponding monosubsti-

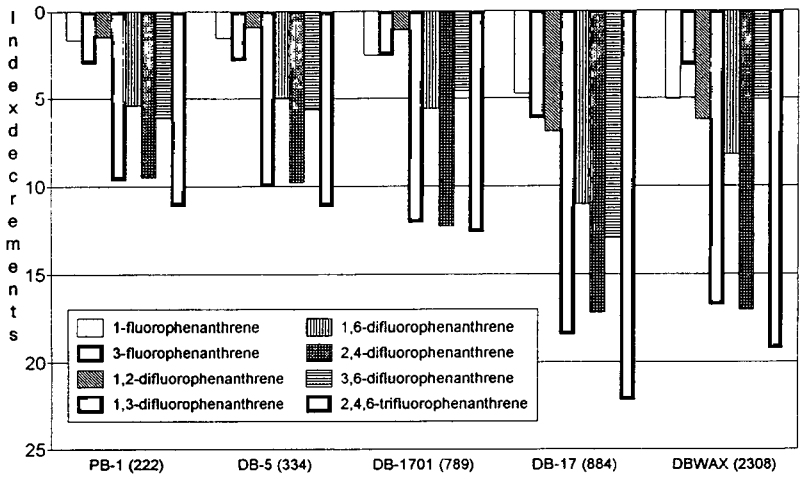

Fig. 3. Index decrements of eight fluorophenanthrenes on five different columns (see Table III).

tuted phenanthrenes would predict. Finally, it must be noted that the order of elution is dependent on the stationary phase. For instance, on methylphenylsilicone (column 4, DB-17), 1,6-difluorophenanthrene elutes earlier than the 3,6-derivative but on a polyethylene glycol phase (column 5, DB-WAX) the opposite is true. Several other such reversals can be seen through inspection of Fig. 3.

The chromatogram in Fig. 4A illustrates the resolution of all eight fluorophenanthrenes (peaks G–O) on DB-17. It is clear that all eight can be used simultaneously as I.S.s on this stationary phase provided that they do not co-elute with sample components. A difference in retention index of about 1 unit (Table I) means that the peaks are fully resolved.

The response of the flame ionization detector was investigated and the molar response calculated (Table I). The theoretical molar response was assumed to be unity for each carbon atom, independent of substitution [15]. Only dibenzofuran displays a lower than theoretical response, which is in line with previous data [16]. No such effect is seen for dibenzothiophene.

The results presented so far indicate that the F-PACs fulfil the criteria listed earlier for I.S.s. To test them under realistic conditions, they were used for the determination of PACs in two kinds of environmental samples.

SRM 1597

This sample consists of the aromatic fraction of a coal tar, dissolved in toluene. The concentrations of ten PAHs are certified by NIST and for eight more an orientation value is given. As only aromatic compounds are present in the solution supplied, no work-up is necessary. The gas chromatogram of SRM 1597 is shown in Fig. 4B, which illustrates how the selection of suitable I.S.s can be performed if a sample solution containing the aromatics to be determined is available. For the early-eluting analytes, 2-fluoro- and 2,2′-difluorobiphenyl (compounds C and E, respectively) were chosen because, as a comparison of Fig. 4A and B shows, they do not interfere with any peaks in the sample. As this is a sample with relatively few analyte peaks, almost any of the fluorinated phenanthrenes investigated here can be used without the problem of co-elution. Compounds G, H, K and O were selected. (In principle, only one of those standards would have been sufficient, but as will be shown in Fig. 5, the use of more than the theoretical minimum number of standards can be useful on occasion.) For the later eluting aromatics, 1,3-difluorobenzo[*c*]phenanthrene (compound P) was added. As shown in Fig. 3C, the analyte and standard peaks are well resolved from each other. For the calculation of the concentration of the analytes, the molar re-

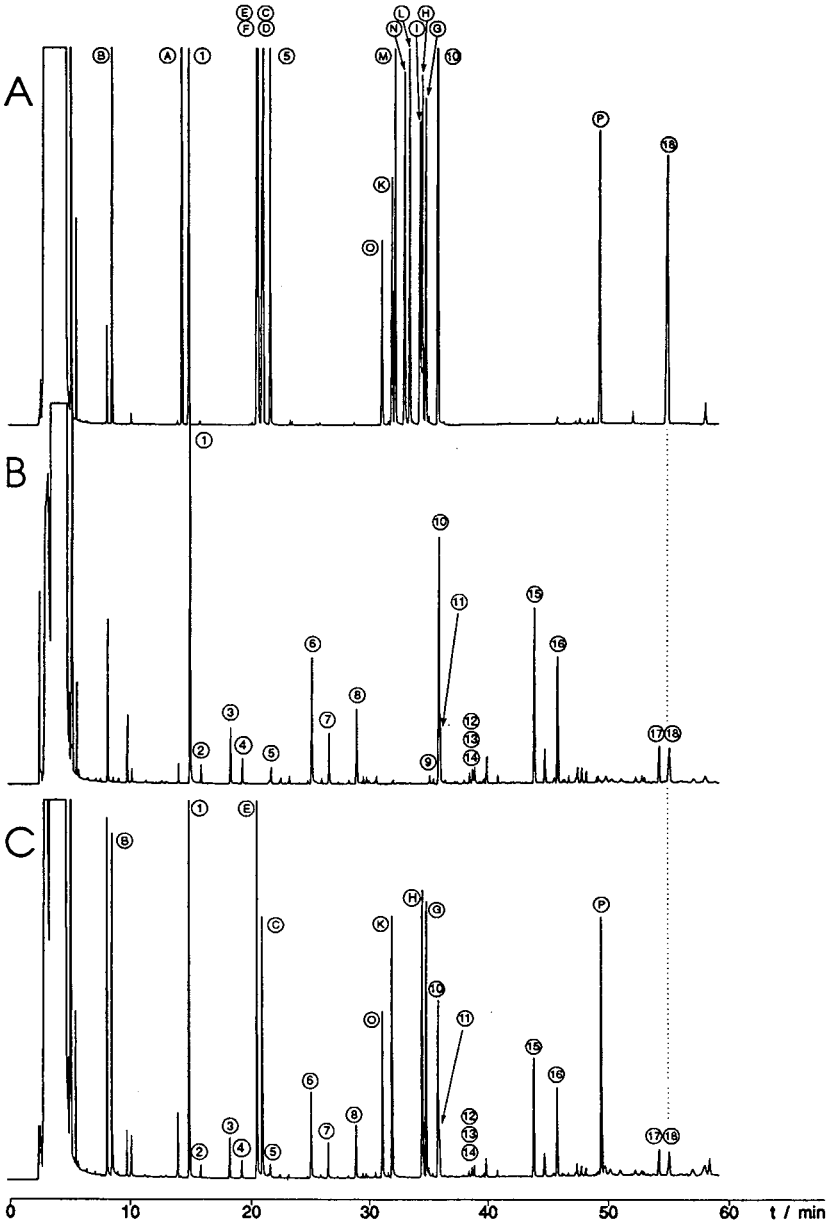

Fig. 4. Selection of the internal standards for the determination of PACs in SRM 1597. (A) Chromatogram of standard solution containing F-PAHs; (B) chromatogram of SRM 1597; (C) chromatogram of a solution containing SRM 1597 and the selected I.S. GC conditions: on-column injection on column 4, temperature programme as in text, flame ionization detection. Peak numbers as in Table IV.

sponse factors determined previously were used. In most instances, the results agree well with the certified concentrations, but there are four values that do not, namely those for biphenyl, dibenzofuran, dibenzothiophene and 4,5-methylenephenanthrene (Table IV). For dibenzofuran and dibenzothiophene the NIST value was calculated using response factors of unity with respect to the nearest I.S. (acenaphthene and 1-methylphenanthrene, respectively), which is un-

TABLE IV

DETERMINATION OF PACs BY USE OF F-PAHs AS INTERNAL STANDARDS IN SRM 1597 AND CHIMNEY ASH

Peak	Compound	Certified value (μg/g)	Recalculated NIST value (see text)	Determined value[a] (μg/g)	Relative deviation from NIST value (%)	Chimney ash[a] (μg/g)
1	Naphthalene	1160 ± 50	–	1172 ± 14	1.0	
2	Benzothiophene	–	–	42.4 ± 1	–	
3	2-Methylnaphthalene[b]	97.1 ± 1.1	–	96 ± 5	−1.1	
4	1-Methylnaphthalene[b]	47.0 ± 0.6	–	47.8 ± 0.9	1.7	
5	Biphenyl[b]	27.0 ± 0.3	–	30 ± 1	11.1	
6	Acenaphthylene[b]	252 ± 1	–	256 ± 2	1.6	
7	Dibenzofuran[b]	88.9 ± 0.5	103.9	103 ± 1	−0.9	
8	Fluorene[b]	136 ± 1	–	133 ± 2	−2.2	
9	Dibenzothiophene[b,c]	23 ± 0.4	27.5	28 ± 1	3.6	
10	Phenanthrene	462 ± 3	–	460 ± 16	−0.4	41 ± 3
11	Anthracene	101 ± 2	–	106 ± 5	4.9	5 ± 1
12	2-Methylphenanthrene	–	–	17 ± 0.6	–	
13	4,5-Methylenephenanthrene[d]	51.3 ± 0.3	–	56 ± 5		
14	1-Methylphenanthrene	–	–	9.1 ± 0.5	–	
15	Fluoranthene	322 ± 4	–	329 ± 8	2.2	118 ± 5
16	Pyrene	235 ± 2	–	238 ± 7[e]	1.3	104 ± 3[e]
17	Benz[*a*]anthracene	98.6 ± 3.6	–	112 ± 8[f,g]		62 ± 3[f,g]
18	Chrysene + triphenylene	83.8	–	86 ± 6	2.6	97 ± 3

[a] Nearest I.S. was used for calculation.
[b] Compound quantified but not certified.
[c] Dibenzothiophene + naphtho[1,2-*b*]thiophene.
[d] Too high owing to co-elution with methylphenanthrene.
[e] Response factor of fluoranthene was used.
[f] Response factor of chrysene was used.
[g] Too high owing to insufficient separation from cyclopenta[*cd*]pyrene.

likely to apply. Under the conditions of the flame ionization detector used the molar response factors for those two compounds were 1.12 and 1.21, respectively. The recalculation of the NIST values using these two values gave the values listed in Table IV, which are in considerably better agreement with our values. For dibenzothiophene, it must additionally be noted that this compound co-elutes with naphtho[1,2-*b*]thiophene on non-polar stationary phases so that the integrated peak area yields the sum of those two compounds.

The SRM is a simple sample because no work-up is needed and the fairly high analyte concentrations and the small number of analytes present, allowing a wide and unproblematic choice of I.S.s. In principle, only one of those standards would have been sufficient, but as shown previously [6], the use of more than the theoretical minimum number of standards can be useful on occasion, especially in case of complex mixtures.

The PAC content of a chimney ash originating from an oil-heated furnace was determined, based on four different I.S.s. For 4,4′-difluorobiphenyl (compound F, Fig. 5B) all the values were always lower than if one of the other standards was used. A possible explanation for this observation is co-elution of standard F with a sample component. Indeed, when the temperature programme was changed, a previously hidden peak emerged from under the peak of the standard (Fig. 5). In such cases where the aromatic fraction is not available for screening for suitable "empty" spaces for standards (Fig. 4 shows a case where this is possible), the addition of several standards is recommended. The con-

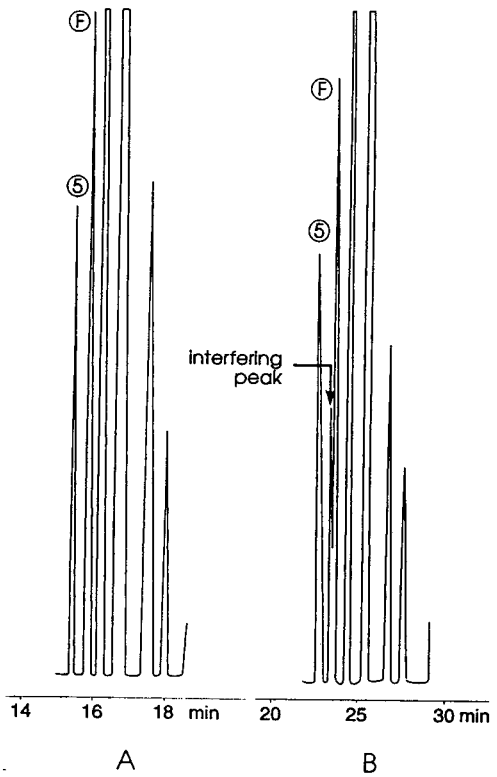

Fig. 5. Chromatogram of a chimney ash with two different temperature gradients: (A) 4 and (B) 2°C/min.

centration values obtained should be the same when calculated with any of the standards; if not, co-elution of the standard with the analyte might be the cause of the problem, invalidating the quantification. Such a co-elution would not be detectable with only one standard (*e.g.*, a per-deuterated derivative).

Chimney ash

A more complex case that requires several work-up steps before the analysis can be done was provided by a chimney ash taken from a furnace fuelled exclusively with paper and wood. In contrast to SRM 1597, the chromatogram of the aromatic fraction of this sample was not available beforehand so the selection of I.S.s had to be based on assumptions. As the PAC pattern is combustion derived, a more complex gas chromatogram than for the coal tar must be expected, making the selection of I.S.s somewhat delicate. As several work-up steps are necessary, we took advantage of the possibility of multiple additions of I.S.s at different points of the work-up that is made available by the fluorinated PACs. The scheme is illustrated in Fig. 2 together with the relevant I.S.s. Three fluorinated I.S.s, one for each ring number, were added to the sample at the beginning of the work-up. Following the Soxhlet extraction with benzene and the reduction of the volume of the extract, two fluorinated phenanthrenes were added and finally, after two liquid chromatographic pretreatment steps, two more I.S.s were added just prior to the GC analysis.

A normal-phase liquid chromatographic separation of the aromatics and long-chain aliphatics, which adsorbed strongly enough to elute with the aromatic fraction from alumina, was necessary in order to obtain a clean gas chromatogram of the PACs.

The results for six PACs are provided in Table IV. They were calculated using the appropriate response factors and were corrected for losses, determined through the use of several I.S.s.

The calculation of the recovery of the initially added I.S., based on 2,2′-difluorobiphenyl and 3-fluorophenanthrene, shows that there is virtually no difference depending on which integration standards were used (Table V). This demonstrates that both of these standards elute in the gas chromatogram free of interferences from sample components. As the chromatogram without the I.S.s is not available, it is not self-evident that there is no co-elution of a sample component with the I.S.s. The data in Table V show that 2,4,6-trifluorophenanthrene, which was added initially to the sample, has the same recovery as the two fluorinated phenanthrenes which were added after the Soxhlet extraction and rotary evaporation (to a volume of 25 ml, Fig. 2). This means that in those early steps, no losses of any consequence occurred. The recovery of all fluorinated phenanthrenes of *ca.* 50% means that about half of the sample components in this volatility region are lost, probably during the reduction in volume using nitrogen. As expected, the more volatile standard compound octafluoronaphthalene was lost to a greater extent (60%) and the less volatile standard, 1,3-difluorobenzo[*c*]phenanthrene, to a lesser

TABLE V

RECOVERIES (%) OF THE INTERNAL STANDARD, CALCULATED USING 2,2′-DIFLUOROBIPHENYL AND 3-FLUOROPHENANTHRENE

Peak	Compound	2,2′-Difluorobiphenyl	3-Fluorophenanthrene	Mean
B	Octafluoronaphthalene	39	40	40
O	2,4,6-Trifluorophenanthrene	52	54	53
P	1,3-Difluorobenzo[*c*]phenanthrene	59	61	60
K	1,3-Difluorophenanthrene	49	50	50
G	1-Fluorophenanthrene	50	51	51

extent (40%) than the phenanthrenes. This hints at evaporative losses during steps involving a reduction in volume. The data also demonstrate how important it is to use standards in the appropriate volatility region for each analyte. It must be cautioned against the use of standards with a volatility that is much different from that of the analytes in question; in other words, the analyte and standard must elute fairly close to each other in the gas chromatogram (on non-polar stationary phases). The results obtained confirm the speculation that it is possible to determine the losses in every step of the work-up procedure in one run if a sufficient number of I.S.s are available.

CONCLUSIONS

The use of fluorinated compounds as standards for the determination of PACs has been demonstrated for two samples. Among the several advantages over the frequently used deuterated PACs is the possibility of using several standards for each ring number, thus allowing the determination of losses in serval work-up steps in one chromatogram. Another benefit is that if a standard by coincidence should co-elute with a sample component, this can easily be detected if multiple standards are used. The fact that the F-PAHs in general elute ahead of their parent compounds could be advantageous in the case of complex PAC patterns, when fractionation according to ring number is necessary: The F-PAHs would then elute in a region where no other components are present. Finally, if a chromatogram without standards is available, there is a wide choice of fluorinated compounds to choose from so that the possibility of co-elution can be avoided altogether.

ACKNOWLEDGEMENTS

Dr. Thomas Class is thanked for making his GC system available. Financial support from the Fonds der Chemischen Industrie is gratefully acknowledged. Dr. S.A. Wise is thanked for a gift of the coal tar standard.

REFERENCES

1 M.L. Lee, M.V. Novotny and K.D. Bartle, *Analytical Chemistry of Polycyclic Aromatic Compounds*, Academic Press, New York, 1981, pp. 17–49.
2 C.F. Poole and S.A. Schuette, *Contemporary Practice of Chromatography*, Elsevier, Amsterdam, 1984, p. 452.
3 D.E. Wells and A.A. Cowan, *J. Chromatogr.*, 279 (1983) 209.
4 J.T. Andersson, *Int. J. Environ. Anal. Chem.*, 48 (1992) 1.
5 J.T. Andersson, *J. Chromatogr.*, 585 (1991) 376.
6 J.T. Andersson and U. Weis, in P. Garrigues and M. Lamotte (Editors), *Polycyclic Aromatic Compounds. Synthesis, Properties, Analytical Measurements, Occurrence, and Biological Effects. PAH XIII*, Gordon and Breach, 1993, p. 85.
7 J. Boutagy and R. Thomas, *Chem. Rev.*, 74 (1974) 87.
8 C.S. Woods and F.B. Mallory, *J. Org. Chem.*, 29 (1964) 3373.
9 M.L. Lee, D.L. Vassilaros, C.M. White and M. Novotny, *Anal. Chem.*, 51 (1979) 768.
10 R.V. Golovnya and B.M. Polanuer, *J. Chromatogr.*, 517 (1990) 67.
11 R.V. Golovnya and T.A. Misharina, *J. High Resolut. Chromatogr. Chromatogr. Commun.*, 3 (1980) 4.
12 U. Müller, P. Dietrich and D. Prescher, *J. Chromatogr.*, 259 (1983) 243.
13 J. Macak, V. Nabivach, P. Buryan and S. Sindler, *J. Chromatogr.*, 234 (1982) 285.
14 J.K. Haken and I.O.O. Korhonen, *J. Chromatogr.*, 265 (1983) 323.
15 H.Y. Tong and F.W. Karasek, *Anal. Chem.*, 56 (1984) 2124.
16 A.D. Jorgensen, K.C. Picel and V.C. Stamoudis, *Anal. Chem.*, 62 (1990) 683.

Journal of Chromatography A, 659 (1994) 163–175
Elsevier Science B.V., Amsterdam

CHROM. 25 581

Determination and in-depth chromatographic analyses of alkaloids in South American and greenhouse-cultivated coca leaves

James M. Moore*, John F. Casale, Robert F.X. Klein and Donald A. Cooper

United States Drug Enforcement Administration, Special Testing and Research Laboratory, 7704 Old Springhouse Road, McLean, VA 22102-3494 (USA)

John Lydon

United States Department of Agriculture, Agricultural Research Services, Weed Science Laboratory, Building 001, Room 236, Beltsville, MD 20705 (USA)

(First received May 28th, 1993; revised manuscript received September 13th, 1993)

ABSTRACT

Methodology is described for the detection and/or determination of cocaine and minor alkaloids in South American coca as well as in greenhouse- and tropical-cultivated field coca of known taxonomy. Coca leaf from Bolivia, Peru, Ecuador and Colombia were subjected to the determination of cocaine, *cis*- and *trans*-cinnamoylcocaine, tropacocaine, hygrine, cuscohygrine and the isomeric truxillines. The greenhouse samples were cocaine-bearing leaves of the genus *Erythroxylum* and included *E. coca* var. *coca*, *E. novogranatense* var. *novogranatense* and *E. novogranatense* var. *truxillense*, and the alkaloids determined were cocaine, ecgonine methyl ester, cuscohygrine, tropacocaine and the cinnamoylcocaines. The tropical-cultivated coca were *E. novogranatense* var. *novogranatense* and *E. coca* var. *coca*. Cocaine and minor alkaloids were isolated from basified powdered leaf samples using a toluene extractant, followed by acid–Celite column chromatography. The isolated alkaloids were determined by capillary gas chromatography with flame ionization or electron-capture detection. Methodology is also presented for the isolation and mass spectral analysis of numerous trace-level coca alkaloids of unknown structure.

INTRODUCTION

It is well-recognized in forensic drug research that the characterization of manufacturing impurities and byproducts present in illicit drugs is useful for intelligence purposes. This may include (a) ascertaining the geographic origin of the drug, (b) doing chemical comparative analyses to determine if different drug seizures are related and derived from a common source and (c) evaluation of the clandestine manufacturing processes for precursor chemical monitoring. The manufacturing impurities and byproducts most studied and reported have been those associated with cocaine, heroin and the amphetamine-type compounds [1–20].

Although most illicit drugs are produced via chemical syntheses, some are derived directly from natural products. Such an example is illicit cocaine, a drug which is isolated from the leaves of the South American coca plant, *Erythroxylum* (*E.*) *coca* var. *coca*, using multiple extraction and purification steps. There have been an increasing number of publications describing the in-depth gas chromatographic (GC) analyses of manufac-

* Corresponding author.

SSDI 0021-9673(93)E1010-W

turing impurities/byproducts in refined illicit cocaine seizures [1,12–34]. However, scant attention has been paid by forensic chemists to the in-depth analysis of *E. coca* var. *coca* or other cocaine-bearing plants, or how their alkaloidal content relates to impurities and byproducts present in refined illicit cocaine.

A review of the literature indicated that virtually all of the quantitative data for coca-leaf alkaloids have been provided for only cocaine and the cinnamoylcocaines [35–44]. Therefore, methodology was developed and described herein that utilizes toluene extraction and column chromatography for the isolation of coca alkaloids from the leaf, followed by their determination using capillary GC (cGC)–flame ionization detection (FID) or cGC–electron-capture detection (ECD). This methodology is suitable for the determination of cocaine and most other known alkaloids in cocaine-bearing plants, including *cis*- and *trans*-cinnamoylcocaine, the isomeric truxillines, tropacocaine, ecgonine methyl ester, cuscohygrine and hygrine. This study encompasses the analyses of coca leaf samples from the field in South America, *i.e. E. coca* var. *coca* (ECVC-SA) and *E. novogranatense* var. *novogranatense* (ENVN-SA), as well as greenhouse-cultivated *E. coca* var. *coca* (ECVC-GH), *E. novogranatense* var. *novogranatense* (ENVN-GH) and *E. novogranatense* var. *truxillense* (ENVT-GH). Tropical-cultivated samples, grown at a site other than South America, included *E. novogranatense* var. *novogranatense* (ENVN-TR) and *E. coca* var. *coca* (ECVC-TR).

Methodology is also described for the isolation of numerous unknown trace-level alkaloids from leaf tissue and the bulk cocaine matrix of South American coca. This was accomplished largely by trap, ion-pairing and liquid–liquid partition column chromatography and acid buffer extractions. Mass spectral data were acquired for about 100 of these suspected alkaloids.

EXPERIMENTAL

Plant material

All leaf material examined in this study contained significant levels of cocaine. While several varieties of cocaine-producing *Erythroxylum* are known, cocaine-bearing leaves are sometimes referred to collectively as coca leaves, regardless of the species/variety of the plant from which they were harvested. Unless referring to a specific species, we use that terminology herein. Leaves analyzed in this study included collections from the field in Bolivia, Peru, Ecuador and Colombia. Other leaves were harvested from coca plants of three different varieties cultivated in a greenhouse environment at the US Department of Agriculture. Also included in this study were leaves from plants cultivated at a tropical site other than South America.

Two batches of leaves originating from Bolivia/Peru and leaves from Colombia were believed to be ECVC-SA and ENVN-SA, respectively. ECVC-SA leaves are the most commonly associated with the clandestine manufacture of illicit refined cocaine. Leaves harvested in Ecuador were of unknown taxonomy. These South American field samples were believed harvested from plants cultivated by local natives. After harvesting, the leaves were sun/air-dried and then sent to our laboratory for analyses. The dried leaves were stored at room temperature for 1–3 years prior to in-depth alkaloid analyses.

Plants grown in a greenhouse at the US Department of Agriculture in Beltsville, MD, USA were ECVC-GH, ENVN-GH and ENVT-GH. Greenhouse cultivars were grown in 1.2–l pots containing seven parts greenhouse potting media (sandy loam) and three parts Promix B1 (Premier Brands, New York, NY, USA) (pH 6.0, 4.1% organic matter). Plants were watered to soil saturation as needed and fertilized with 2.5 g/l of N–P–K–(20:20:20) fertilizer every third week. The plants were approximately 2 years old at the time of harvest. Leaves were air-dried at room temperature for two days and then stored over silica gel at 0°C.

Cultivated at a non-South American tropical site were ENVN-TR and ECVC-TR. These plants were of the same seed stock used in the greenhouse cultivar of the same species (ENVN-GH and ECVC-GH). The soil at the tropical site location was a Halii gravelly sandy loam [classified as Typic Gibbshumox (an oxisol)] containing 6% organic matter (pH 5.4). The site was at an

elevation of 170 m and received a mean annual rainfall of 250 cm. Plants did not receive supplemental watering and were fertilized with 30 kg/ha N–P–K (20:20:20) per month. Plants were about 1.5 years old at time of harvest. Leaves were air-dried at room temperature for 2 days and then stored over silica gel at 0°C.

Solvents, chemicals, standards and materials

All solvents were distilled-in-glass products of Burdick & Jackson Labs. (Muskegon, MI, USA). Heptafluorobutyric anhydride (HFBA) and N-methyl-N-trimethylsilyltrifluoroacetamide (MSTFA), both supplied in 1-ml sealed glass ampules, were obtained from Pierce (Rockford, IL, USA). A 1.0 *M* solution of lithium aluminum hydride ($LiAlH_4$) in diethyl ether and 4-dimethylaminopyridine (DMAP) were supplied by Aldrich (Milwaukee, WI, USA). Cocaethylene, used as methodology internal standard, was prepared by the benzoylation of ecgonine ethyl ester. Hygrine, ethylhygrine, cuscohygrine, ecgonine methyl ester, ecgonine ethyl ester and *trans*-cinnamoylcocaine were synthesized in our laboratory. Dimethyl-μ-truxinate was prepared as described in ref. 18. Pharmaceutical-grade cocaine base and tropacocaine · HCl were obtained from commercial sources. The Celite 545 stationary phase used for column chromatography was obtained from J.T. Baker (Jackson, TN, USA) and was used without any pre-treatment. A pH 4.0 acid phthalate buffer was prepared according to the United States Pharmacopeia XIX [48]. All other chemicals were of reagent-grade quality.

Gas chromatography

Three gas chromatographs were used in this study. All used hydrogen as carrier gas at 30–40 cm/s. A Hewlett-Packard 5890 Series II GC–FID system, operating in a split mode of 20:1 and fitted with a 30 m × 0.25 mm I.D. fused-silica capillary column coated with DB-1 (0.25 μm) (J & W Scientific, Rancho Cordova, CA, USA), was used for the concomitant determination of ecgonine methyl ester, cuscohygrine, tropacocaine, cocaine and *cis*-/*trans*-cinnamoylcocaine in the greenhouse- and tropical-cultivated coca. The oven temperature was programmed as follows: initial temperature, 150°C; initial hold, 1.0 min; program rate, 6.0°C; final temperature, 275°C; final hold, 8.0 min. Injector and detector temperatures of 230 and 280°C, respectively, were maintained. Nitrogen was used as auxiliary gas. A Perkin-Elmer Sigma 2000 GC–FID system was utilized for the analysis of South American-cultivated coca, under conditions similar to those described above.

A Hewlett-Packard 5880A GC–^{63}Ni ECD system, operating in the splitless mode and fitted with two capillary columns, was used for the analyses of the isomeric truxillines and hygrine. Argon–methane (95:5) was used as auxillary gas. Chromatographic conditions for the truxillines analyses are given in refs. 18 and 25. Hygrine was chromatographed on a 15 m × 0.25 mm fused-silica capillary column coated with DB-5 + (0.25 μm). The oven temperature for the hygrine quantitation was programmed as follows: (level 1) initial temperature, 90°C; initial hold, 5.5 min; program rate, 5°C/min; final temperature, 160°C; final hold, 5 min; (level 2) program rate, 4°C/min; final temperature, 275°C; final hold, 10 min. Injector and detector temperatures were both held at 300°C.

Mass spectrometry (MS)

A Hewlett-Packard Model 5971 quadrupole mass-selective detector interfaced with a Hewlett-Packard 5890 Series II gas chromatograph was used in this study. The mass-selective detector was operated in the electron impact ionization mode with an ionization potential of 70 eV, a secondary electron multiplier value of 1541 and at 1.2 scans/s. The GC system was fitted with a 30 m × 0.25 mm I.D. fused-silica capillary column coated with DB-1 (0.25 μm). The oven temperature was programmed as follows: initial temperature, 150°C; initial hold, 1.0 min; program rate, 6.0°C/min; final temperature, 285°C; final time, 11 min. Injector and detector temperatures were maintained at 230 and 280°C, respectively.

Extraction and isolation of coca-leaf alkaloids

Air-dried leaf tissue was powdered with a Wiley mill to pass a 2-mm sieve. If not used immediately, the powder was placed in a screw-

capped glass jar and stored over silica gel at about 0°C.

About 1 g of coca-leaf powder was accurately weighed into a 50-ml centrifuge tube and triturated with 1 ml of an aqueous solution saturated with sodium hydrogencarbonate. To this basified mixture were added 20 ml of water-saturated toluene containing 2.00 mg of cocaethylene internal standard. The tube was heated at 60–65°C for 1 h with occasional mixing. After centrifugation (*ca.* 400 *g*) for 10 min, the toluene supernatant was transferred to a flask. The coca-leaf powder residue in the tube was then extracted with two additional 15-ml aliquots of water-saturated toluene as just described. The three toluene extracts were combined, mixed thoroughly and transferred to a chromatographic column (260 mm × 22 mm) packed with a mixture of 2.0 ml of 0.18 *M* sulfuric acid and 4 g of Celite 545. After passing through the column, the toluene eluate was discarded. An additional 20 ml of water-saturated toluene followed by 20 ml of water-saturated $CHCl_3$ were then added to the column and the eluates discarded. The coca alkaloids were then liberated from the column by the addition of 50 ml of water-saturated $CHCl_3$ containing 250 μl of diethylamine. After adjustment to 50.0 ml, the eluate containing the coca alkaloids, referred to as solution A, was mixed thoroughly with 10 g of anhydrous Na_2SO_4 and saved for alkaloid quantitation (note: for coca-leaf samples with lower alkaloid content, greater sample masses and/or a concentration step may be required).

GC quantitation of isolated alkaloids

Ecgonine methyl ester, cuscohygrine, tropacocaine, cocaine and cis/trans-cinnamoylcocaine. About 2–3 μl of solution A from above was injected in duplicate into the 30-m DB-1 capillary column under chromatographic conditions described above for the Hewlett-Packard 5890 Series II GC–FID system. Quantitative data were obtained using a standard mixture of target alkaloids in 50 ml of chloroform, at the following concentrations: cocaine 0.100 mg/ml, cocaethylene internal standard 0.040 mg/ml, cuscohygrine 0.050 mg/ml, ecgonine methyl ester 0.050 mg/ml and *trans*-cinnamoylcocaine 0.030 mg/ml. The 50 ml of standard solution also contained about 100 μl of diethylamine. Calculations for *cis*-cinnamoylcocaine in samples were based upon peak area for the standard *trans*-cinnamoylcocaine.

If review of a sample chromatogram revealed only trace levels of certain alkaloids, especially tropacocaine, an appropriate aliquot of solution A was reduced in volume (5–10 ×), but not to dryness, *in vacuo* at 45–50°C and then reinjected into the 30-m DB-1 capillary column as described previously.

Truxillines. For determination of the truxillines, an appropriate aliquot (1.0–5.0 ml) from solution A was transferred to a centrifuge tube, containing 5.0–25.0 μg of dimethyl-μ-truxinate internal standard, and evaporated to dryness. To the residue were added 250 μl of chloroform and the tube heated at 75°C for 3 min with occasional vortex mixing. The residue in the tube was then subjected to $LiAlH_4$ reduction followed by HFBA derivatization and cGC–ECD analysis as described in ref. 18. All quantitative calculations for the isomeric truxillines used the dimethyl-μ-truxinate internal standard as reference compound. After using a conversion factor, all results were ultimately reported as % (w/w) truxillines dry relative to the cocaine content of the leaf [25].

Hygrine. For the determination of hygrine, recently developed methodology was used [45]. To a 5.0–10.0-ml aliquot from solution A was added an accurate quantity (approximating suspected levels of hygrine in sample) of ethylhygrine internal standard and the solution extracted with 10–20 ml of a pH 4.0 acid phthalate buffer, discarding the chloroform phase. The buffer phase was made basic by the addition of sodium hydrogencarbonate and then extracted with several small aliquots of chloroform, filtering each extract through anhydrous sodium sulfate. To the combined chloroform extracts was added a minimum amount of HCl and the chloroform evaporated to dryness. The residue was treated with a minimum volume of chloroform followed by reduction with 1 *M* $LiAlH_4$ in diethyl ether and derivatization with HFBA in the presence of DMAP. Quantitative analysis was accomplished by cGC–ECD using a 15-m DB-5 capillary

column under conditions described above. Quantitative data were obtained using a standard mixture of known amounts of hygrine and ethylhygrine internal standard that were subjected to $LiAlH_4$ reduction and HFBA/DMAP derivatization.

Isolation of trace unknown alkaloids from coca leaves

For the mass spectral analyses of trace levels [$< 1\%$ (w/w) relative to cocaine] of suspected alkaloids in the coca leaf matrix, 150–200 g of Peruvian/Bolivian powdered coca leaf was used. Extraction and column chromatographic isolation of the alkaloids were accomplished as described previously, using toluene as extractant and a dilute sulfuric acid–Celite chromatographic column, except material masses and volumes were scaled up to accommodate the increased sample mass. The final Celite column chloroform–alkaloid eluate was dried over sodium sulfate and then reduced in volume under vacuum (50°C) to a syrupy residue.

The residue was reconstituted in 50–100 ml of chloroform and extracted with twice its volume of pH 4.0 acid phthalate buffer. The buffer was back-extracted with two aliquots of chloroform, which were combined with the original chloroform extract and set aside as fraction A. The buffer was made basic with sodium hydrogencarbonate and extracted with several small aliquots of chloroform. The combined chloroform extracts were passed through a glass column (600 mm × 40 mm) packed with a mixture of 25 ml of pH 4.0 acid phthalate buffer and 50 g Celite 545. The eluate was dried over sodium sulfate and then reduced under vacuum (at *ca.* 50°C) to a small volume, identified as fraction B.

The pH 4.0 buffer–Celite column above was eluted with sufficient diethylamine in water-saturated chloroform to liberate any retained alkaloids. The eluate was dried over sodium sulfate and then reduced under vacuum to a small volume, identified as fraction C.

Fraction A from above was passed through a glass column (600 mm × 40 mm) packed with a mixture of 50–75 ml of 1 *M* HCl–1 *M* NaCl and 100–150 g of Celite 545. The eluate was monitored in 10-ml fractions until 100 ml had been collected, which were subsequently identified as fractions D_{1-10}.

The 1 *M* HCl–1 *M* NaCl–Celite column from above was eluted with sufficient diethylamine in water-saturated chloroform to liberate any retained alkaloids. The eluate was dried over sodium sulfate and then reduced under vacuum (40–50°C) to a small volume, identified as fraction E.

Aliquots from each of fractions A–E were evaporated to dryness and the residues treated with 500 μl of chloroform–MSTFA (1:1) at 75°C for 30 min. The derivatized samples were subjected to cGC–MS analyses under conditions already described.

RESULTS AND DISCUSSION

Before a discussion of results, it is prudent to recognize that only four South American coca leaf samples, three greenhouse specimens and two non-South American tropical-cultivated leaf samples were subjected to quantitative analyses in this study. Since it is believed that the alkaloid content of the coca leaf may vary upon a number of factors including the age of the plant/leaf, soil composition, altitude of cultivation, soil composition, longitudinal location, environmental factors and the time lapse between leaf harvesting and analysis, the quantitative results reported herein should be viewed from that perspective. With the analysis of many more samples, the aforementioned factors will play a less significant role in the evaluations of results.

Method accuracy and reproducibility

The quantitative results for the ENVN-GH coca leaf obtained by the method described herein were compared with data obtained using a modification of a direct extraction/dilution procedure. The modification of this latter method [41] involved the quantitative extraction of the alkaloids from 1.500 g of ENVN-GH coca leaf with warm methanol and dilution to volume with chloroform that contained cocaethylene internal standard and diethylamine. The comparative quantitative data for these two methods are given in Table I. Fig. 1 illustrates the alkaloid chromatography for the ENVN-GH leaf using

TABLE I

COMPARATIVE DETERMINATION OF ALKALOIDS IN *E. NOVOGRANTENSE* VAR. *NOVOGRANATENSE* USING TOLUENE *VERSUS* METHANOL EXTRACTION

All quantitative data are reported as the average of duplicate analyses; all chromatographic determinations were the average of duplicate injections. Cocaine quantitative results are reported as % (w/w) relative to air-dried leaf; all other alkaloids are reported as % (w/w) relative to cocaine content. The toluene extraction method is as described in this paper in the Experimental section. The methanol extraction method was a modification of a procedure reported by Solon and Sperling [41].

Alkaloid	Methodology	
	Toluene extraction	Methanol extraction
Cocaine	0.38	0.36
Ecgonine methyl ester	63	?[a]
Cuscohygrine	11	?[b]
Tropacocaine	4.6	?[a]
cis-Cinnamoylcocaine	50	51
trans-Cinnamoylcocaine	170	165

[a] Unable to quantify because of peak interference by compound from coca leaf extract.

[b] Unable to quantify because of absence of cuscohygrine peak, perhaps caused by degradation during extraction or co-adsorption with coca leaf extract in cGC system.

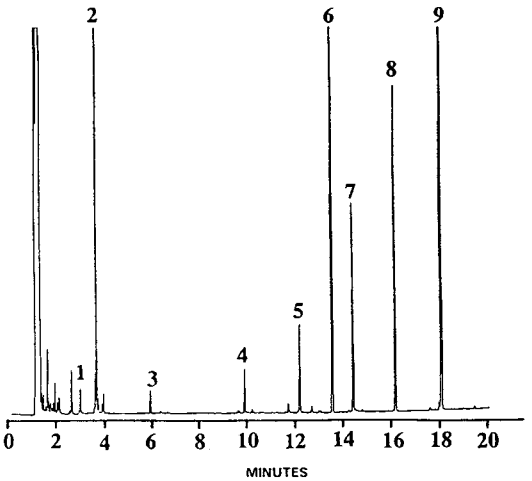

Fig. 1. The cGC–FID chromatogram of major coca alkaloids isolated and determined in greenhouse-cultivated *E. novograntense* var. *novograntense*. Peaks: 1 = ecgonidine methyl ester (2.9 min); 2 = ecgonine methyl ester (3.6 min); 3 = cuscohygrine (5.8 min); 4 = tropacocaine (9.8 min); 5 = unidentified coca alkaloid (12.1 min); 6 = cocaine (13.5 min); 7 = cocaethylene internal standard (14.3 min); 8 = *cis*-cinnamoylcocaine (16.1 min); 9 = *trans*- cinnamoylcocaine (18.0 min).

the method described herein. As seen in Table I, good agreement was found between the two methods for cocaine and *cis*- and *trans*-cinnamoylcocaine content. However, peaks 3 (cuscohygrine) and 5 (unknown hydroxy-substituted alkaloid), seen in Fig. 1, were not present in the chromatogram of the direct dilution [41] method, due probably to some suppression phenomenon. One possibility is irreversible adsorption of these two polar compounds, along with plant components, in the GC–FID injection port. Furthermore, peaks 2 (ecgonine methyl ester) and 4 (tropacocaine) in Fig. 1 could not be determined from the chromatogram of the direct dilution method because of coeluting impurities attributed to non-alkaloidal coca leaf compounds.

As seen in Table I, the direct dilution method using methanol was less than satisfactory for the in-depth analysis of alkaloids in coca leaf. This is evidenced by the non-detection of alkaloids represented by peaks 3 and 5 in Fig. 1. Furthermore, the direct injection of coca leaf extracts into the GC system resulted in interfering peaks due to plant components. Finally, there was evidence that suggested repeated injections of plant extracts into the GC system caused a degradation in column performance.

The efficacy of the truxillines determination referenced herein has been previously determined [18,25]. The accuracy of that methodology was notably enhanced by using the structurally related dimethyl-μ-truxinate as internal standard. Similarly, the hygrine determination employed a structurally related internal standard, namely, ethylhygrine, to improve accuracy. However, as will be discussed subsequently, there was some question as to whether the reported presence of hygrine was due, in part or wholly, to the degradation of cuscohygrine.

The ENVN-GH leaf sample (see Fig. 1) was also subjected to a quantitative reproducibility study for selected alkaloids. A total of seven

sample analyses was accomplished over the period of one week. A sample mass of 1.5 g of coca leaf powder was used for each determination, with a final dilution of 50 ml. The reproducibility results, reported in Table II, were determined to be acceptable for all target alkaloids. As seen, the most reproducible results were for cocaine and *cis*- and *trans*-cinnamoylcocaine. This was not surprising, given their higher levels in coca leaf and the fact that a structurally related internal standard, cocaethylene, was used in their analyses. The data for cuscohygrine may be a reflection of its instability, non-homogeneity in leaf tissue and/or its higher vapor pressure, which may result in losses during the basification and mixing of the coca leaf powder. The results in Table II, as well as in Table I, indicated that when using a sample mass of 1.5 g and a final dilution of 50 ml, the minimum % (w/w) (relative to cocaine) for acceptable reproducibility/accuracy for cuscohygrine and tropacocaine was about 5–10% and 2–4%, respectively. Concentrations below these required a concentration step and/or a greater sample mass.

Alkaloid content of greenhouse- and tropical-cultivated coca leaf

The quantitative results for ECVC-GH, ENVT-GH, ENVN-GH, ENVN-TR and ECVC-TR are found in Table III. In Fig. 1 is the chromatogram used for the determination of alkaloids in the ENVN-GH coca leaf sample. In all cases, a sample mass of 1.000 g and a dilution of 50.0 ml were used. For some samples the inclusion of a concentration step was necessary to enhance chromatographic response and achieve good accuracy for cuscohygrine and tropacocaine. Cocaethylene was used as internal standard for all samples and in the standard mixture.

All compounds listed in Table III, excepting cuscohygrine, are tropane alkaloids. Cuscohygrine, an N-methylpyrrolidine alkaloid, was at significantly higher levels in the two ECVC samples than in either ENVN or ENVT varieties. Conversely, the tropacocaine and *cis*- and *trans*-cinnamoylcocaine content in the ECVC samples was markedly below that of the other varieties. As will be seen, these findings also pertained to South American samples.

Ecgonine methyl ester, when present in illicit refined cocaine samples, may be the result of cocaine hydrolysis during clandestine cocaine manufacture. However, the methodology herein did not produce significant levels of this compound and, therefore, was considered a *bona fide* coca leaf alkaloid. Peak 1 in Fig. 1 was identified as ecgonidine methyl ester, believed to be formed as a result of the thermal degradation of the isomeric truxillines in the GC injection port [18]. The presence of this artifact was more pronounced in samples with higher truxillines content, especially ENVN and ENVT. Because

TABLE II

REPRODUCIBILITY OF QUANTITATIVE RESULTS FOR ALKALOIDS IN GREENHOUSE-CULTIVATED *E. NOVOGRANATENSE* VAR. *NOVOGRANTENSE*

A coca powder sample mass of 1.500 g was used for each analysis, with a final dilution volume of 50 ml. Quantitative result for cocaine was the average of 7 analyses and reported as % (w/w), relative to air-dried coca leaf. Quantitative results for alkaloids other than cocaine were the average of 7 analyses and reported as % (w/w), relative to the cocaine content. All ± results are standard deviations; $n = 7$.

Cocaine	Ecgonine methyl ester	Cuscohygrine	Tropacocaine	Cinnamoylcocaine	
				cis	*trans*
0.371 ± 0.004	62.8 ± 3.4	10.8 ± 1.1	4.60 ± 0.26	50.1 ± 0.8	170.5 ± 1.6

TABLE III

QUANTITATIVE RESULTS FOR COCAINE AND OTHER COCA ALKALOIDS IN GREENHOUSE- AND TROPICAL-CULTIVATED COCA LEAVES

All cocaine results are % (w/w) and are calculated relative to dry leaf mass. Results for all alkaloids, excepting cocaine, are % (w/w) and are calculated relative to cocaine content.

Alkaloid	ECVC-GH[a]	ENVT-GH[b]	ENVN-GH[c]	ENVN-TR[d]	ECVC-TR[e]
Cocaine	0.54	0.60	0.37	0.43	0.67
Ecgonine methyl ester	57	38	63	29	47
Cuscohygrine	57	3.8	11	5.8	61
Tropacocaine	0.3[f]	1.4	4.6	3.8	0.16
cis-Cinnamoylcocaine	7.2	25	50	53	18
trans-Cinnamoylcocaine	18	46	98	170	22

[a] Greenhouse-cultivated *E. coca* var. *coca*.
[b] Greenhouse-cultivated *E. novogranatense* var. *truxillense*.
[c] Greenhouse-cultivated *E. novogranatense* var. *novogranatense*.
[d] Tropical-cultivated *E. novogranatense* var. *novogranatense*.
[e] Tropical-cultivated *E. coca* var. *coca*.
[f] Sample also contained benzoyltropeine, an epimer of tropacocaine, at a level of 1.1% (relative to cocaine content).

of its artifactual presence, quantitative levels of ecgonidine methyl ester were not determined. Perhaps the most unexpected result in Table III was the presence of benzoyltropeine at a level 3 × greater than that for its epimer, tropacocaine (benzoyl-ψ-tropeine). This is believed to be the first report of such a level of benzoyltropeine in coca leaf.

Another compound seen in Fig. 1, but not given in Table III, was peak 5. This peak has yet to be characterized, but preliminary mass spectral analysis suggested it to be a hydroxy-substituted tropane alkaloid, having an apparent molecular mass of 261. Its presence was, by far, the greatest in ENVN-GH. It was also detected at lower levels in ENVN-TR and ENVT-GH, but not in ECVC-GH or ECVC-TR. This compound is believed to be a major new alkaloid.

The truxillines and hygrine were not determined in the greenhouse samples. Their determination in greenhouse coca leaf will be the subject of a future report.

Alkaloid content of South American coca leaf

In-depth alkaloid determinations were also provided for field samples cultivated and harvested in the countries of Peru, Bolivia, Colombia and Ecuador. In Table IV are given the results for cocaine, the cinnamoylcocaines, tropacocaine and cuscohygrine. As seen, the most disparate data belonged to the Colombian leaf, believed to be ENVN. The higher results for the cinnamoylcocaines and tropacocaine, compared to the ECVC cultivars of Peru and Bolivia, were consistent with the data in Table III for greenhouse- and tropical-cultivated coca. Of particular interest in Table IV was the ratio of the cinnamoylcocaine *trans*-to-*cis* isomers. The *trans*/*cis* ratios of the four South American field samples were markedly below that for the greenhouse cultivars in Table III. A smaller ratio was also realized for the tropical-cultivated ECVC in Table III. These results are consistent with previous postulations that the *trans* isomer of cinnamoylcocaine is the first-formed alkaloid and is partially converted to the *cis* isomer via photoisomerization [46]. Presumably, the greenhouse cultivars would not be subjected to the full array of ultraviolet radiation from sunlight as is field-cultivated coca. A higher *trans*/*cis* ratio has also been reported for growth chamber-grown ECVC [44]. An exception to the foregoing was the high *trans*/*cis* ratio for the ENVN-TR coca leaf sample.

The truxilline quantitative data for the South American coca are presented in Table V. Fig. 2

TABLE IV

QUANTITATIVE RESULTS FOR COCAINE AND OTHER COCA ALKALOIDS IN SOUTH AMERICAN-CULTIVATED COCA LEAVES

All cocaine results are % (w/w) and are calculated relative to dry leaf mass. Results for all alkaloids, excepting cocaine, are % (w/w) and are calculated relative to cocaine content.

Country	Cocaine	Cinnamoylcocaine		Tropacocaine	Cuscohygrine
		cis	*trans*		
Bolivia	0.70	8.6	6.0	0.34	78
Peru	0.72	5.8	2.9	0.25	51
Ecuador	0.36	6.6	7.4	1.6	11
Colombia	0.44	28	33	4.9	33

illustrates the chromatography of the truxilline alkaloids present in the Peruvian coca leaf. As seen in Table V the lowest truxilline values were associated with the coca leaf from Peru and Bolivia. These results were consistent with truxilline levels found in illicit refined cocaine hydrochloride seized in those countries [47]. Relative to cocaine, the total truxilline content for the Ecuadoran leaf was 4–5 × higher than that from Peru/Bolivia. The Colombian sample had the highest truxilline levels, the total being more than 60% of its cocaine content. A review of the individual truxilline ratios for the four samples revealed no remarkable differences in their intra-sample truxilline ratios. Such data would only be meaningful, however, if derived from a much larger data base.

In Table VI are the quantitative results for hygrine in South American coca. Fig. 3 illustrates the chromatography of hygrine and ethylhygrine internal standard in the Colombian coca leaf. Both hygrine (peaks 1 and 2) and ethylhygrine (peaks 3 and 4) internal standard are each represented by two peaks. These are the di-HFB derivatives of diastereomeric pairs. These diastereomers are created upon $LiAlH_4$ reduction of hygrine and ethylhygrine to yield hygrinol and ethylhygrinol, respectively [45].

TABLE V

ISOMERIC TRUXILLINE CONTENT OF SOUTH AMERICAN-CULTIVATED COCA LEAVES

All isomeric truxilline results calculated using the μ-isomer as reference standard. All data presented as % (w/w) relative to cocaine.

Truxilline	Bolivia	Peru	Ecuador	Colombia
α-	0.74	0.87	3.51	20.4
β-	0.62	0.74	3.22	14.5
δ-	0.46	0.50	1.82	9.2
ϵ-	0.30	0.35	1.36	6.2
ω-	0.11	0.15	0.84	2.8
γ-	0.11	0.15	0.64	2.5
neo-	0.09	0.11	0.61	2.4
peri-	0.05	0.05	0.33	1.4
ζ-	0.03	0.05	0.50	1.2
epi-	0.02	0.02	0.21	0.64
Total	2.53	2.99	13.04	61.2

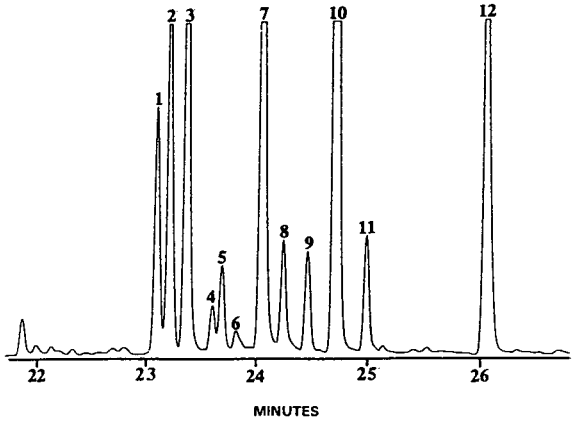

Fig. 2. The cGC–ECD chromatogram of the isomeric truxillines determined in Peruvian coca leaves. Pertinent chromatographic peaks are the result of $LiAlH_4$ reduction of the truxilline followed by derivatization with heptafluorobutyric anhydride to yield a di-O-HFB derivative. Peaks (truxilline isomers): 1 = ϵ- (23.00 min); 2 = δ- (23.21 min); 3 = β- (23.37 min); 4 = *peri-* (23.60 min); 5 = *neo-* (23.69); 6 = *epi-* (23.82 min); 7 = α- (24.06 min); 8 = ω- (24.24 min); 9 = γ- (24.46 min); 10 = μ- internal standard (24.72 min); 11 = ζ- (24.94 min); 12 = heneicosanol internal standard (26.06 min).

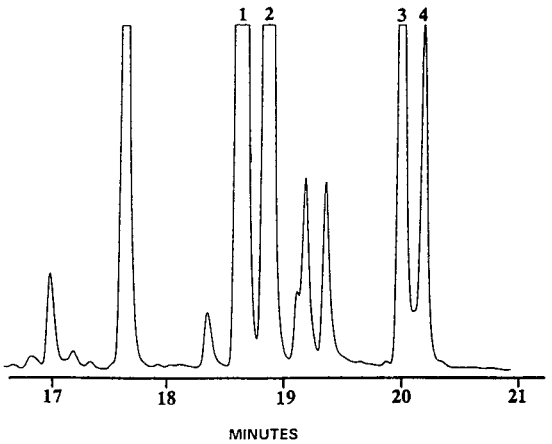

Fig. 3. The cGC–ECD chromatogram of hygrine determined in Colombian coca leaves. Peaks: 1, 2 (18.6 min, 18.8 min) = di-HFB derivatives of hygrinol diastereomers (obtained via $LiAlH_4$ reduction and HFBA derivatization of hygrine); 3, 4 (20.0 min and 20.2 min) = di-HFB derivatives of ethylhygrinol (obtained via $LiAlH_4$ reduction and HFBA derivatization of ethylhygrine internal standard).

These two alcohols each have two asymmetric carbon atoms, accounting for two diastereomeric pairs. The peak areas for each pair were summed for quantitative calculations. Though not seen in Fig. 3, later eluting peaks (28–32 min) in the chromatogram were believed due to the isomeric truxillines.

As seen in Table VI, coca leaf from Peru and Bolivia had the lowest levels of hygrine. In fact, at these low levels the question is raised as to whether these values reflect the true leaf content for hygrine or whether this alkaloid is produced wholly, or in part, from the degradation of cuscohygrine. We have previously observed that, when stored at room temperature for prolonged periods, some powdered coca samples experienced diminution in cuscohygrine content with concomitant increases in the levels of hygrine [47]. In contrast, and unexpectedly, the hygrine content of the Colombian leaf was nearly 25% of the cocaine content. Although it was not believed that this result was an anomaly, the analysis of additional samples will be required for confirmation of this finding.

TABLE VI

HYGRINE CONTENT OF SOUTH AMERICAN-CULTIVATED COCA LEAVES

Results reported as % (w/w) relative to cocaine content of air-dried leaf.

Hygrine (%)			
Bolivia	Peru	Ecuador	Colombia
2.3	1.4	4.2	24

Uncharacterized trace level coca alkaloids

For the detection and characterization of trace-level coca alkaloids, a greater quantity (150–200 g) of basified South American coca leaf powder was subjected to toluene extraction as described under Experimental. Subsequent column chromatographic and buffer extraction work-up yielded fractions A–E (see Experimental). Each fraction was subjected to trimethylsilylation with chloroform–MSTFA and then subjected to cGC–electron impact MS analyses.

In fraction A were cocaine and the bulk of the major coca alkaloids in chloroform. Fraction A

was extracted with a pH 4.0 acid phthalate buffer, which removed cuscohygrine, hygrine and numerous trace-level hydroxy-containing alkaloids. After extraction of the pH 4.0 buffer with several aliquots of chloroform (which were added to fraction A), it was basified and extracted with several more aliquots of chloroform. These extracts were subsequently passed through a pH 4.0 buffer–Celite column and the eluate concentrated to a small volume and identified as fraction B.

Fraction B contained, by far, the bulk of the unknown trace-level alkaloids amenable to cGC analysis. Over 60 trace-level compounds were detected as seen in the reconstructed total-ion chromatogram illustrated in Fig. 4. Of these compounds, about 45 yielded significant fragment ions at m/z 82 and 182, which suggested the presence of a carbomethoxy-substituted tropane moiety, as found in the major coca alkaloids. More than 50 suspected alkaloids contained a trimethylsilyl (TMS) moiety, as evidenced by a significant m/z 73 ion. It was believed that TMS attachment occurred primarily on –OH functions. These findings were are significant, because it suggested these alkaloids would also be amenable to heptafluorobutyrylation and more sensitive detection using cGC–ECD [1].

Alkaloids retained on the pH 4.0 buffer column from above were liberated using chloroform–diethylamine and the eluate reduced to a small volume which was identified as fraction C. Two major alkaloids found in this fraction were ecgonine methyl ester and cuscohygrine. Also present were 15–20 suspected alkaloids, the majority of which yielded a base-peak fragment ion at m/z 84, suggesting the presence of an N-methylpyrrolidine moiety, as in cuscohygrine. Also present in this fraction were compounds that gave ions at m/z 82, 84 and 182, indicating the presence of both N-methylpyrrolidine and carbomethoxy-substituted tropane moieties. Finally, suspected alkaloids were present that yielded a base-peak fragment ion at m/z 82 but did not give the usual accompanying m/z 182 ion. As was seen for fraction B, the majority of the alkaloids in fraction C incorporated at least one TMS group upon derivatization with chloroform–MSTFA.

Fraction A from above was subjected to ion-pairing column chromatography using 1 *M* HCl–1 *M* NaCl–Celite 545 and chloroform as eluent. A collection and examination of the ten 10-ml fractions, identified as fractions D_{1-10}, revealed that most of the trace-level alkaloids were present in the first two fractions. These early-eluting fractions contained more than 25 suspected trace-level alkaloids. More than half of these compounds yielded mass spectral fragment ions at m/z 82 and 182, and only about one-third contained a TMS group. Some of the TMS-substituted alkaloids gave mass spectral ions as high as 495 u. It was not known whether these high-mass ions were molecule or fragment ions.

The compounds that did not ion-pair, and were thus retained on the column from above, were liberated with chloroform–diethylamine and the eluate concentrated to a small volume, identified as fraction E. After MSTFA derivatization, this fraction was subjected to cGC–MS analysis. As expected, the reconstructed total-ion chromatogram was dominated by the presence of cocaine and the isomeric cinnamoylcocaines. Less than five suspected trace-level alkaloids were seen.

Of the more than 100 uncharacterized, trace-level alkaloids and other compounds detected in the above fractions, the possibility that some were artifactual was considered. Since many tropane alkaloids in coca leaf are diesters, their potential for hydrolysis during routine manipulations should be recognized. Furthermore, since a relatively strong organic base (diethylamine) was used in the work-up of alkaloids, the possibility of epimerization could not be discounted. Finally, the action of certain solvents upon some coca alkaloids may result in their N-demethylation. For example, the presence of trace levels of peroxides or other oxidants in some solvents can cause low-yield N-demethylation of cocaine to yield N-norcocaine [47]. After review of the mass spectra for the compounds isolated in fractions A–E from above, it was concluded that the majority of them were *bona fide* alkaloids and not artifactual. Work is ongoing in an attempt to structurally characterize and determine the levels of these 100 or so trace-level coca alkaloids.

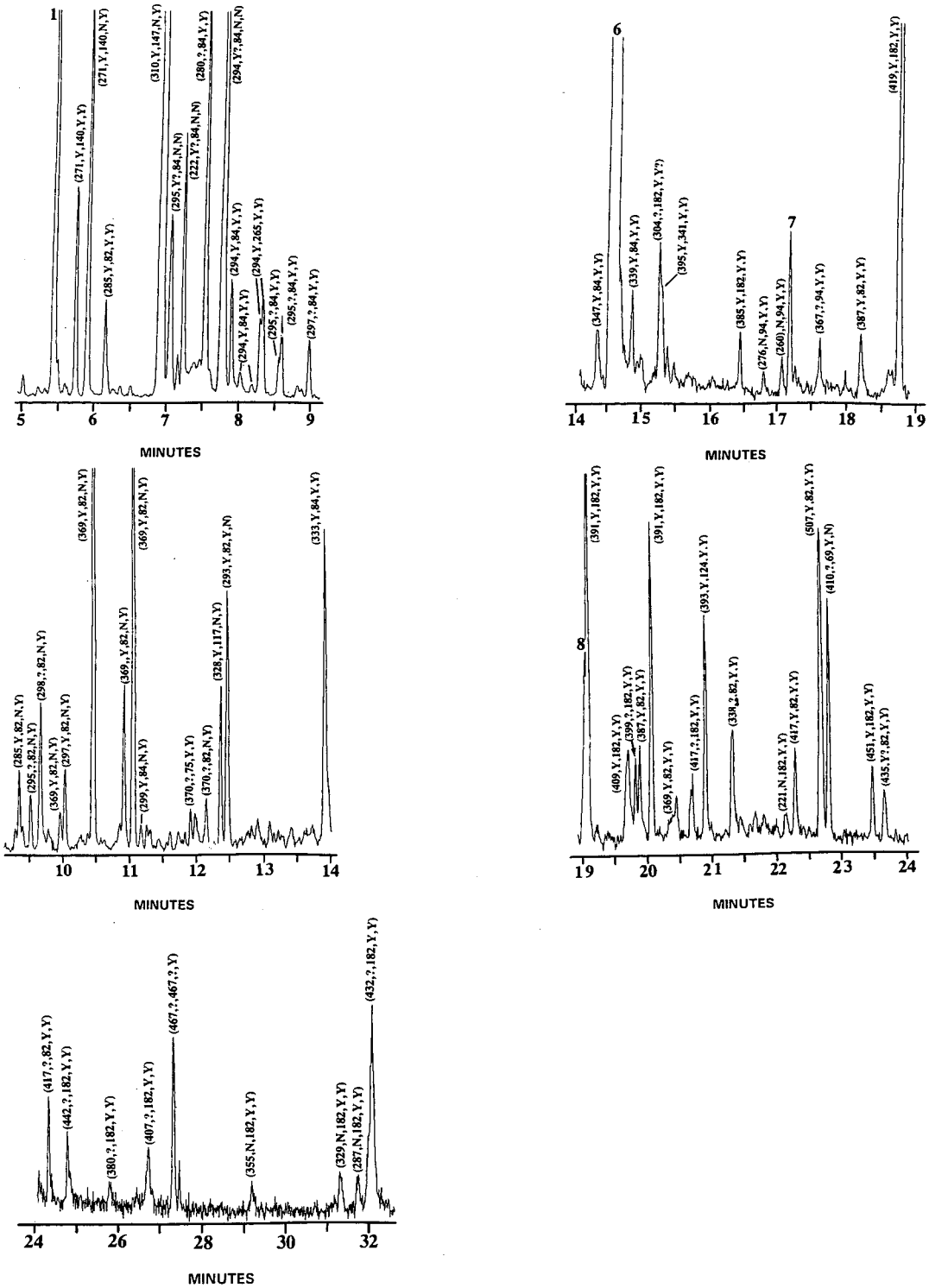

Fig. 4. The reconstructed total-ion chromatogram of suspected trace-level coca alkaloids in Peruvian/Bolivian coca leaves. Key to peak captions: (A, B, C, D, E): A = mass spectral ion of highest mass detected for peak; B = probability of high mass ion being the molecule ion, Y (yes), N (no), ? (unknown); C = mass spectral base peak; D = presence of mass spectral fragment ions m/z 82 and 182 (Y, N, ?); E = alkaloid amenable to trimethylsilalation (Y, N, ?).

CONCLUSIONS

Methodology has been presented that is suitable for the determination of cocaine, *cis*- and *trans*-cinnamoylcocaine, tropacocaine, the isomeric truxillines, ecgonine methyl ester, cuscohygrine and hygrine in South American and greenhouse-cultivated coca leaf. This included the analysis of field samples from Bolivia, Peru, Ecuador and Colombia as well as greenhouse- and tropical-cultivated coca of known taxonomy, including *E. coca* var. *coca*, *E. novogranatense* var. *novogranatense* and *E. novogranatense* var. *truxillense*. Quantitation was accomplished using cGC–FID and–ECD. Methodology was also described for the isolation and mass spectral analysis of about 100 suspected trace level alkaloids of unknown composition from Peru/Bolivian coca leaf.

REFERENCES

1 J.M. Moore, *Forensic Sci. Rev.*, 2 (1990) 79–124.
2 A.M.A. Verweij, *Forensic Sci. Rev.*, 1 (1989) 1–11.
3 A. Sinnema and A.M.A. Verweij, *Bull. Narcotics*, 33 (1981) 37–54.
4 T.S. Cantrell, B. John, L. Johnson and A.C. Allen, *Forensic Sci. Inter.*, 39 (1988) 39–53.
5 I.S. Lurie and S.M. Carr, *J. Liq. Chromatogr.*, 9 (1986) 2485–2509.
6 J.M. Moore, A.C. Allen and D.A. Cooper, *Anal. Chem.*, 58 (1986) 1003–1006.
7 P.J. O'Neil and T.A. Gough, *J. Forensic Sci.*, 30 (1985) 681–691.
8 J.M. Moore, A.C. Allen and D.A. Cooper, *Anal. Chem.*, 56 (1984) 642–646.
9 A.C. Allen, D.A. Cooper, J.M. Moore, M. Gloger and H. Neumann, *Anal. Chem.*, 56 (1984) 2940–2947.
10 I.S. Lurie and A.C. Allen, *J. Chromatogr.*, 317 (1984) 427–442.
11 H. Neumann and M. Gloger, *Chromatographia*, 16 (1982) 261–264.
12 J.G. Ensing and J.C. Hummelen, *J. Forensic Sci.*, 36 (1991) 1666–1687.
13 K.E. Janzen, L. Walter and A.R. Fernando, *J. Forensic Sci.*, 37 (1992) 436–445.
14 J.G. Ensing, C. Racamy and R.A. de Zeeuw, *J. Forensic Sci.*, 37 (1992) 446–459.
15 M. LeBelle, S. Callahan, D. Latham, B.A. Lauriault and C. Savard, *J. Forensic Sci.*, 36 (1991) 1102–1120.
16 J.F. Casale and R.W. Waggoner, *J. Forensic Sci.*, 36 (1991) 1312–1330.
17 I.S. Lurie, J.M. Moore, D.A. Cooper and T.C. Kram, *J. Chromatogr.*, 405 (1987) 273–281.
18 J.M. Moore, D.A. Cooper, I.S. Lurie, T.C. Kram, S. Carr, C. Harper and J. Yeh, *J. Chromatogr.*, 410 (1987) 273–281.
19 T. Lukaszewski and W.K. Jeffery, *J. Forensic Sci.*, 25 (1980) 499–507.
20 C.C. Clark, *Microgram*, 11 (1978) 184–187.
21 J.G. Ensing and R.A. de Zeeuw, *J. Forensic Sci.*, 36 (1991) 1299–1311.
22 J.F. Casale, *Forensic Sci. Inter.*, 47 (1990) 277–287.
23 I.S. Lurie, J.M. Moore, T.C. Kram and D.A. Cooper, *J. Chromatogr.*, 504 (1990) 391–401.
24 M. LeBelle, G. Lauriault, S. Callahan, D. Latham, C. Chiarelli and H. Beckstead, *J. Forensic Sci.*, 33 (1988) 662–675.
25 J.M. Moore, in R.T. Castanguay (Editor), *Proceedings of the International Symposium on the Forensic Aspects of Controlled Substances, March 28–April 1, 1988, Quantico, VA*, Federal Bureau of Investigation, Washington, DC, 1988, pp. 191–192.
26 M.J. LeBelle, S.A. Callahan, D.J. Latham and G. Lauriault, *Analyst*, 113 (1988) 1213–1215.
27 F. Medina, *Microgram*, 12 (1979) 139–144.
28 F.T. Noggle and C.R. Clark, *J. Assoc. Off. Anal. Chem.*, 65 (1982) 756–761.
29 J.M. Moore, in M. Klein, A.V. Kruegel and S.P. Sobol (Editors), *Instrumental Application of Forensic Drug Chemistry*, US Department of Justice, Drug Enforcement Administration, Washington, DC, 1978, pp. 180–201.
30 J.M. Moore, *J. Chromatogr.*, 101 (1974) 215–218.
31 J.M. Moore, *J. Assoc. Off. Anal. Chem.*, 56 (1973) 1199–1205.
32 J.M. Moore and D.A. Cooper, *J. Forensic Sci.*, 38 (1993) 1286–1303.
33 L.M. Brewer and A.C. Allen, *J. Forensic Sci.*, 36 (1991) 697–707.
34 L.D. Baugh and R.H. Liu, *Forensic Sci. Rev.*, 3 (1991) 102–115.
35 C.E. Turner, C.Y. Ma and M.A. Elsohly, *Bull. Narcotics*, 31 (1979) 71–76.
36 C.E. Turner, C.Y. Ma and M.A. Elsohly, *J. Ethnopharmacol.*, 3 (1981) 293–298.
37 B. Holmstedt, E. Jaatmaa, K. Leander and T. Plowman, *Phytochemistry*, 16 (1977) 1753–1755.
38 M. Youssefi, R.G. Cooks and J.L. McLauglin, *J. Am. Chem. Soc.*, 101 (1979) 3400–3402.
39 R.G. Cooks, R.W. Kondrat, M. Youssefi and J.L. McLaughlin, *J. Ethnopharmacol.*, 3 (1981) 299–312.
40 L. Rivier, *J. Ethnopharmacol.*, 3 (1981) 313–335.
41 E. Solon and A.R. Sperling, *Microgram*, 17 (1984) 62.
42 T. Plowman and L. Rivier, *Ann. Bot.*, 51 (1983) 641–659.
43 C.E. Turner, B.S. Urbanek, G.M. Wall and C.W. Waller, in *Cocaine —An Annotated Bibliography*, Vols. I and II, Research Institute of Pharmaceutical Sciences, University of Mississippi, Oxford, MS, 1988.
44 J. Lydon, R.H. Zimmerman and I.M. Fordham, J. Herbs, *Spices Med. Plants*, (1993) in press.
45 J.M. Moore, D.A. Cooper and R.F.X. Klein, unpublished results.
46 E. Leete, *Planta Med.*, 56 (1990) 339–351.
47 J.M. Moore, unpublished results.
48 *United States Pharmacopeia*, XIX, United States Pharmacopeial Convention, Rockville, MD, 1975, p. 654.

Journal of Chromatography A, 659 (1994) 177–183
Elsevier Science B.V., Amsterdam

CHROM. 25 489

High-performance thin-layer chromatographic determination of digoxin and related compounds, digoxigenin bisdigitoxoside and gitoxin, in digoxin drug substance and tablets

Garratt W. Ponder and James T. Stewart*

Department of Medicinal Chemistry, College of Pharmacy, University of Georgia, Athens, GA 30602-2352 (USA)

(First received April 21st, 1993; revised manuscript received August 6th, 1993)

ABSTRACT

A high-performance thin-layer chromatographic (HPTLC) method for the determination of digoxin and its related compounds digoxigenin bisdigitoxoside (DBD) and gitoxin in digoxin drug substance and tablets was developed. Separation of the three compounds was accomplished on a C_{18} wettable reversed-phase plate using water–methanol–ethyl acetate (50:48:2, v/v/v) as the mobile phase. The analytes were determined by densitometry using absorbance for digoxin and fluorescence for the two related compounds. All peaks were quantified by peak-height analysis. Linear regression analysis of the data was performed for all three compounds. The calibration range for digoxin was set at 320–480 ng per 5-mm band, equivalent to 80–120% (w/w) of a 400-ng band load, that for DBD was set at 4–12 ng per 5-mm band, equivalent to 1–3% (w/w) of the digoxin load, and that for gitoxin was set at 0.4–1.6 ng per 5-mm band, equivalent to 0.1–0.4% (w/w) of the digoxin load. The limit of quantification (LOQ) for digoxin was 64 ng per 5-mm band with a limit of detection (LOD) of 8 ng per 5-mm band. The LOQs for both DBD and gitoxin were 0.12 ng per 5-mm band with LODs of 0.4 ng per 5-mm band. The linearity range for the digoxin peak height in the absorbance mode was 0–5000 ng per 5-mm band. The linearity range for DBD and gitoxin peak heights in the fluorescence mode was 0–2000 ng per 5-mm band.

INTRODUCTION

Digoxin is an extremely potent cardiotonic glycoside of the digitalis family that is widely used in modern medicine for its effect on the heart's force and speed of contraction [1]. Gitoxin and digoxigenin bisdigitoxoside (DBD) may be present in Burroughs-Wellcome digoxin. Material made by other processes may have different impurity profiles [2]. Suitable analytical techniques are necessary to detect and determine these compounds in both digoxin drug substance and tablets. Previous methods to assay for these compounds have included GC, HPLC and TLC techniques. The GC methods involve the hydrolysis of the sugar moieties to form the digoxigenin aglycone, which is subsequently trimethylsilylated. However, digoxin, DBD, digoxigenin monodigitoxoside and digoxigenin present in digoxin drug substance are all converted into the same aglycone as digoxin and will artificially inflate the digoxin response due to the formation of identical trimethylsilyl derivatives [3,4]. Methods have been developed using both reversed and normal phases to separate and determine various cardiotonic glycosides from the digitalis family. Analyses to separate drug substances from either metabolites or degradation products have used both isocratic or gradient elution HPLC systems. However, none of these methods can separate and determine the compounds of

* Corresponding author.

0021-9673/94/$07.00
SSDI 0021-9673(93)E0895-2

interest in this paper at the desired levels [5–9]. The TLC procedures vary in their capability to assay these compounds. In general, they do not provide determination at the desired levels and resolution can be a problem. Typically, normal-phase TLC methods give fast development times, but show irreproducible quantification owing to poor resolution. Reversed-phase TLC methods give better resolution of the three compounds, but have long development times and poor precision. Overpressurized reversed-phase TLC methods take only a few minutes, but the technique is not as widely accepted as classical TLC [10]. For none of the TLC methods has the quantitative recovery of these three compounds from commercial digoxin tablets been reported.

A perusal of the current literature indicates that there is no single method for the determination of digoxin and the two related compounds DBD and gitoxin. The USP XXII method uses HPLC to determine digoxin in digoxin tablets and drug substance [11]. The inclusion of DBD in the HPLC assay method for digoxin drug substance and tablets is used as a system suitability test only. A compendial limit test for digoxin drug substance uses a TLC response to gitoxin to provide information about related glycoside levels ($\leq$3%, w/w). Neither of the related compounds is determined at the levels described here. In this paper, a high-performance TLC (HPTLC) method for the determination of the three compounds is reported. The substances are separated on a 100% wettable octadecylsilane HPTLC plate using water–methanol–ethyl acetate (50:48:2, v/v/v) as the mobile phase. The plate is scanned in the absorption mode for digoxin followed by fluorophore development and scanning in the fluorescence mode for DBD and gitoxin.

EXPERIMENTAL

Reagents and chemicals

Digoxin (99% purity) and digoxigenin bisdigitoxoside (92% purity) were supplied by Burroughs-Wellcome (Greenville, NC, USA) and gitoxin (95% purity) by Sigma (St. Louis, MO, USA). Chloroform, absolute methanol and ethyl acetate (J.T. Baker, Phillipsburg, NJ, USA) were of HPLC grade. Ethanol (USP) and concentrated hydrochloric acid (analytical-reagent grade) were obtained from the Central Research Store of the University of Georgia.

Instrumentation

The HPTLC system consisted of a Camag Linomat IV band applicator (Camag Scientific, Wilmington, NC, USA) equipped with a 100-μl syringe and a Camag Densitometric Scanner II operated by a Camag software package (System HPL 2.1 Rev. 7.01) on a Hewlett-Packard Model 9121 microcomputer. The developing chamber and conditioning tray were purchased from Camag. A Model C-31 microbalance (Cahn Instruments, Cerritos, CA, USA) and a Model AE50 balance (Mettler Instruments, Greifensee, Switzerland) were used for weighing.

Preparation of stock solutions

A digoxin stock solution was prepared by weighing 10.0 ± 0.1 mg of the digoxin powder and transferring it into a 50-ml acid-washed light-resistant volumetric flask. Chloroform–methanol (50:50, v/v) was added to volume and mixed by shaking to obtain a 0.2 mg/ml solution of digoxin.

A DBD stock solution was prepared by weighing 1.08 ± 0.05 mg of the powder and placing it in a 100-ml acid-washed light-resistant volumetric flask. Chloroform–methanol (50:50, v/v) was added to volume and mixed by shaking to obtain a 0.1 mg/ml solution of DBD.

A gitoxin stock solution was prepared by weighing 1.05 ± 0.05 mg of the powder and placing it in a 10-ml acid-washed light-resistant volumetric flask. Chloroform–methanol (50:50, v/v) was added to volume and mixed by shaking. A 1-ml volume was pipetted into a 100-ml acid-washed light-resistant volumetric flask. Chloroform–methanol (50:50, v/v) was added to volume to obtain a final concentration of 0.001 mg/ml of gitoxin.

Preparation of calibration solutions

Aliquots of 4.0, 5.0 and 6.0 ml of the digoxin stock solution were accurately pipetted into each of three individual acid-washed 100-ml volumet-

ric flasks, then 1.0, 2.0 and 3.0 ml of the DBD and 1.0, 2.5 and 4.0 ml of the gitoxin stock solutions were added to the flasks, respectively. A 40-ml volume of ethanol–water (50:50, v/v) was added to each flask and the flasks were shaken in a horizontal shaker (Eberbach, Ann Arbor, MI, USA) for 10 min. The flasks were allowed to stand at ambient temperature for an additional 10 min and chloroform–methanol (50:50, v/v) was added to volume.

Preparation of spiked tablet samples

Into each of three 100-ml acid-washed light-resistant volumetric flasks were accurately pipetted 4, 5 and 6 ml of digoxin stock solution, 1, 2 and 3 ml of DBD stock solution and 1, 2.5 and 4 ml of gitoxin stock solution. Each mixture was evaporated to dryness with the aid of a nitrogen flow at ambient temperature. Then, 800 mg placebo 0.125 mg tablet matrix or 500 mg placebo 0.25 mg tablet matrix was accurately weighed and transferred into each flask [12] and 10 ml of chloroform–methanol (50:50, v/v) and 40 ml of ethanol–water (50:50, v/v) were added to each flask. Each flask was shaken in a horizontal mixer for 30 min, then allowed to stand at ambient temperature for a minimum of 10 min. Next, chloroform–methanol (50:50, v/v) was added to volume. Each solution was filtered through a medium-porosity sintered-glass funnel (15 ml) into a clean Büchner flask and 40 μl were spotted on to the HPTLC plate.

Preparation of assay sample from commercial tablets

Either twenty digoxin 0.125-mg tablets or twenty digoxin 0.25-mg tablets were accurately weighed and powdered. An accurately weighed portion of the powder equivalent to 1.0 mg of digoxin was transferred into a 100-ml acid-washed light-resistant volumetric flask and the procedure described above for spiked tablet samples was followed.

Chromatography

A 100% wettable HPTLC plate (10 × 10 cm octadecylsilane) (Merck) was prewashed with absolute methanol and dried with forced air. A 40-μl aliquot of each calibration solution and tablet sample were applied in duplicate as 5-mm bands at the rate of 10 s/μl.

The vertical twin-trough chamber was lined on two sides with saturation pads (Universal Scientific, Atlanta, GA, USA) and equilibrated for no more than 6 min with mobile phase. The plate was developed for 30–35 min, removed and dried with forced heated air for 5–10 min. Each lane was scanned for digoxin peak height using 218 nm in the absorbance mode.

Fluorophore development

After scanning for digoxin, the plate was exposed to HCl vapor for 60 min in a conditioning tray. The plate was then heated in an oven for 30 min at 120°C, allowed to cool for 10 min at ambient temperature and each lane was scanned in the fluorescence mode for DBD and gitoxin peak heights using 365 nm with a K400 cut-off filter.

RESULTS AND DISCUSSION

The structures of the analytes are shown in Fig. 1. Many TLC systems were initially investigated in these studies. Normal-phase HPTLC systems using silica plates and mobile phases containing various proportions of chloroform–methanol, methyl ethyl ketone–toluene, methanol–formamide, cyclohexane–acetone–glacial acetic acid and chloroform–methanol–formamide provided fast development times, but gave inadequate resolution of the three compounds. Reversed-phase HPTLC methods showed more promise, but gave unique problems. Mobile phases consisting of methanol–water and acetonitrile–water were investigated. It was found that methanol–water (70:30, v/v) gave a good resolution of the three compounds, but the development time was 2.5 h with a relative standard deviation (R.S.D.) of peak heights of *ca.* 5–15%.

With the commercial availability of a 100% wettable reversed-phase C_{18} plate, adequate resolution of the three compounds was obtained using a mobile phase of water–methanol–ethyl acetate (50:48:2, v/v/v). The development time

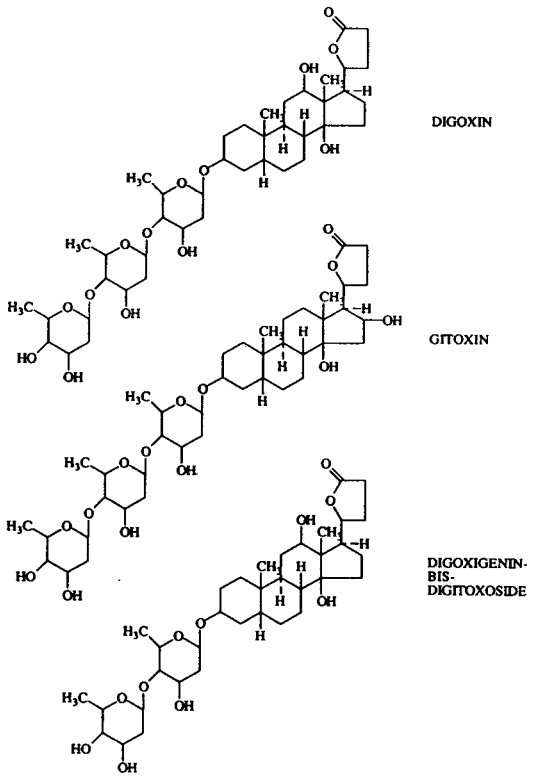

Fig. 1. Structures of analytes.

was improved to 30 min with an R.S.D. of peak heights of ≤5%.

Single-step densitometric scanning and quantification by peak-height analysis of all three analytes on the HPTLC plate was investigated in both the absorbance and fluorescence scanning modes. It soon became apparent that a single-scanning mode was unsuitable for the compounds. There was a linear response for digoxin in the absorbance mode at 218 nm, but DBD and gitoxin were not detectable at the required levels. Therefore, it was decided to investigate fluorescence detection for the three analytes. None of the compounds possessed native fluorescence, so methods to induce fluorescence were examined, including dips such as zirconium tetrachloride, sprays such as chloramine-T–trichloroacetic acid, absolute methanol–sulfuric acid, *p*-toluenesulphonic acid, inorganic acids, hydrogen peroxide, potassium bromide–potassium bromate–hydrochloric acid and vapors such as inorganic acids. Different fluorophores were created which emitted blue to yellow light. The various sprays were not reproducible enough for this study, and the zirconium tetrachloride dip removed the coated phase from the HPTLC plate. The best fluorophore development system that gave repeatable scanning results with sufficient fluorescence to detect the DBD and gitoxin at the required levels was exposure of the developed plate to hydrogen chloride vapor for 60 min followed by heating for 30 min in an oven at 120°C. However, plots of digoxin concentration *versus* fluorescence emission were not linear in its respective calibration range. Therefore, it was necessary to scan digoxin in the absorbance mode (see Fig. 2), develop the fluorophores for DBD and gitoxin and determinate them using the fluorescence mode (see Fig. 3). In this manner, all three compounds were detected and determined at levels within their specified linear ranges.

The coefficient of determination (r^2) in the absorbance mode for digoxin in the range 0–5000 ng per 5-mm band was 0.9912 ($n = 6$), DBD in the fluorescence mode gave $r^2 = 0.9904$ ($n = 7$) in the range 0–2000 ng per 5-mm band and gitoxin in the fluorescence mode gave $r^2 = 0.9986$ ($n = 7$) in the range 0–2000 ng per 5-mm band.

The calibration range for digoxin was set at 320–480 ng per 5-mm band, equivalent to 80–120% (w/w) of a 400-ng band load, that for DBD was set at 4–12 ng per 5-mm band, equivalent to 1–3% (w/w) of the digoxin load, and that for gitoxin was set at 0.4–1.6 ng per 5-mm band, equivalent to 0.1–0.4% (w/w) of the digoxin load. The limit of quantification (LOQ)

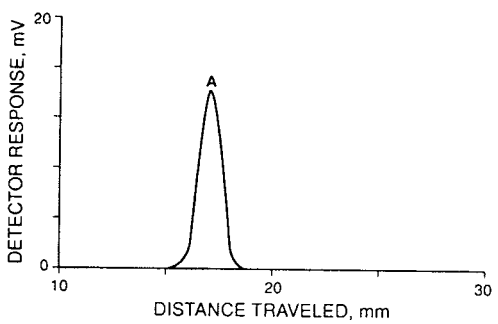

Fig. 2. Typical chromatogram of 400 ng per 5-mm band of digoxin (A) scanned in the absorbance mode at 218 nm.

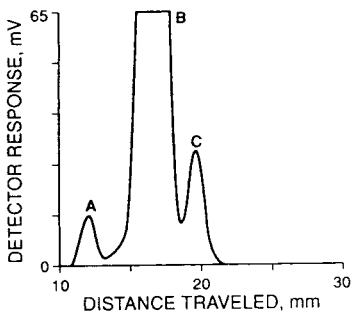

Fig. 3. Typical chromatogram of (A) 1.6 ng per 5-mm band of gitoxin, (B) 400 ng per 5-mm band of digoxin and (C) 12 ng per 5-mm band of DBD, after induced fluorescence and scanned in the fluorescence mode at 365 nm with a K400 filter.

for digoxin was 64 ng per 5-mm band with a limit of detection (LOD) of 8 ng per 5-mm band. The LOQs for both DBD and gitoxin were 0.12 ng per 5-mm band with LODs of 0.04 ng per 5-mm band.

Recovery data for spiked samples of the analytes at the three concentrations of each analyte employed for the calibration graphs are given in Table I for both the 0.125- and 0.25-mg placebo digoxin tablet matrices. Analysis of variance (ANOVA) tests run on the recovery data from spiked and commercial tablet samples showed that there was no significant difference between the data across plate lots and on analysis days at the 95% confidence level.

Actual commercial digoxin tablets were assayed for digoxin, DBD and gitoxin content using the HPTLC method described here. The results are given in Table II. The digoxin levels were within 90–105% (w/w) of the labeled amount established following the USP XXII digoxin monograph [11]. The DBD and gitoxin levels were also within the allowable ranges except for tablets C and D, which were beyond the stated date of expiration and the DBD levels were elevated compared with in-date digoxin tablets (A, B, E and F). However, the DBD levels in the out-of-date tablets are still below the 3.0% (w/w) upper limit specified in the USP XXII monograph.

The assay was unaffected by exposure of the plate to light, longer plate development times and a lined *versus* unlined developing chamber. It is important that the mobile phase be prepared fresh daily. A temperature of 22 ± 1°C was necessary as higher temperatures gave faster

TABLE I

RECOVERY DATA FOR DIGOXIN, DIGOXIGENIN BISDIGITOXOSIDE (DBD) AND GITOXIN FROM SPIKED PLACEBO DIGOXIN 0.125- AND 0.25-mg TABLET MATRICES

Analyte	Amount loaded (ng per 5-mm band)	Mean recovery (%)			
		0.125-mg matrix[a]	R.S.D. (%)	0.25-mg matrix[b]	R.S.D. (%)
Digoxin	320	99.84 ± 2.30	2.30	99.64 ± 0.12	0.12
	400	100.20 ± 0.62	0.62	100.33 ± 1.22	1.21
	480	100.27 ± 2.20	2.19	99.35 ± 0.16	0.16
DBD	4[c]	98.99 ± 1.53	1.55	96.25 ± 0.13	0.14
	8[c]	98.91 ± 1.92	1.94	96.45 ± 0.22	0.23
	12[c]	97.78 ± 3.05	3.12	97.42 ± 0.54	0.55
Gitoxin	0.4[d]	96.46 ± 2.92	3.03	94.37 ± 0.19	0.20
	1.0[d]	96.65 ± 2.10	2.17	94.35 ± 0.07	0.07
	1.6[d]	97.16 ± 3.04	3.13	97.35 ± 3.31	3.40

[a] Placebo tablet matrix used in 0.125-mg digoxin formulation. Results are means ± S.D. ($n = 10$).
[b] Placebo tablet matrix used in 0.25-mg digoxin formulation. Results are means ± S.D. ($n = 18$).
[c] Equivalent to 1, 2 and 3% (w/w) of digoxin level at 400 ng per 5-mm band.
[d] Equivalent to 0.1, 0.25 and 0.4% (w/w) of digoxin level at 400 ng per 5-mm band.

TABLE II

HPTLC ASSAY OF COMMERCIAL DIGOXIN TABLETS FOR DIGOXIN AND RELATED COMPOUNDS

Tablet	Labeled amount of digoxin (mg)	Analyte	Amount found (mg)	Recovery (%)
A	0.125	Digoxin	0.127 ± 0.003[a]	101.84 ± 2.27[b]
		DBD	<0.001	<1.0[c]
		Gitoxin	<0.0001	<0.1[d]
B	0.125	Digoxin	0.123 ± 0.005[e]	99.02 ± 3.01[e]
		DBD	<0.001	<1.0
		Gitoxin	<0.0001	<0.1
C	0.125	Digoxin	0.126 ± 0.002[e]	100.65 ± 2.03[e]
		DBD	0.0014 ± 0.0001	1.13 ± 0.09[f]
		Gitoxin	<0.0001	<0.1
D	0.25	Digoxin	0.249 ± 0.006[e]	99.4 ± 2.5[e]
		DBD	0.003 ± 0.0004	1.24 ± 0.17
		Gitoxin	<0.0002	<0.1
E	0.25	Digoxin	0.246 ± 0.004[g]	98.6 ± 1.5[g]
		DBD	<0.002	<1.0
		Gitoxin	<0.0002	<0.1
F	0.25	Digoxin	0.251 ± 0.006[h]	100.36 ± 2.43[h]
		DBD	<0.002	<1.0
		Gitoxin	<0.0002	<0.1

[a] Mean ± S.D. ($n = 15$).
[b] Mean ± S.D. ($n = 15$).
[c] % (w/w) of DBD based on digoxin content; value is below quantifiable level ($n = 16$).
[d] % (w/w) of gitoxin based on digoxin content; value is below quantifiable level ($n = 16$).
[e] $n = 6$.
[f] Mean ± S.D. ($n = 6$).
[g] $n = 10$.
[h] $n = 15$.

development but incomplete resolution of bands. If the chamber pre-equilibration time was longer than 6 min, curved bands resulted on plate development. A fluorophore development time of 30 min at 120°C was preferred for the method as longer times showed decreases in fluorescence intensity for the gitoxin band but increases in fluorescence intensity for the DBD band. A 40-μl band loading gave the best detection with minimum diffusion of the analyte bands. The absorbance of the digoxin band at 218 nm was stable for up to 11 h and the fluorescence of the DBD and gitoxin bands was stable for up to 14 h. Standards and samples must be developed and scanned on the same plate for optimum accuracy and precision.

In conclusion, an accurate and precise HPTLC method has been developed for the simultaneous determination of digoxin, DBD and gitoxin in both digoxin drug substance and commercial digoxin tablets. The analytes are separated on a 100% wettable octadecylsilane plate and assayed for digoxin by absorbance densitometry and DBD and gitoxin by fluorescence densitometry.

ACKNOWLEDGEMENT

The authors are grateful for the financial support of and stimulating discussions with the personnel at Burroughs-Wellcome.

REFERENCES

1 W.O. Foye, *Principles of Medicinal Chemistry*, Lea and Febiger, Philadelphia, PA, 3rd ed., 1989, p. 363.

2 K. Holmes, Burroughs-Wellcome, Greenville, NC, personal communication, 1989.
3 A.H. Kibbe and O.E. Aracys, *J. Pharm. Sci.*, 62 (1973) 1703.
4 W.E. Wilson, S.A. Johnson, W.H. Perkins and J.E. Ripley, *Anal. Chem.*, 39 (1967) 40.
5 B. Sener, N. Evren, M. Ozguven, F. Bingol and A. Mutlugil, *J. Pharm. Belg.*, 42 (1987) 188.
6 B. Pekic, S.M. Petrovic and B. Slavica, *J. Chromatogr.*, 268 (1983) 237.
7 H. Kaizuka and K. Takahashi, *J. Chromatogr.*, 258 (1983) 135.
8 M.C. Castle, *J. Chromatogr.*, 115 (1975) 437.
9 E. Mincsovics, T.J. Szekely, M. Hoznek, Z. Vegh, I. Zambo, G. Szepesi and E. Tyihak, *Anal. Chem. Symp. Ser.*, 10 (1982) 427.
10 P. Horvath, G. Szepesi, M. Hoznek, Z. Vegh and E. Mincsovics, in R.E. Kaiser (Editor), *Proceedings of the International Symposium on Instrumental High Performance Thin-Layer Chromatography*, Institute of Chromatography, Bad Dürkheim, 2nd ed., 1982, p. 295.
11 *The United States Pharmacopeia, XXII Revision*, United States Pharmacopeial Convention, Rockville, MD 1990, p. 438.
12 *Physicians' Desk Reference*, Medical Economics, Montvale, NJ, 46th ed., 1992, p. 783.

Journal of Chromatography A, 659 (1994) 185–189
Elsevier Science B.V., Amsterdam

CHROM. 25 573

Determination of pteroic acid by high-performance thin-layer chromatography

Contribution to the investigation of 7,8-dihydropteroate synthase

Rainer Bartels and Lothar Bock*

Borstel Research Institute, Parkallee 4a, D-23845 Borstel (Germany)

(First received July 9th, 1993; revised manuscript received September 20th, 1993)

ABSTRACT

A TLC method was developed that allows the evaluation of the 7,8-dihydropteroate synthase reaction via determination of the stable pteroic acid (PtA), obtained by chemical oxidation of the enzymatic product dihydropteroic acid (H_2PtA). Using amino-bonded HPTLC plates and solution of 52% acetonitrile in 100 m*M* Tris–HCl buffer (pH 8.6) as the mobile phase it is possible to separate all enzyme substrates and competitively formed drug analogues of PtA from the oxidized enzymatic product. The method allows the detection of PtA at levels down to 0.5 ng/μl.

INTRODUCTION

The reaction shown in Fig. 1 is catalysed by 7,8-dihydropteroate synthase (SYN) (EC 2.5.1.15) of the folate pathway. Our interest was in the isolation of this enzyme from different organisms and in the investigation of its inhibition. Several methods for following this enzymatic reaction have been published: a biological detector system [1] and chromatographic systems (TLC, HPLC), analysing radiolabelled [2], fluorescent [3] or UV-absorbing compounds [4,5]. Other workers have described chromatographic separation techniques for different pteroyl derivatives, which were detected by radiolabelling [6] or a biological overlay technique [7,8]. For the detection of pteroic acid only, these procedures are difficult in handling and quantification, and especially the expenditure of time is high. Hitherto we employed a time-consuming HPLC method [5] for low-level detection and a TLC method [3] measuring a

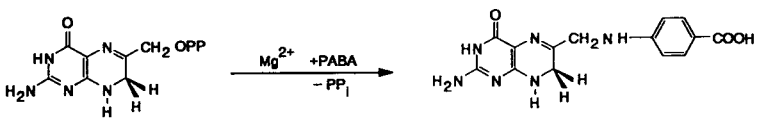

Fig. 1. Reaction catalysed by 7,8-dihydropteroate synthase. 7,8-Dihydropteridine alcohol pyrophosphate, enzymatically formed in a preceding reaction, is converted into 7,8-dihydropteroic acid by incorporation of *p*-aminobenzoic acid.

* Corresponding author.

0021-9673/94/$07.00
SSDI 0021-9673(93)E1008-N

fluorescent product that could not be quantified. The HPTLC method described here, however, combines fast enzyme detection with quantitative measurements and is adaptable to the study of the enzyme's inhibition by different drugs.

EXPERIMENTAL

Materials

The chemicals used were of analytical-reagent grade and were purchased from Merck (Darmstadt, Germany), as were amino-bonded HPTLC plates (20 × 10 cm). Pteroic acid (PtA) applied as a standard was obtained from Aldrich (Steinheim, Germany) and acetonitrile (ACN) from Baker (Gross-Gerau, Germany). 3,4-Dimethyl-5-sulphaisoxazole (SA) and its PtA analogue N^1-5-(3,4-dimethylisoxazolyl)-N^4-(6-pterinylmethyl)sulphanilamide (Pt-SA) were synthesized in our laboratory according to ref. 9. For chromatographic measurements, a Nanomat III, a horizontal development chamber (20 × 10 cm) and a TLC Scanner II working with CATS software 3.12, obtained from Camag (Muttenz, Switzerland) were used.

Methods

For system development and subsequent investigations 7,8-dihydropteroic acid (H_2PtA), pteroic acid (PtA), 7,8-dihydropteridine alcohol (H_2PtOH) and *p*-aminobenzoic acid (PABA) were used singly and in artificial mixtures. For the optimization of the mobile phase the method of Issaq and Seburn [10] was applied. To determine R_F values and for the determination of PtA, the diffuse reflectance signal at 280 nm was used.

As PtA is much more stable than the SYN product H_2PtA, the latter was oxidized to PtA according to ref. 4. However, we avoided trichloroacetic acid (coprecipitation of PtA and protein). Further, the excess of the oxidizing agent was destroyed by 1,4-dithiothreitol (DTT) (6 mmol/l). The volumes of the reagents were adapted to the amount of PtA. Samples of 1 μl were applied to the TLC plates (20 × 10 cm) and developed horizontally at room temperature in an unsaturated chamber.

RESULTS AND DISCUSSION

Previous HPLC experiments using amino-bonded phases indicated a good separation of PtA. As the instability (hydrolysis) of this column material does not disturb TLC, amino-bonded HPTLC plates were selected. The two mobile phases fulfilling the requirements of the optimization method were Tris–HCl buffer + $CaCl_2$, which allowed the separation of PABA from the rest of the reaction mixture, and an aqueous solution of ACN (>75% ACN), which separated PABA and H_2PtOH from stationary H_2PtA and PtA. These experiments resulted in the selection of 100 m*M* Tris–HCl (pH 8.6) containing 120 m*M* $CaCl_2$ as mobile phase A and 65% ACN in 100 m*M* Tris–HCl (pH 8.6) as mobile phase B. Mixtures of 0, 25, 50, 75 and 100% A in B were prepared as mobile phases. Fig. 2 shows the R_F values for four chromatographic runs. The mixture with 75% A was not tested because of the expected similarity to the runs with 100% and 50% A. A solvent composition in the range 10–30% mobile phase A gave a good separation of all components. Table I shows the calculated compositions of the liquid phases. However, the actual concentration of $CaCl_2$ was lower than the calculated value. Some time after mixing, opacity was observed in liquid

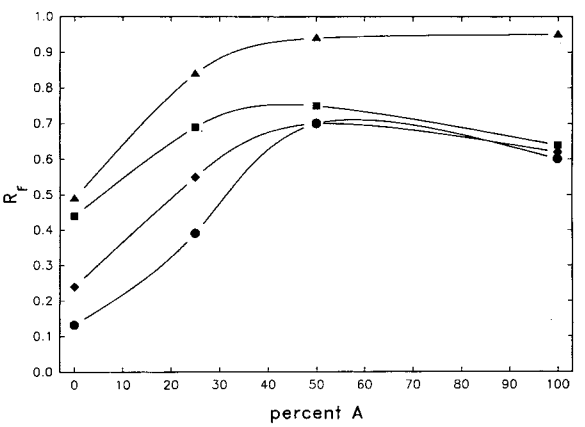

Fig. 2. Plot of R_F values *vs.* mobile phase composition. Amino-bonded HPTLC plates. ○ = PtA; ◆ = H_2PtA; □ = H_2PtOH; ▲ = PABA. Mobile phase A: 100 m*M* Tris–HCl (pH 8.6)–120 m*M* $CaCl_2$. Mobile phase B: 65% ACN in 100 m*M* Tris–HCl (pH 8.6).

TABLE I

COMPOSITIONS OF MOBILE PHASES

Solvent	A (%)	B (%)	Calculated mobile phase composition		
			ACN (%)	$CaCl_2$ (m*M*)	Tris–HCl (m*M*)
1	100	0	0	120	100
2	50	50	32.5	60	100
3	25	75	48.75	30	100
4	0	100	65	0	100

phases containing higher concentrations of ACN, indicating a decreased solubility of $CaCl_2$. Experiments with increasing $CaCl_2$ concentrations in the mobile phase using $CaCl_2$-impregnated and normal HPTLC plates showed that the addition of $CaCl_2$ influenced the R_F values only up to 5 m*M*. Higher concentrations were detrimental for the separation effect and for the peak symmetries on the impregnated plates. Hence $CaCl_2$ was not necessary for a good separation with the ranges of solvent composition used. In experiments with ACN-containing phases, solvent demixing resulted in a secondary solvent front [11]. The separation of the solutes was observed to occur below the secondary front. Therefore, in subsequent experiments the R_F values were calculated on the basis of this front and were labelled as R_x values.

Fig. 3 shows the R_x values at different Tris–HCl buffer concentrations in 52% ACN at pH 8.6. Lower buffer concentrations reduced the distance between the peaks. Concentrations above 40 m*M* were sufficient for baseline separation. To establish the pH dependence of the separation, a set of nineteen mobile phases were tested. Each phase was composed of 52% ACN and 100 m*M* Tris–HCl or phosphate buffer, with different pH values. Fig. 4 shows a plot of R_x *vs.* pH. The R_x values show differences in the influence of the buffer species. Phosphate buffers above pH 6.5 did not separate all compounds satisfactorily. Nevertheless, a separation over the total range of pH tested is possible. Fig. 5 shows an example using 100 m*M* Tris–HCl (pH 8.6) and 52% ACN.

The inhibition studies present an additional

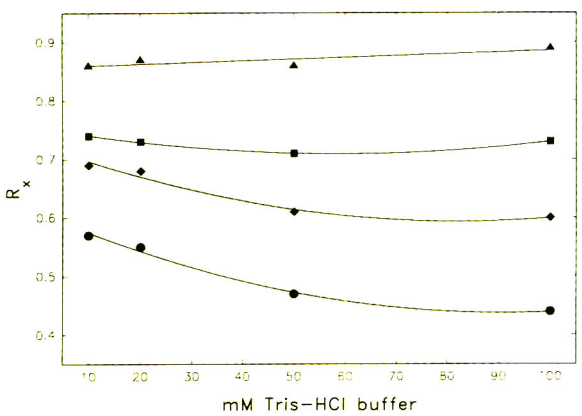

Fig. 3. Plot of R_x values *vs.* concentration of Tris–HCl buffer. Amino-bonded HPTLC plates. Symbols as in Fig. 2.

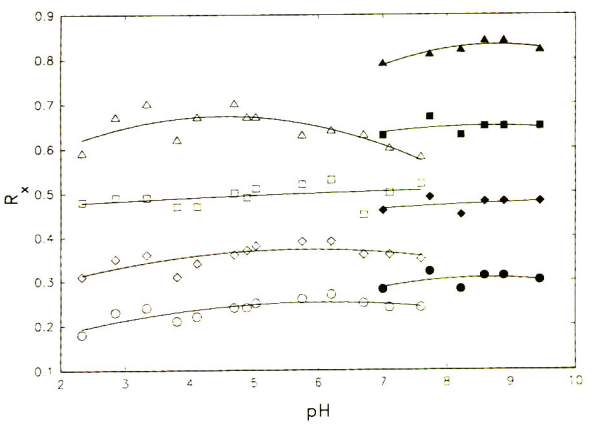

Fig. 4. Plot of R_x values *vs.* pH. Mobile phase: 52% ACN in 100 m*M* buffers of Tris–HCl (closed symbols) and phosphate (open symbols). Amino-bonded HPTLC plates. ●, ○ = PtA; ◆, ◇ = H_2PtA; ■, □ = H_2PtOH; ▲, △ = PABA.

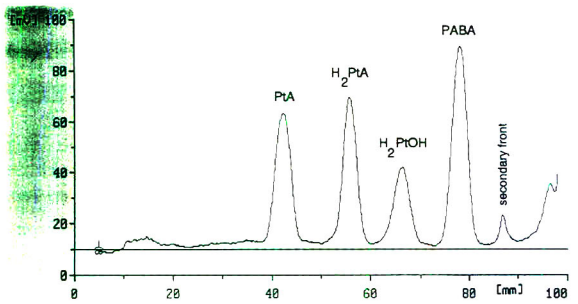

Fig. 5. Separation of PtA, H_2PtA, H_2PtOH and PABA on an amino-bonded HPTLC plate using 52% ACN in 100 m*M* Tris–HCl (pH 8.6) as mobile phase; 280 nm.

problem. It has been shown that the inhibition of *Escherichia coli* SYN by sulphonamides leads to the production of PtA analogues (Pt-SA) containing sulphonamides instead of PABA [9]. Therefore, two more solutes (Sa, Pt-SA) had to be separated. An analogue with 3,4-dimethyl-5-sulphaisoxazole (SA) was synthesized and analysed together with all the other substrates and the sulphonamide using the liquid phase described above. PtA was perfectly separated from all other solutes (Fig. 6).

Finally, it was difficult to examine samples quantitatively in the presence of proteins. After direct application of aqueous solutions, adsorption of PtA on the protein was observed, resulting in a disturbed chromatographic separation. Alkalinization of the sample by addition of 10 *M* NaOH was ineffective. Whereas the absorption of protein could be overcome, strong adsorption to magnesium hydroxide was ob-

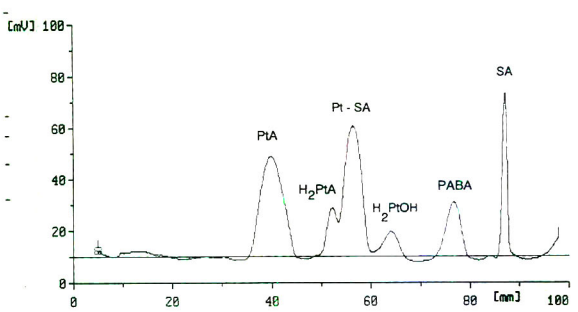

Fig. 6. Separation of PtA, H_2PtA, H_2PtOH, PABA, SA and Pt-SA on amino-bonded HPTLC plates using 52% ACN in 100 m*M* Tris–HCl (pH 8.6) as mobile phase; 280 nm.

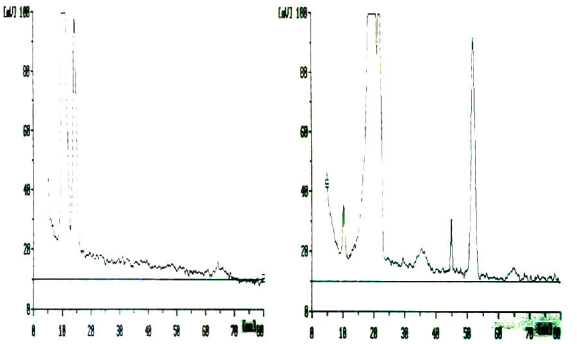

Fig. 7. Separation of PtA in the presence of protein. Untreated TLC plate on the left and spotted plate (1 μl of 1 *M* NaOH) on the right; 280 nm.

served that was not reversible by the addition of EDTA (*note:* magnesium ions are necessary for the enzyme reaction). However, this problem could be overcome as follows: before the sample was applied, the application point was directly alkalinized with 1 μl of 1 *M* NaOH ("spotting"). This procedure had two effects: first, the adsorption of PtA on the protein was terminated (up to 5 mg/ml of protein were tested), and second, the PtA peak was focused (Fig. 7). The shape of the calibration graph depends on the kind of sample application. The "spotting" of the TLC plate described above led to a non-linear dependence. However, a linear relation-

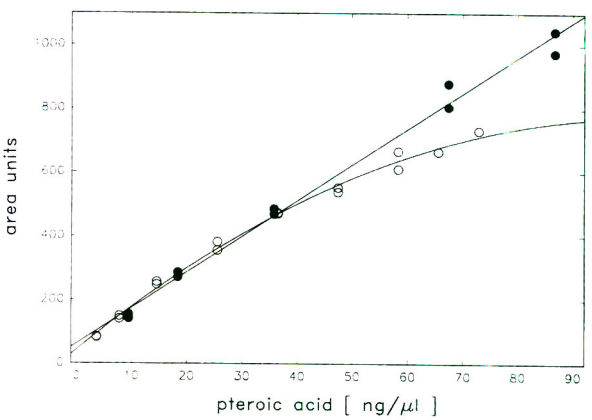

Fig. 8. Calibration graphs for the determination of pteroic acid. Plot of area units *vs.* concentration of PtA (ng/μl). ● = Aqueous solution of PtA: $y = 97.79 + 9.08x$, $r = 0.985$, S.D. = 41.44, $n = 18$. ○ = Spotted samples of PtA: $y = 42.77 + 14.21x - 0.069x^2$, $r = 0.997$, S.D. = 17.87, $n = 16$.

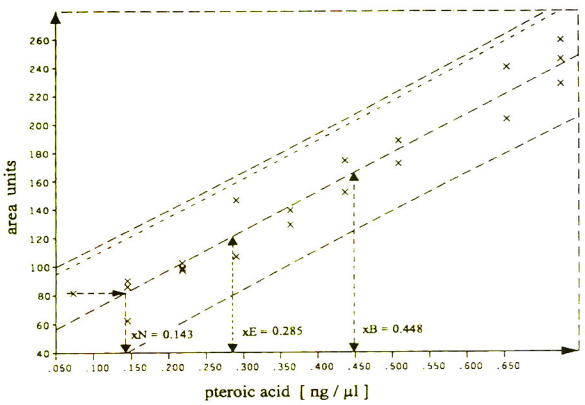

Fig. 9. Statistical calculation of the limit of determination [12]. xN = Limit of detection; xE = limit of identification; xB = limit of determination.

ship was obtained using solutions with pH < 9 (if another sample preparation is preferred, *e.g.*, solid-phase extraction) and untreated plates (Fig. 8). Sample treatment affects the shape of the PtA spot obtained. The untreated samples showed larger oval areas, whereas the "spotted" samples were separated into higher loaded bands instead of spots. For both preparations the determination limit of PtA was <0.5 ng/µl as determined by a serial dilution tests (Fig. 9). Samples containing 700 ng/µl were evaluated, but a suitable upper limit was 70 ng/µl. A linear relationship (area units/pteroic acid) is obtained in the lower range up to 7 ng/µl for both preparations.

CONCLUSIONS

The proposed HPTLC method is practical for the rapid detection of the SYN enzyme. The sensitivity is in the lower micromolar (ng/µl) range. The accessible pH range is large, and the system is tolerant to changes in the acetonitrile content in the mobile phase. It is possible to separate PtA from all other substrates of the SYN enzyme reaction and at least from one PtA analogue and its contaminating sulphonamide. The disadvantage of the method is the low dynamic range. To detect higher concentrations of PtA or enzyme concentrations, appropriate dilution of the sample is necessary. Higher sensitivity for biological systems [1,6,7] could be achieved by a concentration step using solid-phase extraction. Further, on-line automation should be feasible.

REFERENCES

1 G.H. Miller, P.H. Doukas and J.K. Seydel, *J. Med. Chem.*, 15 (1972) 700–706.
2 R. Ferone and S. Webb, in W. Pfleiderer (Editor), *Chemistry and Biology of Pteridines*, Walter de Gruyter, New York, 1976, pp. 61–71.
3 L. Bock, W. Butte, M. Richter and J.K. Seydel, *Anal. Biochem.*, 86 (1978) 238–251.
4 M. Wiese, J.K. Seydel, H. Pieper, G. Krüger, K.R. Noll and J. Keck, *Quant. Struct.–Act. Relat.*, 6 (1987) 164–172.
5 R. Bartels and L. Bock, in E. Tyihák and Gy. Hajós (Editors), *Proceedings of the 3rd International Conference on Biochemical Separations, Sopron, September 30–October 4, 1991*, pp. 43–44.
6 J.A. Blair and E. Dransfield, *Biochem. J.*, 123 (1971) 907.
7 I. Schlie and L. Janecke, *Z. Naturforsch., B*, 26 (1971) 1260.
8 F. Kreuzig, *Z. Anal. Chem.*, 255 (1971) 126.
9 L. Bock, G.H. Miller, K.-J. Schaper and J.K. Seydel, *J. Med. Chem.*, 17 (1974) 23–28.
10 H.J. Issaq and K.E. Seburn, *J. Liq. Chromatogr.*, 12 (1989) 3121–3128.
11 D. Nurok, *Chem. Rev.*, 89 (1989) 363–375.
12 A. Bahr, S. Hippich and M. Kolb, *Program: Nachweisgrenze Erfassungsgrenze Bestimmungsgrenze nach DIN 32645*, Fachhochschule Aalen, Aalen, 1992.

Journal of Chromatography A, 659 (1994) 191–197
Elsevier Science B.V., Amsterdam

CHROM. 25 588

Adsorption chromatography on cellulose

XI. Chiral separations with aqueous solutions of cyclodextrins as eluents

Huynh Thi Kieu Xuan and M. Lederer*

Institut de Chimie Minèrale et Analytique, Université de Lausanne, Boîte Postale 115, Centre Universitaire, CH-1015 Lausanne (Switzerland)

(First received July 7th, 1993; revised manuscript received September 23rd, 1993)

ABSTRACT

The system cellulose–aqueous α-cyclodextrin was investigated for chiral separations of tryptophan, methyltryptophans and fluorotryptophans by thin-layer and paper chromatography. The chiral effects are essentially additive (for cellulose and α-cyclodextrin), hence some large R_F differences can be obtained for enantiomeric pairs. There is also a temperature effect, with an increase in ΔR_F values as the temperature is decreased.

INTRODUCTION

Thin-layer chromatographic (TLC) separations of enantiomers have been found to be of interest and two reviews [1,2] have summarized the extensive work published and its application to purity control. We have investigated the chiral properties of cellulose in paper and thin-layer chromatography [3–7] and our interest was centred on understanding adsorption on cellulose.

In this paper we report on chromatography using cellulose as adsorbent and aqueous solutions of cyclodextrins as eluents. Separations using a chiral adsorbent and a chiral eluent together have been reported by several workers.

Fujita *et al.* [8,9] seem to have been the first, using a tartrate ester linked to Sephadex as the stationary phase and 0.3 *M* disodium L-tartrate as eluent. Davankov *et al.* [10] considered theoretically the copper–amino acid type of chiral selector in the stationary and the mobile phase. They concluded that "Enantioselectivity of chiral chromatographic systems appears to be a complex function of the enantioselectivity effects of the selector–selectand adduct formation in both the mobile and stationary phases, as well as of the phase distribution of these adducts, unless the chiral selector resides entirely in one of these phases . . . The reciprocity relationship for mutual chiral selector–selectand recognition which are known to be valid for their association in solutions and for diastereomeric salt crystallization do not necessarily hold for chiral chromatographic systems".

The chiral selectivity of cyclodextrins has been summarized by Menges and Armstrong [11] and involves the size of the cavity of the cyclodextrin and hydrogen bonding between the hydroxyl groups of the cyclodextrin and the included molecule. We have to consider another parameter in our system: the cyclodextrin must not be strongly adsorbed on cellulose otherwise it cannot be used readily as constituent of the eluent.

* Corresponding author.

0021-9673/94/$07.00
SSDI 0021-9673(93)E1014-Q

For our work only α-cyclodextrin, which moves to an R_F of 0.91 on paper and about 0.8 on cellulose thin layers, was suitable, β- and γ-cyclodextrins being fairly strongly adsorbed. The work reported here deals mainly with substituted tryptophans, which separate well with aqueous solvents on microcrystalline cellulose layers [3,6].

EXPERIMENTAL

Standard paper and thin-layer chromatographic techniques were used as reported in a previous paper [6]. The cyclodextrins used were obtained from Fluka (Buchs, Switzerland).

RESULTS

Reaction of iodine vapour with substituted tryptophans in the presence of α-cyclodextrin

In absence of α-cyclodextrin, iodine vapour produces pale brown spots on a white background irrespective of the type of cellulose used as the support. This reaction is about as sensitive as the reaction with ninhydrin. If left for prolonged periods in iodine vapour (*e.g.*, overnight), a black spot on a grey background is produced.

In the presence of α-cyclodextrin on cellulose layers, grey-black spots develop in a few seconds and these spots are very stable. Fig. 1 shows typical chromatograms after more than 60 days. We determined the sensitivity of this reaction for tryptophan and found that 5 ng can still be detected. This is about the lowest level generally detected by reagents in TLC.

Attempts to isolate the compound formed by mixing tryptophan in 1 *M* NaCl with α-cyclodextrin and adding iodine were unsuccessful. On Whatman 3MM paper the spots became intensely blue and not black and they disappeared within a few minutes. In the absence of NaCl or another salt sensitive coloration was not obtained. We suggest that it is a form of charge-transfer reaction involving the tryptophan, α-cyclodextrin, a salt and the cellulose support.

α-Cyclodextrin has been reported previously in conjunction with iodine vapour for the detection of lipids in TLC [12], but we could not find any reference to the reaction of tryptophan.

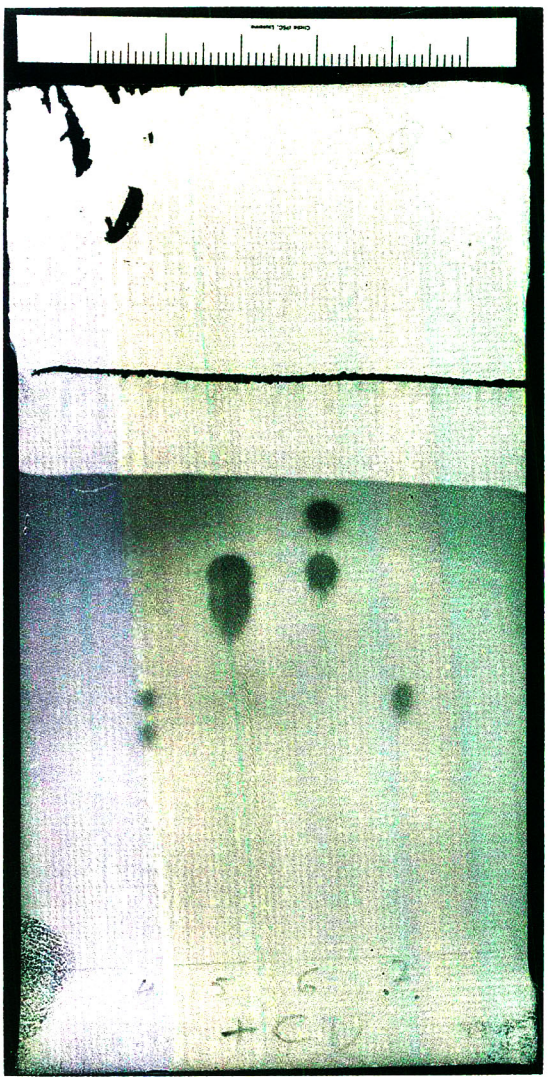

Fig. 1. Chromatogram of DL-methyltryptophans on native cellulose (Macherey–Nagel Cel-300) thin layers developed with aqueous 1 *M* NaCl containing 4% of α-cyclodextrin at room temperature (20–22°C). From left to right: 4-, 5-, 6- and 7-methyltryptophan. The thin layer was exposed to iodine vapour for a few seconds and then stored for over 60 days in the laboratory without a noticeable change in the intensity of the spots.

Effect of α-cyclodextrin concentration

We developed chromatograms with solutions of 1 *M* NaCl containing 1–10% of α-cyclodextrin. Table I shows the results obtained on microcrystalline cellulose (Merck 5577) and on "native" cellulose (Macherey–Nagel Cel-300). There is an increase in the separation from 1 to

TABLE I

EFFECT OF α-CYCLODEXTRIN CONCENTRATION ON THE R_F VALUES OF ENANTIOMERS OF SUBSTITUTED TRYPTOPHANS SEPARATED ON CELLULOSE THIN LAYERS WITH AQUEOUS α-CYCLODEXTRIN–1 *M* NaCl SOLUTIONS AT 22°C

Thin layer	Compound	α-Cycylodextrin (%)											
		0		1		2		4		6		10	
		R_F	ΔR_F	R_F	ΔR_F	R_F	ΔR_F	R_F	ΔR_F	R_F	ΔR_F	R_F	ΔR_F
Merck 5577 microcrystalline cellulose	Trp L-	0.41	0.07	0.40	0.09	0.41	0.10	0.48	0.12	0.47	0.13	0.59	0.12
	D-	0.48		0.49		0.51		0.60		0.60		0.67	
	4-Methyl-Trp L-	0.22	0.10	0.31	0.10	0.33	0.09	0.24	0.11	0.28	0.11	0.29	0.11
	D-	0.32		0.41		0.42		0.35		0.39		0.40	
	5-Methyl-Trp L-	0.25	0.08	0.24	0.09	0.32	0.10	0.41	0.13	0.47	0.11	0.52	0.11
	D-	0.33		0.33		0.42		0.54		0.58		0.63	
	6-Methyl-Trp L-	0.24	0.07	0.26	0.12	0.32	0.16	0.46	0.19	0.52	0.17	0.58	0.16
	D-	0.31		0.38		0.48		0.65		0.69		0.74	
	7-Methyl-Trp L-	0.26	0.07	0.26	0.08	0.28	0.07	0.28	0.08	0.32	0.08	0.34	0.07
	D-	0.33		0.34		0.35		0.36		0.40		0.41	
	4-Fluoro-Trp L-	0.30	0.08	0.19	0.09	0.21	0.10	0.34	0.11	0.42	0.10	0.44	0.12
	D-	0.38		0.28		0.31		0.45		0.52		0.56	
	5-Fluoro-Trp L-	0.35	0.06	0.33	0.08	0.38	0.08	0.42	0.09	0.46	0.08	0.56	0.05
	D-	0.41		0.41		0.46		0.51		0.54		0.61	
	6-Fluoro-Trp L-	0.32	0.09	0.35	0.11	0.40	0.14	0.43	0.17	0.49	0.16	0.57	0.15
	D-	0.41		0.46		0.54		0.60		0.65		0.72	
Macherey–Nagel Cel-300 native cellulose	Trp L-	0.56	0.02	0.53	0.03	0.58	0.04	0.60	0.07	0.60	0.06	0.62	0.07
	D-	0.58		0.56		0.62		0.67		0.66		0.69	
	4-Methyl-Trp L-	0.40	0.05	0.45	0.06	0.49	0.06	0.51	0.06	0.37	0.07	0.33	0.08
	D-	0.45		0.51		0.55		0.57		0.44		0.41	
	5-Methyl-Trp L-	0.43	0.04	0.42	0.05	0.50	0.05	0.58	0.06	0.60	0.06	0.61	0.07
	D-	0.47		0.47		0.55		0.64		0.66		0.68	
	6-Methyl-Trp L-	0.43	0.03	0.42	0.06	0.51	0.11	0.63	0.12	0.65	0.10	0.67	0.11
	D-	0.46		0.48		0.62		0.75		0.75		0.78	
	7-Methyl-Trp	0.50		0.46		0.43		0.47		0.44		0.47	
	4-Fluoro-Trp L-	0.48	0.04	0.34	0.07	0.37	0.07	0.38	0.06	0.50	0.07	0.47	0.09
	D-	0.52		0.41		0.44		0.44		0.57		0.56	
	5-Fluoro-Trp	0.51		0.49		0.53		0.58		0.57		0.57	
	6-Fluoro-Trp L-	0.48		0.47	0.05	0.53	0.06	0.60	0.11	0.60	0.10	0.60	0.13
	D-			0.52		0.59		0.71		0.70		0.67	

4% of α-cyclodextrin. The R_F difference between the two enantiomers does not increase measurably above 4% of cyclodextrin.

On "native" cellulose the separation of the enantiomers is slight, *e.g.*, an R_F difference of 0.02 between D- and L-tryptophan, whereas the difference on microcrystalline cellulose is 0.07. By comparing the behaviours on the two layers it is possible to obtain an estimate of the effect due to the α-cyclodextrin. It can be seen that the chiral effect due to the cellulose and that due to the α-cyclodextrin are essentially additive. On both layers an eluent containing 4% of α-cyclodextrin yields an increase in the R_F value with a difference of 0.05 for D,L-tryptophan.

The effect of different substituents and the position of the substituent is considerable in this system. Qualitatively it correlates with the data of Menges and Armstrong [11], who studied cyclodextrin-bonded phases in HPLC with 1% triethylammonium acetate at pH 5.1 as the eluent. There are several high R_F differences such as for 6-methyltryptophan ($\Delta R_F = 0.19$) and for 6-fluorotryptophan ($\Delta R_F = 0.17$), and there is a general increase for all the substituted tryptophans which were examined.

Effect of concentration of NaCl in the eluent

Table II shows the R_F values obtained on microcrystalline and "native" cellulose when the NaCl concentration was varied from 0 to 1 *M*, keeping the concentration of cyclodextrin at 4% throughout. There is a small but measurable salt

TABLE II

EFFECT OF CONCENTRATION OF NaCl ON R_F VALUES OF ENANTIOMERS OF SUBSTITUTED TRYPTOPHAN SEPARATED ON CELLULOSE THIN LAYERS WITH AQUEOUS 4% α-CYCLODEXTRIN–NaCl SOLUTIONS AT 22°C

Thin layer	Compound	NaCl concentration (M)							
		0		0.1		0.5		1	
		R_F	ΔR_F	R_F	ΔR_F	R_F	ΔR_F	R_F	ΔR_F
Merck 5577 microcrystalline cellulose	Trp L-	0.50	0.04	0.53	0.10	0.48	0.10	0.48	0.12
	D-	0.54		0.63		0.58		0.60	
	4-Methyl-Trp L-	0.27	0.09	0.45	0.09	0.38	0.10	0.24	0.11
	D-	0.36		0.54		0.48		0.35	
	5-Methyl-Trp L-	0.40	0.09	0.45	0.11	0.39	0.10	0.41	0.13
	D-	0.49		0.56		0.49		0.54	
	6-Methyl-Trp L-	0.43	0.16	0.48	0.17	0.44	0.18	0.46	0.19
	D-	0.59		0.65		0.62		0.65	
	7-Methyl-Trp L-	0.30	0.07	0.37	0.07	0.30	0.08	0.28	0.08
	D-	0.37		0.44		0.38		0.36	
	4-Fluoro-Trp L-	0.37	0.08	0.32	0.09	0.25	0.09	0.34	0.11
	D-	0.45		0.41		0.34		0.45	
	5-Fluoro-Trp L-	0.43	0.06	0.49	0.06	0.42	0.09	0.42	0.09
	D-	0.49		0.55		0.51		0.51	
	6-Fluoro-Trp L-	0.40	0.16	0.50	0.13	0.46	0.13	0.43	0.17
	D-	0.56		0.63		0.59		0.60	
Macherey–Nagel Cel-300 native cellulose	Trp L-	0.63	0.04	0.64	0.05	0.64	0.04	0.60	0.07
	D-	0.67		0.69		0.68		0.67	
	4-Methyl-Trp L-	0.45	0.05	0.57	0.05	0.55	0.05	0.51	0.06
	D-	0.50		0.62		0.60		0.57	
	5-Methyl-Trp L-	0.61	0.05	0.63	0.06	0.61	0.04	0.58	0.06
	D-	0.66		0.69		0.65		0.64	
	6-Methyl-Trp L-	0.65	0.08	0.65	0.09	0.66	0.08	0.63	0.12
	D-	0.73		0.74		0.74		0.75	
	7-Methyl-Trp	0.53		0.54		0.51		0.47	
	4-Fluoro-Trp L-	0.57	0.04	0.45	0.07	0.41	0.06	0.38	0.06
	D-	0.61		0.52		0.47		0.44	
	5-Fluoro-Trp	0.63		0.65		0.61		0.58	
	6-Fluoro-Trp L-	0.64	0.08	0.65	0.08	0.61	0.09	0.60	0.11
	D-	0.72		0.73		0.70		0.71	

effect both for the R_F values in general and for the ΔR_F values for a chiral pair. The optimum results were obtained with 1 M NaCl.

Effect of temperature

In previous work [3] on the separation of enantiomers in the absence of α-cyclodextrin in the range −10 to 63°C, the R_F values increased with increase in temperature but the chiral effect remained almost constant, diminishing only slightly at the highest temperature (63°C) and in the presence of high salt concentrations (*e.g.*, in 4.7 M LiCl).

In eluents containing α-cyclodextrin there is a large temperature effect, as shown in Table III. With an increase in temperature from 8 to 60°C the ΔR_F values can change as much as fivefold (*e.g.*, for 6-methyltryptophan on Macherey–Nagel Cel-300 cellulose from 0.15 at 8°C to 0.03

TABLE III

EFFECT OF THE TEMPERATURE OF DEVELOPMENT ON THE R_F VALUES OF ENANTIOMERS OF SUBSTITUTED TRYPTOPHANS SEPARATED ON CELLULOSE THIN LAYERS WITH AQUEOUS 4% α-CYCLODEXTRIN–1 *M* NaCl SOLUTION

Thin layer	Compound	8°C		22°C		40°C		60°C	
		R_F	ΔR_F	R_F	ΔR_F	R_F	ΔR_F	R_F	ΔR_F
Merck 5577 microcrystalline cellulose	Trp L-	0.35	0.16	0.48	0.12	0.56	0.08	0.62	0.08
	D-	0.51		0.60		0.64		0.70	
	4-Methyl-Trp L-	0.28	0.11	0.24	0.11	0.44	0.11	0.56	0.06
	D-	0.39		0.35		0.55		0.62	
	5-Methyl-Trp L-	0.29	0.12	0.41	0.13	0.46	0.08	0.55	0.07
	D-	0.41		0.54		0.54		0.62	
	6-Methyl-Trp L-	0.31	0.21	0.46	0.19	0.50	0.13	0.59	0.10
	D-	0.52		0.65		0.63		0.69	
	7-Methyl-Trp L-	0.20	0.08	0.28	0.08	0.39	0.06	0.51	0.04
	D-	0.28		0.36		0.45		0.55	
	4-Fluoro-Trp L-	0.14	0.10	0.34	0.11	0.32	0.10	0.44	0.08
	D-	0.24		0.45		0.42		0.52	
	5-Fluoro-Trp L-	0.31	0.08	0.42	0.09	0.50	0.06	0.59	0.05
	D-	0.39		0.51		0.56		0.64	
	6-Fluoro-Trp L-	0.35	0.17	0.43	0.17	0.53	0.11	0.60	0.08
	D-	0.52		0.60		0.64		0.68	
Macherey–Nagel Cel-300 native cellulose	Trp L-	0.48	0.09	0.60	0.07	0.69	0.04	0.73	0.02
	D-	0.57		0.67		0.73		0.75	
	4-Methyl-Trp L-	0.42	0.07	0.51	0.06	0.59	0.06	0.68	0.03
	D-	0.49		0.57		0.65		0.71	
	5-Methyl-Trp L-	0.46	0.07	0.58	0.06	0.64	0.05	0.69	0.04
	D-	0.53		0.64		0.69		0.71	
	6-Methyl-Trp L-	0.49	0.15	0.63	0.12	0.68	0.08	0.73	0.03
	D-	0.64		0.75		0.76		0.76	
	7-Methyl-Trp L-	0.39	0.03	0.47		0.57		0.67	
	D-	0.42							
	4-Fluoro-Trp L-	0.28	0.08	0.38	0.06	0.50	0.07	0.61	0.03
	D-	0.36		0.44		0.57		0.64	
	5-Fluoro-Trp L-	0.48	0.03	0.58		0.66		0.71	
	D-	0.51							
	6-Fluoro-Trp L-	0.50	0.12	0.60	0.11	0.67	0.05	0.70	0.04
	D-	0.62		0.71		0.72		0.74	

at 60°C). Further, high ΔR_F values are possible at low temperatures ($\Delta R_F = 0.21$ for 6-methyltryptophan at 8°C on Merck 5577 layers). The effect of temperature on the enantiomer separation varies considerably with the substituent and its position and there is always a decrease with increase in temperature.

The best results shown in Table III are as good as the best separations obtained by Günther [2] on chiral plates.

Paper chromatography

The chiral separations obtained on cellulose paper are usually of the same order as those obtained in TLC with "native" cellulose and as paper has a lower plate number not many baseline separations can be obtained [5]. It was therefore considered of interest to try eluents containing α-cyclodextrin as high ΔR_F values were recorded.

Table IV gives the R_F values on Whatman

TABLE IV

R_F VALUES OF SUBSTITUTED TRYPTOPHANS DEVELOPED ON WHATMAN NO. 3MM PAPER WITH AQUEOUS 1 *M* NaCl CONTAINING 4% OF α-CYCLODEXTRIN

Time, 7 h; distance moved, 25 cm; temperature, 20–22°C; R_F value of α-cyclodextrin front, 0.91.

Compound	R_F	ΔR_F
L-Trp	0.54	0.07
D-Trp	0.63	
DL-4-Methyl-Trp	0.38 0.44	0.06
DL-5-Methyl-Trp	0.53 0.61	0.08
DL-6-Methyl-Trp	0.60 0.69	0.09
DL-7-Methyl-Trp	0.46 (single spot)	0
DL-4-Fluoro-Trp	0.46 0.53	0.07
DL-5-Fluoro-Trp	0.51 (single spot)	0
DL-6-Fluoro-Trp	0.52 0.64	0.12

3MM paper; ΔR_F values identical with those on Macherey–Nagel Cel-300 thin layers were obtained. A number of enantiomeric pairs (as indicated in Table IV) yield baseline separations with a development of 20–25 cm in 5–7 h. The reaction with iodine vapour is different to that on thin layers, as already discussed.

Effect of Cu^{2+} ions on chiral separations with α-cyclodextrin

In a previous paper [7] we reported that the chiral discrimination of tryptophan and substituted tryptophans on cellulose is diminished when an excess of Cu^{2+} ions ($CuSO_4$ as eluent) is present in the eluent. Table V shows that the same occurs when α-cyclodextrin is used for chiral separations. It seems that complexation of the NH_2 and COOH groups interferes with the chiral interactions not only with cellulose but also with α-cyclodextrin.

CONCLUSIONS

Davankov *et al.* [10] pointed out that systems with a chiral support and a chiral eluent are complex owing to the numerous equilibria that are possible in solution and on the support. Our results with the cellulose–aqueous α-cyclodextrin system show a general but only qualitative additivity of the chiral separation effects, that is, the ΔR_F values are always larger on microcrystalline cellulose, which has a strong chiral discrimination, than on native cellulose.

However, in addition to this general trend there is a considerable change in R_F values in the presence of α-cyclodextrin and there is a strong temperature dependence for the chiral separations. This permits a wide choice of conditions for separations between the enantiomers and also between numerous substituted tryptophans which do not separate without α-cyclodextrin. The reaction of iodine vapour with thin-layer

TABLE V

R_F VALUES OF SUBSTITUTED TRYPTOPHANS ON CELLULOSE THIN LAYERS DEVELOPED WITH AQUEOUS α-CYCLODEXTRIN SOLUTION CONTAINING $CuSO_4$

Thin layer	Compound	R_F	
		4% α-cyclodextrin + 0.05 *M* $CuSO_4$	0.05 *M* $CuSO_4$
Merck 5577 microcrystalline cellulose	L-Trp	0.60	0.70
	D-Trp	0.63	0.74
	DL-4-Methyl-Trp	0.47	0.48
	DL-5-Methyl-Trp	0.60 0.64	0.50 0.53
	DL-6-Methyl-Trp	0.68	0.52
	DL-7-Methyl-Trp	0.53	0.54
	DL-4-Fluoro-Trp	0.57	0.55
	DL-5-Fluoro-Trp	0.61	0.57
	DL-6-Fluoro-Trp	0.63	0.56
Macherey–Nagel Cel-300 native cellulose	L-Trp	0.61	0.56
	D-Trp	0.63	0.58
	DL-4-Methyl-Trp	0.45	0.43
	DL-5-Methyl-Trp	0.62	0.50
	DL-6-Methyl-Trp	0.66	0.48
	DL-7-Methyl-Trp	0.52	0.51
	DL-4-Fluoro-Trp	0.54	0.51
	DL-5-Fluoro-Trp	0.57	0.52
	DL-6-Fluoro-Trp	0.60	0.51

plates developed with an aqueous NaCl–α-cyclodextrin mixture yields a colour reaction which seems to be as good as the best yet reported.

REFERENCES

1 J. Mertens and R. Bhushan, *J. Pharm. Biomed. Anal.*, 8 (1990) 259.
2 K. Günther, in J. Sherma and B. Fried (Editors), *Handbook of TLC*, Marcel Dekker, New York, 1991, pp. 541–591.
3 A.O. Kuhn, M. Lederer and M. Sinibaldi, *J. Chromatogr.*, 469 (1989) 253.
4 M. Lederer, *J. Chromatogr.*, 510 (1990) 367.
5 M. Lederer, *J. Chromatogr.*, 604 (1992) 55.
6 T.K.X. Huynh and M. Lederer, *J. Chromatogr.*, 635 (1993) 346.
7 T.K.X. Huynh and M. Lederer, *J. Chromatogr.*, 645 (1993) 185.
8 M. Fujita, Y. Yoshikawa and H. Yamatera, *Chem. Lett.*, (1975) 473.
9 M. Fujita, Y. Yoshikawa and H. Yamatera, *Chem. Commun.*, (1975) 941.
10 Y.A. Davankov, A.A. Kurganov and T.M. Ponomareva, *J. Chromatogr.*, 452 (1988) 309.
11 R.A. Menges and D.W. Armstrong, in S. Ahuja (Editor), *Chiral Separations by Liquid Chromatography (ACS Symposium Series*, No. 471), American Chemical Society, Washington, DC, 1991, p. 67.
12 I.M. Hais and K. Macek (Editors), *Paper Chromatography*, Academic Press, New York, 1963, p. 797.

Journal of Chromatography A, 659 (1994) 199–204
Elsevier Science B.V., Amsterdam

CHROM. 25 574

Capillary electrophoresis instrumentation as a bench-top viscometer

Michael S. Bello[☆], Roberta Rezzonico and Pier Giorgio Righetti[*]

Faculty of Pharmacy and Department of Biomedical Sciences and Technologies, University of Milan, Via Celoria 2, Milan 20133 (Italy)

(First received July 27th, 1993; revised manuscript received September 20th, 1993)

ABSTRACT

A simple and reliable method is proposed for measuring the viscosities of different solutions by using standard capillary zone electrophoresis equipment. The capillary is first filled with, *e.g.*, a liquid of known viscosity and then the solution under analysis is pumped through it at a constant pressure drop and constant temperature. The migration time of the boundary between the two liquids from the injection port to the detector is carefully measured and the experimental data are entered in a derived modified Poiseuille equation for calculating the unknown viscosity. Viscosities of small analytes (*e.g.*, sucrose solutions) and of macromolecular solutions (*e.g.*, methylcellulose) could be assessed with a precision of the order of 3%. The boundary between the two liquids is usually detected by refractive index gradients, even in the presence of non-UV-absorbing species. With very minute refractive index variations, the boundary is easily detected by spiking one of the two solutions with traces of a strongly UV-absorbing compound (*e.g.*, riboflavin).

INTRODUCTION

One of the most recent trends in the mass separation of macromolecules (notably proteins and nucleic acids) in capillary electrophoresis (CE) is the use of capillaries filled with viscous polymer solutions, according to an original idea first proposed by Bode [1] and De Gennes [2]. Such polymer solutions can be extremely viscous, and the separation (especially with nucleic acids) seems to be directly correlated with the viscosity of such solutions [3,4]. Therefore, simple and reliable methods allowing the rapid assessment of the viscosity of a given solution used in biochemical separations are highly desirable. Whereas sophisticated (and very expensive) viscometers are commonly found in laboratories dealing with polymer science, they are rarely to be seen in a biochemical laboratory. We report here a simple and efficient procedure by which a standard instrument for capillary electrophoresis can be used as a bench-top viscometer.

The possibility of measuring the viscosity of a liquid by measuring its velocity in a tube of known diameter is well known and follows from the classical Poiseuille equation [5,6]. However, to put this method into practice one needs tubing, a pump with connections, a marker and a detector. Fortunately, a CE unit contains all these components and hence can be used for viscosity measurements. In the Theory section we derive an approximate equation for calculating the time taken by the boundary between two liquids to migrate from one end of the capillary

* Corresponding author.
☆ Permanent address: Institute of Macromolecular Compounds, Bolshoi 31, 199004 St. Petersburg, Russian Federation.

0021-9673/94/$07.00
SSDI 0021-9673(93)E1007-M

to the UV window. The Experimental section describes a procedure developed to measure the viscosity of a liquid by means of a Waters Quanta 4000 CE unit. Measured viscosities were compared with those given in tables and measured by a standard technique.

THEORY

Consider a capillary of total length L, distance between the entrance end and the UV window l and inner diameter d (Fig. 1). Assume that the capillary was initially filled with a liquid having viscosity η_1 and that this liquid is replaced with another liquid with a viscosity η_2 under a pressure drop Δp. Obviously, the time it takes to replace the first liquid in the capillary by the second one depends on the viscosities of both liquids. In order to obtain a quantitative relationship between the time and the viscosities we have to solve the following problems: (1) what is the velocity of the liquid inside the capillary as a function of time?; and (2) how long does it take the boundary between the liquids to reach the UV window and how is this time related to the viscosity of the liquids?

As an approximation, we assume that the boundary between the two liquids is flat and does not disperse when flowing down the capillary. Let the boundary be located at a distance x from the entrance end of the capillary (see Fig. 1) at time t. The velocity of the boundary is, obviously, equal to the average cross-sectional velocity, which must be the same at any cross-section of the capillary but can vary in time. The average cross-sectional velocity of the viscous

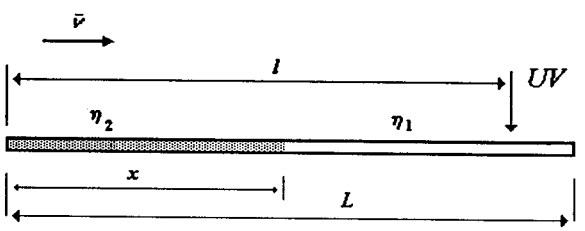

Fig. 1. Scheme of the experimental set-up for measuring viscosities in a CZE unit. L = total capillary length; l = distance between capillary entrance and detector (UV); x = coordinate of the boundary between the two liquids of viscosities; $\bar{v}$ = average cross-sectional velocity.

fluid flowing in a tube is given by the Poiseuille equation [5,6].

In accordance with the assumptions made above, we apply the Poiseuille law separately to both parts of the capillary filled with the two liquids:

$$\bar{v} = \frac{\Delta p_1 d^2}{32(L-x)\eta_1} \qquad (1)$$

$$\bar{v} = \frac{\Delta p_2 d^2}{32x\eta_2}$$

where $\bar{v}$ is the average cross-sectional velocity, x is the coordinate of the boundary between the liquids and Δp_1 and Δ_{p2} are the pressure drops on the parts of the capillary occupied by the first and the second liquid, respectively. Eqn. 1 transforms to

$$\bar{v} = \frac{\Delta p d^2}{32[\eta_2 x + \eta_1(L-x)]} \qquad (2)$$

where Δp is the total pressure drop, equal to the sum of the partial pressure drops. This equation relates the average velocity of the liquid in the capillary with the instantaneous position of the boundary.

The velocity $\bar{v}$ is also the velocity of the boundary between liquids and is given by $\bar{v} = \mathrm{d}x/\mathrm{d}t$. After substituting this expression into eqn. 2 one obtains a differential equation, integration of which gives the following relationship between the boundary migration time and its position along the capillary axis:

$$t = \frac{32Lx\eta_1}{\Delta p d^2}\left[\frac{x}{2L}\left(\frac{\eta_2}{\eta_1} - 1\right) + 1\right] \qquad (3)$$

This equation can be used for estimating the time necessary to replace one liquid in the capillary with another. Setting $x = L$ in eqn. 3 gives

$$t_s = \frac{16L^2}{\Delta p d^2}(\eta_2 + \eta_1) \qquad (4)$$

where t_s is the time during which the boundary is moving within the capillary.

For $x = l$, eqn. 4 easily transforms to

$$\frac{l}{2L}\cdot\eta_2+\left(1-\frac{l}{2L}\right)\eta_1=\frac{\Delta t\,\Delta p d^2}{32Ll} \quad (5)$$

where Δt is the time during which the boundary is migrating from the entrance of the capillary to the detector window.

Eqn. 5 allows one to calculate the viscosity of one of the liquids if the viscosity of the other liquid, time Δt and other parameters are known. The capillary length L and the distance between the capillary entrance and the UV window can be easily measured. The pressure drop can be read from a display and the capillary diameter is usually given by the manufacturer or can be measured as suggested in ref. 7. The only unknown parameter to be determined experimentally is the time Δt.

Often the boundary between two liquids can be registered by a UV detector, as the latter is also sensitive to the difference in refractive index. Thus, for example, boundaries between distilled water and the buffer or water and sucrose solution are visible. If the boundary is invisible, a small amount of a light-adsorbing substance should be added.

EXPERIMENTAL

A Waters Quanta 4000 capillary electrophoresis system (Millipore, Milford, MA, USA) was used. Capillaries were obtained from Polymicro Technologies (Phoenix, AZ, USA). The inner diameter of the capillary was determined according to ref. 7 by using a software package [8] and found to be $d = 75.4 \pm 0.4$ μm. The temperature was read from a Digiterm Quartz 1505 thermometer (Hanhart, Schwenningen, Germany) installed in the vicinity of the capillary.

In order to demonstrate the possibility of using the CE unit for viscosity measurements, three solutions of different viscosities were used. A 0.5% methylcellulose (Methocel A4-M; Dow Chemical, Midland, MI, USA) solution was prepared by a hot-water method and centrifuged for 45 min in a Biofuge (Heraus Sepatech, Am Kalkberg, Germany) at 51 000 g. A 30% sucrose (Merck, Darmstadt, Germany) solution was prepared. Riboflavin-5′-phosphate (Bio-Rad, Richmond, CA, USA) was used to reveal the boundaries between distilled water and Methocel solution.

Viscosity measurements on the polymer solution were performed on a Bohlin VOR Rheometer (Bohlin Rheologi, Lund, Sweden).

In order to measure the viscosity of a liquid, a capillary of $L = 0.982$ m and $l = 0.909$ m was installed in the Waters Quanta 4000 unit. The entrance end of the capillary was positioned in the vial with the first liquid and the capillary was filled with a liquid by applying a pressure (purge on) of $\Delta p = 5.53 \cdot 10^4$ N m^{-2}. After a certain time sufficient to fully replace the liquid in the capillary, the vial was changed and the pressure was applied again. The moment of turning on the pump and the moment when the boundary passed by the UV window were monitored. The vial was then replaced with the first one and the procedure was repeated several times.

RESULTS

Fig. 2 illustrates the described procedure for the measurement of the time Δt necessary for the boundary between the sucrose solution and distilled water to pass the distance between the entrance of the capillary and the UV window. The capillary was initially filled with distilled water. Then the capillary entrance was placed in the vial with the sucrose solution and the pressure was applied at time t_p. The upper meander-type line represents the light absorbance signal received from detector 1 during pumping. At the beginning the light absorbance is constant and corresponds to that of the water. The transition to a low level of the UV signal shows the boundary between distilled water and the sucrose solution. The difference in the amplitude of the detector signal is probably caused by the difference in the refractive indices of water and the sucrose solution. The inflection point of the curve is associated with the position of the boundary and by measuring its coordinate one finds the time t_b at which the boundary passes the UV window. The time t_p of the start of purging can be assessed by either a chronometer or by recording the current signal. This signal is shown below the UV signal in Fig. 2. The peculiarity of the CE unit we used is that the

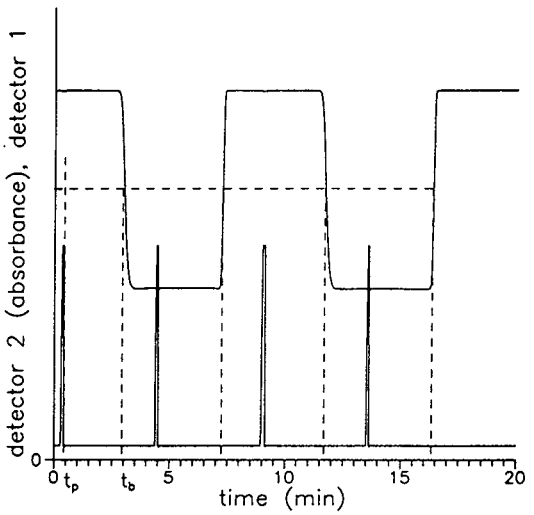

Fig. 2. Procedure for measurement of the boundary migration time. The upper meandering curve is given by the UV detector as the water–sucrose boundary passes through it (probably caused by differences in refractive indices between the two liquids; detector 1). The lower peaks (detector 2) are produced as spikes in the current signal when the lid of the box containing the capillary is opened or closed (this signal is taken as the start of boundary migration, *i.e.*, zero time). The graph shows the passage of four consecutive starting signals and of four consecutive boundaries.

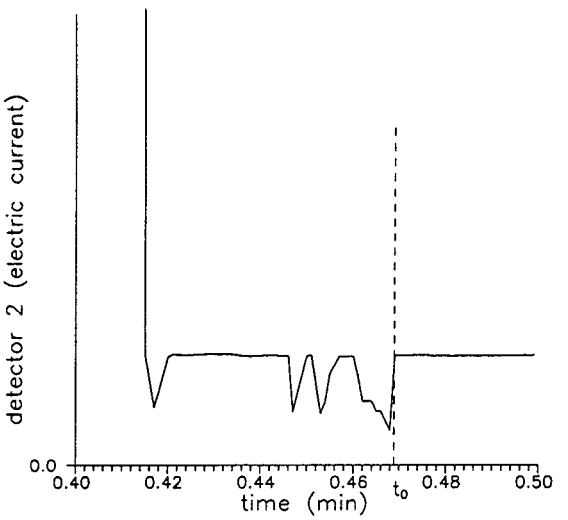

Fig. 3. Example of the spikes in the current signal produced by the up and down movement of the loading carousel. The last of this train of spikes is used as a marker for the start of the pumping of the viscous solution inside the capillary (*i.e.*, zero migration time).

current signal (detector 2) gives spikes when the box containing the capillary is opened and closed and when the carousel moves up and down. Spikes corresponding to the opening of the box are shown in Fig. 2. Spikes corresponding to the motion of the carousel have a lower amplitude, as shown in Fig. 3. The latest of these spikes was used as a marker for the moment when the pump had been turned on. In our experiments the button "Purge" had been pressed immediately after the carousel had moved to its normal position. Thus, t_b was found as a coordinate of the inflection point of the UV signal curve (detector 1) and t_p was found as a coordinate of the last spike on the detector 2 signal. Finally, we obtain the time interval during which the boundary was migrating between the capillary entrance and the UV window as $\Delta t = t_b - t_p$.

Table I presents times Δt and relative viscosities for the sucrose solution calculated from the run shown in Fig. 2. The value of the relative viscosity measured by means of a rotating viscometer is 3.0 and agrees well with the data presented in Table I. The error of the measurements depends on the accuracy of the pressure readings, edge effects, especially for viscous liquids, and on the precision with which time Δt is determined.

In our case we cannot expect the experimental error to be less than 3–4% and therefore we include only two valid decimal digits for the measured viscosities.

Viscosity measurements on distilled water were performed in order to compare the experimental data with those presented in ref. 9. We used two vials, one of which contained

TABLE I

RELATIVE VISCOSITY OF THE 30% SUCROSE SOLUTION AT 27.5°C MEASURED BY MEANS OF THE CE UNIT

Substitution	Δt (min)	η/η_w
Water–solution	2.55	3.1
Solution–water	2.72	3.0
Water–solution	2.57	3.1
Solution–water	2.7	3.0

TABLE II

MEASUREMENTS OF THE VISCOSITY OF WATER AT DIFFERENT TEMPERATURES OF THE AMBIENT AIR

T (°C)	Δt (min)	$\sigma_{n-1} \cdot 10^3$ (min)	$\eta_m \cdot 10^3$ (kg m^{-1} s^{-1})	$\eta_w \cdot 10^3$ (kg m^{-1} s^{-1})	ε (%)
27.5	1.26	3	0.83	0.84	1.2
30.3	1.2	11	0.79	0.8	1.3
26	1.32	7.7	0.87	0.87	0

distilled water and the other a 0.01% solution of riboflavin. It was assumed that such a low concentration of riboflavin would not change the solution viscosity. Table II presents times Δt representing average values for three series of measurements. The series of measurements were performed on different days and at different temperatures T. Table II also gives the standard deviations, σ_{n-1}, for the times Δt, the measured viscosities, η_m, the viscosity of water, η_w, taken directly from ref. 9 or obtained by linear interpolation and the percentile difference, ε, between the measured and standard values. It is seen that the agreement between measured and standard values is fairly good.

Table III presents the results for viscosity measurements on the polymer solution. Δt_1 denotes the time Δt measured when water was replaced with methylcellulose solution and Δt_2 that when water replaced methylcellulose. The

TABLE III

VISCOSITY MEASUREMENTS ON THE METHYLCELLULOSE (MC) SOLUTION

Substitution	Δt_1 (min)	Δt_2 (min)
Water–MC	13.4	
MC–water		15.6
Water–MC	13.44	
Water–MC	13.6	
MC–water		15.96
Water–MC	14.1	
MC–water		16.9
Δt (min)	13.6	16.2
σ (min)	0.32	0.67

calculated viscosities are $21 \cdot 10^{-3}$ and $22 \cdot 10^{-3}$ kg m^{-1} s^{-1}, respectively. These data are in good agreement, but the standard deviation of the boundary migration time is three times lower when the more viscous liquid replaces the less viscous liquid. The agreement with the viscosity obtained by using the standard viscometer is not so good: the measured viscosity was $16 \cdot 10^{-3}$ kg m^{-1} s^{-1}. However, this discrepancy can be attributed to the non-Newtonian properties of the polymer solution.

DISCUSSION

The precise assessment of the migration of a boundary was adopted long ago in separation science for measuring the physico-chemical properties of a solute. An example is the analytical ultracentrifuge, in which the velocity of a boundary of a sedimenting protein was used to assess the sedimentation coefficient and, in turn, the molecular mass of such a macromolecule. It should be noted that the spreading of such a boundary with time (seen as a sedimenting peak, obtained as the first derivative of a sigmoidal transition from a zone of pure solvent to a solute zone) was also used for the precise measurement of the diffusion coefficient of the macromolecular analyte. In an analogous fashion, measurement of the velocity of protein boundaries in an electric field was used for the determination of the free mobilities of proteins in the Tiselius moving boundary unit. In both techniques (centrifugal and electric fields), perhaps the most complex part of the instrumentation was the bulky optical bench used for revealing (and photographing) such boundaries. While present-day analysts might be unaware of such a discipline, the observation of boundaries was a complex problem and developed into an almost independent science. In the early days, Svedberg and Jette [10] made use of the fluorescence of colourless proteins when irradiated from the side by UV radiation. Subsequently, Svedberg and Tiselius [11] adopted a direct UV absorption method for tracking sedimenting protein zones. The method finally adopted, however, was based on the deviation of light at the boundary, due to sharp refractive index variations, as proposed in

1902 by Abegg and Gaus [12]. The methodology finally adopted was the Schlieren observation technique, introduced in 1937 by Tiselius [13] in electrokinetic processes. Soon after, Philpot [14] reported a self-registering Schlieren optics arrangement for the ultracentrifuge, which was later improved by Longsworth [15] and Svensson [16]. Just to give an idea of the complexity of such systems, in the analytical ultracentrifuge the sedimenting peak is obtained by the synchronous mechanical movement of a horizontal edge and a vertical plate placed on the optical bench, which transform the boundary (a sigmoidal curve) into a Gaussian profile.

In the present method also a precise assessment of the transit time of a boundary between two liquids is used for a physico-chemical measurement, namely the viscosity of a solution. Fortuitously we did not have to spend considerable time in implementing complex Schlieren optics for observing such boundaries, as the miniaturized, yet very powerful, UV detection system normally present in CE units was found to be adequate for recording such signals. We have noted that, even when both liquids are UV transparent, the refractive index variation at the boundary if often sufficient for generating a signal at the detector (see the meandering pattern in Fig. 2). Even when the signal tends to vanish (due to minute increments in refractive index) it is still possible to detect the boundary by adding traces of a strongly UV-absorbing substance (*e.g.*, riboflavin) to one of the two liquids. This is a simple, yet effective, method proposed as early as 1899 by Masson [17].

An additional advantage of the suggested procedure is that only very small volumes of the analyte liquid are necessary for a satisfactory viscosity measurement.

ACKNOWLEDGEMENTS

The authors thank Dr. Scandroglio (Millipore, Vimodrone, Italy) for generous help. This work was supported in part by the Progetto Finalizzato Chimica Fine II (CNR, Rome) and by a grant from the European Community (Biomed 1, Area III: Human Genome Analysis).

REFERENCES

1 H.J. Bode, *Anal. Biochem.*, 83 (1977) 204–210 and 364–371.
2 P.G. De Gennes, *Scaling Concepts in Polymer Physics*, Cornell University Press, Ithaca, NY, 1979.
3 M. Chiari, M. Nesi, M. Fazio and P.G. Righetti, *Electrophoresis*, 13 (1992) 690–697.
4 J.L. Viovy and T. Duke, *Electrophoresis*, 14 (1993) 322–329.
5 R.B. Bird, W.E. Stewart and E.N. Lightfoot, *Transport Phenomena*, Wiley, New York, 1960.
6 F.M. White, *Viscous Fluid Flow*, McGraw-Hill, San Francisco, 1974.
7 M.S. Bello, M. Chiari, M. Nesi, P.G. Righetti and M. Saracchi, *J. Chromatogr.*, 625 (1992) 323–330.
8 M.S. Bello, E.I. Levin and P.G. Righetti, *J. Chromatogr.*, 652 (1993) 329–336.
9 R. Weast (Editor), *CRC Handbook of Chemistry and Physics*, CRC Press, Boca Raton, FL, 67th ed., 1986–1987, p. F-37.
10 T. Svedberg and E.R. Jette, *J. Am. Chem. Soc.*, 45 (1923) 954–960.
11 T. Svedberg and A. Tiselius, *J. Am. Chem. Soc.*, 48 (1926) 2272–2276.
12 R. Abegg and W. Gaus, *Z. Phys. Chem.*, 40 (1902) 737–745.
13 A. Tiselius, *Trans. Faraday Soc.*, 33 (1937) 524–531.
14 J.S.L. Philpot, *Nature*, 141 (1938) 283–285.
15 L.G. Longsworth, *Chem. Rev.*, 30 (1942) 323–343.
16 H. Svensson, *Ark. Kemi Mineral. Geol.*, 22A (1946) 1–156.
17 O. Masson, *Philos. Trans. Roy. Soc. London, Ser. A*, 192 (1899) 331–340.

Journal of Chromatography A, 659 (1994) 205–208
Elsevier Science B.V., Amsterdam

CHROM. 25 752

Short Communication

Fan-induced heating

R.I. Meacham, B.A. Buffham*, D.W. Drott and G. Mason

Department of Chemical Engineering, Loughborough University of Technology, Loughborough, Leicestershire LE11 3TU (UK)

(First received September 20th, 1993; revised manuscript received November 19th, 1993)

ABSTRACT

A method is described in which the temperature of a chromatograph oven can be controlled over a range of 20°C above ambient temperature by controlling the power input to the fan.

INTRODUCTION

Temperature control of chromatographs just above ambient temperature poses special problems. The quantity of heat that must be supplied to balance losses is relatively small and yet must be supplied by a heating and control system that is designed to supply enough power for the chromatograph to heat up quickly and to operate up to, say, 500°C. In the early days of chromatography, control systems were designed that supplied power for part of each mains electricity cycle. For example, Ashbury *et al.* [1] used a modified Brown amplifier and a large thyratron to do just this. The famous Pye Model 104 chromatograph of the 1960s used solid-state circuitry to accomplish phase-angle control (Fig. 1a). Nowadays phase-angle control is frowned upon because it can introduce disturbances into the electricity mains and adversely affect the performance of digital electronic equipment.

This problem can be overcome by using circuitry that switches current on or off at the zero-volts part of the electrical cycle. A control circuit decides what proportion of the time the power shall be on. A thyristor stack can then be used to switch the power on and off. Two ways of doing this are illustrated in Fig. 1b and c. At low temperature the heater is only on for a small proportion of the time. It is easy to detect this happening. Fig. 2 shows pulses of power being supplied to the heater of a modern chromatograph to maintain its temperature at 40°C. Current flowing to the heater was detected by an inductive power meter. A potentiometric chart recorder was connected across a resistor connected across the terminals of the power meter. Although the electrical noise problem is solved, the power input is very uneven.

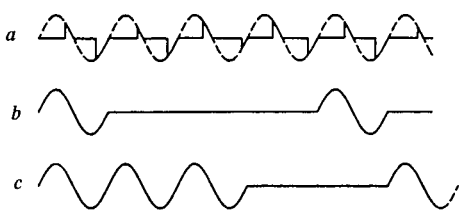

Fig. 1. Three ways of regulating power input: (a) phase-angle control; (b) single cycle; (c) fast cycle.

* Corresponding author.

0021-9673/94/$07.00
SSDI 0021-9673(93)E1233-P

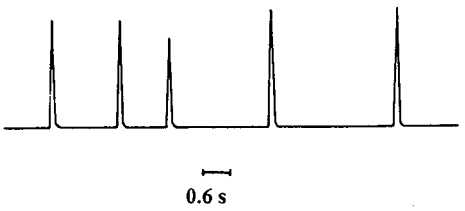

Fig. 2. Pulses of power being supplied to the heater of a modern chromatograph when operated at a relatively low temperature (40°C).

An approach used in the design of some modern chromatographs to aid operation at temperatures not much above ambient is to exchange air between the oven and its surroundings. This can be done via a motor-driven flap whose other purpose is to allow rapid cooling.

We have developed qualitative [2] and absolute [3] gas chromatographic methods based on measuring the small changes in flow rate that are caused by sorption and desorption, *i.e.* the "sorption effect". In these methods a pressure difference is measured with a sensitive pressure transducer. Thermal fluctuations at *any* point in the column cause pressure fluctuations that are sensed by the transducer as "thermal noise". This is in stark contrast to conventional gas chromatography where such fluctuations may cause band spreading but do not usually reveal themselves as signal noise. In capillary chromatography they can sometimes be seen on the chromatogram [4]. Flow-rate methods are worse affected by thermal noise than are conventional chromatographic measurements. Tests of several modern chromatographs proved none of them to perform as well for our purposes as the obsolete Pye Model 104. This machine has phase-angle control, no deliberate exchange of air with the surroundings and is insulated with substantial Marinite (asbestos cement) blocks.

Thermal noise can be reduced [5] by preventing exchange of air between the oven and its surroundings and by designing [6] the oven so that there is no temperature difference between the heater and the circulating air. This eliminates hot eddies. As part of this latter investigation, two methods of supplying power to the heater were devised that do not use phase-angle control; they can easily be implemented in the laboratory and adapted for most chromatographs.

There remains the problem of operating at just above atmospheric temperature. In this range the power input of the air-circulating fan in the chromatograph is sufficient to raise the temperature about 20°C. In this paper, we show that the temperature can be controlled satisfactorily just above ambient by controlling the power input to the fan. Our interest is in making sorption-effect measurements near ambient conditions, but the method will work just as well for conventional chromatography.

FAN HEATING

Baseline noise in sorption-effect chromatography has proved [5,6] to be a sensitive test of oven performance. We have demonstrated [5] the effect on noise of changing the fan speed by changing the motor voltage. We have also described [6] the use of a variable autotransformer (Variac) with negative-feedback temperature control to vary the power input to the *heater* in a chromatograph. These elements provide the basis for a method of controlling the oven temperature by varying the power dissipated by the fan.

The Pye Model 104 chromatograph has a two-speed fan. The speed is changed by switching between tappings on a transformer. The blades of the fan increase the temperature of the air inside the oven because of friction. The Pye Model 104 oven will attain a temperature about 17°C above ambient with the fan at full speed and about 12°C above on the low-speed setting. There is a range of fan speed above the speed at which the fan stalls for which the oven performance is satisfactory, so it is possible to control the temperature by varying the fan speed.

In the work reported here, a Variac adjusts the power supplied to the *fan* to maintain the oven temperature. A Eurotherm 821 three-term electronic controller is used to adjust the rotor position of the Variac by means of a servo motor and gear box. The temperature in the oven is sensed by a platinum resistance thermometer. The controller compares the measured value

with its set point and adjusts the Variac to eliminate the error. The Variac supplies power to the fan motor and thus adjusts the fan speed to keep the temperature constant. Almost all the mechanical energy produced by the fan motor is dissipated as heat in the oven. Full details of the servo-system are reported elsewhere [6]. Depending on the design of the motor, there are many ways of controlling fan speed. It was convenient to use the servo-driven Variac "because it was there" but also because the motor was suitable for voltage speed control. The chromatograph could still be used in the usual way by connecting the thermometer to the chromatograph's own controller and setting the fan speed manually. The limits of this system are that the fan will stop if the voltage is too low and if the fan speed is too fast there are problems with random temperature fluctuations caused by the air turbulence. The fan motor voltage at zero controller input was adjusted to the minimum at which the fan kept moving by moving the Variac shaft gear relative to the gearbox output-shaft gear. The maximum speed could be set by a controller adjustment that limits the maximum output.

The three-term (PID, proportional, integral, derivative) Eurotherm 821 controller has 12-bit resolution (4096 divisions) over the configured temperature range. This was altered from 0–500°C to 0–100°C by reconfiguring the controller in set-up mode to give 40 divisions per degree instead of 8 divisions per degree. Two resistors, 1 kΩ and 1.5 kΩ, were connected in series across the controller output terminals to act as a potential divider and the servo control-system input was connected across the 1 kΩ resistor. This meant that instead of the controller output being 0 (0%)–5 V (100%) and giving the corresponding Variac arm movement (162° ≈ 130 V a.c.) via the servo control unit, the controller output becomes 0 (0%)–2 V (100%) thereby reducing the maximum arc through which the arm can move to approximately 65° (≈50 V a.c.). The change in the output of the Variac to a 1% change in the control signal is 0.5 V a.c. with this modification compared to 1.3 V a.c. with the previous [6] configuration.

There are several recognised ways [7,8] of finding initial controller settings to be used as the starting point and improved by trial and error. The methods involve simple tests whose object is to give an idea of the system dynamics. One such is to measure "the process reaction curve" obtained by making a step change in the voltage applied to the fan motor. The reaction curve (Fig. 3) looks like the sum of two exponential rises to limits, one being a rapid but modest rise the other being a slow but much larger rise. What is probably happening is that the power supply to the circulating air starts to change the air temperature rapidly but that heat then starts to be used to heat the heavy oven walls thus slowing the process. In these circumstances (no dead time) it would be expected [7,8] that proportional (or proportional-plus-integral) control could be used with high gain (and high reset rate if integral action is employed). The absence of any effective dead time was confirmed by increasing the gain. In the presence of dead time, this would make the temperature oscillate. It was not possible to cause oscillations. With the controller set to the most favourable control settings found, the temperature is only controllable within half a degree of setpoint but the drift is slow and little thermal noise is seen in sorption-effect measurements. The setpoint may be only a few degrees above ambient temperature (most commercial ovens have a minimum operating temperature that is ten degrees or so above ambient). Unless the oven application requires a very accurately set temperature this is not a problem. The advantage of this system for sorption-effect chromatography is that the temperature changes are smooth and slow and do not

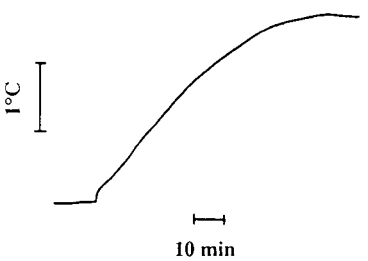

Fig. 3. A process reaction curve showing the temperature rise caused by a step change in the voltage applied to the heater fan of a Pye Model 104 chromatograph. There is no dead time.

disturb the flow as would the power pulses shown in Fig. 2. The temperature change while a chromatogram is recorded is very small. The system could perhaps be used in conjunction with a conventional heater for operation at higher temperatures. A constant voltage could be applied to the conventional heating element to set the temperature roughly. The fan speed could then be used to fine tune the temperature. It would also be possible to programme the temperature by programming the controller set point.

REFERENCES

1 G.K. Ashbury, A.J. Davies and J.W. Drinkwater, *Anal. Chem.*, 29 (1957) 918–925.
2 B.A. Buffham, G. Mason and R.I. Meacham, *J. Chromatogr. Sci.*, 24 (1986) 265–269.
3 B.A. Buffham, G. Mason and R.I. Meacham, *Proc. Roy. Soc. Lond.*, A440 (1993) 291–301.
4 F. Munari and S. Trestianu, *J. Chromatogr.*, 279 (1983) 457–472.
5 R.I. Meacham, M.J. Heslop, B.A. Buffham and G. Mason, *J. Chromatogr. Sci.*, 31 (1993) 409–415.
6 R.I. Meacham, B.A. Buffham, G. Mason and D.W. Drott, *Trans. Instn. Chem. Engrs., A., Chem. Eng. Res. Des.*, 72 (1994), in press.
7 D.R. Coughanowr and L.B. Koppel, *Process Systems Analysis and Control*, McGraw-Hill, New York, 1965.
8 T.C. Wherry and E.C. Miller, in R.H. Perry and C.H. Chilton (Editors), *Chemical Engineers' Handbook*, McGraw-Hill, New York, 5th ed., 1973, Section 22, pp. 24–27.

Journal of Chromatography A, 659 (1994) 209–212
Elsevier Science B.V., Amsterdam

CHROM. 25 538

Short Communication

Sensitivity enhancement in dynamic "off-line" supercritical fluid extraction

Jiří Vejrosta*, Alena Ansorgová and Milena Mikešová

Institute of Analytical Chemistry, Academy of Sciences of the Czech Republic, Veveří 97, 611 42 Brno (Czech Republic)

Keith D. Bartle

University of Leeds, School of Chemistry, Leeds LS2 9JT (UK)

(First received April 14th, 1993; revised manuscript received August 1st, 1993)

ABSTRACT

A method for analytical supercritical fluid extraction in "off-line" mode was developed with the aim of obtaining maximum sensitivity, *i.e.* maximally concentrated solute solutions after extraction without further concentration steps. Dry deposition on the inner capillary wall was used, followed by rinsing of the trapped solutes using a minimum volume of the solvent. For the case of an inert support (glass beads) spiked with fluoranthene, the reproducible minimal volume of the solvent was determined and the influence of flow velocity in the trapping capillary was studied.

INTRODUCTION

At present, supercritical fluid extraction (SFE) is one of the fastest developing analytical sample preparation techniques [1,2]. Among the problems encountered in SFE, efficient trapping of analytes from the depressurized supercritical fluid is still difficult to achieve. Two modes of SFE, "on-line" and "off-line", are practised. When comparing these methods, the overall higher sensitivity of the "on-line" mode and the reproducibility of sampling in "off-line" mode have been emphasized. One way to increase the sensitivity in "off-line" SFE is to decrease the solvent volume in which extracted analytes are dissolved, so as to avoid further concentration steps, during which serious losses of solutes can occur. At the same time the high trapping efficiency must be maintained. This paper reports a new approach to trapping in SFE.

Analyte trapping into a liquid solvent [3–7] is one of three commonly used collection methods. The end of the restrictor is immersed in a vial filled with liquid solvent, in which the analytes are to be trapped, and the decompressed fluid bubbles through the liquid and vents to the atmosphere. The liquid solvent (usually methylene chloride, methanol or hexane) must be compatible with the analytes of interest and the flow of the decompressed fluid maintained below a certain limit, at which violent bubbling of the liquid solvent can lead to analyte loss. The vial is often cooled to decrease solvent evaporation.

* Corresponding author.

0021-9673/94/$07.00
SSDI 0021-9673(93)E0961-S

The solvent volumes used in this method are usually larger than 1 ml.

Collection on solid sorbents [8–12] may involve three trapping mechanisms —cryogenic trapping, adsorption and absorption. Chromatographic solid supports are mainly used as packing material. The recoveries of analytes depend on the combination of trapping and rinsing efficiencies. The solvent volumes in this case are also rarely less than 1 ml.

Trapping on solid surfaces is the best way to decrease the solvent volume and obtain more concentrated solutions in dynamic SFE, without further concentration steps. The reason why this collection method is not used more widely follows from the character of the expanding solute–fluid mixture, in which the formation of solute particles [13] and aerosols has been confirmed. Inefficient trapping in an open glass bulb [14] of 100 ml volume is hardly surprising.

On the other hand, this collection system is successfully used in "on-line" SFE–GC, in which analytes are cryogenically focused on the wall of metal or fused-silica capillaries. The question thus arises as to why this method is not also used in "off-line" dynamic SFE. The aim of this work is to verify this approach, in which flash heating after cryogenic focusing is replaced by solvent rinsing of analytes from capillary walls into a glass microvial.

EXPERIMENTAL

The device used in the work is schematically shown in Fig. 1. A personal computer-based syringe pump HP 5001 (Laboratory Devices, Prague, Czech Republic) is connected through an on–off valve to the extraction vessel, which is inserted into a thermostatically controlled aluminium tube. The temperature was maintained at 50°C in all experiments. The internal volume of the extraction vessel was approximately 2.5 ml, but in all cases a replaceable cartridge of internal volume 0.6 ml was used. The cartridge was packed with glass beads (∅ *ca.* 0.2 mm) held in place by glass wool plugs. The glass beads were spiked with standard solutions of fluoranthene in tetrachloromethane. The absolute amounts of fluoranthene were in the range 5–20 μg.

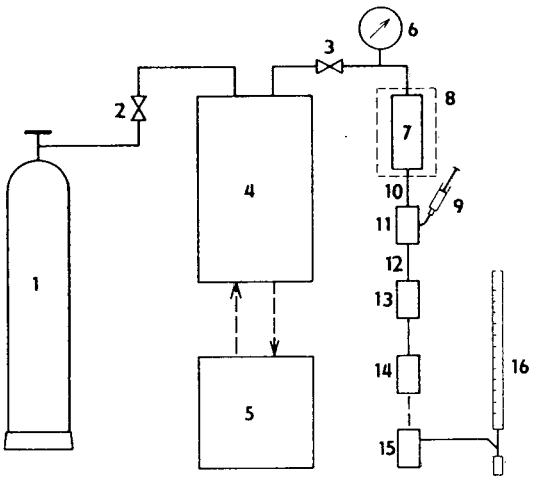

Fig. 1. Schematic diagram of SFE device. 1 = Tank of CO_2; 2,3 = "on–off" valves; 4 = syringe pump; 5 = personal computer; 6 = pressure gauge; 7 = extraction cell; 8 = metal (aluminium) oven; 9 = syringe; 10 = restrictor; 11 = connecting union; 12 = trapping capillary; 13 = heater; 14 = cryofocuser; 15 = vials, 16 = bubble flowmeter.

Supercritical pressures were maintained inside the extraction cartridge by using capillary restrictor–fused-silica tubing (I.D. 17 μm, lengths from 10 to 25 cm).

The sample trap (see Fig. 2) consisted of fused-silica tubing (30 cm × 500 μm I.D.) into which the capillary restrictor was inserted through the connection union. This allowed injection of an arbitrary amount of a suitable solvent to wash out the trapped analytes into a glass microvial. The flow-rate of CO_2 was measured by a bubble flowmeter at ambient conditions. All GC–flame ionization detection (FID) analyses were performed by using a CHROM-5 gas chromatograph (Laboratory Devices) on a packed SE-30 column.

RESULTS AND DISCUSSION

The proposed analyte collection method for "off-line" SFE consists of two steps: the trapping of the analytes onto an inner surface of the capillary (*ca.* 500 μm I.D.) and their subsequent washing from the capillary inner surface by a

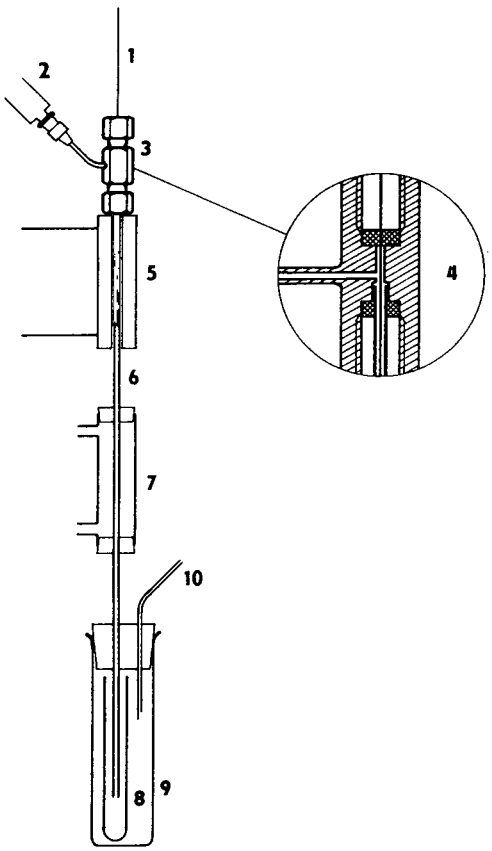

Fig. 2. Schematic representation of the trapping system. 1 = Restrictor; 2 = syringe; 3 = connecting union; 4 = detailed inner configuration of the connecting union; 5 = heater; 6 = trapping capillary; 7 = cryofocuser; 8,9 = vials; 10 = output of CO_2.

small volume of solvent into a glass microvial. There are several experimental parameters on which the efficiency of the entire process could depend and which can be summarized as follows:

(a) Parameters related to the trapping step: (1) type of sample and its matrix concentration; (2) extraction conditions (type of extracting fluid, pressure, temperature); (3) type of restrictor used; (4) linear velocity of gas in the trapping capillary; (5) length and diameter of the trapping capillary; (6) surface properties and temperature.

(b) Parameters related to the rinsing step: (7) type of solvent; (8) volume of solvent used for rinsing; (9) timing of rinsing process.

The two steps cannot be studied separately, and only the efficiency of the entire process can be determined. In this preliminary work, the influence of the linear velocity of the expanding gas in the trapping capillary on the percentage recovery of fluoranthene has been studied.

TABLE I

DEPENDENCE OF PERCENTAGE RECOVERIES ON LINEAR VELOCITIES IN THE TRAPPING CAPILLARY AT DIFFERENT PRESSURES

Restrictor length 30 cm, spiked amount 5 μg.

Pressure (MPa)	Linear velocity (cm/s)	Extraction time (min)	Recovery (%)
13.8	102	40	99
16.6	136	20	97
19.4	157	15	101
22.0	201	10	95
24.6	212	10	94

The percentage recoveries in Tables I and II are averages of two extractions, and the concentration of fluoranthene in each extracted sample was determined as an average of three subsequent analyses. Different linear velocities were obtained through different extraction pressures (Table I) or by the use of restrictors of different length (Table II). In both cases up to linear velocities of *ca.* 2 m/s, fluoranthene was practically quantitatively trapped. The spiked amount of fluoranthene was 5 μg (Table I) and was

TABLE II

DEPENDENCE OF PERCENTAGE RECOVERIES ON LINEAR VELOCITIES IN THE TRAPPING CAPILLARY AT DIFFERENT RESTRICTOR LENGTHS

Pressure 22.0 MPa, spiked amount of fluoranthene 20 μg.

Restrictor length (cm)	Linear velocity (cm/s)	Extraction time (min)	Recovery (%)
25	113	20	98
20	126	15	100
15	151	15	96
10	253	10	97

increased to 20 μg (Table II) with no effect on resulting recoveries. The rinsing solvent volume was 100 μl.

The reproducibility of this collection mode was determined by ten repeated extractions, keeping all parameters at constant values (linear velocity ≈ 1 m/s, spiked amount 20 μg). When 100 μl of tetrachloromethane were used, an average percentage recovery 96% with R.S.D. 3.4% was obtained.

The same series of experiments were performed with a washing volume of 50 μl with effectively the same results. This value is the practical limiting volume when a capillary of *ca.* 500 μm I.D. is used, and repeated analyses must be carried out.

CONCLUSIONS

A new method of analyte collection after off-line SFE is proposed. A fused-silica capillary (*ca.* 500 μm I.D.) was used as the trap, followed by analyte rinsing with a small volume of appropriate solvent (*ca.* 100 μl). The method proved to be efficient for the quantitative trapping of a test substance (fluoranthene) (*ca.* 95%). Quantitative rinsing of fluoranthene with a smaller volume of tetrachloromethane (50 μl) from the trapping capillary resulted in an increase in the concentration within the solution.

Future work will involve the application of this technique to samples of varying volatilities. The influence of a number parameters, discussed above, must also be tested.

REFERENCES

1 S.B. Hawthorne, *Anal. Chem.*, 62 (1990) 633A–642A.
2 T.L. Chester, J.D. Pinkston and D.E. Raynie, *Anal. Chem.*, 64 (1992) 153R–170R.
3 S.B. Hawthorne and D.J. Miller, *Anal. Chem.*, 59 (1987) 1705–1708.
4 V. Lopez-Avila, N.S. Dodhiwala and W.S. Beckert, *J. Chromatogr. Sci.*, 28 (1990) 468–476.
5 N. Alexandrou and J. Pawliszyn, *Anal. Chem.*, 61 (1989) 2770–2778.
6 S.K. Nam, S. Kapila, D.S. Viswanath, T.E. Clevenger, J. Johansson and A.F. Yanders, *Chemosphere*, 19 (1989) 33–38.
7 S.K. Nam, S. Kapila, A.F. Yanders and R.K. Puri, *Chemosphere*, 20 (1990) 871–880.
8 M.M. Schantz and S.N. Chesler, *J. Chromatogr. Sci.*, 363 (1986) 397–401.
9 J.L. Hedrick and L.T. Taylor, *J. High Resolut. Chromatogr.*, 13 (1990) 312–316.
10 L.J. Mulcahey, J.L. Hedrick and L.T. Taylor, *Anal. Chem.*, 63 (1991) 2225–2232.
11 R.M. Smith and M.D. Burford, *J. Chromatogr.*, 600 (1992) 175–181.
12 J.M. Levy, R.M. Ravey, R.K. Houck and M. Ashraf-Khorassani, *Fresenius' J. Anal. Chem.*, 344 (1992) 517–520.
13 R.D. Smith, J.L. Fulton, R.C. Petersen, A.J. Kopriva and B.W. Wright, *Anal. Chem.*, 58 (1986) 2057–2064.
14 B.W. Wright, Ch. W. Wright, R.W. Gale and R.D. Smith, *Anal. Chem.*, 59 (1987) 38–44.

Journal of Chromatography A, 659 (1994) 213–216
Elsevier Science B.V., Amsterdam

CHROM. 25 605

Short Communication

Gas chromatographic determination of organobromine micropollutants in air and water

Uno Mäeorg*, Lilli Paama and Heino Kokk

Institute of Chemical Physics, Tartu University, Str. Jakobi 2, EE-2400 Tartu (Estonia)

(First received April 27th, 1993; revised manuscript received September 29th, 1993)

ABSTRACT

A gas chromatographic method for the determination of organic halogen flame retardant compounds such as 1,1,3-tribromopropane (TBP) in the presence of bromoform and α-bromobutyric acid (BBA) in the presence of butyric acid in air and water was developed. The proposed method is appropriate; the determination limits for TBP are 0.5 μg l^{-1} when sampling 20 l of air and 0.1 mg l^{-1} when sampling 100 ml of water and those for BBA are 0.2 μg l^{-1} when sampling 120 l of air and 0.5 mg l^{-1} when sampling 100 ml of water.

INTRODUCTION

Organic halogen compounds (OHCs) are important chemicals in the manufacture of plastics, flame retardants, drugs, insecticides, etc. [1]. The allowable concentrations of some important OHCs such as 1,1,3-tribromopropane (TBP) and α-bromobutyric acid (BBA) have not been fixed and the determination of these compounds is not sufficiently described [2,3].

In this paper we describe a gas chromatographic method for the determination of TBP in the presence of bromoform and BBA in the presence of butyric acid in air and water. For sampling of air pollutants solid adsorbents were used and water samples were concentrated by liquid–liquid extraction.

* Corresponding author.

EXPERIMENTAL

Instruments

A Biochrom I Model 7 and a Tsvet 152 gas chromatograph equipped with a flame ionization detector were used. The columns used (glass) were as follows: (A) 3 m × 3 mm I.D. packed with 3% XE-60 on Chromaton N-Super, 100–120 mesh (Lachema, Brno, Czech Republic); (B) 3 m × 2 mm I.D. packed with 3.5% PDEAS on Chromaton N-Super, 100–120 mesh (Lachema).

Gas chromatographic conditions

For the determination of TBP column A was used. The temperatures were isothermal at 150°C for the column and 250°C for the injector and detector. The flow-rates were carrier gas (nitrogen) 30, hydrogen 30 and air 300 ml min^{-1}.

0021-9673/94/$07.00
SSDI 0021-9673(93)E1030-4

For the determination of BBA column B was used. The temperatures were isothermal at 175°C for the column and 250°C for the injector and detector. The flow rates were carrier gas (nitrogen) 20, hydrogen 30 and air 300 ml min^{-1}. The volume injected was always 2 μl.

For the sampling of OHC air pollutants, a special glass collecting device containing solid adsorbents (silica gel, charcoal) was used, in which desorption with organic solvents also can be carried out [4].

Chemicals

Silica gel of 50–200 mesh (Lachema) and charcoal of 100–150 mesh (Reakhim, Russian Federation) were purified according to the procedure described by Paama *et al.* [4].

TBP, BBA, 1-decanol, bromoform, butyric acid and myristic acid were of analytical-reagent grade. Ethanol, diethyl ether and hexane were of pure grade and distilled before use. All chemicals were purchased from Reakhim.

The concentrations of the standard solutions (in ethanol) of TBP, 1-decanol, myristic acid were 100 μg ml^{-1} and those of BBA, bromoform and butyric acid were 10 μg ml^{-1}.

Air analysis

For the preparation of standard gas mixtures of OHC, dynamic methods developed earlier [4–7] were used. Air was drawn through the sampling device at a rate of 0.7–1.0 l min^{-1}. The micropollutants TBP and BBA were adsorbed on 150–200 mg of silica gel (in a tube). The subsequent desorption was carried out with 4 ml of ethanol. Then 1 ml of internal standard solution (100 μg ml^{-1}) was added to the solution of desorbed micropollutants and gas chromatographic analysis was carried out under the conditions described above.

Water analysis

For the determination of TBP in water, the samples (100 ml) were extracted with 4 ml of *n*-hexane, then 1 ml of internal standard (1-decanol) solution (100 μg ml^{-1}) was added and 2-μl volumes of the extracts were injected into the gas chromatograph.

For the determination of BBA in water, the samples (100 ml) were extracted (pH 2) with 4 ml of diethyl ether, then 1 ml of internal standard (myristic acid) solution (100 μg ml^{-1}) was added and the gas chromatographic analysis was carried out.

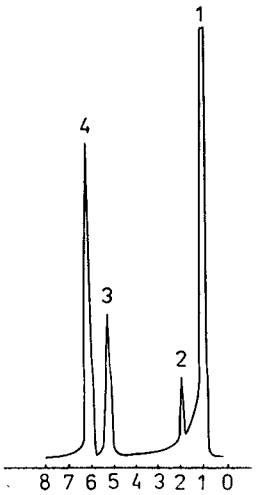

Fig. 1. Gas chromatographic separation of a solution of bromoform (2), TBP (3) and *n*-decanol (internal standard) (4) in ethanol (1). For conditions, see text. Time scale in min.

Calibration graphs for these analyses were obtained by co-injection of the analyte compounds and the internal standards.

RESULTS AND DISCUSSION

The retention times (t'_R) and separation factors (R_s) for the compounds investigated were calculated (see Figs. 1 and 2 and Table I). The results

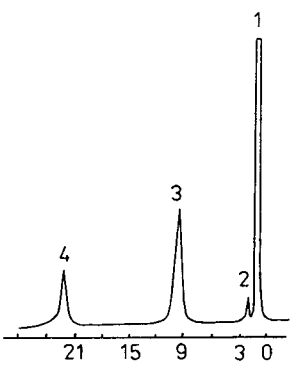

Fig. 2. Gas chromatographic separation of a solution of butyric acid (2), BBA (3) and myristic acid (internal standard) (4) in ethanol (1). For conditions see text. Time scale in min.

TABLE I

RETENTION TIMES AND SEPARATION FACTORS FOR GAS CHROMATOGRAPHIC DETERMINATION OF TBP IN PRESENCE OF BROMOFORM AND BBA IN PRESENCE OF BUTYRIC ACID

Column	Substance	Retention time, t'_R (min)	Separation factor, R_s [a]
A	(1) TBP	5.5	5.8 (1–2)
	(2) Bromoform	2.3	7.3 (2–3)
	(3) *n*-Decanol (internal standard)	6.5	1.6 (1–3)
B	(4) BBA	11.3	6.3 (4–5)
	(5) Butyric acid	1.8	9.3 (5–6)
	(6) Myristic acid (internal standard)	21.3	1.9 (4–6)

[a] Compound numbers in parentheses.

in Table I show that the separation of TBP in the presence of bromoform and BBA in the presence of butyric acid was satisfactory.

A dynamic method was developed for the preparation of a standard gas mixture of TBP, bromoform, BBA and butyric acid [4]. The diffusion tubes contained the pure compounds that were used to prepare the standards. The gas mixing system was maintained at a constant temperature (±0.02°C) for the diffusion tubes and carrier gas. Measurement of the actual diffusion rate was easily achieved. The basic principle of operation is the gravimetric measurement of the mass loss from the device. The volumetric flow through the gas mixing system was monitored using flow meters.

The concentration of TBP in the standard gas mixture was 0.44–29.48 $\mu g\ l^{-1}$ and that of BBA

TABLE II

RESULTS OF GAS CHROMATOGRAPHIC DETERMINATION OF TBP IN AIR AND WATER

Sample	Concentration of TBP in standard gas mixture ($\mu g\ l^{-1}$) or in water ($mg\ l^{-1}$)	Sample volume of air (l) or water (ml)	Measured concentration ($P = 0.95$, $n = 5$) [a]			
			$\bar{C}$	S_c	S_r (%)	$\pm\frac{tS}{\sqrt{n}}$ [b]
Air ($\mu g\ l^{-1}$)	0.44	20	0.45	0.09	0.20	0.11
	3.25	10	3.30	0.41	0.13	0.52
	7.78	10	7.72	0.83	0.11	1.03
	14.08	10	14.40	1.49	0.10	1.86
	29.48	5	29.32	2.80	0.09	3.48
Water ($mg\ l^{-1}$)	0.10	100	0.09	0.017	0.19	0.021
	0.25	100	0.24	0.03	0.13	0.040
	0.50	100	0.51	0.06	0.11	0.072
	1.00	100	1.02	0.10	0.10	0.13
	2.00	100	1.98	0.16	0.08	0.20

[a] $\bar{C}$ = Mean result ($n = 5$); C_c = standard deviation; S_r = relative standard deviation.
[b] Confidence limit.
[c] Concentration of bromoform = 5.5–10.0 $\mu g\ l^{-1}$.
[d] Concentration of bromoform = 10 $mg\ l^{-1}$.

TABLE III

RESULTS OF GAS CHROMATOGRAPHIC DETERMINATION OF BBA IN AIR AND WATER

Sample	Concentration of TBP in standard gas mixture ($\mu g\ l^{-1}$) or in water ($mg\ l^{-1}$)	Sample volume of air (l) or water (ml)	Measured concentration ($P = 0.95$, $n = 5$) [a]			
			$\bar{C}$	S_c	S_r (%)	$\pm\frac{tS}{\sqrt{n}}$ [b]
Air ($\mu g\ l^{-1}$)	0.42	100	0.40	0.048	0.12	0.06
	2.10	100	2.20	0.28	0.13	0.35
	9.20	10	9.0	0.81	0.09	1.08
	16.40	10	15.8	1.51	0.10	1.87
Water ($mg\ l^{-1}$)	0.25	100	0.24	0.034	0.14	0.04
	0.50	100	0.52	0.062	0.12	0.08
	1.0	100	0.98	0.108	0.11	0.01
	2.0	100	2.02	0.20	0.10	0.02
	4.0	100	3.90	0.35	0.09	0.04

[a,b] See Table II.
[c] Concentration of butyric acid = 5 $\mu g\ l^{-1}$.
[d] Concentration of butyric acid = 2 $mg\ l^{-1}$.

was 0.42–16.40 $\mu g\ l^{-1}$. The concentration of bromoform was 5.5–10 $\mu g\ l^{-1}$ and that of butyric acid 5.0 $\mu g\ l^{-1}$.

Satisfactory results were obtained for the determination of TBP and BBA in air (Tables II and III). The relative standard deviation was 0.09–0.20% [8].

The concentration of TBP in the water samples was 0.10–2.00 $mg\ l^{-1}$ and that of BBA was 0.25–0.40 $mg\ l^{-1}$. The concentration of bromoform in the water was 10 $mg\ l^{-1}$ and that of butyric acid was 2 $mg\ l^{-1}$ (Tables II and III). The relative standard deviation for the determination of TBP and BBA in water samples was 0.09–0.19%.

CONCLUSIONS

The proposed gas chromatographic method is appropriate for the determination of the micropollutants TBP and BBA in air and water. The determination limits for the gas chromatographic determination of TBP in the presence of bromoform are 0.5 $\mu g\ l^{-1}$ when sampling 20 l of air and 0.1 $mg\ l^{-1}$ when sampling 100 ml of water. The determination limits for the gas chromatographic determination of BBA in the presence of butyric acid are 0.2 $\mu g\ l^{-1}$ when sampling 120 l of air and 0.50 $mg\ l^{-1}$ when sampling 100 ml of water.

REFERENCES

1 G.C. Tesoro, *J. Polym. Sci.*, 13 (1978) 273.
2 K. Bayermann, *Organic Trace Analysis*, Ellis Horwood, Chichester, 1984.
3 B.V. Gidaspov, I.G. Zenkevitch and A.A. Rodin, *Usp. Khim.*, 58 (1989) 1409.
4 L.A. Paama and H.J. Kokk, *Zh. Anal. Khim.*, 40 (1985) 2062.
5 Y.L. Haldna, H.J. Kokk, A.E. Anijalg and M.O. Steinberg, *Russ. Pat.*, 814444 (1980).
6 L.A. Paama, U.J. Mäeorg and H.J. Kokk, *Zh. Anal. Khim.*, 43 (1988) 904.
7 L. Paama, H. Kokk and U. Mäeorg, in H. Meinander (Editor), *Textiles and Composites '92*, Technical Research Centre of Finland (VTT), Espoo, 1992, p. 133.
8 J.C. Miller and J.N. Miller, *Statistics for Analytical Chemistry*, Wiley, New York, 1988.

Journal of Chromatography A, 659 (1994) 217–222
Elsevier Science B.V., Amsterdam

CHROM. 25 575

Short Communication

Sheathless capillary electrophoresis–electrospray ionization mass spectrometry using 10 μm I.D. capillaries: analyses of tryptic digests of cytochrome *c*

Jon H. Wahl, David C. Gale and Richard D. Smith*

Chemical Methods and Separations Group, Chemical Sciences Department, Pacific Northwest Laboratory, Richland, WA 99352 (USA)

(First received July 22nd, 1993)

ABSTRACT

The analyses of tryptic digest of proteins present a difficult challenge to the analytical chemist due to the wide range of molecular masses and hydrophobicities of the peptides produced. In this study, we demonstrate the separation of tryptic digests of bovine, *Candida krusei* and equine cytochrome *c* using a new electrospray ionization (ESI) interface for CE–MS that does not require additional sheath make-up fluid or mechanical assistance to aid the ESI process. The utility of this new CE–ESI-MS interface is demonstrated using a 10 μm I.D. CE capillary where the injected sample amounts are in the 30 femtomole (of protein) region. The CE electroosmotic flow rates when aminopropylamine treated capillaries are utilized are in the 10 nl/min region for a relatively conductive buffer system (0.01 *M* ammonium acetate–acetic acid buffer system, pH 4.4 and a 300 V/cm field strength).

INTRODUCTION

In the development of analytical techniques for biochemical identification and quantitation, intense effort has been directed to increased solute detectability and sensitivity, because sample size is often limited or obtained at great effort. The application of capillary electrophoresis (CE) to biochemical analyses has led to increasing demand for detection methods that are more sensitive and that provide component information. In principle, mass spectrometry (MS) is recognized as a nearly ideal detector for analytical separations; however, in practice it has not generally been considered adequately sensitive when compared with techniques such as laser induced-fluorescence [1–3] or electrochemical detection [4]. For CE, these methods have demonstrated detection limits at the zeptomole (10^{-21} mole) level; however, compound identification is generally determined by comparison between standard and unknown solute electrophoretic mobilities, which requires a high degree of precision. Consequently, a major advantage of MS detection for CE is that component identification can readily be achieved without the need for precise mobility measurements.

Presently, the technique that is used to interface CE with MS is often a critical feature for the success or failure of a CE–MS experiment. Electrospray ionization (ESI) has gained accept-

* Corresponding author.

0021-9673/94/$07.00
SSDI 0021-9673(93)E1005-K

ance as the interface method of choice to combine CE with MS. This acceptance is due to the variety of approaches that have been developed for CE-ESI–MS interfaces, which allow the CE separation to occur relatively unperturbed by the method of establishing and maintaining electrical contact at the CE capillary terminus. In the first CE–MS interface reported electrical contact was made by the use of silver metal deposition onto the fused-silica capillary terminus [5]. The metalized capillary terminus served to define the CE field strength along the capillary and also as the electrospray electric field by having the terminus at a voltage of 3 to 5 kV relative to the mass spectrometer inlet. In a subsequent design, a coaxial sheath liquid was introduced; this served to establish the electrical contact with the CE effluent and facilitate the electrospray process [6]. Another variation on the CE–MS interface was introduced by Henion and co-workers [7], in which a liquid-junction was used to establish electrical contact with the analytical capillary and provide an additional make-up flow to the buffer. A disadvantage of both the latter two approaches is that they depend upon an additional flow of liquid that contains charge-carrying species, which will generally degrade solute detectability and sensitivity [8]. The relative contributions to the electrospray ion current arising from the sheath flow become greater as the capillary I.D. is decreased. Because improving CE–MS sensitivity is generally recognized as an important goal to the further utility of CE–MS in biological analyses, interest remains in the development of more sensitive CE–MS instrumentation based upon alternative interface designs that are simple, versatile and more reliable. In this report we demonstrate the utility of CE–ESI-MS using a chemically modified 10 μm I.D. capillary for the analysis of tryptic digests of three proteins using a new ESI interface that does not use a liquid sheath, but has similarities to the first CE–MS interface design.

EXPERIMENTAL

In this work, a fused-silica capillary of 10 μm I.D., *ca.* 150 μm O.D., and approximately 50 cm in length was utilized (Polymicro Technologies, Phoenix, AZ, USA). The inner wall of the capillary was chemically treated with 3-aminopropyltrimethoxysilane (Aldrich, Milwaukee, WI, USA) [8,9], in a manner similar to that described by Bruin *et al.* [10], and previously reported by Lukacs [11]. To taper the outlet of the analytical capillary, the polyimide coating was removed from approximately one centimeter of the capillary terminus, and the exposed fused silica was etched with a 40% hydrofluoric acid solution (Aldrich). The buffer system used in the experiments was a 0.01 *M* ammonium acetate–acetic acid solution, pH 4.4. The CE electrical field strength used for all experiments is -300 V cm^{-1}.

The capillary electrophoresis instrument used for this work was constructed at our laboratory and has been discussed previously [8,9]. The CE system is interfaced to a modified Sciex TAGA 6000E triple quadrupole mass spectrometer (Thornhill, Ontario, Canada) through an electrospray ionization interface as previously described [12]. The mass spectrometer was scanned from m/z 600–1200 in 2-m/z steps at 0.6 s/scan in all experiments. The electrospray interface was constructed by applying a silver conductive coating (Epoxy Technology, Billerica, MA, USA) to the analytical capillary terminus. In addition, a gold conductive coating has also been successfully demonstrated for use in the electrospray interface [13]. The electrospray is produced using a potential difference of approximately $+2.5$ kV between the capillary terminus and the MS sampling orifice. Coaxial to the analytical capillary, a sheath gas of sulfur hexafluoride (SF_6) was used to suppress corona discharge. The CE–ESI-MS interface region is schematically illustrated in Fig. 1.

The samples chosen for this work were tryptic digests of bovine, *Candida krusei* and equine cytochrome *c*. The proteins were used as purchased (Sigma, St. Louis, MO, USA) without further purification. The tryptic digests utilized an enzyme-to-substrate ratio of approximately 1:25 in 0.05 *M* ammonium bicarbonate (pH 8.3) solution at 37°C for 18 h. Electrokinetic injection at -20 V cm^{-1} for approximately 5 s for each digest was utilized for the separations, which consumed approximately 30 femtomoles of original protein.

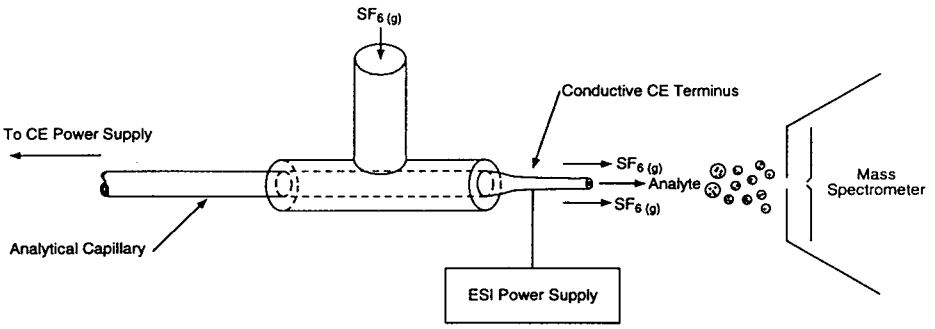

Fig. 1. Schematic illustration of the electrospray ionization interface used for the CE–ESI-MS experiments. See text for further discussion.

RESULTS AND DISCUSSION

The complex mixture of peptides produced from the tryptic digestion of proteins presents a difficult challenge to the analytical chemist due to the wide range of solute molecular masses and hydrophobicities encountered. The proper choice of a buffer system is essential to achieve a successful separation. Moreover, the success of the CE–ESI-MS analysis depends upon many factors, including the electrospray interface, buffer composition, and solute interaction with the inner surface of the analytical capillary. Specifically in CE–ESI-MS, analyte detectability and sensitivity can vary significantly with buffer composition and concentration. In general, the optimum analyte signal obtained for CE–ESI-MS occurs when volatile buffer systems are utilized at the lowest practical concentration. Conversely, when large quantities of ionic buffer species are delivered to the electrospray source, the analyte is not efficiently ionized by the electrospray process, and analyte detectability is greatly reduced. As a result, the ideal ionization process for a CE–ESI-MS system occurs when the number of charge carrying species to the ESI source is supplied at a rate that is equal to or less than that necessary to maintain the maximum electrospray current normally achievable. Previously, we have demonstrated that the use of small I.D. capillaries offers a simple method to control the number of ionic species entering the electrospray source during a CE–ESI-MS experiment [8,9].

The total ion electropherograms obtained from the tryptic digests of bovine, *Candida krusei* and equine cytochrome *c* and using this new CE–ESI-MS interface are shown in Fig. 2. Each separation utilized a 0.01 *M* ammonium acetate–acetic acid buffer system (pH 4.4) and a 10 μm I.D. analytical capillary. From Fig. 2, each analysis was complete within six minutes, although greater separation resolution could have been obtained using longer capillaries. From the mass spectrometric data, however, peaks corresponding to singly or multiply protonated molecular ions of the individual tryptic fragments can be isolated. For example, shown in Fig. 3 are examples of extracted ion electropherograms for the individual tryptic fragments YIPGTK (*m/z* 678), which is a tryptic fragment common to all three proteins, EDLIAYLK (*m/z* 964), which is common to bovine and equine cytochrome *c*, and MAFGGLK (*m/z* 723), which is specific to *Candida krusei* cytochrome *c*. The three extracted ion electropherograms show additional solute zones of the same *m/z* as the tryptic fragments. These additional zones are likely due to collisional dissociation of other tryptic fragments or intact protein during transport into the MS.

An important characteristic of ESI is that under appropriate conditions intact molecular ions are formed with little dissociation, unless created during transport into the MS. As a result, molecular mass measurements for large biomolecules that exceed the instrumental MS mass range can be obtained because their ESI mass spectra generally consist of a distribution of molecular ion charge states that are in the MS

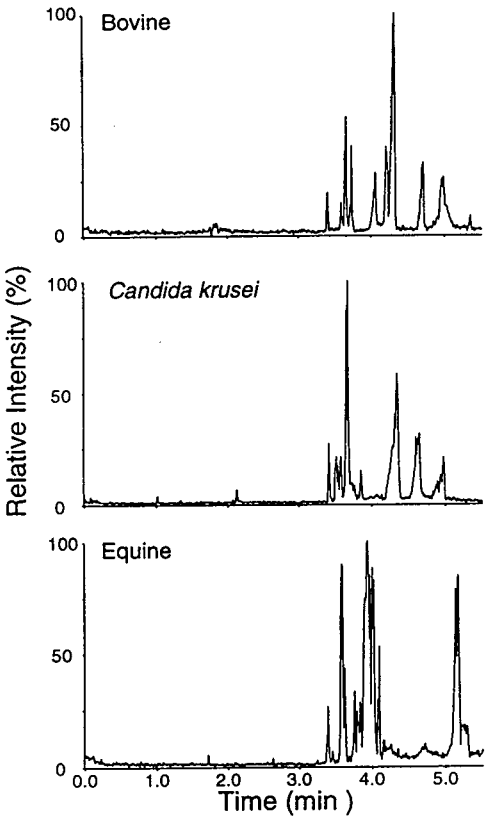

Fig. 2. Total ion electropherograms obtained from tryptic digests of bovine, *Candida krusei* and equine cytochrome *c* . Separation conditions: 0.01 *M* ammonium acetate–acetic acid buffer system, pH 4.4; capillary: 10 μm I.D., 50 cm in length and chemically modified with 3-aminopropyltrimethoxysilane; electric field, -300 V cm^{-1}; injection: 5 s at -1 kV; concentration of original proteins: *ca.* 750 μg/ml; mass spectrometer: scanning from *m/z* 600–1200, 2-*m/z* steps, 0.6 s/scan.

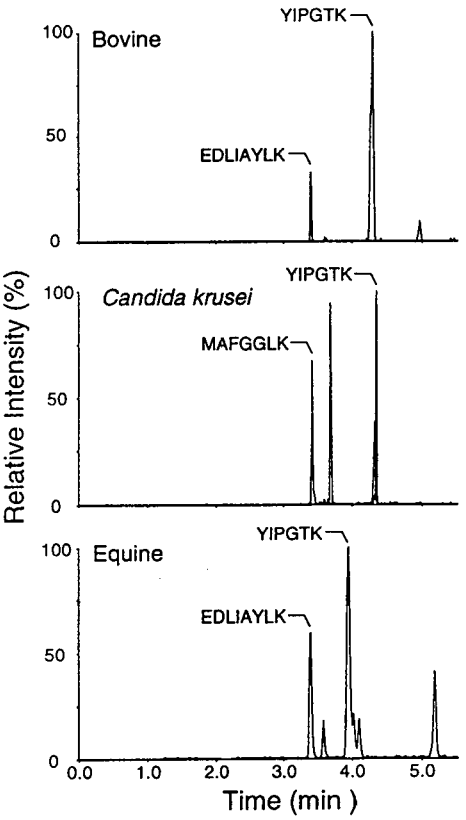

Fig. 3. Extracted ion electropherograms obtained from Fig. 2 for the individual tryptic fragments YIPGTK (*m/z* 678), which is a tryptic fragment common to all three proteins, EDLIAYLK (*m/z* 964), which is common to bovine and equine cytochrome *c*, and MAFGGLK (*m/z* 723), which is specific to *Candida krusei* cytochrome *c*. The additional solute zones of the same *m/z* as the tryptic fragments are likely due to incomplete digestion and fragmentation of other tryptic fragments occurring during transport to the mass spectrometer.

mass range [14,15]. This distribution of molecular ion charge states for peptides and proteins, which generally arises from protonation of basic residue sites for positive ion ESI, yields a distinctive pattern of peaks due to the discrete nature of the electronic charge, where adjacent peaks vary by one charge. Generally, the peptides that result from a tryptic digest produce singly and doubly charged molecular ions during the ESI process. To determine the molecular mass of a specific solute zone in a separation, this extremely small charge state distribution must first be recognized, which may be difficult because the distribution may not be within the instrumental mass range or because additional mass spectra peaks, which exist due to dissociation in the MS interface, may interfere. This lack of a definable charge distribution can make mass spectra assignment and component identification ambiguous unless higher MS resolution is used to determine exact molecular ion charge states. Fortuitously, the use of the silver conductive CE terminus can produce silver adducts (addition of *ca.* 108 u) with each molecular species. These adducts are formed at the electrospray tip where the oxidation of silver occurs in a manner de-

scribed previously [16]. As a result, the charge state for a known or unknown MS peak may be determined when silver adducts are present without the necessity of greatly degrading sensitivity to obtain resolution sufficient for molecular ion charge state determination. From the charge state information the actual molecular mass of the tryptic fragment can be determined within the precision of the MS measurement and with greater accuracy than with contaminant adduction such as sodium, which may not be resolved under all CE–ESI-MS conditions. For example, the mass spectra obtained from the bovine tryptic fragments of TGQAPGFSYTDANK (M_r 1457), which is observed at 3.7 min in the electropherogram, and of KTGQAPGFSYTDANK (M_r 1585), which is observed at 4.1 min, are illustrated in Fig. 4. The

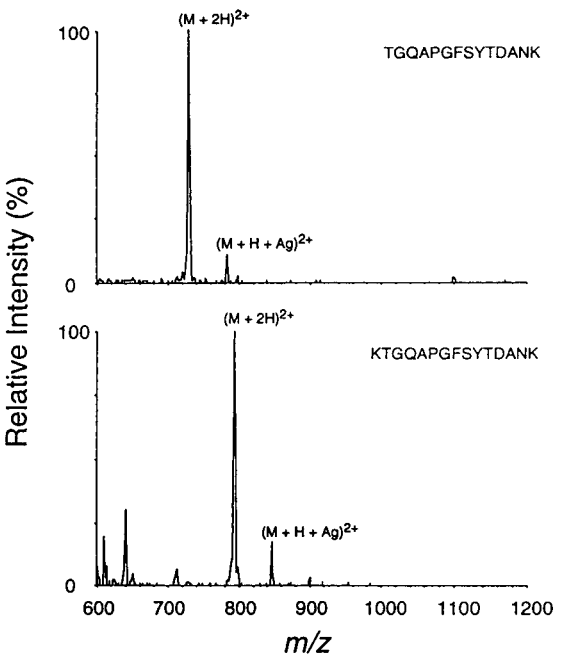

Fig. 4. Mass spectra obtained from the bovine tryptic fragments of TGQAPGFSYTDANK (M_r 1457, observed at 3.7 min) and of KTGQAPGFSYTDANK (M_r 1585, observed at 4.1 min). The singly charged species of both solutes is greater than can be observed with the MS instrument used However, because of the silver capillary terminus, both mass spectra show an additional peak that is approximately 54 greater than the base peak. Consequently, the base peak in each mass spectra is presumed to be the doubly charged molecular ion, $(M + H + Ag)^{2+}$.

molecular mass of both solutes is greater than can be observed with the MS instrument used; consequently, the singly charged species can not be detected, but the doubly charged species is observed. Moreover, because of the silver capillary terminus, both mass spectra show an additional peak that is approximately 54 m/z units greater than the molecular ion. As a result, the base peak in each mass spectrum is presumed to be the doubly charged molecular ion because this second peak is a multiple of two greater relative to silver (*ca.* 108 u) addition. Accordingly, the use of a silver-metalized capillary terminus has the advantage that exact charge states may be determined for solutes under certain conditions.

CONCLUSIONS

The results shown in this report demonstrate several important findings. First, this new CE–ESI–MS interface can produce and maintain a stable electrospray signal during a CE–ESI–MS experiment without additional sheath or make-up fluid or mechanical assistance to aid the ESI process. The absence of these additional liquids should offer improved solute detectability and sensitivity in CE–ESI–MS because of improved solute ionization efficiency. Second, the use of a silver conductive CE terminus can allow the exact determination of a charge state for a peak in a mass spectra; however, these additional peaks in the mass spectra may make mixture determination more problematic. Finally, the combination of this new ESI interface with small I.D. capillaries (10 μm) in CE–ESI–MS analyses illustrates that low nl/min effluent flow rates can be electrosprayed directly from a conductive CE capillary terminus. These low CE flow rates permit the ESI–MS to function as a mass sensitive detector, where the ESI current is limited by the rate of delivery of charge carrying species in solution to the ESI source. Consequently, a constant analyte sensitivity is to be expected within the linear dynamic range of the MS detector [8]. These initial results demonstrate a simple and versatile electrospray interface design, which appears to offer increased solute detectability and sensitivity [13], for the use in ultrasensitive peptide and protein analyses.

ACKNOWLEDGMENT

This research is supported by internal exploratory research and the Director, Office of Health and Environmental Research, U.S. Department of Energy. Pacific Northwest Laboratory is operated by Battelle Memorial Institute for the US Department of Energy, through contract DE-AC06-76RLO 1830.

REFERENCES

1 T.F. Cheng and N.J. Dovichi, *Science*, 242 (1988) 562.
2 J.V. Sweedler, J.B. Shear, H.A. Fishman and R.N. Zare, *Anal. Chem.*, 63 (1991) 496.
3 L. Hernandez, J. Escalana, N. Joshi and N. Guzman, *J. Chromatogr.*, 559 (1991) 183.
4 R.A. Wallingford and A.G. Ewing, *Anal. Chem.*, 61 (1989) 98.
5 J.A. Olivares, N.T. Nguyen, C.R. Yonker and R.D. Smith, *Anal. Chem.*, 59 (1987) 1230.
6 R.D. Smith, C.J. Barinaga and H.R. Udseth, *Anal. Chem.*, 60 (1988) 1948.
7 M.D. Lee, W. Mück, J.D. Henion and T.R. Covey, *J. Chromatogr.*, 458 (1988) 313.
8 J.H. Wahl, D.R. Goodlett, H.R. Udseth and R.D. Smith, *Electrophoresis*, 14 (1993) 448.
9 J.H. Wahl, D.R. Goodlett, H.R. Udseth and R.D. Smith, *Anal. Chem.*, 64 (1992) 3194.
10 G.L.M. Bruin, R. Huisden, J.C. Kraak and H. Poppe, *J. Chromatogr.*, 480 (1989) 339.
11 K.D. Lukacs, *Diss. Abstr. Int.*, 44 (1983) 3766.
12 R.D. Smith, H.R. Udseth, C.J. Barinaga and C.G. Edmonds, *J. Chromatogr.*, 559 (1991) 197.
13 J.H. Wahl, D.C. Gale, S.A. Hofstadler, H.R. Udseth and R.D. Smith, presented at the *41st Conference on Mass Spectrometry and Allied Topics, San Francisco, CA, May 1993*; paper ThP 226.
14 J.B. Fenn, M. Mann, C.K. Meng and S.F. Wong, *Mass Spectrom. Rev.*, 9 (1990) 37.
15 R.D. Smith, J.A. Loo, R.R. Ogorzalek Loo, M. Busman and H.R. Udseth, *Mass Spectrom. Rev.*, 10 (1991) 359.
16 A.T. Blades, M.G. Ikonomou and P. Kebarle, *Anal. Chem.*, 63 (1991) 2109.

Journal of Chromatography A, 659 (1994) 223
Elsevier Science B.V., Amsterdam

CHROM. 25 676

Discussion

Isotachophoresis of polyols in borate buffer solutions

J.C. Reijenga

Faculty of Chemical Engineering, Eindhoven University of Technology, P.O. Box 513, 5600 MB Eindhoven (Netherlands)

(Received September 6th, 1993)

In a recent Short Communication in this journal [1], Atamas and Troitsky reported on the electrophoresis of polyols in boric acid solutions. In Fig. 1, experimental data of isotachophoretic mobility *vs.* pH are fitted to a model equation. The major systematic difference between the model and experiment in all four examples indicates that the model presented requires adjustment, especially in view of the following three considerations.

(1) In isotachophoresis it is not uncommon for the pH of the isotachophoretic zones to differ substantially from the pH of the leading electrolyte buffer [2].

(2) The existence of the following equilibria regarding the interaction between diols and boric acid was published many years ago [3,4]:

$$H_3BO_3 + H_2O \rightleftharpoons B(OH)_4^- + H^+ \quad (1)$$

$$B(OH)_4^- + \text{diol} \rightleftharpoons \text{diolB}(OH)_2^- + 2H_2O \quad (2)$$

$$\text{diolB}(OH)_2^- + \text{diol} \rightleftharpoons \text{diol}_2B^- + 2H_2O \quad (3)$$

$$\text{diolB}(OH)_2^- + H^+ \rightleftharpoons \text{diolBOH} + H_2O \quad (4)$$

(3) In addition, mobility differences between, *e.g.*, glucose and rhamnose, also determined by Frahn *et al.* [5] and Consden *et al.* [6], are readily explained by the following additional equilibrium:

$$2B(OH)_4^- + \text{glucose} \rightleftharpoons \text{glucose}(B(OH)_2^-)_2 + 4H_2O \quad (5)$$

as glucose has two pairs of adjacent hydroxyl groups, both orientated in the same direction, whereas rhamnose has only one.

The first can contribute considerably but it remains to be seen which of these aspects will predominate.

REFERENCES

1 S.P. Atamas and G.V. Troitsky, *J. Chromatogr.*, 644 (1993) 407.
2 F.M. Everaerts, Th.P.E.M. Verheggen and J.L. Beckers, *Isotachophoresis, Theory, Instrumentation and Application* (*Journal of Chromatography Library*, Vol. 6), Elsevier, Amsterdam, 1976.
3 H.S. Isbell, J.F. Brewster, N.B. Holt and H.L. Frush, *J. Res. Natl. Bur. Stand.*, 40 (1948) 129.
4 J. Boëseken, *Adv. Carbohydr. Chem.*, 4 (1949) 189.
5 J.L. Frahn and J.A. Mills, *Chem. Ind. (London)*, (1956) 578.
6 R. Consden and W.M. Stainer, *Nature*, 169 (1952) 783.

0021-9673/94/$07.00
SSDI 0021-9673(93)E1120-O

Journal of Chromatography A, 659 (1994) 224
Elsevier Science B.V., Amsterdam

CHROM. 25 677

Discussion

Isotachophoresis of polyols in borate buffer solutions —a reply

S.P. Atamas

Crimean Medical Institute, Department of Biochemistry, Bulv. Lenina 5/7, 333 670 Simferopol (Ukraine)

(Received October 18th, 1993)

Referring to Reijenga's comments [1] concerning our paper in this journal [2], I should like to state that the data in Fig. 1 relate to ionophoretic but not isotachophoretic mobility. It is evident that boundary mobilities in isotachophoresis and in free electrophoresis differ from each other. Hence the first of the three considerations presented is not relevant.

In addition, the model equation discussed is empirical and does not explain the real mechanism of interaction between polyols, boric acid and water.

Since these interactions are not simple, as follows from the second and the third considerations of Dr. Reijenga and from many other sources, the model empirical equation fitting experimental data also cannot be simple. We tried to select the simplest of all possible versions which are accurate enough. However, the final equation obtained is still too complicated.

We consider that our model fitting is adequate, as can be seen in Fig. 1. However, we would be grateful to anybody who can find a better model equation for the experimental data.

REFERENCES

1 J.C. Reijenga, *J. Chromatogr.*, 659 (1994) 223.
2 S.P. Atamas and G.V. Troitsky, *J. Chromatogr.*, 644 (1993) 407.

0021-9673/94/$07.00
SSDI 0021-9673(93)E1119-K

Journal of Chromatography A, 659 (1994) 225
Elsevier Science B.V., Amsterdam

CHROM. 25 643

Book Review

HPLC detection: newer methods, edited by G. Patonay, VCH, Weinheim, 1992, IX + 236 pp., price DM 158, £ 65, ISBN 0-89573-372-7, 3-527-28219-X.

The book is focused on new detection methods in HPLC, including several coupled techniques. Conventional detection methods in HPLC can give only very limited information and are not useful for peak identification, which is the most important aspect of chromatographic separations. Useful information for peak identification is provided by a combination of chromatography with detectors providing structural information, and this has been the driving force behind the development of effective coupled techniques. Selective detection capability is also of major importance because separations of complex mixtures are sometimes very difficult but selective detection provides much simpler chromatograms for the desired analytes. Therefore, new detection techniques are required to establish such capabilities in HPLC. The purpose of this book is to introduce and discuss newer detection methods in HPLC, and the Editor and the contributors have succeeded in accomplishing this primary purpose.

In Chapter 1, laser-based detection is discussed. Lasers are the most promising and powerful tool for HPLC detection but still very few are commercially available because of the difficulty of providing them at an economic cost. This chapter treats selective detection using lasers. Chapter 2 discusses an unusual detection method using luminescence, especially focusing on the luminescence detection of lanthanides.

Chapter 3 treats detection methods using chemiluminescence. Postcolumn reactions using ozone-induced bioluminescence and electroluminescence make highly selective and sensitive detection possible at picomole or femtomole levels. In Chapter 4, the authors discuss the use of near-infrared (NIR) radiation for HPLC detection. NIR fluorescence after labelling using a laser diode is mainly discussed.

The popular electrochemical detection method in HPLC is discussed in Chapter 5. Details of the method such as the theory, mobile phase requirements, electrodes, cell design and various detection modes are discussed. Another method using lasers appears in Chapter 6, in which photothermal detectors are introduced. Applications and future prospects are discussed.

The most popular coupled techniques in separation sciences are Fourier transform (FT) IR and MS combined with chromatography. Recent efforts and instrumentation in HPLC–FT-IR are introduced in Chapter 7 and HPLC–MS in Chapter 8. FT-IR detection in HPLC can be divided into two alternative interface approaches, solvent elimination and the flow cell. Both are well reviewed in this chapter. MS is the only universal detection technique in HPLC, although the refractive index method is also categorized as universal, but its very low sensitivity hinders future possibilities. Both chapters are well written but the discussions cover the same ground as in other books on HPLC detection.

An unusual detection technique using NMR is described in Chapter 9. NMR is the most powerful tool for organic identification but the difficulty of combining it with HPLC is obvious because of mobile phase interference and its low sensitivity. Impressive results from several research groups are reviewed.

Overall, this book is a valuable new source of information on the latest developments in HPLC detection techniques, and it is highly recommended for graduate students, technicians and researchers using HPLC.

Toyohashi (Japan) Kiyokatsu Jinno

SSDI 0021-9673(93)E1126-K

Journal of Chromatography A, 659 (1994) 226–227
Elsevier Science B.V., Amsterdam

CHROM. 25 712

Book Review

Handbook of derivatives for chromatography, by K. Blau and J.M. Halket, Wiley, New York, 2nd ed., 1993, XXII + 369 pp., price £ 65.00 ISBN 0-471-92699-X.

This is really a handbook of methods, reagents, chemicals and detection approaches suitable for a large variety of organics and inorganics in all forms of chromatography, for all forms of chromatography. There is no discussion of the applicability of any of these reagents or approaches/methods for applications in HPCE or other forms of electrophoresis. The first edition of this outstanding handbook was published in 1977 or thereabouts, and it was very well received. This edition is much better and will, one predicts, be even more well received, if that is possible. The book is very practically oriented, containing a wealth of useful and usable information about how to choose reagents for various areas of chromatography, for various classes of organics/inorganics, for various detection needs, with tables throughout, specific chemistries throughout, and (!) with exact details of procedures, even with comments on pitfalls in each procedure. It also contains know-how to actually carry out the derivatizations, once recommended.

The book is nicely divided into about 16 individual chapters, each of which could almost stand on its own as a separate review article on that particular topic. However, the book is much more than just a collection of chapters that delineate and list available derivatizing reagents and procedures for various classes of reactions, such as esterification, acylation, silylation, alkylation, ketone–base condensations, cyclic derivatization, and so forth. Because, it also contains other chapters that summarize available derivatization approaches for UV-absorbing derivatives, fluorescent derivatives, and so forth. In addition, it contains still further chapters that discuss ion-pair extraction approaches in chromatography, derivatizations for fast-atom bombardment MS, derivatives for supercritical fluid chromatography, derivatives for GC–MS, and also post-chromatographic derivatization approaches. Finally, the book wraps itself in-between two outstanding chapters, the first and the last. These deal with a guide to the handbook and the selection of derivatives and then practical considerations in using the reactions and reagents provided in the prior chapters.

The book contains specific discussions and descriptions of reaction/derivatization procedures, conditions, temperatures, times, amounts of reagents, work-up of reactions, amounts injected, and so forth. It can be used as almost a cook-book of how to perform specific derivatizations, for specific substrates/analytes, with specific reagents and conditions cited throughout. There are comments about the specific conditions where needed, not too many, not too convoluted or involved, but just thorough enough to assist the reader in using the procedures reproduced.

There are tables and tables of specific chemical reagents cited for derivatization of various classes of compounds for chromatography, *and* then specific line equations of individual reaction chemistries. Both prove most helpful to those with an organic bent or interest, as well as chromatographic interests. At times, specific chemical (line) equations of reagents, analytes, conditions, products and so forth are missing, such as in the chapter dealing with post-column reaction chemistries. Too many times one reads about specific approaches that could be used in chromatographic derivatizations, but only words were used to describe the chemistry involved, rather than actual chemical reactions and struc-

SSDI 0021-9673(93)E1180-8

tures. The index is fine, it is very detailed, one can find almost anything described anywhere in the book. The Table of Contents is thorough, so that one can find individual topic areas with ease and go right to those sections. The figures are well done, chromatograms are easy to understand, photographs, schematics, and diagrams are replete throughout the book. There are photos of actual instrumentation, post-column reactor designs, photochemical apparatus, and so forth. The book is quite complete and replete with illustrations, tables of reagents, substrates, reaction conditions, and references. The references are incredibly thorough, exhaustive, extremely complete, up-to-date, and well cited throughout each and every chapter. There are almost, not quite, too many references and literature citations provided.

This is not a book that one reads late at night over a warm glass of milk or tea. Rather, it is a book that one keeps in the laboratory or on the office-laboratory bookshelf, and then pulls down when it is time to decide which reagent would be best for a specific application in chromatography and why that reagent above all others. It is really a *handbook* of chemistry for chromatography, to be used by able and experienced practitioners of chromatography, with perhaps some experience already in derivatization areas. They now need to use other derivatization approaches for perhaps different analytes and/or different types of chromatography. The book is somewhat unique, it is not a book that will teach people how to do HPLC or supercritical fluid chromatography or GC, but rather it is a book that will help us to perform reaction chemistry for chromatography. It does *not* discuss specific aspects of HPLC, GC or supercritical fluid chromatography, but rather discusses how chemistry can be used to improve the utility and applicability of these separation techniques. It may not even be a book that people will read to teach themselves how to perform, in general, derivatizations for chromatography, until they need a specific application of such approaches. It is perhaps hard to imagine anyone, other than reviewers and/or experts in these areas, actually setting out and sitting down to read this book cover-to-cover, just to learn more about derivatizations for chromatography. That does *not* detract from the worth and value of the book —for these things are inherent within its pages. Rather, if you are going to purchase the book, it will not be for a specific course or reading pleasure, but rather to use as a reference tool, to cite on occasions for proposals and reviews or research papers, and more importantly, to use on a regular or irregular basis as the need arises for specific problems, analyses, analytes, and reaction chemistries. Clearly the book is highly recommended for such specific needs and intents, if not just to add to one's professional library.

Boston, MA (USA) Ira S. Krull

Journal of Chromatography A, 659 (1994) 228
Elsevier Science B.V., Amsterdam

CHROM. 25 669

Book Review

Chromatography of polymers —Characterization by SEC and FFF (ACS Symposium Series, No. 521), edited by T. Provder, American Chemical Society, Washington, DC, 1993, XIII + 337 pp., price US$ 94.95, ISBN 0-8412-2625-3. This work reports a symposium held at the 202nd National Meeting of the American Chemical Society, New York, August 25–30, 1991.

Significant advances in the chromatographic characterization of polymers by size-exclusion chromatography (SEC) and field flow fractionation (FFF) are described. The work consists of 22 chapters arranged in four groupings, the first on FFF, the remainder on SEC. The chapters on SEC concern fundamental considerations, viscometric detection and some high-temperature applications to polymers.

Current developments in FFF methods (sedimentation, flow FFF and thermal FFF) make up the first grouping. Sedimentation techniques are applied to perfluorocarbon emulsions while this technique and flow FFF are applied to nanometre size particles. Again using lattices narrow and broad molecular mass distributions are determined followed by a review of thermal FFF. The final two FFF contributions concern the analysis of co-polymers and the determination of the gel content of electron beam irradiated polymers.

Fundamental considerations of SEC first establish the critical conditions for compositional polymer separation followed by a validation of a single-parameter calibration curve, and a quantitative determination of specific refractive index increments by SEC. Multidetection SEC for compositional determination and quantitative end group analysis using spectroscopy and SEC complete the grouping.

Viscometric detection in SEC includes two contributions on a strategy for interpreting multidetector SEC data, the quantitative nature of single-capillary viscometric measurements, the use of various solvent systems and the determination of absolute number-average molecular masses of copolymers and mixed homopolymers.

The final section reports high-temperature SEC, three chapters consider applications to polyolefins, the others to various forms of copolymers of vinylpyrrolidone, to cotton fibre and to aggregated polysaccharides.

The chapters include a vast amount of information on FFF and SEC which has developed in the last few years. The work as the majority of works on the topic is largely mathematical in nature. The volume will be of interest to the serious worker rather than the casual reader. The chapters provided by active researchers each include moderate bibliographies in many cases containing references to the authors' previous works thus allowing ready access to a particular area.

Kensington, N.S.W. (Australia) J.K. Haken

SSDI 0021-9673(93)E1127-L

Journal of Chromatography

Request for Manuscripts

Ralph Riggin and Gregory Davis will edit a special, thematic issue of the *Journal of Chromatography* entitled "**Analytical Biotechnology**". Both reviews and research articles will be included.

Topics such as the following will be covered:

- Sequencing
- Host Cell Protein Determination
- Peptide Mapping
- Electrophoretic Methods
- Capillary Electrophoresis/Electrokinetic Chromatography
- Protein Mass Spectrometry
- Glycoprotein Characterization
- High-Speed Separations
- Chromatographic Methods
- Residual DNA Determination
- Immunochemical Assays
- Moisture Determination

Potential authors of reviews should contact Roger Giese, Editor, prior to any submission. Address: Mugar Building Rm 122, Northeastern University, Boston, MA 02115, USA; tel.: (617) 373-3227; fax: (617) 373-8720.

The deadline for receipt of submissions is **April 30, 1994**. Manuscripts submitted after this date can still be published in the Journal, but then there is no guarantee that an accepted article will appear in this special, thematic issue. Four copies of the manuscript, citing this issue, should be submitted to the Editorial Office, Journal of Chromatography, P.O. Box 681, NL-1000 AR Amsterdam, The Netherlands. All manuscripts will be reviewed and acceptance will be based on the usual criteria for publishing in the *Journal of Chromatography*.

Environmental Analysis

Techniques, Applications and Quality Assurance

Edited by **D. Barceló**

Techniques and Instrumentation in Analytical Chemistry Volume 13

Three aspects of environmental analysis are treated in this book:

- the use of various analytical techniques
- their applications to trace analysis of pollutants, mainly organic compounds
- quality assurance aspects, including the use of certified reference materials for quality control of the entire analytical process.

The book will serve as a general reference for post-graduate students as well as a practical reference for environmental chemists who need to use the analytical techniques for environmental studies. Analytical chemists needing information on the complexity of environmental sample matrices and interferences will also find this an invaluable reference.

Contents: Part 1. Field Sampling Techniques and Sample Preparation. 1. Sampling techniques for air pollutants (R. Niessner). 2. Sample handling strategies for the analysis of organic contaminants from environmental samples (M.-C. Hennion, P. Scribe). 3. Extraction, clean-up and recoveries of persistent trace organic contaminants from sediment and biota samples (D.E. Wells).
Part 2. Application Areas. 4. Current developments in the analysis of polychlorinated biphenyls (PCBs) including planar and other toxic metabolites in environmental matrices (D.E. Wells). 5. Official methods of analysis of priority pesticides in water using gas chromatographic techniques (D. Barceló). 6. Coupled-column reversed phase liquid chromatography as a versatile technique for the determination of polar pesticides (E.A. Hogendoorn, P. van Zoonen). 7. Liquid chromatographic determination of phenols and substituted derivatives in water samples (G. Marko-Varga). 8. HPLC methods for the determination of mycotoxins and phycotoxins (J.F. Lawrence, P.M. Scott). 9. Determination of radionuclides in environmental samples (V. Valkovic).
Part 3. Quality Assurance and Reference Materials. 10. Quality assurance in environmental analysis (W.P. Cofino). 11. Certified reference materials for the quality control of measurements in environmental monitoring (E.A. Maier). 12. Standard reference materials for the determination of trace organic constituents in environmental samples (S.A. Wise).

ELSEVIER SCIENCE B.V.

Part 4. Emerging Techniques. 13. Application of fluorescence spectroscopic techniques in the determination of PAHs and PAH metabolites (F. Ariese, C. Gooijer, N.H. Velthorst). 14. Characterization of surfactants in water by desorption ionization methods (F. Ventura). 15. Utilization of various LC-MS interfacing systems in environmental analysis; application to polar pesticides (M.H. Lamoree, R.T. Ghijsen, U.A.Th. Brinkman). 16. Hyphenated techniques applied to the speciation of organometallic compounds in the environment (O.F.X. Donard, R. Ritsema). 17. The potential of capillary electrophoresis in environmental analysis (M.W.F. Nielen).
Subject index.

© 1993 660 pages Hardbound
Price: Dfl. 465.00 (US $ 265.75)
ISBN 0-444-89648-1

ORDER INFORMATION

For USA and Canada
ELSEVIER SCIENCE INC.
P.O. Box 945
Madison Square Station
New York, NY 10160-0757
Fax: (212) 633 3880

In all other countries
ELSEVIER SCIENCE B.V.
P.O. Box 330
1000 AH Amsterdam
The Netherlands
Fax: (+31-20) 5862 845

US$ prices are valid only for the USA & Canada and are subject to exchange rate fluctuations; in all other countries the Dutch guilder price (Dfl.) is definitive. Customers in the European Community should add the appropriate VAT rate applicable in their country to the price(s). Books are sent postfree if prepaid.

Analytical Applications of Circular Dichroism

Edited by **N. Purdie** and **H.G. Brittain**

Techniques and Instrumentation in Analytical Chemistry Volume 14

Circular dichroism is a special technique which provides unique information on dissymmetric molecules. Such compounds are becoming increasingly important in a wide variety of fields, such as natural products chemistry, pharmaceutics, molecular biology, etc. The content of this book has been selected in order to feature the unique aspects of circular dichroism, and how these strengths can be of assistance to workers in the field.

Substantial discussions have been provided regarding the particular phenomena associated with dissymmetric compounds which give rise to the circular dichroism effect. Reviews are also given of the type of instrumentation available for the measurement of these effects. A number of chapters cover the wide range of applications illustrating the power of the method.

Owing to its broad appeal, the book will be of interest to workers in all areas of chemistry and pharmaceutical science.

Contents:

© 1994 360 pages Hardbound
Price: Dfl. 355.00 (US $ 202.75)
ISBN 0-444-89508-6

ORDER INFORMATION

For USA and Canada
ELSEVIER SCIENCE INC.
P.O. Box 945
Madison Square Station
New York, NY 10160-0757
Fax: (212) 633 3880

In all other countries
ELSEVIER SCIENCE B.V.
P.O. Box 330
1000 AH Amsterdam
The Netherlands
Fax: (+31-20) 5862 845

US$ prices are valid only for the USA & Canada and are subject to exchange rate fluctuations; in all other countries the Dutch guilder price (Dfl.) is definitive. Customers in the European Community should add the appropriate VAT rate applicable in their country to the price(s). Books are sent postfree if prepaid.

ELSEVIER SCIENCE B.V.

PUBLICATION SCHEDULE FOR THE 1994 SUBSCRIPTION

Journal of Chromatography A and *Journal of Chromatography B: Biomedical Applications*

MONTH	O 1993	N 1993	D 1993	J	F	
Journal of Chromatography A	652/1 652/2 653/1	653/2 654/1 654/2 655/1	655/2 656/1 + 2 657/1 657/2	658/1 658/2 659/1 659/2	660/1 + 2 661/1 + 2 662/1 662/2	The publication schedule for further issues will be published later.
Bibliography Section						
Journal of Chromatography B: Biomedical Applications				652/1	652/2 653/1	

INFORMATION FOR AUTHORS

(Detailed *Instructions to Authors* were published in *J. Chromatogr. A*, Vol. 657, pp. 463–469. A free reprint can be obtained by application to the publisher, Elsevier Science B.V., P.O. Box 330, 1000 AH Amsterdam, Netherlands.)

Types of Contributions. The following types of papers are published: Regular research papers (full-length papers), Review articles, Short Communications and Discussions. Short Communications are usually descriptions of short investigations, or they can report minor technical improvements of previously published procedures; they reflect the same quality of research as full-length papers, but should preferably not exceed five printed pages. Discussions (one or two pages) should explain, amplify, correct or otherwise comment substantively upon an article recently published in the journal. For Review articles, see inside front cover under Submission of Papers.

Submission. Every paper must be accompanied by a letter from the senior author, stating that he/she is submitting the paper for publication in the *Journal of Chromatography A* or *B*.

Manuscripts. Manuscripts should be typed in **double spacing** on consecutively numbered pages of uniform size. The manuscript should be preceded by a sheet of manuscript paper carrying the title of the paper and the name and full postal address of the person to whom the proofs are to be sent. As a rule, papers should be divided into sections, headed by a caption (*e.g.*, Abstract, Introduction, Experimental, Results, Discussion, etc.) All illustrations, photographs, tables, etc., should be on separate sheets.

Abstract. All articles should have an abstract of 50–100 words which clearly and briefly indicates what is new, different and significant. No references should be given.

Introduction. Every paper must have a concise introduction mentioning what has been done before on the topic described, and stating clearly what is new in the paper now submitted.

Experimental conditions should preferably be given on a *separate* sheet, headed "Conditions". These conditions will, if appropriate, be printed in a block, directly following the heading "Experimental".

Illustrations. The figures should be submitted in a form suitable for reproduction, drawn in Indian ink on drawing or tracing paper. Each illustration should have a caption, all the *captions* being typed (with double spacing) together on a *separate sheet*. If structures are given in the text, the original drawings should be provided. Coloured illustrations are reproduced at the author's expense, the cost being determined by the number of pages and by the number of colours needed. The written permission of the author and publisher must be obtained for the use of any figure already published. Its source must be indicated in the legend.

References. References should be numbered in the order in which they are cited in the text, and listed in numerical sequence on a separate sheet at the end of the article. Please check a recent issue for the layout of the reference list. Abbreviations for the titles of journals should follow the system used by *Chemical Abstracts*. Articles not yet published should be given as "in press" (journal should be specified), "submitted for publication" (journal should be specified), "in preparation" or "personal communication".

Vols. 1–651 of the *Journal of Chromatography*; *Journal of Chromatography, Biomedical Applications* and *Journal of Chromatography, Symposium Volumes* should be cited as *J. Chromatogr.* From Vol. 652 on, *Journal of Chromatography A* (incl. Symposium Volumes) should be cited as *J. Chromatogr. A* and *Journal of Chromatography B: Biomedical Applications* as *J. Chromatogr. B*.

Dispatch. Before sending the manuscript to the Editor please check that the envelope contains four copies of the paper complete with references, captions and figures. One of the sets of figures must be the originals suitable for direct reproduction. Please also ensure that permission to publish has been obtained from your institute.

Proofs. One set of proofs will be sent to the author to be carefully checked for printer's errors. Corrections must be restricted to instances in which the proof is at variance with the manuscript.

Reprints. Fifty reprints will be supplied free of charge. Additional reprints can be ordered by the authors. An order form containing price quotations will be sent to the authors together with the proofs of their article.

Advertisements. The Editors of the journal accept no responsibility for the contents of the advertisements. Advertisement rates are available on request. Advertising orders and enquiries can be sent to the Advertising Manager, Elsevier Science B.V., Advertising Department, P.O. Box 211, 1000 AE Amsterdam, Netherlands; courier shipments to: Van de Sande Bakhuyzenstraat 4, 1061 AG Amsterdam, Netherlands; Tel. (+31-20) 515 3220/515 3222, Telefax (+31-20) 6833 041, Telex 16479 els vi nl. *UK*: T.G. Scott & Son Ltd., Tim Blake, Portland House, 21 Narborough Road, Cosby, Leics. LE9 5TA, UK; Tel. (+44-533) 753 333, Telefax (+44-533) 750 522. *USA and Canada*: Weston Media Associates, Daniel S. Lipner, P.O. Box 1110, Greens Farms, CT 06436-1110, USA; Tel. (+1-203) 261 2500, Telefax (+1-203) 261 0101.

Analytical Abstracts Now on CD-ROM!

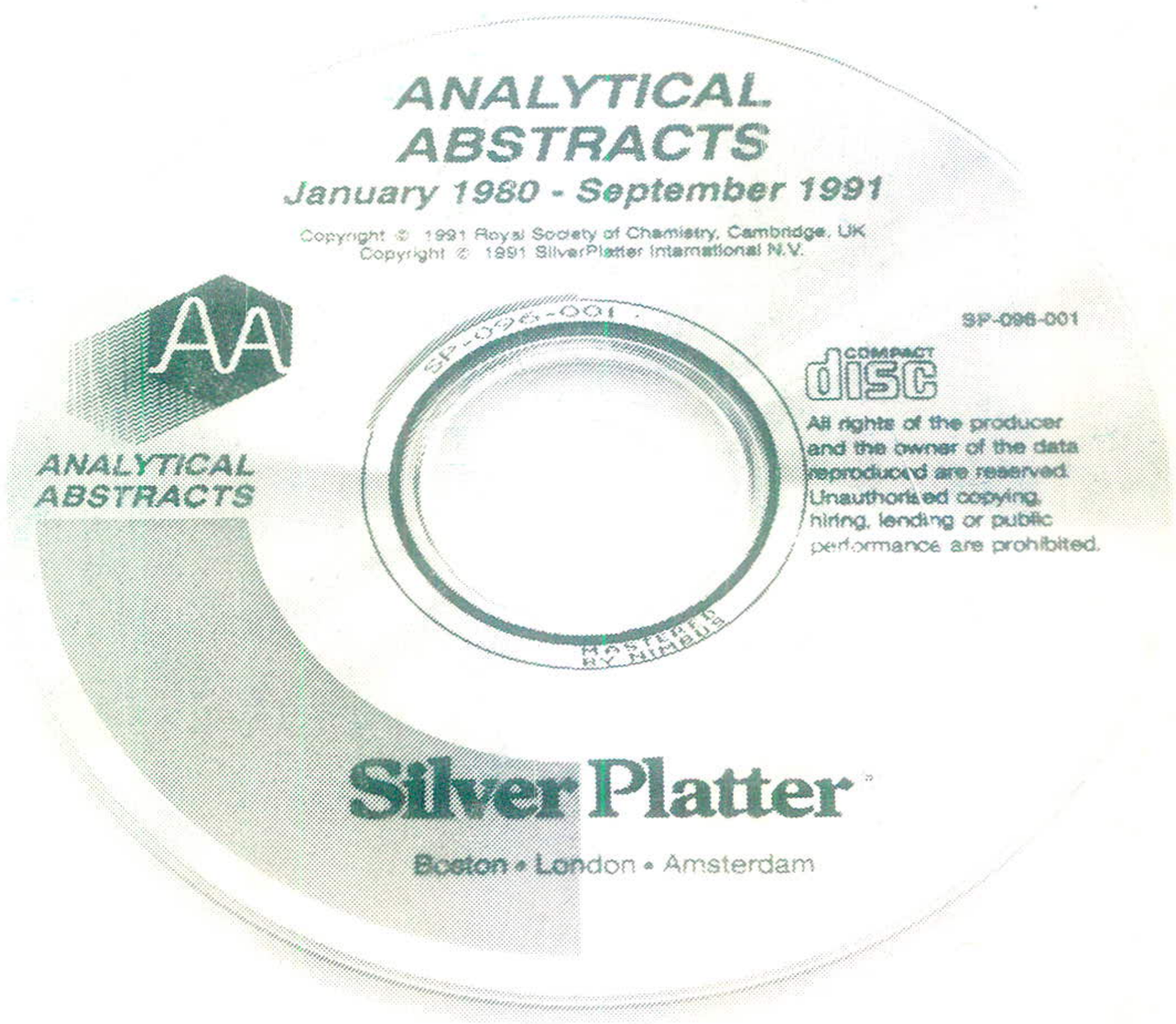

Available in Macintosh™ and IBM Compatible Formats

The premier source of current awareness information in analytical chemistry is now available on a single SilverPlatter CD-ROM.

Analytical Abstracts on CD-ROM features:

- Approximately 140,000 items from 1980 onwards
- Easy to use SilverPlatter software
- Quarterly updates with more than 3,000 items
- Unlimited searching – no additional costs

Special Discount for Hardcopy Subscribers

Contact us today for further information and a FREE demo disk.

Judith Barnsby, Royal Society of Chemistry,
Thomas Graham House, Science Park, Milton Road,
Cambridge CB4 4WF, United Kingdom
Tel: +44 (0) 223 420066 Fax: +44 (0) 223 423623
Telex: 818293 ROYAL

AA

ROYAL SOCIETY OF CHEMISTRY
Information Services